



Consiglio Nazionale
delle Ricerche



UNIVERSITÀ DEGLI STUDI DI NAPOLI

“FEDERICO II”

Department of Biology



PhD in Biology 35th Cycle

PhD Thesis

***Characterization of the Capnophilic Lactic Fermentation
pathway and molecular approaches in the hyperthermophilic
bacterium Thermotoga neapolitana***

Tutors

Prof. Sergio Esposito
Prof. Angelo Fontana
Dr. Giuliana d'Ippolito

PhD Student

Nunzia Esercizio

Table of Contents

Abstract	3
<i>Lists of Publications.....</i>	4
1. Introduction.....	5
1.1 Taxonomy of <i>Thermotoga neapolitana</i>	7
1.2 Dark fermentation pathway in <i>T.neapolitana</i>	9
1.3 Capnophilic lactic fermentation in <i>T.neapolitana</i>	11
1.4 Goal of the project.....	13
1.5 Structure of the thesis.....	13
1.6 References	17
2. Fermentation of Biodegradable Organic Waste by the Family Thermotogaceae	22
3. Effect of Cultivation Parameters on Fermentation and Hydrogen Production in the Phylum Thermotogae.....	49
4. CO₂-Induced Transcriptional Reorganization: Molecular Basis of Capnophilic Lactic Fermentation in <i>Thermotoga Neapolitana</i>	84
5.Improvement of CO₂ and Acetate Coupling into Lactic Acid by Genetic Manipulation of the Hyperthermophilic Bacterium <i>Thermotoga Neapolitana</i>	96
6. Evidence for a pentose phosphate pathway in the hyperthermophilic anaerobic bacterium <i>Thermotoga neapolitana</i>.....	109
7. Occurrence of Capnophilic Lactic Fermentation in the Hyperthermophilic Anaerobic Bacterium <i>Thermotoga</i> sp. Strain RQ7.....	125
8. Effect of inorganic sulfured sources on CLF pathway in <i>Thermotoga neapolitana</i>.....	139
9. Adaptive laboratory evolution of <i>Thermotoga neapolitana</i> in minimal medium containing glucose as unique organic source.....	165
10.Electrostimulation of Hyperthermophile <i>Thermotoga Neapolitana</i> Cultures.....	176
11. Conclusion and future perspectives.....	187

Abstract

Capnophilic lactic fermentation (CLF) is a novel anaplerotic pathway recently identified and patented in the anaerobic hyperthermophilic bacterium *Thermotoga neapolitana*. The CO₂-activated mechanism enables a non-competitive synthesis of hydrogen and L-lactic acid at high yields from sugar-based waste and renewable feedstocks, which makes it economically attractive for development of sustainable biotechnological processes. Starting from the transcriptional modification induced by CO₂ in *T. neapolitana* cultures using an RNA-seq approach, this study shows a massive metabolic rearrangement of the central carbon metabolism along with the activation of replenishing mechanisms that increase the availability of reducing equivalents necessary to support the concomitant production of hydrogen and lactic acid by CLF pathway. The analysis of the differentially expressed genes allowed the selection of possible candidates for the genetic manipulation of *T. neapolitana*. The development of a specific transformation strategy allowed to the heterologous expression of the *acs* gene that increased the fixation rate of CO₂ into lactic acid, thus in the mutant strain ACS03. During this study, we also found that *Thermotoga* sp. RQ7 is the closest parental strain of *T. neapolitana* and the only naturally competent strain of the genus *Thermotoga*. This strain, originally isolated from marine sediment in the Azores, is also able to operate CLF and thus, is proposed as candidate for further implementation of the CLF applications.

On the basis of evidence in the transcriptomic analysis suggesting the possible switch from the classical Embden-Meyerhof-Parnas pathway to the alternative Entner-Doudoroff or oxidative pentose phosphate pathway, a biosynthetic study performed in this PhD thesis by using NMR and GC-MS techniques highlighted the possible activation of the pentose phosphate pathway in *T. neapolitana* under CO₂. In addition, investigation of variation of the culture media highlighted the effect of sulfur compounds and nitrogen source on the production of lactic acid and hydrogen by CLF.



Lists of Publications

1. d'Ippolito G, Landi S, **Esercizio N.**, Lanzilli M, Vastano M, Dipasquale L, Pradhan N and Fontana A. CO₂-Induced Transcriptional Reorganization: Molecular Basis of Capnophilic Lactic Fermentation in *Thermotoga neapolitana*. *Front. Microbiol.* **2020**, 11:171. doi: 10.3389/fmicb.2020.00171
2. **Esercizio, N.**; Lanzilli, M.; Vastano, M.; Landi, S.; Xu, Z.; Gallo, C.; Nuzzo, G.; Manzo, E.; Fontana, A.; d'Ippolito, G. Fermentation of Biodegradable Organic Waste by the Family *Thermotogaceae*. *Resources*. **2021**, 10, 34. <https://doi.org/10.3390/resources10040034>
3. Lanzilli, M.; **Esercizio, N.**; Vastano, M.; Xu, Z.; Nuzzo, G.; Gallo, C.; Manzo, E.; Fontana, A.; d'Ippolito, G. Effect of Cultivation Parameters on Fermentation and Hydrogen Production in the Phylum *Thermotogae*. *Int. J. Mol. Sci.* **2021**, 22, 341. <https://doi.org/10.3390/ijms22010341>
4. **Esercizio, N.**; Lanzilli, M.; Vastano, M.; Xu, Z.; Landi, S.; Caso, L.; Gallo, C.; Nuzzo, G.; Manzo, E.; Fontana, A.; et al. Improvement of CO₂ and Acetate Coupling into Lactic Acid by Genetic Manipulation of the hyperthermophilic Bacterium *Thermotoga neapolitana*. *Microorganisms* **2021**, 9, 1688. <https://doi.org/10.3390/microorganisms9081688>
5. G. d'Ippolito, G. Squadrito, M. Tucci, **N. Esercizio**, A. Sardo, M. Vastano, M. Lanzilli, A. Fontana, P. Cristiani, Electrostimulation of hyperthermophile *Thermotoga neapolitana* cultures, *Bioresource Technology*, **2021**, Volume 319, 2021,124078, ISSN 0960-8524, doi.org/10.1016/j.biortech.2020.124078.
6. **Esercizio, N.**; Lanzilli, M.; Landi, S.; Caso, L.; Xu, Z.; Nuzzo, G.; Gallo, C.; Manzo, E.; Esposito, S.; Fontana, A.; et al. Occurrence of Capnophilic Lactic Fermentation in the Hyperthermophilic Anaerobic Bacterium *Thermotoga sp.* Strain RQ7. *Int. J. Mol. Sci.* **2022**, 23, 12049. <https://doi.org/10.3390/ijms231912049>

Manuscripts in preparation

- I. Effect of inorganic sulfured sources on Capnophilic Lactic Fermentation pathway in *Thermotoga neapolitana*
Esercizio, N. et al
- II. Evidence for a pentose phosphate pathway in the hyperthermophilic anaerobic bacterium *Thermotoga neapolitana*
Esercizio, N. et al
- III. Adaptive laboratory evolution of *Thermotoga neapolitana* in minimal medium containing glucose as unique organic source
Esercizio, N. et al

1. Introduction

Hydrogen is considered central player for the implementation of green alternative to the traditional use of fossil fuels for energy production. Oxidation of hydrogen by internal-combustion engines or fuel cells produces only water, thus the gas is considered a clean and renewable energy vector, potentially of unlimited abundance.

Hydrogen is also the side product of biological processes through three major mechanisms named biophotolysis, photofermentation and anaerobic fermentation (Chong et al., 2009; Boodhun et al., 2017; Dincer et al., 2018; Staffel et al., 2019; Esercizio et al., 2021b). In this context, Dark Fermentation (DF) is currently recognized as a promising and attractive way of anaerobic fermentation to produce the so-called biological hydrogen or biohydrogen at high yield from a wide range of organic feedstock (**Fig.1**) (Chong et al., 2009; Ntaikou et al., 2010; Khanna et al., 2012; Abreu et al., 2016; Soares et al., 2020; Esercizio et al., 2021b).

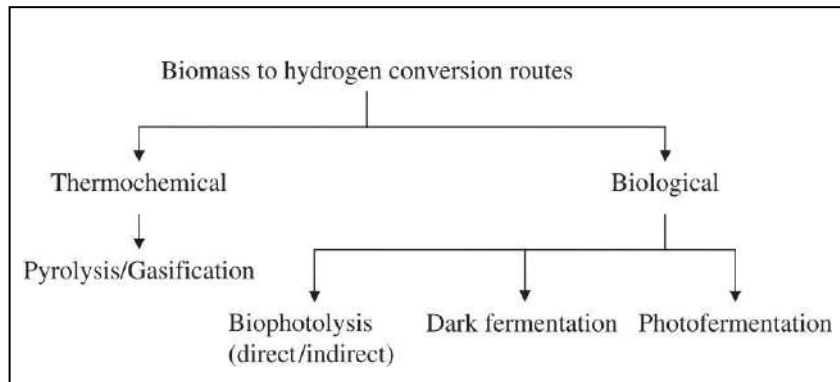


Fig.1 Schematic representation of the main hydrogen production routes from Manish et al., 2008

The thermophilic and hyperthermophilic bacteria of the *Thermotogacea* family can ferment a wide range of sugar-based waste and release of high hydrogen with yields close to the theoretical value of 4 mole of hydrogen *per* mole of sugar expected by the Thauer equation (Thauer et al., 1977; Huber et al., 1986; Jannash et al., 1988; Balk et al., 2002; Huber et al., 2006; Eriksen et al., 2011; Cappelletti et al., 2014; Esercizio et al., 2021b). In addition to the high hydrogen yield, fermentation processes based on these hyperthermophilic bacteria is attractive for a number of technical advantages that include (1) the low risk of contamination even in the absence of costly and energy-demanding

sterilization procedures, (2) the increased solubility of complex substrates such as lignocellulosic waste, (3) the favorable hydraulic retention time and organic loading rate, and (4) the reduction of cooling costs (Khanna et al., 2012).

In the past years, among the members of *Thermotoga spp*, special attention has been given to *Thermotoga neapolitana* that operates an unprecedented fermentation process called capnophilic lactic fermentation (CLF). This mechanism is induced by CO₂ and requires an unusual pathway of non-photosynthetic fixation. By CLF, *T. neapolitana* is able to recycle exogenous CO₂ by coupling it to acetate and synthesize lactic acid. The process does not affect rate and yield of the hydrogen production, thus offering a fermentation model competitive to dark fermentation (Dipasquale et al., 2014; d'Ippolito et al., 2014; Pradhan et al., 2017). CLF occurrence in *T. neapolitana* allows to consider this bacterium a very promising candidate for biotechnological processes aimed to couple energy production (hydrogen), CO₂ valorization (synthesis of L-lactic acid) and waste treatment (sugar-based fermentation). In this context, CLF potential has been funded by the European Horizon 2020 project “BioRECO₂VER” that focused on development of sustainable biotechnological processes for the capture of CO₂ and its conversion into industrial products.

1.1 Taxonomy of *Thermotoga neapolitana*

T. neapolitana was isolated and identified in a shallow submarine hot spring near Lucrino, in the Bay of Naples in 1986 (**Fig.2**). The bacterium, together with *T. maritima*, *T. petrophila*, *T. naphthophila*, *Thermotoga* sp. EMP, *Thermotoga* sp. A7A, *Thermotoga* sp. RQ2 and sp. RQ7 is member of the genus *Thermotoga*, one of the two taxonomic branches of the family *Thermotogaceae* that include also *P. lettingae*, *P. thermarum*, *P. elfii*, *P. subterranea*, and *P. hypogea*, which belong to the new genus *Pseudothermotoga* (Bhandari and Gupta 2014; Belahbib et al., 2018; Esercizio et al., 2021b).

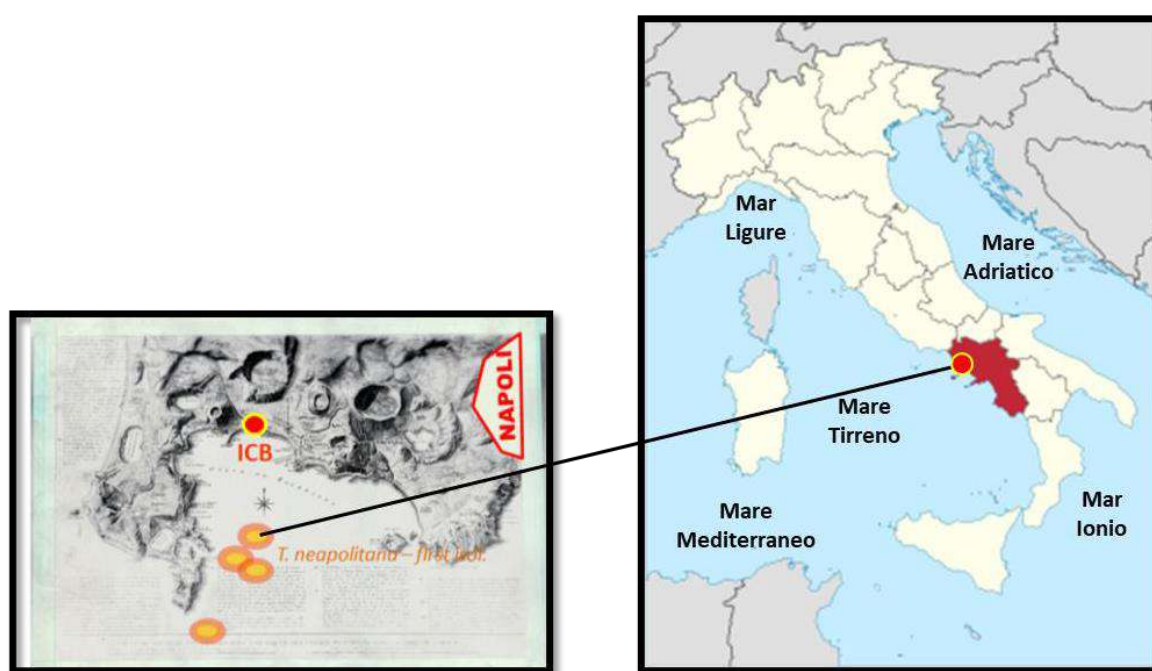


Fig. 2 Geographical indication of the *Thermotoga neapolitana* isolation point. The proximity between the isolation point and the Institute of Biomolecular Chemistry is observable.

All the member of the family *Thermotogaceae* are anaerobic, hyperthermophilic, gram-negative, rod-shaped bacteria, surrounded by a sheath-like structure called “toga”, made of peptidoglycan that wrap and protect the whole prokaryotic cell, and isolated from geothermal environments, oil reservoirs, submarine hot springs, and continental solfataric springs, with optimal growth

temperature in the range of 77–80°C (**Fig.3**) (Huber et al. 1986; Balk et al. 2002, Fardeau et al. 1997, Jannasch et al. 1988, Windberger et al. 1989, Jeanthon et al. 1995, Ravot et al. 1995, Takahata et al. 2001).

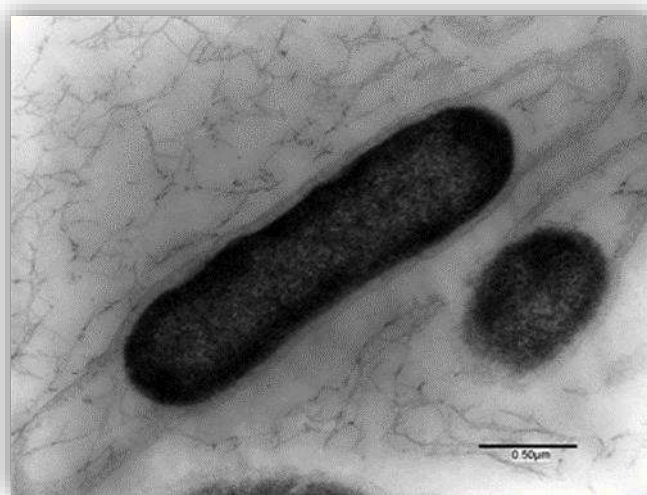
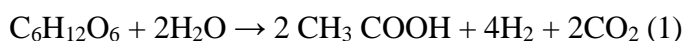


Fig. 3 Microscope image of bacteria belonging to the family *Thermotogaceae*.

A large number of *Thermotoga* and *Pseudothermotoga* species are recognized as good candidates for bio-hydrogen production via dark fermentation, with efficient fermentation performances using different sugars as carbon sources, including simple monosaccharides (hexoses and pentoses) and complex polysaccharides (e.g., starch, lactose, sucrose, and cellobiose) (d'Ippolito et al., 2020; Esercizio et al., 2021b). They can generate H₂ close to the Thauer limit for anaerobic fermentation (i.e., 4 mol H₂/mol glucose), CO₂, acetate, and other minor products such as lactic acid, ethanol, and alanine (Huber et al., 2006; Thauer et al., 1977). Although the metabolic mechanisms underlying the production of hydrogen and value-added products are all yet to be clarified, the advantageous properties of *Thermotoga* spp make them promising candidates for biotechnological applications.

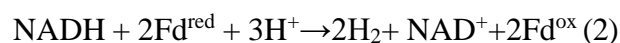
1.2 Dark fermentation pathway in *Thermotoga neapolitana*

The reactions for glucose conversion to hydrogen and acetate are thermodynamically more favorable at high temperature, with high biogas yields, thus explaining the great potential of thermophiles in biotechnological application (Khanna et al., 2012). According to the classical dark fermentation equation (1), 4 mole of hydrogen per mole of sugar consumed into glycolytic process are theoretically produced, with acetic acid and CO₂ as the byproducts (Thauer et al., 1977):



Since chemotropic production of H₂ requires H⁺ as electron acceptor, there is a direct relationship between the biogas yield and the type of the organic acid produced during the fermentation. In fact, hydrogen yields are optimized only when all glucose is converted to acetate because NADH and electrons are fully consumed to produce the energy carrier, while no H₂ is produced when lactic acid is the organic product released in the medium. The enzymatic complex responsible for the high bio-hydrogen yields achieved by *Thermotoga* spp. is the heterotrimeric [FeFe]-hydrogenase. Hydrogenases (H₂ase), present in many anaerobic bacteria, constitute a family of flavoprotein multimeric enzymes able to reduce protons to H₂. The β subunit accepts electrons from NADH, and the γ subunit transfers electrons from the β subunit to the catalytic α subunit. The catalytic site (the so-called H cluster) shows a complex Fe-S structure and requires the specific action of three highly conserved proteins to be assembled (Albertini et al., 2014). The endergonic reduction is energetically unfavorable, and in fact the reaction of H₂ production is influenced by physiological conditions such as pH, cell growth rate and H₂ partial pressure. Moreover, in this reaction, the hydrogenase complex oxidizes ferredoxin, cyclically produced by pyruvate:ferredoxin

oxidoreductase (PFOR) during the oxidation of pyruvate to acetyl coenzyme A, and transferred electrons to protons to form molecular H₂ (Oh et al., 2011). This mechanism has been called “electro-bifurcating”, since it couples the unfavorable endoergonic reduction of H⁺ to hydrogen by oxidation of NADH to the favorable exergonic oxidation of reduced ferredoxin (Thauer et al., 1977; LI et al., 2008; Schut & Adams, 2009). The overall hydrogenase reaction is summarized in the following Equation (2):



This novel type of energy conservation system elucidated for the first time in *T.maritima* is responsible for the production of H₂ close to the Thauer limits also in *T.neapolitana*, since sequence analysis of H₂ase of *T.maritima* showed 90% homology with that of *T.neapolitana* (**Fig.4**).

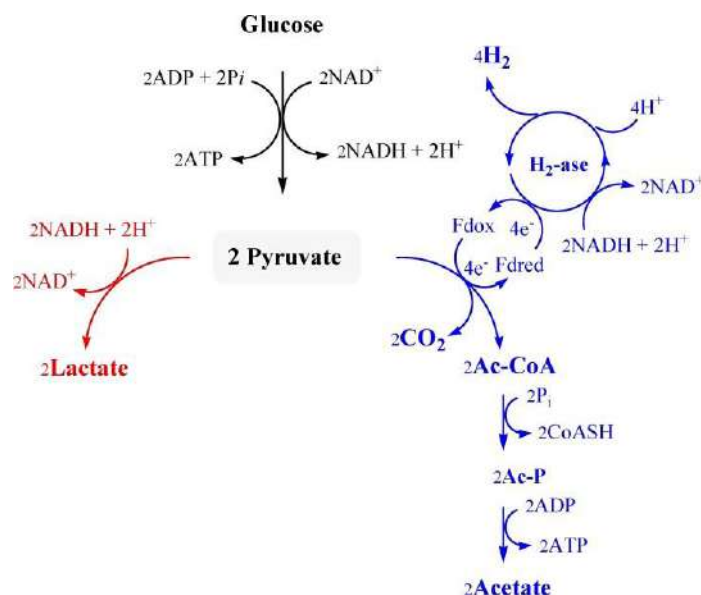


Fig. 4 Hydrogen production in *T.neapolitana* through Dark fermentation model from Pradhan et al., 2015

According to the electron-bifurcating mechanism, hydrogen yields via dark fermentation can therefore be affected also by both NADH or reduced Fd concentration available in the cell (Schut & Adams, 2009). *Thermotoga* spp. harvests energy mainly by glycolysis via the Embden-Meyerhoff pathway (EMP) (d'Ippolito et al., 2010), although an activation of 15% of the Entner–Doudoroff pathway (ED) has been described in *T.maritima*, and a possible activation of the Entner–Doudoroff pathway (ED) or the pentose phosphate pathway has been proposed active in *T.neapolitana* (Selig et al., 1997; d'Ippolito et al., 2020). EMP is the most common route for the oxidation of glucose (or other carbon sources) to pyruvate, and to provide energy to the cell in form of ATP and reducing equivalents (NADH). Pyruvate can undergo to terminal oxidation to acetate or can be diverted away for the synthesis of other organic substrates, as lactate that is produced by lactate dehydrogenase (LDH) with NADH oxidation, or for the biosynthesis in form of acetyl-CoA. Lactate levels reported during fermentation by *Thermotoga* species vary from trace amounts up to levels rivaling those of acetate (Schönheit, 1995; Anshuman et al., 2005; Khanna et al., 2012; Schut & Adams, 2009; Wu et al., 2006).

1.3 Capnophilic lactic fermentation in Thermotoga neapolitana

Capnophilic lactic fermentation (CLF) is a novel anaplerotic pathway described for the first time in *T. neapolitana* and represent the first example of non-autotrophic sequestration of CO₂ in hyperthermophilic bacteria (Dipasquale et al., 2014). The process is triggered under CO₂-saturated atmosphere (capnophilic means “requiring CO₂”) and it is based on the coupling reaction of exogenous acetate produced during fermentation and CO₂, to produce L-lactic acid without affecting hydrogen production (Dipasquale et al., 2014; d'Ippolito et al., 2014; Nuzzo et al., 2019). The reactions involved belongs to two-branches of *Thermotoga* metabolism: the first part includes the catabolic steps from sugars to pyruvate by glycolysis, and then the conversion of the pyruvate

obtained to acetyl-CoA catalyzed by pyruvate:ferredoxin oxidoreductase (PFOR) enzyme, which generates also reduced ferredoxin, available for the hydrogen production by the heterotrimeric [FeFe]-hydrogenase, as in the classical Dark fermentation (Fig. 5). Acetyl-CoA was then converted into acetate and ATP through the combined activities of PTA (phosphate acetyltransferase; EC 2.3.1.8) and ACK (acetate kinase; EC 2.7.2.1) enzymes (Dipasquale et al., 2014; d'Ippolito et al., 2020; Esercizio et al., 2021) (Fig. 5). The second part is supported by the reversible activities of both ACK-PTA system and PFOR complex stimulated by CO₂, able to coupling exogenous CO₂ and acetate and convert them again into pyruvate. Then the activation of lactate dehydrogenase enzyme (LDH) leads to the synthesis of L-lactic acid (Dipasquale et al., 2014; d'Ippolito et al., 2014-2020; Pradhan et al., 2016) (Fig. 5).

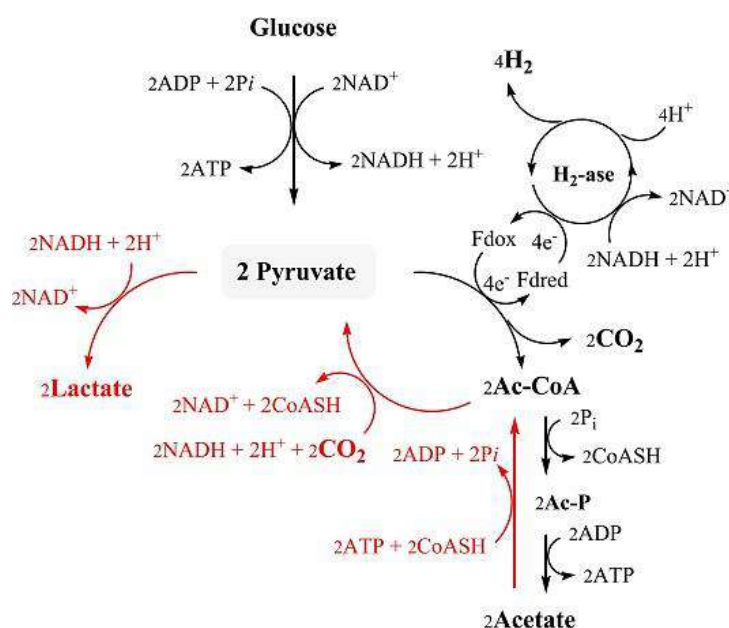
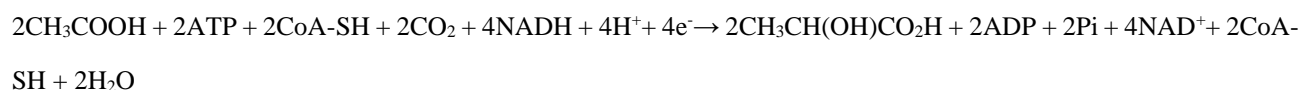


Fig. 5 Schematic representation of Capnophilic lactic fermentation in *T. neapolitana*, from Pradhan et al., 2015. Catabolic branch (black arrows); anabolic branch (red arrows).

The overall reaction is summarized in the following Equation (3):



This non-competitive synthesis of hydrogen and lactic acid at high yields represent an attractive process for biotechnological application, since it offers a biological mechanism to convert CO₂ into value-added products and to produce biohydrogen at the same time. Biochemically, the key node that holds up this interesting process, and that is the basis of this PhD study, is represented by the source of the reducing power required to support the concomitant production of hydrogen and lactic acid. It is commonly known that both hydrogen and lactic acid synthesis are NADH-dependent reactions (d'Ippolito et al., 2020). Therefore, an additional NADH pool is needed to satisfy the CO₂-induced process. However, to date, the absence of molecular and biochemical studies on this metabolic pathway had not allowed to clarify the entire mechanism. Screening of eight species of the genus *Thermotoga* (*T. neapolitana*, *T. neapolitana* subsp. *capnolactica*, *T. maritima*, *T. naphthophila*, *T. petrophila*, *T. caldifontis*, *T. hypogea*, *T. profunda*) and four species of the genus *Pseudothermotoga* (*P. elfii*, *P. lettingae*, *P. subterranea*, *P. thermarum*) revealed that CLF pathway is exclusive of *T. neapolitana* metabolism (Dipasquale et al., 2018).

1.4 Goal of the PhD research project

The PhD aims to ameliorate our understanding of the metabolism in the hyperthermophilic bacterium *T. neapolitana* when subjected to CLF conditions. Specific objectives concern the glucose catabolic pathways and the crosstalk between CLF pathway and energy conservation mechanisms. At the same time, the biggest challenge is the development of tools for the genetic manipulation of *T. neapolitana* in order to both achieve functional and molecular characterization of the CLF pathway and pave the way for developments in genetic engineering and synthetic biology in this family of microorganisms.

1.5 Structure of the thesis

The chapters in this thesis are written in scientific publication format, since most of the results obtained during the PhD have been already published. Each chapter focuses on a specific topic, and they are not arranged by date of publication, but rather according to a sequence that allows a greater

understanding of all the aspects treated in the PhD project. The flow that binds the different chapters is showed in **Figure 6**:

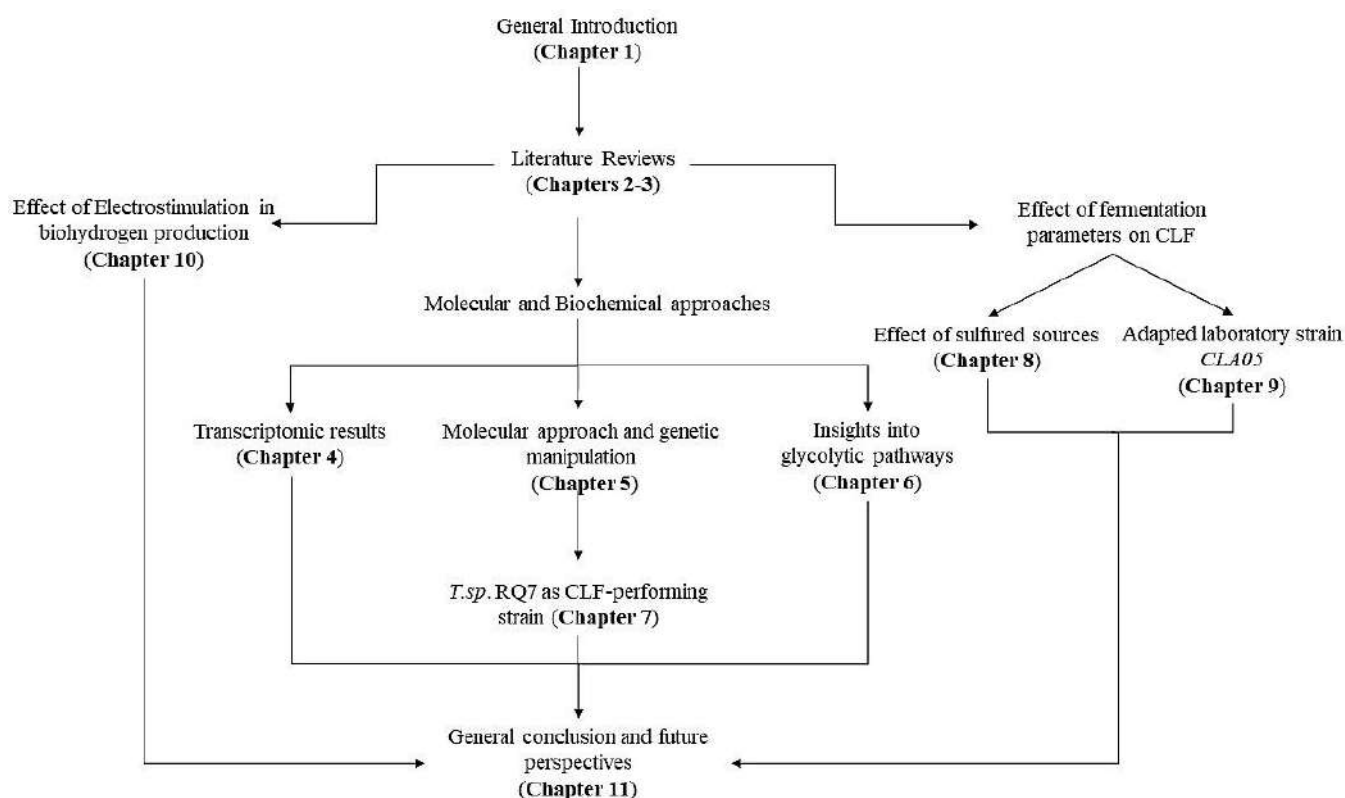


Fig. 6 Schematic outline of the thesis.

The present thesis is composed of eleven chapters:

Chapter 1: Introduction. The first chapter provides a general introduction of *T.neapolitana* metabolism and taxonomy and a brief summary of scope of the study.

Chapter 2-3: Literature reviews. In these two chapters, I reviewed the potential of biotechnological application of the member of the phylum *Thermotogae*. In particular, Chapter 2 describes the ability of Thermotogales to ferment a wide range of biodegradable organic wastes in view of their use in microbial processes for the bio-based circular economy.



Chapter 3 gives an overview of all the cultivation parameters affecting fermentation rate and products in order to explore increase of bio-hydrogen and value-added products yields in the phylum *Thermotogae*.

Chapter 4: Transcriptomic results. This chapter reports the results of the transcriptional analysis carried out in *T.neapolitana*. The transcriptional modification occurred under CO₂-saturated atmosphere was analyzed by an RNA-seq approach. The data contribute to a first molecular characterization of the CLF pathway and provide a list of differentially expressed genes available for further studies.

Chapter 5: Molecular approach and genetic manipulation. This chapter aims to describe the efforts made to develop an efficient transformation strategy in *T. neapolitana subsp. capnolactica*, and the first phenotypic characterization of the mutant strain ACS03. The heterologous expression of a *Thermus thermophilus* AMP-AcetylCoA synthetase (ACS; EC 6.2.1.1) has been designed in order to boost the coupling reaction from CO₂ and acetyl-CoA to lactic acid.

Chapter 6: Insights into glycolytic pathways. This section is focused on the possible metabolic switch from the classical Embden-Meyerhof-Parnas glycolytic pathway to alternative glycolytic routes, as Entner-Doudoroff and/or Pentose Phosphate pathways in *T. neapolitana* under CLF conditions. The up-regulation of the first steps of these pathways under CO₂ suggested a possible involvement in the production of extra equivalents of biological reductants to sustain the CLF reactions.

Chapter 7: *T.sp.* RQ7 as CLF-performing strain. The chapter concerns the activation of CLF in *Thermotoga sp.* RQ7. This bacterium is the closest taxonomic strain of *T. neapolitana* and shows natural competence. The identification of *T. sp.* strain RQ7 as a CLF- performing strain opens the possibility of clarifying the molecular mechanism of CLF pathway by molecular manipulation.



Consiglio Nazionale
delle Ricerche



Chapter 8: Effect of sulfured sources: The chapter presents the effect of sulfur sources on CLF pathway in *T. neapolitana*. Since *T. neapolitana* was isolated in solfataric environment, sulfur compounds have already been described as important factors in the optimization of the fermentation process in terms of kinetic and end-products.

Chapter 9: Effect of yeast extract. The chapter summarizes the attempt to adapt *T. neapolitana* subsp. *capnolactica* in a minimal medium without yeast extract and tryptone as extra source of carbon and nitrogen in order to evaluate the effects of these supplements on the fermentation parameters under CO₂.

Chapter 10: Effect of Electrostimulation. This chapter reports the effect of electrostimulation on the biofilm formation and on the metabolism in *T. neapolitana* the experiments were carried out in a single-chamber electrochemical bioreactor and aimed to test possible increase in biohydrogen production under CLF conditions.

Chapter 11: Conclusion and future perspectives. This section draws the main conclusions of this PhD study and provides insights into future perspectives

.

1.6 References

- M. L. Chong, V. Sabaratnam, Y. Shirai, and M. A. Hassan, “Biohydrogen production from biomass and industrial wastes by dark fermentation,” *International Journal of Hydrogen Energy*, vol. 34, no. 8, pp. 3277–3287, May **2009**.
- B. S. F. Boodhun, A. Mudhoo, G. Kumar, S. H. Kim, and C. Y. Lin, “Research perspectives on constraints, prospects and opportunities in biohydrogen production,” *Int. J. Hydrogen Energy*, vol. 42, no. 45, pp. 27471–27481, **2017**.
- I. Dincer and C. Acar, “Smart energy solutions with hydrogen options,” *Int. J. Hydrogen Energy*, vol. 43, no. 18, pp. 8579–8599, May **2018**.
- I. Staffell et al., “The role of hydrogen and fuel cells in the global energy system,” *Energy Environ. Sci.*, vol. 12, no. 2, pp. 463–491, **2019**.
- N. Esercizio et al., “Fermentation of biodegradable organic waste by the family *Thermotogaceae*,” *Resources*, vol. 10, no. 4, **2021 (b)**.
- I. Ntaikou, G. Antonopoulou, and G. Lyberatos, “Biohydrogen production from biomass and wastes via dark fermentation: A review,” *Waste and Biomass Valorization*, vol. 1, no. 1, pp. 21–39, Mar. **2010**.
- N. Khanna and D. Das, “Biohydrogen production by dark fermentation,” *Wiley Interdiscip. Rev. Energy Environ.*, vol. 2, no. 4, pp. 401–421, **2012**.
- A. A. Abreu, F. Tavares, M. M. Alves, and M. A. Pereira, “Boosting dark fermentation with co-cultures of extreme thermophiles for biohydrogen production from garden waste,” *Bioresour. Technol.*, vol. 219, pp. 132–138, Nov. **2016**.
- J. F. Soares, T. C. Confortin, I. Todero, F. D. Mayer, and M. A. Mazutti, “Dark fermentative biohydrogen production from lignocellulosic biomass: Technological challenges and future prospects,” *Renew. Sustain. Energy Rev.*, vol. 117, no. January 2019, **2020**.
- R. K. Thauer, K. Jungermann, and K. Decker, “Energy Conservation in Chemotrophic Anaerobic Bacteria,” *Am. Soc. Microbiol. Vol.*, **1977**.

- R. Huber et al., “*Thermotoga maritima* sp. nov. represents a new genus of unique extremely thermophilic eubacteria growing up to 90°C,” *Arch. Microbiol.*, vol. 144, no. 4, pp. 324–333, **1986**.
- H. W. Jannasch, R. Huber, S. Belkin, and K. O. Stetter, “*Thermotoga neapolitana* sp. nov. of the extremely thermophilic, eubacterial genus *Thermotoga*,” *Arch. Microbiol.*, vol. 150, no. 1, pp. 103–104, **1988**.
- M. Balk, J. Weijma, and A. J. M. Stams, “*Thermotoga lettingae* sp. nov., a novel thermophilic, methanol-degrading bacterium isolated from a thermophilic anaerobic reactor,” *Int. J. Syst. Evol. Microbiol.*, vol. 52, no. 4, pp. 1361–1368, **2002**.
- R. Huber and M. Hannig, “*Thermotogales*,” *The Prokaryotes*, pp. 899–922, **2006**.
- N. T. Eriksen, M. L. Riis, N. K. Holm, and N. Iversen, “H₂ synthesis from pentoses and biomass in *Thermotoga* spp.,” *Biotechnol. Lett.*, vol. 33, no. 2, pp. 293–300, Feb. **2011**.
- M. Cappelletti, Davide Zannoni, and B. O. Anne Postec, “Members of the Order *Thermotogales*: From Microbiology to Hydrogen Production,” *Microb. BioEnergy Hydrog. Prod. Adv. Photosynth. Respir.*, vol. 38, pp. 321–347, **2014**.
- L. Dipasquale, G. D’Ippolito, and A. Fontana, “Capnophilic lactic fermentation and hydrogen synthesis by *Thermotoga neapolitana*: An unexpected deviation from the dark fermentation model,” *Int. J. Hydrogen Energy*, vol. 39, no. 10, pp. 4857–4862, **2014**.
- G. d’Ippolito, L. Dipasquale, and A. Fontana, “Recycling of Carbon Dioxide and Acetate as Lactic Acid by the Hydrogen-Producing Bacterium *Thermotoga neapolitana*,” *ChemSusChem*, vol. 7, no. 9, pp. 2678–2683, **2014**.
- N. Pradhan et al., “Hydrogen and lactic acid synthesis by the wild-type and a laboratory strain of the hyperthermophilic bacterium *Thermotoga neapolitana* DSMZ 4359T under capnophilic lactic fermentation conditions,” *Int. J. Hydrogen Energy*, vol. 42, no. 25, pp. 16023–16030, **2017**.
- V. Bhandari and R. S. Gupta, *The Phylum Thermotogae*. **2014**.

- H. Belahbib et al., “Towards a congruent reclassification and nomenclature of the thermophilic species of the genus *Pseudothermotoga* within the order *Thermotogales*,” *Syst. Appl. Microbiol.*, vol. 41, no. 6, pp. 555–563, **2018**.
- M.-L. Fardeau et al., “*Thermotoga hypogea* sp. nov., a Xylanolytic, Thermophilic Bacterium from an Oil-Producing Well,” vol. 147, no. 4, pp. 51–56, **1997**.
- E. Windberger, R. Huber, A. Trincone, H. Fricke, and K. O. Stetter, “*Thermotoga thermarum* sp. nov. and *Thermotoga neapolitana* occurring in African continental solfataric springs,” *Arch. Microbiol.*, vol. 151, no. 6, pp. 506–512, **1989**.
- C. Jeanthon et al., “*Thermotoga subterranea* sp. nov., a new thermophilic bacterium isolated from a continental oil reservoir,” *Arch. Microbiol.*, vol. 164, no. 2, pp. 91–97, **1995**.
- G. Ravot et al., “*Thermotoga elfii* sp. nov., a novel thermophilic bacterium from an African oil-producing well,” *Int. J. Syst. Bacteriol.*, vol. 45, no. 2, pp. 308–314, **1995**.
- Y. Takahata, M. Nishijima, T. Hoaki, and T. Maruyama, “*Thermotoga petrophila* sp. nov. and *Thermotoga naphthophila* sp. nov., two hyperthermophilic bacteria from the Kubiki oil reservoir in Niigata, Japan,” *Int. J. Syst. Evol. Microbiol.*, vol. 51, no. 5, pp. 1901–1909, **2001**.
- G. d’Ippolito et al., “CO₂-Induced Transcriptional Reorganization: Molecular Basis of Capnophilic Lactic Fermentation in *Thermotoga neapolitana*,” *Front. Microbiol.*, vol. 11, **2020**.
- M. Albertini et al., “The proton iron-sulfur cluster environment of the [FeFe]-hydrogenase maturation protein HydF from *Thermotoga neapolitana*,” *Int. J. Hydrogen Energy*, vol. 39, no. 32, pp. 18574–18582, **2014**.
- Y. K. Oh, S. M. Raj, G. Y. Jung, and S. Park, “Current status of the metabolic engineering of microorganisms for biohydrogen production,” *Bioresour. Technol.*, vol. 102, no. 18, pp. 8357–8367, **2011**.
- F. Li, J. Hinderberger, H. Seedorf, J. Zhang, W. Buckel, and R. K. Thauer, “Coupled ferredoxin and crotonyl coenzyme A (CoA) reduction with NADH catalyzed by the butyryl-

- CoA dehydrogenase/Etf complex from *Clostridium kluyveri*,” *J. Bacteriol.*, vol. 190, no. 3, pp. 843–850, **2008**.
- G. J. Schut and M. W. W. Adams, “The iron-hydrogenase of *Thermotoga maritima* utilizes ferredoxin and NADH synergistically: A new perspective on anaerobic hydrogen production,” *J. Bacteriol.*, vol. 191, no. 13, pp. 4451–4457, **2009**.
 - N. Pradhan et al., “Hydrogen production by the thermophilic bacterium *Thermotoga neapolitana*,” *International Journal of Molecular Sciences*, vol. 16, no. 6. MDPI AG, pp. 12578–12600, Jun. 04, **2015**.
 - G. d’Ippolito et al., “Hydrogen metabolism in the extreme thermophile *Thermotoga neapolitana*,” *Int. J. Hydrogen Energy*, vol. 35, no. 6, pp. 2290–2295, **2010**.
 - M. Selig, K. B. Xavier, H. Santos, and P. Schönheit, “Comparative analysis of Embden-Meyerhof and Entner-Doudoroff glycolytic pathways in hyperthermophilic archaea and the bacterium *Thermotoga*,” *Arch. Microbiol.*, vol. 167, no. 4, pp. 217–232, **1997**.
 - P. Schönheit and T. Schäfer, “Metabolism of hyperthermophiles,” *World J. Microbiol. Biotechnol.*, vol. 11, no. 1, pp. 26–57, Jan. **1995**.
 - Anshuman, K.; Mike, M.; Brenda, J. H₂: The energy source for the 21st century. *Technovation* **2005**, 25, 569–585.
 - Wu, S.Y.; Hung, C.H.; Lin, C.N.; Chen, H.W.; Lee, A.S.; Chang, J.S. Fermentative H₂ production and bacterial community structure in high-rate anaerobic bioreactors containing silicone immobilized and self-flocculated sludge. *Biotechnol. Bioeng.* **2006**, 93, 934–946.
 - G. Nuzzo, S. Landi, N. Esercizio, E. Manzo, A. Fontana, and G. D’Ippolito, “Capnophilic lactic fermentation from *Thermotoga neapolitana*: A resourceful pathway to obtain almost enantiopure L-lactic acid,” *Fermentation*, vol. 5, no. 2, **2019**.



Consiglio Nazionale
delle Ricerche



- N. Esercizio et al., “Improvement of CO₂ and acetate coupling into lactic acid by genetic manipulation of the hyperthermophilic bacterium *Thermotoga neapolitana*,” *Microorganisms*, vol. 9, no. 8, **2021**.
- N. Pradhan et al., “Model development and experimental validation of capnophilic lactic fermentation and hydrogen synthesis by *Thermotoga neapolitana*,” *Water Res.*, vol. 99, no. April, pp. 225–234, **2016**.
- L. Dipasquale, N. Pradhan, and G. Ippolito, “Potential of Hydrogen Fermentative Pathways in Marine Thermophilic Bacteria: Dark Fermentation and Capnophilic Lactic Fermentation in *Thermotoga* and *Pseudothermotoga* Species,” in *Grand Challenges in Marine Biotechnology*, *Grand Challenges in Biology and Biotechnology*, **2018**, pp. 217–235.

2. Fermentation of Biodegradable Organic Waste by the family Thermotogaceae

Nunzia Esercizio¹, Mariamichela Lanzilli ¹, Marco Vastano¹, Simone Landi², Zhaohui Xu³, Carmela Gallo¹, Genoveffa Nuzzo¹, Emiliano Manzo¹, Angelo Fontana ^{1,2} and Giuliana d'Ippolito ^{1,*}

¹ Institute of Biomolecular Chemistry (ICB), Consiglio Nazionale delle Ricerche (CNR), Via Campi Flegrei 34, 80078 Pozzuoli, Italy

² Laboratory of Bio-Organic Chemistry and Chemical Biology, Department of Biology, University of Naples "Federico II", Via Cinthia, 80126 Napoli, Italy

³ Department of Biological Sciences, Bowling Green State University, Bowling Green, OH 43403, USA









* Correspondence: gdippolito@icb.cnr.it; Tel.: +39-0818675096

Citation:

Esercizio, N.; Lanzilli, M.; Vastano, M.; Landi, S.; Xu, Z.; Gallo, C.; Nuzzo, G.; Manzo, E.; Fontana, A.; d'Ippolito, G. Fermentation of Biodegradable Organic Waste by the Family *Thermotogaceae*. *Resources* **2021**, 10, 34.

Review

Fermentation of Biodegradable Organic Waste by the Family *Thermotogaceae*

Nunzia Esercizio ¹, Mariamichela Lanzilli ¹, Marco Vastano ¹, Simone Landi ², Zhaohui Xu ³, Carmela Gallo ¹, Genoveffa Nuzzo ¹, Emiliano Manzo ¹, Angelo Fontana ^{1,2} and Giuliana d'Ippolito ^{1,*}

- ¹ Institute of Biomolecular Chemistry, National Research Council of Italy, Via Campi Flegrei 34, 80078 Pozzuoli, Italy; n.esercizio@icb.cnr.it (N.E.); m.lanzilli@icb.cnr.it (M.L.); marco.vastano@gmail.com (M.V.); carmen.gallo@icb.cnr.it (C.G.); nuzzo.genoveffa@icb.cnr.it (G.N.); emanzo@icb.cnr.it (E.M.); afontana@icb.cnr.it (A.F.)
- ² Department of Biology, University of Naples "Federico II", Via Cinthia, I-80126 Napoli, Italy; simone.landi@unina.it
- ³ Department of Biological Sciences, Bowling Green State University, Bowling Green, OH 43403, USA; zxu@bgsu.edu
- * Correspondence: gdippolito@icb.cnr.it

Abstract: The abundance of organic waste generated from agro-industrial processes throughout the world has become an environmental concern that requires immediate action in order to make the global economy sustainable and circular. Great attention has been paid to convert such nutrient-rich organic waste into useful materials for sustainable agricultural practices. Instead of being an environmental hazard, biodegradable organic waste represents a promising resource for the production of high value-added products such as bioenergy, biofertilizers, and biopolymers. The ability of some hyperthermophilic bacteria, e.g., the genera *Thermotoga* and *Pseudothermotoga*, to anaerobically ferment waste with the concomitant formation of bioproducts has generated great interest in the waste management sector. These biotechnologically significant bacteria possess a complementary set of thermostable enzymes to degrade complex sugars, with high production rates of biohydrogen gas and organic molecules such as acetate and lactate. Their high growth temperatures allow not only lower contamination risks but also improve substrate solubilization. This review highlights the promises and challenges related to using *Thermotoga* and *Pseudothermotoga* spp. as sustainable systems to convert a wide range of biodegradable organic waste into high value-added products.

Keywords: *Thermotoga*; *Pseudothermotoga*; thermophilic bacteria; fermentation; hydrogen; lactic acid; waste valorization; added-value products



Citation: Esercizio, N.; Lanzilli, M.; Vastano, M.; Landi, S.; Xu, Z.; Gallo, C.; Nuzzo, G.; Manzo, E.; Fontana, A.; d'Ippolito, G. Fermentation of Biodegradable Organic Waste by the Family *Thermotogaceae*. *Resources* **2021**, *10*, 34. <https://doi.org/10.3390/resources10040034>

Academic Editors: Ezio Riggi,
Raffaella Maria Balestrini and
Edoardo Marco Napoli

Received: 23 February 2021

Accepted: 9 April 2021

Published: 13 April 2021

Publisher's Note: MDPI stays neutral with regard to jurisdictional claims in published maps and institutional affiliations.



Copyright: © 2021 by the authors. Licensee MDPI, Basel, Switzerland. This article is an open access article distributed under the terms and conditions of the Creative Commons Attribution (CC BY) license (<https://creativecommons.org/licenses/by/4.0/>).

1. Introduction

Biodegradable organic waste from industrial processes provide versatile carbon-rich feedstocks that can be efficiently converted into high-value products and biofuels [1–3]. As described in the 2018 EU Bioeconomy Strategy report [4], the economic value of biodegradable waste is starting to be recognized by agricultural, forestry, chemical, and energy sectors. With the development of the bioeconomy, the demand for these secondary products is likely to increase, changing the economic conditions of production. More than 3300 megatonnes of residual biomass are estimated to be generated annually from barley, maize, rice, soybean, sugar cane, and wheat. In Europe only, 900 megatonnes of wastepaper, food, and plant materials are generated each year. In the fisheries sector, about 40 megatonnes of fish may be discarded each year during European commercial fishing; in the forestry sector, woody biomass residues have been estimated to be 5100 megatonnes per year globally [4].

From the perspective of constructing a circular economy based on biowaste, it is important to support the development of industrial symbiosis for feed materials, i.e., one

industry's waste becomes the starting material for another. One example is the treatment of waste and residues for energy production, including the production of biogas through anaerobic digestion of biowaste and wastewater [5–9] as well as the integrated production of chemical products and bioenergy in biorefineries [10,11]. The food processing industry is exploring the potential of recovering the energy contained in food residues on site [12–14]. A typical fermentation process consists of the controlled digestion of biodegradable materials under anaerobic conditions in closed reactors, at temperatures suitable for mesophilic or thermophilic bacteria. Fermentation products include (1) digested solids that can be used as a soil conditioner; (2) biogas that can be consumed directly or refined for higher levels of demands, such as fuels for vehicles.

In this framework, special attention has been paid to fermentation processes in which biowaste is treated for generating hydrogen gas [15,16]. Hydrogen represents a promising bioenergy fuel since it is clean, renewable, abundant, and cheap; it produces only water as the end-product when used as a fuel, without any pollutants [17–19]. Dark fermentation operated by anaerobic thermophilic bacteria is an attractive way to produce biohydrogen because of the high biogas evolution yields and the versatile feedstocks [17,18,20–24]. Among extreme thermophilic bacteria, members of the order *Thermotogales* have proven to be promising candidates due to high H₂ yields that are close to theoretical values and the ability of some members to recycle produced CO₂ into lactic acid synthesis [25–35]. These bacteria are capable of fermenting not only simple and pure sugars but also complex carbon sources with various production rates [36–41].

This review focuses on the potential of the members of the order *Thermotogales* to ferment biodegradable organic waste. Feedstock pretreatments and their effects on cultural parameters are also discussed [24,42–44]. With the development of molecular and biochemical tools applicable to extremophilic bacteria, it has been possible to demonstrate the involvement of specific enzymes and putative pathways in the uptake and degradation processes [45–47], offering new routes in the evaluation of the application of these biological systems.

The examined substrates discussed here are divided into four groups, based on their main constituents and relative origins: food waste, lignocellulosic waste, glycerol, and microalgal biomass. Their main characteristics, compositions, utility, and fermentation processes involving *Thermotogaceae* family members are discussed in subheadings, and the best results are summarized in tables. It provides a concise and precise description of the experimental results, their interpretation as well as the conclusions drawn from the studies.

2. *Thermotogaceae* Family: Features and Roles in Sugar Fermentation

2.1. General Characteristics

The phylum *Thermotogae* represents a critical node in the phylogenetic tree of bacteria. Bhandari and Gupta's classification was taken as a model because it was based on genomic data from several *Thermotogae* species, and the molecular markers were identified to estimate the relationship within the phylum [48]. Recently, with the significant advances in modern taxonomy practices, Belahbib et al. [49] have proposed some changes to Bhandari and Gupta's classification system. Nowadays, the phylum *Thermotogae*, comprising of mesophilic, thermophilic and hyperthermophilic bacteria, has more than 52 species belonging to four orders: *Thermotogales*, *Kosmotogales*, *Petrotogales* and *Mesoacidotogales* [50]. The order of *Thermotogales* includes two families, *Thermotogaceae* and *Fervidobacteriaceae*, and their species are distinguished by the shared presence of conserved sequences [48–50]. The family *Thermotogaceae* contains two genera, *Thermotoga* and *Pseudothermotoga*, which are anaerobic, rod-shaped bacteria, surrounded by a sheath-like structure called “toga”, resulting in large periplasmic spaces at the poles of each rod [28,48]. The genus *Thermotoga* retains the species *T. maritima*, *T. neapolitana*, *T. petrophila*, *T. naphthophila*, *Thermotoga* sp. EMP, *Thermotoga* sp. A7A, and *Thermotoga* sp. RQ2, while *P. lettingae*, *P. thermarum*, *P. elfii*, *P. subterranea*, and *P. hypogea* belong to the new genus *Pseudothermotoga* [28,48,49]. Members of the *Thermotogaceae* family have been isolated from geothermal environments across the

globe, including oil reservoirs, submarine hot springs, and continental solfataric springs, with their optimal growth temperature in the range of 77–80 °C [28]. They can reduce elemental sulfur and use hexoses, pentoses, disaccharides, glucans, xylans, glucomannan, galactomannan, pectin, chitin, and amorphous cellulose as main substrates during fermentation [28,48]. *Thermotoga* species generate H₂ close to the Thauer limit for anaerobic fermentation (i.e., 4 mol H₂/mol glucose), CO₂, acetate, and other minor products such as lactic acid, ethanol, and alanine [28,51]. According to the classical model of fermentation referred to as dark fermentation (DF), *Thermotoga* spp. harvest energy mainly by glycolysis via the Embden–Meyerhoff–Parnas pathway (EMP), although a simultaneous activation of 15% of the Entner–Doudoroff pathway (ED) has been described [25,52]. EMP is the most common route for oxidation of glucose (and other hexoses) and to supply energy (ATP), reducing equivalents (NADH), and pyruvate, which undergoes terminal oxidation (acetate) or is used for biosynthesis (e.g., acetyl-CoA) [25,53,54]. Moreover, some members of the *Thermotogaceae* family possess an unprecedented anaplerotic mechanism, called capnophilic lactic fermentation (CLF), that represents the first example of biological non-autotrophic sequestration of CO₂ in hyperthermophilic bacteria, more advantageous than classical dark fermentation regarding the production of hydrogen through degradation of carbon substrates [32,33,55–57]. This process is activated during glucose fermentation under CO₂ sparging, and it is based on the coupling of acetate and CO₂ derived from glycolysis to produce enantiopure L-lactic acid without affecting H₂ yields [32,33,55,56,58–60]. This mechanism was extensively studied in *Thermotoga neapolitana*, and only a few members of the *Thermotoga* and *Pseudothermotoga* genera operated this CO₂ recycling mechanism [34]. Under CLF conditions, the bacteria also shift their glucose utilization through downregulation of EMP, activation of ED and/or OPP pathways, and the upregulation of some bifurcating enzymes that could supply NADH in these metabolic processes [60].

These advantageous properties of *Thermotoga* spp., i.e., valorization and transformation of biodegradable organic waste with H₂ production and, in some cases, the sequestration of CO₂ to recover energy and generate value-added products, have positioned these bacteria as promising candidates in the biotechnological field. In addition, many of their enzymes are capable of deconstructing complex biomass into basic components for fermentation [46,61]. Although biohydrogen production from hyperthermophilic bacteria is far from an industrial scale application, these studies provide common knowledge about the potential of the family *Thermotogaceae*, fueling interest in future exploration.

2.2. Fermentation of Pure Monosaccharides and Polysaccharides

Members of the *Thermotogaceae* family can ferment a wide range of mono- and polysaccharides as carbon and energy sources. In the identification processes of each new *Thermotoga* species, the authors tested a panel of pure monosaccharides to analyze strain adaptability and discovered potential alternative carbon sources for these organisms [28,36,37,62–69]. In the past a few years, independent work also evaluated the effects of monosaccharides on fermentation end-product yields, mainly in *T. maritima* and *T. neapolitana*. Glucose is the preferred substrate, and it produces the greatest amount of hydrogen, with yields higher than 3.5 mol/mol glucose [36,38,70–73]. Using other sugars as the sole carbon source, such as arabinose, fructose, mannose, galactose and ribose, resulted in similar hydrogen production rates in both species (H₂ yields around 3 mol/mol sugar) [28,36,58,73–77]. Variations in sugar concentration seem to remarkably affect the H₂ production and substrate utilization in *T. neapolitana* [72]; in *T. maritima*, lower H₂ yields have been observed (around 1.1 ± 0.1 mol H₂/mol xylose) [77].

Thermotoga spp. can also metabolize pure di- and tri-saccharides, such as sucrose, lactose, maltose and cellobiose, and polysaccharides including starch, glycogen, carboxymethyl cellulose (CMC) and cellulose [28,72,73,77–84]. The ability to hydrolyze and ferment a wide range of polysaccharides represents the basis of the great potential and versatility for biodegradable organic waste valorization by the family *Thermotogaceae*.

Cellobiose was tested with *T. maritima* at the concentration of 12.5 mmol/L, resulting in 100 mmol/L of hydrogen [77]. At the end of the fermentation, 3.6 ± 0.2 mol H₂/mol sugar was obtained, even though only 49% of the cellobiose was consumed (Table 1), suggesting that cellobiose is a difficult substrate to hydrolyze and may require a different modulation of enzyme activity. Improvements in hydrolysis of cellulosic materials and in H₂ production are possible by cocultivating *T. maritima* with *Caldicellulosiruptor saccharolyticus* [77].

Regarding sucrose, studies with *T. neapolitana* showed that the fermentation process was similar to that using glucose [72,73]. In Ngo et al., sucrose consumption rate, acetic and lactic acid production rates were comparable in batch cultures with and without pH control. A slight increase in H₂ yield was observed in sucrose-based culture (Table 1) [72]. The same trend was observed under the CLF condition in sucrose fermentation, producing 2.56 ± 0.1 mol of H₂, 25.12 ± 1.43 mM of acetate, and 16.95 ± 1.34 mM of lactic acid per mole of glucose equivalent (Table 1) [73].

Fermentation of laminarin led to H₂ yield (3.70 ± 0.17 mol per mole glucose eq) and acetic acid production (28.75 ± 0.81 mM) in *T. neapolitana* sp. *capnolactica* (*T. nea clf*) culture, similar to glucose and sucrose fermentation. However, LA level (7.60 ± 0.27 mM) was two times lower (Table 1) [73].

On CMC, a clear reduction of H₂ and organic acid production was observed in *T. nea clf* because this substrate is poorly metabolized [73,82]. Nguyen et al. described the capability of *T. neapolitana* and *T. maritima* to grow on CMC [82]. Only 95.5 ± 4.8 mL and 96.4 ± 4.8 mL H₂/g glucose eq. were produced by *T. maritima* and *T. neapolitana* growing on CMC, while 187.1 ± 9.4 and 174.5 ± 8.7 mL H₂/g glucose eq. were produced by the two strains, respectively, when growing on starch. (Table 1) [82].

The same effect was observed in *T. neapolitana* subsp. *capnolactica* growing on CMC, with a H₂ yield of 2.05 ± 0.13 mol H₂, 3.40 ± 0.30 mM of AA, and 1.18 ± 0.05 mM of LA per mol of glucose eq. In contrast to other sugars, only 10% of CMC was consumed after 72 h of fermentation, indicating that CMC should probably be pretreated to improve its accessibility to the cells [73]. No growth was observed with *P. elfii* growing on sucrose and CMC [85].

Several papers reported that *T. maritima* and *T. neapolitana* were able to degrade cellulose [17,22,86], which stimulated further research on the topic. Nguyen et al. [82] showed a drastic decrease in H₂ yields in both *T. neapolitana* and *T. maritima* growing on cellulose, with only 27.8 ± 1.3 mL H₂/g glucose eq. for *T. maritima* and 30.7 ± 1.5 mL H₂/g glucose eq. for *T. neapolitana*, suggesting that pretreatment is needed to better ferment this substrate (Table 1) [82]. In Nguyen et al. [81], pure cellulose was pretreated with three different chemical methods, acid (H₂SO₄), alkali (NaOH), and ionic liquid ([C4mim] Cl, 1-butyl-3-methylimidazolium chloride). Ionic liquid turned out to be the most effective pretreatment agent, with 18% of cellulose dissolution [81]. N₂ sparging leads to an improved H₂ production rate in *T. neapolitana* growing on cellulose, reaching 1280 ± 58.0 mL H₂/L culture and 2.20 ± 0.10 mol H₂/mol glucose eq., compared to 1.22 ± 0.067 mol H₂/mol glucose eq. without sparge; this demonstrates the feasibility of using cellulose and other complex feedstocks in *Thermotoga* fermentation [81].

Table 1. Fermentation of pure polysaccharides by *Thermotoga* spp.

Substrate	Strain	T (°C)	Start pH	Mixing Speed (rpm)	Gas Sparge	Reactor Volume (mL)	Working Volume (mL)	Substrate Consumption (mmol/L)	H ₂ yield (mol H ₂ /mol sugar)	Organic acids Production (mM)	Ref.
Sucrose	<i>T.nea cf</i>	80	7.5	250	CO ₂	3800	500	23.30 ± 0.69	2.56 ± 0.1	AA 25.12 ± 1.43 LA 16.95 ± 1.34	[73]
Laminarin	<i>T.nea cf</i>	80	7.5	250	CO ₂	3800	500	24.73 ± 0.40	3.70 ± 0.17	AA 28.75 ± 0.81 LA 7.60 ± 0.27	
CMC	<i>T.nea cf</i>	80	7.5	250	CO ₂	3800	500	2.75 ± 0.25	2.05 ± 0.13	AA 3.40 ± 0.30 LA 1.18 ± 0.05	
Sucrose	<i>T.nea</i>	75	7.5 pH control	300	N ₂	3000	1000	14.69 ± 0.06	4.95 ± 0.25	AA 25.66 LA 1.69	[72]
			7.5 w/o pH control					13.78 ± 0.70	3.52 ± 0.18	AA 23.97 LA 2.5	
Cellulose pretreated with [C4mim] Cl	<i>T.nea</i>	80	7.5	150	N ₂ w/o N ₂	120	40	-	2.20 ± 0.1 1.22 ± 0.067	-	[81]
Cellulose	<i>T.nea</i>	80	7.5	-	N ₂	120	50	10.18 ± 0.08	30.7 ± 1.5 *	AA 4.09	[82]
	<i>T.mar</i>	75	6.5					8.82 ± 0.07	27.8 ± 1.3 *	AA 3.20	
Starch	<i>T.nea</i>	80	7.5	-	N ₂	120	50	5.51 ± 0.09	174 ± 8.7 *	AA 22.04	
	<i>T.mar</i>	75	6.5					6.01 ± 0.09	187 ± 9.4 *	AA 24.34	
CMC	<i>T.nea</i>	80	7.5	-	N ₂	120	50	6.80 ± 0.08	96.4 ± 4.8 *	AA 8.97	
	<i>T.mar</i>	75	6.5					6.99 ± 0.08	95.5 ± 4.8 *	AA 9.75	
Cellobiose	<i>T.mar</i>	70	7.2	90	N ₂	120	50	6.125	3.60 ± 0.2	-	[77]

All the experiments have been performed in batch, with substrate load of 5g/L. AA, acetic acid; LA, lactic acid; CMC, carboxymethyl cellulose. *T.nea cf.*, *Thermotoga neapolitana* subsp. *capnolactica*; *T.nea.*, *Thermotoga neapolitana*; *T.mar.*, *Thermotoga maritima*. H₂ yield column: * mL/g.

3. Biodegradable Organic Waste

Biodegradable organic waste represents the main end-products from agro-industrial processes and nowadays serve as popular feedstocks for anaerobic fermentation [1–3]. These biomass materials contain carbohydrates, lipids, lignocellulosic compounds and proteins, which provide a balanced supply of carbon, nitrogen, sulfur, minerals, vitamins, and other small molecules [14]. Over the years, organic biomass has acquired an increasingly important role because of their abundance and low costs. Originally considered the “waste” of industrial processes, they represent a new economic opportunity to enhance energy production [1–3,6,9,10,13].

3.1. Food Waste

Food waste is generated by the entire food system, from production to processing and to consumption, although there are considerable uncertainties about the estimated quantities related to different stages. Food waste comes from various sources including agro-industrial processes, households, and the hospitality sector. It is generally composed by carbohydrates, protein, lipids and inorganic compounds, in variable proportions depending on the source of the food waste. Their accumulation associated to population growth has become a serious problem [87]. The food processing industries are exploring the potential of recovering the energy contained in food residues on-site, through biogas production or in dedicated combined heat and power plants. Anaerobic digestion is an effective way to manage food waste, with advantages like low costs, less residual waste and production of biohydrogen [10–12,88]. Of the food waste available, only some of it will be discussed in this review based on their applications in *Thermotoga* fermentation.

3.1.1. Fruit and Vegetable Waste

Fruit and vegetable waste (FVW) is the most abundant waste obtained in wholesale markets. These substrates are mainly composed of carbohydrates, cellulose, and hemicellulose, making them good candidates to produce biohydrogen [89–91]. It is already known that these compounds are used to produce biogas and to reduce landfill maintenance costs due to their high organic content and good degradability [5,39,89–91]. Moreover, no special pretreatments are required for these substrates, simply the reduction in size with an electric blender and subsequent filtration and homogenization. This procedure guarantees the absence of extremophilic and/or halotolerant microflora that are able to produce H_2 , and allows for better sugar solubilization. Saidi et al. studied fruit and vegetable waste fermentation with *T. maritima*, using a simplified medium containing natural seawater as the inorganic compound source [39]. Under this experimental condition, 3.89 ± 0.05 mol H_2 /mol hexose, 1.96 mol AA/mol C6 and 1.2 ± 0.2 mmol LA/L were obtained (Table 2) [39].

Carrot pulp is a vegetable residue obtained in carrot juice production, thus available in large quantities as a by-product. It is composed of a soluble water fraction (30%) consisting of sucrose, glucose and fructose, and a considerable amount of insoluble nonstarchy polysaccharides (NSP) (30–40% of the total dry matter) derived from cell wall hemicellulose and pectin [75,92]. Glucose was the most abundant residue in the NSP fraction, while in much lower concentrations were arabinose, galactose, mannose, rhamnose, xylose, and galacturonic acid derived from pectin [75,92]. Both the untreated material and the hydrolysate fraction were tested in *T. neapolitana* fermentation, and the importance of pretreatment was highlighted. After the enzymatic hydrolysis of the insoluble polysaccharide fraction by cellulases, the soluble sugar content in the total liquid hydrolysate increased, for example, 160 g of dry matter produced 4.0 g/L of sucrose, 39.2 g/L of glucose and 14.0 g/L of fructose. However, 30% of the initial dry matter remained insoluble [75]. *T. neapolitana* only fermented the hydrolyzated form, producing 2.4 mol H_2 /mol C6, 1.1 mol AA/mol C6, and 0.30 mol LA/mol C6 (Table 2). A reduction of sugar consumption rate was observed compared to pure sugar fermentation, maybe due to the insoluble residual fraction that can inhibit fermentation [75].

Potato steam peels (PSP) derive from the potato processing industry. This waste is rich in starch, and it is available in large quantities. It is generally used for animal feeding but is now regarded as a potential substrate in biohydrogen production [93]. In fact, a life cycle assessment showed that it is more beneficial to primarily use PSP to produce hydrogen and use protein-rich solids in animal feed, rather than using potato steam peels directly [94]. Mars et al. described H_2 production during *T. neapolitana* fermentation with potato steam peels as the carbon source [95]. Different pretreatment states of PSP were used as organic substrates (untreated PSP, PSP-H1 and PSP-H2). Untreated PSP is composed of 39% starch, 3.8% nitrogen, and 8.5% ash. PSP treated with alpha-amylase and then clarified, referred to as PSP-H1, contains soluble dextrans, 21 mM glucose, 7 mM acetate, and 25 mM lactate. PSP-H1 further hydrolyzed with amyloglucosidase and clarified, referred to as PSP-H2, contained 407 mM glucose, 10 mM acetate, and 33 mM lactate [95]. Untreated PSP led to an H_2 yield of 3.8 mol H_2 /mol glucose units with 1.80 mol AA/mol glucose units and 0.2 mol LA/mol glucose units by *T. neapolitana* (Table 2) [95]. This high hydrogen yield based on starch content in PSP could be an overestimation because other unidentified substrates in PSP may have also been consumed. Using PSP-H1 and PSP-H2, a decrease of all product yields was observed (PSP-H1: 2.6 mol H_2 /mol glucose, 1.20 mol AA/mol glucose. PSP-H2: 3.3 mol H_2 /mol glucose, 1.50 mol AA/mol glucose) [95]. Therefore, untreated PSP may be a suitable alternative to the use of hydrolysates.

Onion waste (OW) is the result of industrial onion (*Allium cepa* L.) cultivation, harvesting and processing. Nowadays onions are the second most important horticultural crop worldwide after tomatoes. The increase in onion demand over the years has led to an increase in onion waste production, representing an environmental concern. They are not suitable for fodder because of their aroma, and neither can they serve as an organic fertilizer because of the rapid development of phytopathogenic agents. Onion waste mainly includes undersized, malformed, diseased or damaged bulbs as well as onion skins, outer fleshy scales and roots that are generated during industrial peeling [96]. However, since onions are rich in several groups of plant compounds, such as dietary fibers (DF), fructo-oligosaccharides (FOS) and flavonoids, they have many benefits to human health [96]. An alternative solution could be their biological conversion into bioenergy and high value-added products (food and pharmacological ingredients, biogas, fertilizers, etc.) [41,97–99]. Up to 65% of the dry weight of onion waste is composed of nonstructural carbohydrates, including fructose (114 ± 1.4 mmol/L), glucose (137.5 ± 0.9 mmol/L) and sucrose (21 ± 0.7 mmol/L) [41]. They also contain sulfur, proteins, minerals, cellulose (7 ± 1.4 g/L), hemicellulose (3 ± 1.9 g/L), and essential oils. H_2 production was evaluated in *T. maritima* using onion waste alone or in combination with other FVW to provide additional nutrients for growth. Substrates were cut with an electric blender into small pieces, filtered and then homogenized [41]. Using a simplified medium containing natural seawater, cysteine-HCl and NH_4Cl as inorganic nitrogen source, *T. maritima* metabolized 60% of the carbohydrates contained in onion waste to produce 124 ± 2.5 mmol H_2 /L (yield of 3.76 ± 0.5 mol H_2 /mol C6), 65 ± 2.7 mmol AA/L (yield of 1.97 mol AA/mol C6), and 10 ± 1.1 mmol LA/L [41].

To enhance H_2 production, several experiments were carried out by combining different amounts of onion waste (0–200 mL) and 100 mL of other fruit and vegetable waste (FVW). The increase in onion waste levels significantly improved substrate consumption (69.8% without OW and 79% with 200 mL of OW), H_2 yield (3.24 ± 0.5 mol H_2 /mol C6 without OW and 3.75 ± 0.8 mol H_2 /mol C6 with 200 mL of OW), and acetate yield (1.67 mol AA/mol C6 without OW and 1.99 mol AA/mol C6 with 200 mL of OW) [41]. An economical and efficient H_2 production process was finally obtained by the removal of inorganic nitrogen sources and a surplus of onion waste (400 mL) (Table 2) [41].

3.1.2. Fish Waste

Supplemented of fish waste (FW) can be used to overcome the low nitrogen content in fruit and vegetable waste to sustain *T. maritima* cultures [40]. The fish waste from sardines

represents a highly biodegradable product. It is available in large quantities and rich in nitrogen, making it a good candidate to balance the C/N ratios in growth media. The reduction of C/N ratio by increasing fish waste counterparts (range 0–250 mL) significantly enhanced substrate consumption (from 69.85% at 47 C/N ratio to 96% at 12 C/N ratio), H₂ yield (from 3.24 ± 0.1 at 47 C/N ratio to 3.87 ± 0.1 at 12 C/N ratio), and organic acids production (AA: 56 ± 1.5 mmol/L at 47 C/N ratio to 99.5 ± 2.6 mmol/L at 12 C/N ratio; LA: 10.1 ± 1.1 mmol/L at 47 C/N ratio to 33.4 ± 2.9 mmol/L at 12 C/N ratio) [40]. In this example, a net increase of H₂ production was observed, resulting in 285 ± 2.9 mmol/L of H₂ (yield of 3.86 mol H₂/mol hexose) with 148 ± 3.5 mmol/L of AA (yield of 1.94 mol AA/mol C6) and 49 ± 1.3 mmol/L of LA (Table 2) [40].

3.1.3. Rice straw

Rice straw is produced as a by-product of rice production, and represents one of the major lignocellulosic industrial residues in the world [100]. It is the vegetative part of the rice plants (*Oryza sativa* L.), cut at grain harvest or after. It may be burned, ploughed down as a soil improver, used as a feed for livestock or to produce biofuels such as bioethanol [101]. It is composed of 41.4% cellulose, 19.6% hemicellulose, 22.8% total lignin (3% acid-soluble lignin and 19.8% acid-insoluble lignin), and 10.9% ash [102]. Over the years, different chemical pretreatments (e.g., thermal NH₃, thermal dilute H₂SO₄, combined pretreatments) were investigated to improve the conversion of residues to fermentable compounds, thus improving their utility in anaerobic digestion [103–105]. Korean rice straw has been used as a growth substrate for *T. neapolitana* [102]. To reduce the percentage of lignin in the matrix and to release the more accessible sugars contained in the cellulose and hemicellulose, a combined protocol consisting of two steps was proposed [102,106,107]. Rice straw particles and 10% ammonium hydroxide solution were thoroughly mixed and autoclaved at 121 °C for 60 min. Then the water-washed solid fractions were hydrolyzed with 1.0% sulfuric acid under autoclaving condition at 121 °C for 50 min, and the hydrolysate mixture was finally neutralized by 5 N of NaOH solution before its use as a carbon source [102,107]. After hydrolysis, the solid fraction consisted of 62.6% glucose, 3.04% xylose, and 5.29% lignin, whereas the liquid fraction was composed of 3.93% glucose and 16.16% xylose. Moreover, 78% of the lignin was removed, and an effective hemi-cellulose hydrolysis of 81.6% was observed. The liquid fraction was then used for the fermentation: 85.4% of the rice straw was consumed, including 95.7% of the xylose conversion and 73.0% of the glucose conversion. H₂ production was 112.38 ± 7.66 mL/L, with a yield of 2.7 mmol H₂/g straw (Table 2) [102]. Compared with the untreated form (not shown) and other chemical pretreatments, hydrogen production was noticeably increased, demonstrating that the combination of an efficient pretreatment and the capability of *T. neapolitana* to completely metabolize glucose and xylose can offer many advantages in rice straw valorization. Inhibitory effects on the growth rate due to chemical reagents used in the hydrolytic treatment should be overcome for industrial exploitation of this process.

Table 2. Fermentation of food waste by *Thermotoga* spp.

Substrate	Matrix Components	Sugar Components	Pretreatment Type	Pretreatment Method	Substrate Load (g/L)	Strain	T (°C)	Start pH	Mixing Speed (rpm)	Volume tot. (mL)	Working Volume (mL)	H ₂ yield (mol/mol sugar)	Organic Acids Yield (mol/mol sugar)	Organic Acids (g/L)	Ref.
Carrot pulp	Glucose, fructose, sucrose, polysaccharides	Glucose, fructose	Enzymatic	Enzymes	10	<i>T.nea</i>	72	6.8/7	350	2000	1000	2.7	AA 1.3 LA 0.17	AA 7.20 LA 1.34	[75]
												2.4	AA 1.1 LA 0.30	AA 10.79 LA 4.08	
Rice straw	Cellulose, hemicellulose, lignin	Glucose, xylose	Untreated	-	10	<i>T.nea</i>	75	7.5	150	120	40	2.27 ± 0.01	-	-	[102]
			Chemical	NH ₃								2.68 ± 0.02			
				H ₂ SO ₄								2.61 ± 0.01			
				Combined NH ₃ /H ₂ SO ₄								2.70 ± 0.01			
Potato steam peels	Starch	Glucose	Enzymatic	Enzymes	10	<i>T.nea</i>	75	6.9	350	2000	1000	3.8	AA 1.8 LA 0.20	-	[95]
Molasses	Glucose, fructose, sucrose	Glucose, fructose, sucrose	-	-	20	<i>T.nea</i>	77	8.5	100	116	40	2.6 ± 0.1	AA 1.5	-	[38]
Cheese whey	Lactose, proteins, lipids	Lactose	-	-	12.5	<i>T.nea</i>	77	8.5	100	116	40	2.4 ± 0.1	AA 1.0	-	
Fruit and vegetable waste	Cellulose, hemicellulose	Glucose	Mechanical	Shredding	8.1	<i>T.mar</i>	80	7	150	2200	1100	3.89	AA 1.96	AA 5.39	[39]
					20 (plus FW)					2500		3.86	AA 1.94	AA 12.28 LA 5.49	[40]
Onion waste	Glucose, fructose, sucrose, cellulose, hemicellulose	Glucose, fructose, sucrose	Mechanical	Shredding	200 * OW	<i>T.mar</i>	80	7	150	2500	1100	3.76 ± 0.5	AA 1.97	AA 5.33 LA 1.12	[41]
					400 * OW 100 * FVW							3.67 ± 0.8	AA 1.85	AA 9.27 LA 1.96	

All the experiments have been performed in batch cultures. H₂ yields, mol H₂/mol sugars; *T.nea*, *Thermotoga neapolitana*; *T.mar.*, *Thermotoga maritima*; FW, Fish waste; OW, Onion waste; FVW, Fish vegetable waste. Substrate load column: * mL.

3.1.4. Molasses

Molasses is one of the main products of the sugar cane or sugar beet industry, commonly used to produce alcohol and food flavoring. It is mainly composed of glucose, fructose and sucrose, and high amounts of organic nitrogen, vitamins and salts [108–112]. It can be employed without any pretreatments, avoiding additional nitrogen sources like yeast extract and peptone in hydrogen production by fermentative bacteria [111]. *T. neapolitana*, *T. maritima*, *T. naphthophila* and *T. petrophila* were able to produce H_2 from molasses with both suspended and immobilized cells, and in particular *T. neapolitana* showed comparable yields to pure glucose under the same conditions [38]. The fermentation process in complete medium leads to efficient H_2 production of 2.6 ± 0.1 mol H_2 /mol C6 and acetic acid production of 1.5 mol AA/mol C6 (Table 2) [38]. The removal of vitamins, micronutrients, tryptic soy broth, yeast extract, $MgCl_2$, and $CaCl_2$ from the growth medium of *T. neapolitana* achieved a 70% reduction of medium cost, without significant loss of performance in molasses fermentation (2.95 ± 0.09 mol H_2 /mol C6 and 1.0 mol AA/mol C6) [38]. These findings were confirmed by Frascari et al., who developed a kinetic model of biohydrogen production by molasses fermentation in *T. neapolitana*, in which several parameters were considered as fundamental to further optimize the fermentation process, such as the effects of H_2 , O_2 and substrate inhibition [113].

3.1.5. Cheese Whey

Cheese whey is the wastewater originating from the precipitation and removal of milk casein during cheese-making. It represents a renewable resource in the food industry for its high lactose content. The milk type used in the cheese production (cow, goat, sheep, buffalo, and other mammals) influences the characteristics of the produced cheese whey. For example, bovine whey contains 70–80% lactose, 9% proteins, 8–20% minerals and other minor components, such as some hydrolyzed peptides of k-casein, lipids and bacteria [114]. Due to its high organic content, it cannot be directly discharged into water bodies and is not easily treatable in municipal/consortium purification plants, thus becoming an environmental problem for the dairy industry [115]. Cheese whey is commonly used as direct animal feed, or to be produced as protein and lactose powders for human food and livestock feed. Biological treatment involving the microbial conversion of the lactose contained in cheese whey represents one of the best approaches to obtain value-added products, such as organic acids, bioalcohols, gases (e.g., hydrogen, methane) and bioplastics [116]. Cheese whey was evaluated as the substrate for selected *Thermotoga* spp. (*T. neapolitana*, *T. maritima*, *T. naphthophila* and *T. petrophila*) to better resist high H_2 concentrations [38]. In terms of H_2 production rate, *T. neapolitana* was markedly superior to the other three strains, obtaining 2.4 ± 0.1 mol H_2 /mol glucose eq. in complete medium (Table 2). The use of minimal medium supported neither growth nor H_2 production of *T. neapolitana*, probably because the protein content of the cheese whey was not readily usable [38]. Kinetic studies in Frascari et al. showed that immobilized and suspended cells performed similarly in cheese whey-based reactors [113].

3.2. Lignocellulosic Waste

Lignocellulosic waste arises from agricultural and wood industries, and represent the largest renewable feedstock for industrial fermentation [117–124]. Lignocellulosic materials are composed of heterogeneous polysaccharides derived from the photosynthesis process representing a potentially inexpensive carbon source of hexose and pentose sugars. More than 90% of plant dry weight is composed of cellulose (30–60%) and hemicelluloses (20–40%). Cellulose is a complex carbohydrate consisting of monomeric glucose units, and hemicelluloses are polysaccharides consisting of different pentose and hexose sugars units (mainly xylose, arabinose, glucose, and galactose). Cellulose and hemicelluloses form the structural components of plant cell walls, providing mechanical resistance and protection against pathogens. They tightly bound to lignin (10–25%), which is a class of cross-linked polymers rich in aromatic subunits, relatively hydrophobic and heterogeneous, with differ-

ent degrees of polymerization [120,125,126]. The major hurdle in the industrial exploitation of lignocellulosic waste as an energy feedstock comes from the need to first hydrolyze them and then remove the lignin from the cellulose and hemicellulose by economical and efficient processes [122,123,126,127]. Due to its hydrophobic and heterogeneous nature, lignin is resistant to acid and base hydrolysis, representing an obstacle for accessing the fermentable polysaccharides for biogas production. Moreover, lignin contains certain oligosaccharides and phenolic compounds that can act as growth inhibitors, representing another significant obstacle during the degradation of the cell walls [10,126,128].

Several chemical, physical, biochemical, and biological pretreatments have been proposed over the years to increase the biodegradation of lignocellulosic compounds and release their fermentable parts [10,42,44,81,118,126,129–131]. Hyperthermophilic bacteria are known to ferment the lignocellulosic biomass because they contain many relevant thermostable glycoside hydrolases [10,61,86,130]. The high growth temperatures also promote partial detachment of lignin from the hemicellulose–cellulose assembly and the degradation of growth inhibitors [81,129,130,132].

3.2.1. Miscanthus Waste

Miscanthus is a woody rhizomatous C4 perennial grass which represents an advantageous lignocellulosic energy crop adapted to various bioenergy processes, replacing fossil fuel resources. It combines high biomass production per hectare in various climates, suitable biomass composition for various thermochemical or biochemical conversions, and a positive environmental footprint (lowest water requirement, lowest N, P, and K fertilization, low greenhouse gas emissions, low invasiveness, etc.) [133]. About 62.5% of the total dry matter consists of cellulose and hemicellulose, whose main components are glucans and xylans. The total lignin content of the grass is around 25.0%, consisting mainly of acid-insoluble compounds, which makes a pretreatment step mandatory [129,130].

There have been several studies comparing different pretreatments to make *Miscanthus* biomass fermentable by *Thermotoga* spp. In early studies on *P. elfii*, the best *Miscanthus* hydrolysate was obtained involving a combination of mechanical extrusion and incubation with sodium hydroxide. The pretreatment caused a substantial delignification of the biomass and significantly improved C5 and C6 sugars, reaching a final monosaccharide concentration around 32 g/L in the hydrolysate [129]. *P. elfii* could grow on *Miscanthus* hydrolysates, consuming glucose and xylose simultaneously, and reaching high hydrogen (82.2 mM) and acetic acid (42.4 mM) production, even slightly higher than growing on glucose [129]. The *Miscanthus* fermentation was also demonstrated in *T. neapolitana* cultures [130]. Based on the previous work, different alkali pretreatments were investigated to reduce lignin insoluble fractions in the hydrolysates. The NaOH incubation at 85 °C for 16 h was found to be the optimal condition. Afterwards, enzymatic hydrolysis with cellulases was performed at 50 °C for 24 h to facilitate the release of arabinose, glucose, and xylose. *T. neapolitana* grown on 14 g/L of hydrolysate gave 3.2 mol H₂/mol C₆, 1.4 mol AA/mol C₆, and 11.2 mmol LA/L (Table 3), demonstrating the efficiency of these pretreatment steps in *Thermotoga* spp. fermentation [130]. When hydrolysate concentrations exceeding 28 g/L, the H₂ and acetate yields substantially dropped to 2.0 mol H₂/mol C₆ and 1.1 mol AA/mol C₆, since the fermentability of the substrate was reduced [130].

3.2.2. Garden Waste

Garden and park waste are generated from the maintenance of private gardens and public parks, and represent an economic substrate to produce biohythane (a mixture of hydrogen and methane, usually with 10 to 25% hydrogen in volume) and hydrogen via anaerobic dark fermentation [77,134,135]. In general, we can identify three major components: an organic fraction from garden grass, small bushes containing an undefined organic content and inorganic elements (on a dry matter basis, 0.6% N, 0.1% P, and 1.0% K), and ash, whose content is related to the amount of soil present. On an annual base, wet

garden waste contains 40% water, 30% organic matter, 30% ash, and a low content of trace elements (Cd, Cr, Cu, Hg, Ni, Pb, and Zn) [136].

Abreu et al. [77] estimated biohydrogen production by *T. maritima* from garden waste with a glucans/xylans ratio of 3:1 and a lignin content higher than 30% [77]. To develop a sustainable process, the biomass was homogenized, and no harsh chemical pretreatments were performed. H₂ production from garden waste by *T. maritima* reached 45.1 ± 4.6 L of H₂ per Kg of organic matter with 3.8 ± 0.2 mmol/L of AA (Table 3) [77]. These results were not very encouraging in comparison to data obtained using pure sugars, suggesting the inability of *T. maritima* to ferment the more recalcitrant fraction of the garden waste. Therefore, efficient pretreatments are needed to make the waste more accessible to fermentation.

3.2.3. Paper Sludge

Paper sludge is a solid industrial waste, arising from the paper industry which can be partially used in cement as a Supplementary Material [137,138]. Landfilling and incineration are also common handling options. However, companies from different sectors are looking for new solutions to reduce costs and their impact on the environment. Wastepaper sludge is becoming an economical and profitable material that can be used, after hydrolysis, in green technologies; for example, as a substrate for microbial fermentation to obtain hydrogen. This is due to its chemical and mineralogical composition: besides its low sulfate content, it is rich in minerals (calcium, silicon and aluminum etc.), proteins (22–52%), lignin (20–58%), carbohydrates (0–23%), lipids (2–10%), and cellulose (2–8%) [139]. The first example of paper sludge fermentation was reported for *P. elfii* [137]. The hydrolysate was obtained after digestion for 48 h using a chemical-enzymatic approach involving H₂SO₄, resulting in 12.8 g/L of glucose and 2.4 g/L of xylose [137]. To search for the medium components for optimal hydrogen production, the bacterium was cultivated in different conditions with defined and complex media. Data demonstrated that *P. elfii* grew on paper sludge hydrolysate. In complex medium, hydrogen production, sugar consumption and acetate production rates were similar to glucose fermentation (approximately 30 mM of H₂, 15mM of glucose consumption, 15mM of AA and less than 5mM of LA on paper sludge). Only a slight reduction in hydrogen production was observed without salts (less than 20 mM of H₂), while a net decrease in both hydrogen and acetate production, together with the glucose consumption rate (approximately 11 mM of H₂ and 7 mM of AA with 6 mM of glucose consumed) was observed without yeast extract, indicating that this component was essential for optimal results [137]. The hydrogen production rate on paper sludge hydrolysate was around 48% of the theoretical hydrogen yield of 4 mol of hydrogen/mol of C6 sugar, suggesting that there were still possibilities to improve the biomass pretreatments and cultural conditions to utilize this waste (Table 3) [137].

Table 3. Fermentation of lignocellulosic waste and microalgal biomass by *Thermotogaceae*.

Substrate	Matrix Components	Sugar Components	Pretreatment type	Pretreatment Method	Substrate Load (g/L)	Strain	T (°C)	Start pH	Mixing Speed (rpm)	Volume tot. (mL)	Working Volume (mL)	H ₂ Yield (mol/mol sugars)	Organic Acid(g/L)	Ref.
<i>Miscanthus</i>	Cellulose, hemicellulose, lignin	Glucose, xylose	Mechanical, chemical	Extrusion NaOH	14	<i>T.nea</i>	80	7	350	2000	1000	3.2	AA 10.29 LA 1.25	[130]
			Chemical, enzymatic	NaOH enzymes	10	<i>P.elfii</i>	65	8	-	100	30	60.36 *	AA 3.52	[129]
Garden waste	Glucans, Xylans, lignin	Glucans, xylans	Mechanical	Shredding	5	<i>T.mar</i>	70	7.2	90	120	50	41.5 **	AA 0.31	[77]
Paper sludge	Proteins, lignin, carbohydrates, lipids, cellulose	Glucose, xylose	Chemical, enzymatic	H ₂ SO ₄ -enzymes	11	<i>P.elfii</i>	65	7.2	100	30	-	-	-	[137]
<i>Chlamydomonas reinhardtii</i>	Starch	Glucose	Enzymatic	Enzymes	5	<i>T.nea</i>	75	7/7.4	150	120	40	2.5 ± 0.3	-	[140]
<i>Thalassiosira weissflogi</i>	Protein, chryso-laminarins	Chrysolaminarins	Chemical	MeOH	2	<i>T.nea</i>	80	7.5/8	250	3800	500	1.9 ± 0.1	AA 1.57 LA 0.112	[141]

All the experiments have been performed in batch cultures. Pretreatment protocols are described in the appropriate sections. H₂ yields, mol H₂/mol sugars; *T.nea*, *Thermotoga neapolitana*; *T.mar*, *Thermotoga maritima*; *P.elfii*, *Pseudothermotoga elfii*. H₂ yield column: * mL/L; ** L/Kg.

3.3. Glycerol

Crude glycerol is the major by-product of the biodiesel industry, generated by base-catalyzed transesterification during the biodiesel production processes [142]. It represents a green, biodegradable and abundant feedstock that can be widely used in pharmaceuticals, cosmetics, soaps, toothpastes, paints, and other commercial products [71,143]. Since around 1 kg of glycerol waste is generated for every 10 kg of biodiesel produced, its abundance has increased due to the dramatic growth of the biodiesel industry, although its economic value has decreased in the last few years [142]. Developing advanced sustainable systems is essential to a wider range of applications of crude glycerol without increasing the refining costs [144]. The classical refining processes, such as filtration, chemical additions, and fractional vacuum distillation are sometimes too expensive for small and middle-sized producers [145,146]. From this perspective, economic and alternative ways of using crude glycerol have been studied, like fatty acid production, animal feed, biological conversion [144,146–150]. Among these options, anaerobic digestion to biogas (e.g., methane and hydrogen) production from fermentative microorganisms represents a promising approach, which produces high levels of biogas in small reactors and enjoys several advantages, such as low nutrient requirements, energy savings, and generation of a stabilized digestate [142–144,151]. The chemical compositions of crude glycerol are not well defined and are dependent on the parent feedstock and biodiesel production processes, e.g., the type of catalyst used, the transesterification efficiency, recovery efficiency of the biodiesel and other impurities [144,146]. Generally, every feedstock contains around 50–60% (wt) of glycerol, 12 to 16% of alkalis, especially in the form of alkali soaps and hydroxides, 15 to 18% of methyl esters, 8 to 12% of methanol, and 2 to 3% of water [146]. In addition to methanol and soaps, crude glycerol also contains Ca, Mg, P, or S [146], K, Na, C, N, and proteins (0.05 to 0.44%), etc. [142]. The impurities present in the raw substrate, such as spent catalysts, salts after neutralization, residual methanol, methyl esters, oil/fat, soap and free fatty acids, have to be removed to make the substrate suitable for further applications [146,152]. As a carbon source, glycerol was tested for biohydrogen production via anaerobic fermentation by thermophilic bacteria. Since glycerol is a more reduced compound compared to other substrates like glucose or xylose, it has the potential to generate more NADH and H₂ during catabolism [153].

Some controversies exist concerning the ability of *Thermotogaceae* family members to utilize glycerol. Early studies reported that *T. maritima* contained the coding sequences for a complete pathway for glycerol uptake, although glycerol had to enter into the cell by diffusion in other strains (e.g., *T. neapolitana*), [154–156]. Therefore, a putative degradation pathway based on the *T. maritima* genome was proposed, i.e., glycerol enters the cell either by diffusion or facilitated transportation and enters glycolysis via glycerol-3-phosphate. The involvement of a glycerol kinase and an uncharacterized NAD⁺ or FAD-dependent multimeric glycerol-3-phosphate dehydrogenase has been hypothesized [154].

Two research groups experimented with the possibility of fermenting glycerol in *T. maritima*, *T. neapolitana*, and *P. elfii*, obtaining conflicting results. Eriksen et al. observed growth only if glycerol was supplemented simultaneously with one or more sugars; none of the three species grew if glycerol was the sole carbon source (data not shown) [36]. The surplus of NADH generated during glycerol conversion may influence the activity of the bifurcating hydrogenases present in these bacteria. In fact, 2 mol of NADH and 2 mol of reduced ferredoxin were produced in glycerol conversion, changing the conventional stoichiometric ratio for hydrogenase activity from 1:2 to 1:1 [153,157,158].

The capability of *T. neapolitana* to ferment glycerol waste was also demonstrated by Ngo et al. [151]. Before use, crude glycerol waste was pretreated to avoid inhibition of bacterial growth by removing the solvents present (e.g., methanol and/or ethanol) by rotary evaporation at 45 °C, and the solid fraction was precipitated by centrifugation at 15,000 rpm for 15 min [151]. H₂ yield was around 1.97 ± 0.09 mol H₂/mol glycerol, obtained without any other modification. Several cultural parameters were also important to enhance glycerol fermentation, including pH, N₂ sparging, sodium chloride concentration and yeast

extract. Under specific conditions (i.e., N_2 sparging and buffering agent), H_2 could reach 2.7 ± 0.1 mol H_2 /mol glycerol; considerable production of acetic acid was also observed (22.35 ± 1.05 mmol/L) (Table 4) [151]. Another study [71] confirmed this ability with pure and waste glycerol, obtaining 1.3 ± 0.06 mol H_2 /mol of glycerol waste consumed and a percentage of acetic and lactic acid comparable to pure glycerol results (data not shown) [71]. During fermentation, more acetic acid than lactic acid was produced, implying that the H_2 -acetate pathway predominated over the lactate one [70].

Again, in the study of Maru et al. [153], both *T. neapolitana* and *T. maritima* metabolized pure glycerol and produced H_2 at 2.65 mol H_2 /mol glycerol for *T. neapolitana* and 2.75 mol H_2 /mol glycerol for *T. maritima* (Table 4) [153]. In order to improve glycerol fermentation, cultural conditions were optimized in *T. maritima* by testing the glycerol content, yeast extract concentration, and pH control. Maximum H_2 yields were 2.86 mol H_2 /mol glycerol for *T. neapolitana* and 2.84 mol H_2 /mol glycerol for *T. maritima* in the optimized conditions [154].

3.4. Microalgal Biomass

Microalgae are photosynthetic unicellular organisms living individually, in chains or groups in a wide range of aquatic habitats; they can tolerate different light intensities, temperature, salinity and pH values [159]. They can be cultured in large scale by different methods and conditions, and represent a potential feedstock for the coproduction of different forms of energy. Several species were recently investigated as a fuel source since they contain large quantities of lipids useful for biodiesel production [159,160]. For example, marine diatoms contain up to 50% of lipids per biomass dry weight [161]. Moreover, to valorize all microalgal biomass components, the soluble polysaccharides of photosynthetic biomass could play an important role for biohydrogen production through DF [140].

T. neapolitana can metabolize different microalgal biomass. Nguyen et al. [140] and Dipasquale et al. [141] studied *T. neapolitana* fermentation on the biomasses of *Chlamydomonas reinhardtii* and *Thalassiosira weissflogi* respectively [140,141]. In the former case, algal biomass was pretreated in two different ways (heat-HCl and Termamyl enzyme) to disrupt the algal cell walls and release starch for fermentation [140]. Termamyl enzyme pretreatment, performed by a thermostable α -amylase from *Bacillus licheniformis* at 90°C for 30 min, was the most effective process to optimize the hydrolysis [140]. This pretreatment maximized H_2 yield (2.5 ± 0.3 mol H_2 /mol glucose eq) when compared to that obtained with other pretreatment methods (<2.2 mol H_2 /mol glucose eq) or with pure starch fermentation (1.5 ± 0.1 mol H_2 /mol glucose eq) (Table 3) [140].

In the latter study [141], chemical extraction with MeOH was performed on the *Thalassiosira weissflogi* biomass to separate the water-soluble fraction from the lipid fraction [141]. The aqueous diatom extracts mainly contained 0.4 g/L protein and 2.3 g/L sugar eqs (chrysolaminarins). Although 81.8% of sugars in microalgal extract were consumed in 48 h of fermentation by *T. neapolitana*, H_2 yields (1.9 ± 0.1 mol H_2 /mol glucose eq) (Table 3) were lower in comparison to those obtained from complex and simple sugars (around 2.7 mol H_2 /mol glucose eq.) [141]. The co-occurring decrease of lactate and acetate production suggested a minor availability of pyruvate in cultures of *T. neapolitana* on diatom extracts (Table 3) [141].

Depending on the origin of microalgal biomass, targeted strategies could be adopted to optimize the fermentation medium or to increase the carbohydrate content.

Table 4. Fermentation of glycerol by *Thermotoga* spp.

Substrate	Pretreatment Type	Pretreatment Method	Substrate Load (g/L)	Strain	T (°C)	Start pH	Mixing Speed (rpm)	Reactor Volume (mL)	Working Volume (mL)	H ₂ Yield (mol H ₂ /mol Sugar)	Organic Acids (g/L)	Ref.
Pure glycerol	-	-	5	<i>T.nea</i> <i>T.mar</i>	80	7.5	200	120	25	$\frac{2.65}{2.75}$	-	[153]
Biodiesel waste (1% glycerol)	Mechanical	Evaporation, centrifugation	5	<i>T.nea</i>	80	7.5	-	120	40	2.70 ± 0.10	AA 1.85	[151]
Pure glycerol	-	-	2.5	<i>T.nea</i> <i>T.mar</i>	80	8	200	120	25	$\frac{2.86}{2.84}$	AA 2.21 LA 1.74	[154]
Biodiesel waste (1% glycerol)	Mechanical	Evaporation, centrifugation	3	<i>T.nea</i>	75	7.5	-	120	40	1.3 ± 0.06	-	[71]

All the experiments have been performed in batch cultures. AA, acetic acid; LA, lactic acid.

4. Molecular Basis of Sugar Catabolism and Hydrolytic Enzymes in the Family *Thermotogaceae*

In recent years, several bacterial genomes of genus *Thermotoga* were sequenced (e.g., *T. maritima*, *T. neapolitana*, *T. thermarum*, RQ7), revealing their versatility in utilizing various organic carbon sources [162–166]. Many members of the family *Thermotogaceae* possess all the genes needed for glucose catabolism by EMP, ED and OPP pathways (Supplemental Table S1), as also supported by the presence of key enzymes, such as phosphofructokinase (PFK, E.C. 2.7.1.11), 2-dehydro-3-deoxyphosphogluconate aldolase (KDPG aldolase, E.C. 4.1.2.14), and 6-phosphogluconate dehydrogenase (6PDGH, E.C. 1.1.1.44) [54]. Interestingly, these pathways showed an environmental-dependent activation mechanism in *T. neapolitana*, because the insufflation of CO₂ instead of N₂ induced the upregulation of the genes involved in ED and OPP [60]. Another peculiarity of some *Thermotogales* members (e.g., *T. maritima*) is the presence of an unconventional triosephosphate isomerase (TIM, E.C. 5.3.1.1) linked to phosphoglycerate kinase (PGK, E.C. 2.7.2.3). This anomalous association leads to a bifunctional tetrameric protein, which showed an increased stability and catalytic activity at high temperatures [167].

On the other hand, *Thermotogaceae* showed the presence of genes involved in monosaccharides conversion to glucose inducing an alternative flux to EMP and ED, enabling *Thermotogaceae* to use alternative sugar substrate sources [168–170]. Examples of these are uronate isomerase (E.C. 5.3.1.12), xylose isomerase (E.C. 5.3.1.5), mannose-1-phosphate guanylyltransferase (E.C. 2.7.7.22), phosphomannomutase (E.C. 5.4.2.8), mannose-6-phosphate isomerase (E.C. 5.3.1.8) and others. These enzymes could operate in the conversion of monosaccharides to glucose and/or glycolysis intermediates. *Thermotogaceae* also possess enzymes related to glucuronic and galacturonic acid metabolism, which provide an additional and specific feed into the ED pathway.

Different species of *Thermotogaceae* prefer different monosaccharides. Experiments performed using mixtures of glucose, fructose, arabinose, and xylose displayed similar behaviors in *T. neapolitana* and *T. maritima* which clearly catabolized glucose and xylose instead of arabinose, while *T. RQ2* quickly consumed fructose [76]. In this context, it is not surprising to find in *Thermotogaceae* genomes the entire regulons for monosaccharide metabolism and the ABC transporters for the import/export of simple and complex sugars [76]. The fine regulation of these mechanisms leads to efficient catabolism of the sugar substrates [60,163,171].

Common components of fruit and vegetable waste are galactose and rhamnose [76,163]. As showed in Supplemental Table S1, the entire set of enzymes, related to Leloir pathway, were encoded by *Thermotogaceae* genomes. This pathway is specifically involved in the galactose metabolism. These enzymes include aldose 1-epimerase (E.C. 5.1.3.3), galactokinase (E.C. 2.7.1.6), galactose 1-phosphate uridylyl-transferase (E.C. 2.7.7.12), phosphoglucomutase (E.C. 5.4.2.2) and UDP-glucose 4-epimerase (E.C. 5.1.3.2), converting galactose to glucose 6-phosphate. The ability of *Thermotogales* in rhamnose metabolism was defined by the presence of rhamnose isomerase (E.C. 5.3.1.14), rhamulose kinase (E.C. 2.7.15), and rhamulose 1-phosphate aldolase, resulting in the biosynthesis of dihydroxyacetone phosphate and lactaldehyde [172]. Interestingly, this metabolic pathway is connected to both glycolysis and lactate dehydrogenase metabolism. The rhamnose metabolism pathway is totally absent in the genus *Pseudothermotoga* [76].

Complex sugars from different sources such as plant and algal biomass were also efficiently metabolized by *Thermotogaceae* [73,95,129,130,140]. Plant storage polysaccharides as well as starch and sucrose could be easily used as the carbon source by using enzymes such as α -amylase, α -glucosidase, pullulanase, and others (Supplemental Table S2). Starch is composed by α -glucose residues mainly linked by α -1,4/1,6 glycosidic bonds. The two main high molecular weight components of starch are the linear polymer amylose and the branched polymer amylopectin [173]. *Thermotogaceae* genomes reported the complex set of depolymerizing enzymes able to catalyze the catabolism of both linear and branched starch polymers (Supplemental Table S2). Non-reducing ends are attacked by

enzymes such as hydrolases, β -amylase producing small oligosaccharides, while enzymes capable of hydrolyzing α -1,6 glycosidic bonds in pullulan are defined pullulanases [173]. These enzymes ensure degradation and linearization of complex polysaccharides into a monosaccharide unit. Intriguingly, although starch is a rare carbon source in deep marine environments, especially in a hot thermal vent, extremophiles repeatedly showed starch-hydrolyzing genes in their genomes, suggesting starch as an important carbon source for their metabolism [173]. Homologous starch catabolic enzymes have been identified and characterized in a number of hyperthermophilic genera, namely *Pyrococcus*, *Thermococcus*, *Sulfolobus*, *Pyrodictium* [173].

Lignocellulosic biomass represents a recalcitrant source of organic compound that requires a number of enzymatic processes to depolymerize [174]. The ability of *Thermotogaceae* to metabolize cellulose and hemicellulose is related to the presence of a number of cellulolytic and hemicellulolytic enzymes. Examples of these are β -glucosidase, α -arabinofuranosidase, endo-1,3- β -xylanase, endo-1,4- β -xylanase, endo-1,4- β -mannanase etc., (Supplemental Table S2). In particular, the lignocellulosic biomass showed the presence of mannans which represent a specific form of storage and cell wall polysaccharide [175]. *Thermotogaceae* showed the presence of a number of genes involved in mannans catabolism, namely mannonate dehydratase, D-mannonate oxidoreductase, α - and β -mannosidases. Microarray analyses revealed a dramatic reorganization of *Thermotogaceae* transcriptomes when bacterial growth on a polysaccharide mix was compared to the growth on glucose. These data connected the ability of *Thermotogaceae* to ferment individual carbohydrates to the versatile set of ABC transporters [76]. The hemicellulolytic enzymes from *T. neapolitana* were tested to solubilize lignocellulosic products from barley straw and corn bran, which improved the yield of fermentable sugars up to 65% compared to traditional systems [86]. *T. maritima* cellulase has also been overexpressed in tobacco and *Arabidopsis* chloroplasts to maximize the production of this cellulolytic enzyme [175]. The biomass of brown algae and diatoms, particularly polysaccharides such as sucrose and laminarin, were easily fermented by *Thermotogaceae* [73]. It is worth pointing out that genes coding for laminarinase, endoglucanase (β 1 \rightarrow 3 and β 1 \rightarrow 4), glucosidase (α and β), and similar enzymes are frequently noticed in *Thermotogaceae* genomes. Interesting differences were reported between *Thermotoga* and *Pseudothermotoga* genomes, regarding polysaccharide catabolic enzymes (Supplemental Table S2). The ability of *Thermotogales* to use microalgal biomass as an organic source could be confirmed by the presence of genes related to lipid catabolism, such as lipase (CTN_RS06200), glycoside hydrolase 4 related to glycolipids and sphingolipids (CTN_RS09115), and α -galactosidase related to glycolipids (CTN_RS06915).

5. Conclusions and Future Perspective

Biodegradable organic waste is a promising carbon source to be exploited in a more circular and sustainable worldwide economy. Their abundance and heterogeneity in terms of compositional and structural features, associated to their origins, allow them to be widely used for biogas production, mainly biohydrogen, biofuels such as bioethanol, and value-added products (acetic acid, lactic acid, etc.). In the last few years, microbial anaerobic fermentation has become a promising way to obtain high production yields of bioenergy and green chemicals, and hyperthermophilic bacteria capable of metabolizing complex sugars via a dark fermentation process represent the new frontier of biotechnological development. The hyperthermophilic family *Thermotogaceae*, including the *Thermotoga* and *Pseudothermotoga* genera, are recognized for their ability to produce H_2 from many complex substrates.

This review demonstrates that *Thermotoga* and *Pseudothermotoga* spp. have an enormous biotechnological potential in fermenting organic waste originated from food, glycerol, lignocellulosic, and microalgal biomasses. In particular, *T. maritima*, *T. neapolitana* and *P. elfii* have been recognized as the best candidates in this scientific landscape. Their ability to degrade complex substrates is due to their unique metabolic and genomic features.

Many studies have been performed to find the best employment strategies and to identify putative transporters, enzymes, pathways, limiting factors, and pretreatment methods. The extreme growth temperatures of these bacteria not only reduce contamination by environmental bacteria but also make complex substrates easier to solubilize, avoiding, in some cases, the pretreatment step, which helps to preserve major components of the substrates and increase their availability.

Several studies were carried out to investigate the effect of different mechanical, thermal, chemical, and biological pretreatment methods on biodegradable organic waste to develop more sustainable processes. They can also include the combined use of different substrates to balance nutritional requests. The synergistic activities of two strains may also be exploited to metabolize complex substrates. For example, *C. saccharolyticus* can provide thermostable cellulolytic and xylanolytic enzymes, allowing the growth on complex lignocellulosic carbon sources and the co-metabolization of a wide range of monosaccharides including both pentose and hexose sugars. On the other hand, *T. maritima* and *T. neapolitana* can grow either on various C5 and C6 sugars, starch, glycogen, or complex organic substrates with hydrogen yields close to the maximum theoretical values. Co-cultivating *C. saccharolyticus* and *Thermotoga* can maximize the utilization of cellulosic substrates while ensuring optimal H₂ yield.

The collective knowledge we gained so far will allow us to experiment with several waste fermentation strategies with members of the *Thermotogaceae* family. The existence of unprecedented pathways, like the capnophilic lactic fermentation pathway discovered in *T. neapolitana*, which pairs CO₂ and acetate to produce lactic acid at high yields and at the same time detoxifies the environment from CO₂, further illustrates the great potentials of the *Thermotoga* and *Pseudothermotoga* genera in establishing a sustainable economy based on waste elimination and exploitation.

Supplementary Materials: The following are available online at <https://www.mdpi.com/article/10.3390/resources10040034/s1>, Table S1: List of *Thermotogales* genes related to glycolytic pathways. Data have been exported from Ensembl Bacteria database; Table S2: List of *Thermotogales* genes related to organic catabolism. Data have been exported from Ensembl Bacteria database.

Author Contributions: Conceptualization, G.d. and N.E.; writing—original draft preparation, N.E., M.L., M.V., bioinformatic analysis, S.L.; writing—review and editing, all authors; editing and revision, Z.X.; supervision, G.d.; funding acquisition and project administration, A.F. and G.d. All authors have read and agreed to the published version of the manuscript.

Funding: This research was funded by BioRECO2VER Project, through the European Union's Horizon 2020 Research and Innovation Programme under Grant Agreement No. 760431.

Institutional Review Board Statement: Not applicable.

Informed Consent Statement: Not applicable.

Data Availability Statement: Not applicable.

Acknowledgments: The authors would like to thank Lucio Caso (CNR-ICB) for the technical support in preparing the manuscript.

Conflicts of Interest: The authors declare no conflict of interest. The funding agencies gave their permissions to the publication of manuscript.

References

1. Perea-Moreno, M.A.; Samerón-Manzano, E.; Perea-Moreno, A.J. Biomass as renewable energy: Worldwide research trends. *Sustainability* **2019**, *11*, 863. [CrossRef]
2. Wainaina, S.; Awasthi, M.K.; Sarsaiya, S.; Chen, H.; Singh, E.; Kumar, A.; Ravindran, B.; Awasthi, S.K.; Liu, T.; Duan, Y.; et al. Resource recovery and circular economy from organic solid waste using aerobic and anaerobic digestion technologies. *Bioresour. Technol.* **2020**, *301*, 122778. [CrossRef] [PubMed]
3. Muthu, S. *Recycling of Solid Waste for Biofuels and Bio-Chemicals*; Obulisamy, P., Heimann, K., Muthu, S., Eds.; Springer: Berlin/Heidelberg, Germany, 2016.

4. European Commission Updated Bioeconomy Strategy. Available online: https://ec.europa.eu/knowledge4policy/publication/updated-bioeconomy-strategy-2018_en (accessed on 12 April 2021).
5. Bouallagui, H.; Touhami, Y.; Ben Cheikh, R.; Hamdi, M. Bioreactor performance in anaerobic digestion of fruit and vegetable wastes. *Process. Biochem.* **2005**, *40*, 989–995. [\[CrossRef\]](#)
6. Kapdan, I.K.; Kargi, F. Bio-hydrogen production from waste materials. *Enzym. Microb. Technol.* **2006**, *38*, 569–582. [\[CrossRef\]](#)
7. Lin, C.Y.; Lay, C.H.; Sen, B.; Chu, C.Y.; Kumar, G.; Chen, C.C.; Chang, J.S. Fermentative hydrogen production from wastewaters: A review and prognosis. *Int. J. Hydrogen Energy* **2012**, *37*, 15632–15642. [\[CrossRef\]](#)
8. Nasir, I.M.; Ghazi, T.I.M.; Omar, R. Production of biogas from solid organic wastes through anaerobic digestion: A review. *Appl. Microbiol. Biotechnol.* **2012**, *95*, 321–329. [\[CrossRef\]](#)
9. Atelge, M.R.; Krisa, D.; Kumar, G.; Eskicioglu, C.; Nguyen, D.D.; Chang, S.W.; Atabani, A.E.; Al-Muhtaseb, A.H.; Unalan, S. Biogas Production from Organic Waste: Recent Progress and Perspectives. *Waste Biomass Valorization* **2020**, *11*, 1019–1040. [\[CrossRef\]](#)
10. Lee, S.Y.; Sankaran, R.; Chew, K.W.; Tan, C.H.; Krishnamoorthy, R.; Chu, D.-T.; Show, P.-L. Waste to bioenergy: A review on the recent conversion technologies. *Bmc Energy* **2019**, *1*, 1–22. [\[CrossRef\]](#)
11. Kumar, P.; Gnansounou, E.; Raman, J.K.; Baskar, G. *Refining Biomass Residues for Sustainable Energy and Bioproducts*; Elsevier: Amsterdam, The Netherlands, 2019.
12. Dung, T.N.B.; Sen, B.; Chen, C.C.; Kumar, G.; Lin, C.Y. Food waste to bioenergy via anaerobic processes. *Energy Procedia* **2014**, *61*, 307–312. [\[CrossRef\]](#)
13. Pham, T.P.T.; Kaushik, R.; Parshetti, G.K.; Mahmood, R.; Balasubramanian, R. Food waste-to-energy conversion technologies: Current status and future directions. *Waste Manag.* **2015**, *38*, 399–408. [\[CrossRef\]](#)
14. Alibardi, L.; Cossu, R. Effects of carbohydrate, protein and lipid content of organic waste on hydrogen production and fermentation products. *Waste Manag.* **2016**, *47*, 69–77. [\[CrossRef\]](#)
15. Boodhun, B.S.F.; Mudhoo, A.; Kumar, G.; Kim, S.H.; Lin, C.Y. Research perspectives on constraints, prospects and opportunities in biohydrogen production. *Int. J. Hydrogen Energy* **2017**, *42*, 27471–27481. [\[CrossRef\]](#)
16. Staffell, I.; Scamman, D.; Velazquez Abad, A.; Balcombe, P.; Dodds, P.E.; Ekins, P.; Shah, N.; Ward, K.R. The role of hydrogen and fuel cells in the global energy system. *Energy Environ. Sci.* **2019**, *12*, 463–491. [\[CrossRef\]](#)
17. Chong, M.L.; Sabaratnam, V.; Shirai, Y.; Hassan, M.A. Biohydrogen production from biomass and industrial wastes by dark fermentation. *Int. J. Hydrogen Energy* **2009**, *34*, 3277–3287. [\[CrossRef\]](#)
18. Pradhan, N.; Dipasquale, L.; D'Ippolito, G.; Panico, A.; Lens, P.N.L.; Esposito, G.; Fontana, A. Hydrogen production by the thermophilic bacterium *Thermotoga neapolitana*. *Int. J. Mol. Sci.* **2015**, *16*, 12578–12600. [\[CrossRef\]](#) [\[PubMed\]](#)
19. Dincer, I.; Acar, C. Smart energy solutions with hydrogen options. *Int. J. Hydrogen Energy* **2018**, *43*, 8579–8599. [\[CrossRef\]](#)
20. Ntaikou, I.; Antonopoulou, G.; Lyberatos, G. Biohydrogen production from biomass and wastes via dark fermentation: A review. *Waste Biomass Valorization* **2010**, *1*, 21–39. [\[CrossRef\]](#)
21. Khanna, N.; Das, D. Biohydrogen production by dark fermentation. *Wiley Interdiscip. Rev. Energy Environ.* **2012**, *2*, 401–421. [\[CrossRef\]](#)
22. Raj, S.M.; Talluri, S.; Christopher, L.P. Thermophilic Hydrogen Production from Renewable Resources: Current Status and Future Perspectives. *Bioenergy Res.* **2012**, *5*, 515–531. [\[CrossRef\]](#)
23. Pawar, S.S.; Van Niel, E.W.J. Thermophilic biohydrogen production: How far are we? *Appl. Microbiol. Biotechnol.* **2013**, *97*, 7999–8009. [\[CrossRef\]](#)
24. Kothari, R.; Kumar, V.; Pathak, V.V.; Ahmad, S.; Aoyi, O.; Tyagi, V.V. A critical review on factors influencing fermentative hydrogen production. *Front. Biosci. Landmark* **2017**, *22*, 1195–1220. [\[CrossRef\]](#)
25. Schönheit, P.; Schäfer, T. Metabolism of hyperthermophiles. *World J. Microbiol. Biotechnol.* **1995**, *11*, 26–57. [\[CrossRef\]](#) [\[PubMed\]](#)
26. Van Ooteghem, S.A.; Beer, S.K.; Yue, P.C. Hydrogen production by the thermophilic bacterium *Thermotoga neapolitana*. *Appl. Biochem. Biotechnol. Enzym. Eng. Biotechnol.* **2002**, *98–100*, 177–189. [\[CrossRef\]](#)
27. Shao, W.; Wang, Q.; Rupani, P.F.; Krishnan, S.; Ahmad, F.; Rezaia, S.; Rashid, M.A.; Sha, C.; Din, M.F. Biohydrogen production via thermophilic fermentation: A prospective application of *Thermotoga* species. *Energy* **2020**, *197*. [\[CrossRef\]](#)
28. Huber, R.; Hannig, M. Thermotogales. *Prokaryotes* **2006**, 899–922. [\[CrossRef\]](#)
29. Turner, P.; Mamo, G.; Karlsson, E.N. Potential and utilization of thermophiles and thermostable enzymes in biorefining. *Microb. Cell Fact.* **2007**, *6*. [\[CrossRef\]](#)
30. Blumer-Schuetz, S.E.; Kataeva, I.; Westpheling, J.; Adams, M.W.; Kelly, R.M. Extremely thermophilic microorganisms for biomass conversion: Status and prospects. *Curr. Opin. Biotechnol.* **2008**, *19*, 210–217. [\[CrossRef\]](#)
31. Arora, R.; Behera, S.; Kumar, S. Bioprospecting thermophilic/thermotolerant microbes for production of lignocellulosic ethanol: A future perspective. *Renew. Sustain. Energy Rev.* **2015**, *51*, 699–717. [\[CrossRef\]](#)
32. Pradhan, N.; Dipasquale, L.; d'Ippolito, G.; Fontana, A.; Panico, A.; Pirozzi, F.; Lens, P.N.L.; Esposito, G. Model development and experimental validation of capnophilic lactic fermentation and hydrogen synthesis by *Thermotoga neapolitana*. *Water Res.* **2016**, *99*, 225–234. [\[CrossRef\]](#)
33. Pradhan, N.; Dipasquale, L.; D'Ippolito, G.; Fontana, A.; Panico, A.; Lens, P.N.L.; Pirozzi, F.; Esposito, G. Kinetic modeling of fermentative hydrogen production by *Neapolitana*. *Int. J. Hydrogen Energy* **2016**, *41*, 4931–4940. [\[CrossRef\]](#)

34. Dipasquale, L.; Pradhan, N.; Ippolito, G.; Fontana, A. Potential of Hydrogen Fermentative Pathways in Marine Thermophilic Bacteria: Dark Fermentation and Capnophilic Lactic Fermentation. In *Thermotoga and Pseudothermotoga Species*; Elsevier: Cham, Switzerland, 2018; pp. 217–235.
35. Okonkwo, O.; Lakaniemi, A.M.; Santala, V.; Karp, M.; Mangayil, R. Quantitative real-time PCR monitoring dynamics of *Thermotoga neapolitana* in synthetic co-culture for biohydrogen production. *Int. J. Hydrogen Energy* **2018**, *43*, 3133–3141. [\[CrossRef\]](#)
36. Eriksen, N.T.; Riis, M.L.; Holm, N.K.; Iversen, N. H₂ synthesis from pentoses and biomass in *Thermotoga* spp. *Biotechnol. Lett.* **2011**, *33*, 293–300. [\[CrossRef\]](#)
37. Cappelletti, M.; Davide, Z.; Anne Postec, B.O. Members of the Order *Thermotogales*: From Microbiology to Hydrogen Production. *Microb. Bioenergy Hydrog. Prod. Adv. Photosynth. Respir.* **2014**, *38*, 321–347. [\[CrossRef\]](#)
38. Cappelletti, M.; Bucchini, G.; De Sousa Mendes, J.; Alberini, A.; Fedi, S.; Bertin, L.; Frascari, D. Biohydrogen production from glucose, molasses and cheese whey by suspended and attached cells of four hyperthermophilic *Thermotoga* strains. *J. Chem. Technol. Biotechnol.* **2012**, *87*, 1291–1301. [\[CrossRef\]](#)
39. Saidi, R.; Liebgott, P.P.; Gannoun, H.; Ben Gaida, L.; Miladi, B.; Hamdi, M.; Bouallagui, H.; Auria, R. Biohydrogen production from hyperthermophilic anaerobic digestion of fruit and vegetable wastes in seawater: Simplification of the culture medium of *Thermotoga maritima*. *Waste Manag.* **2018**, *71*, 474–484. [\[CrossRef\]](#)
40. Saidi, R.; Liebgott, P.P.; Hamdi, M.; Auria, R.; Bouallagui, H. Enhancement of fermentative hydrogen production by *Thermotoga maritima* through hyperthermophilic anaerobic co-digestion of fruit-vegetable and fish wastes. *Int. J. Hydrogen Energy* **2018**, *43*, 23168–23177. [\[CrossRef\]](#)
41. Saidi, R.; Hamdi, M.; Bouallagui, H. Hyperthermophilic hydrogen production in a simplified reaction medium containing onion wastes as a source of carbon and sulfur. *Environ. Sci. Pollut. Res.* **2020**. [\[CrossRef\]](#)
42. Ravindran, R.; Jaiswal, A.K. A comprehensive review on pre-treatment strategy for lignocellulosic food industry waste: Challenges and opportunities. *Bioresour. Technol.* **2016**, *199*, 92–102. [\[CrossRef\]](#)
43. Galbe, M.; Wallberg, O. Pretreatment for biorefineries: A review of common methods for efficient utilisation of lignocellulosic materials. *Biotechnol. Biofuels* **2019**, *12*, 1–26. [\[CrossRef\]](#) [\[PubMed\]](#)
44. Sayara, T.; Sánchez, A. A review on anaerobic digestion of lignocellulosic wastes: Pretreatments and operational conditions. *Appl. Sci.* **2019**, *9*, 4655. [\[CrossRef\]](#)
45. Connors, S.B.; Montero, C.I.; Comfort, D.A.; Shockley, K.R.; Johnson, M.R.; Chhabra, S.R.; Kelly, R.M. An Expression-Driven Approach to the Prediction of Carbohydrate Transport and Utilization Regulons in the Hyperthermophilic Bacterium *Thermotoga maritima*. *J. Bacteriol.* **2005**, *187*, 7267–7282. [\[CrossRef\]](#)
46. Connors, S.B.; Mongodin, E.F.; Johnson, M.R.; Montero, C.I.; Nelson, K.E.; Kelly, R.M. Microbial biochemistry, physiology, and biotechnology of hyperthermophilic *Thermotoga* species. *Fems Microbiol. Rev.* **2006**, *30*, 872–905. [\[CrossRef\]](#)
47. Chhabra, S.R.; Shockley, K.R.; Connors, S.B.; Scott, K.L.; Wolfinger, R.D.; Kelly, R.M. Carbohydrate-induced differential gene expression patterns in the hyperthermophilic bacterium *Thermotoga maritima*. *J. Biol. Chem.* **2003**, *278*, 7540–7552. [\[CrossRef\]](#) [\[PubMed\]](#)
48. Bhandari, V.; Gupta, R.S. Molecular signatures for the phylum (class) *Thermotogae* and a proposal for its division into three orders (*Thermotogales*, *Kosmotogales* ord. Nov. and *Petrotogales* ord. Nov.) containing four families (*Thermotogaceae*, *Fervidobacteriaceae* fam. Nov., *Kosmotoga*. *Antonie Van Leeuwenhoek Int. J. Gen. Mol. Microbiol.* **2014**, *105*, 143–168. [\[CrossRef\]](#) [\[PubMed\]](#)
49. Belahbib, H.; Summers, Z.M.; Fardeau, M.L.; Joseph, M.; Tamburini, C.; Dolla, A.; Ollivier, B.; Armougom, F. Towards a congruent reclassification and nomenclature of the thermophilic species of the genus *Pseudothermotoga* within the order *Thermotogales*. *Syst. Appl. Microbiol.* **2018**, *41*, 555–563. [\[CrossRef\]](#) [\[PubMed\]](#)
50. Reysenbach, A.-L. Phylum BII. *Thermotogae* phylum. In *Bergey's Manual of Systematic Bacteriology*; Springer: New York, NY, USA, 2002.
51. Thauer, R.K.; Jungermann, K.; Decker, K. Energy Conservation in Chemotrophic Anaerobic Bacteria. *Bacteriol. Rev.* **1977**, *41*, 809. [\[CrossRef\]](#)
52. Selig, M.; Xavier, K.B.; Santos, H.; Schönheit, P. Comparative analysis of Embden-Meyerhof and Entner-Doudoroff glycolytic pathways in hyperthermophilic archaea and the bacterium *Thermotoga*. *Arch. Microbiol.* **1997**, *167*, 217–232. [\[CrossRef\]](#)
53. Romano, A.H.; Conway, T. Evolution of carbohydrate metabolic pathways. *Res. Microbiol.* **1996**, *147*, 448–455. [\[CrossRef\]](#)
54. Flamholz, A.; Noor, E.; Bar-Even, A.; Liebermeister, W.; Milo, R. Glycolytic strategy as a tradeoff between energy yield and protein cost. *Proc. Natl. Acad. Sci. USA* **2013**, *110*, 10039–10044. [\[CrossRef\]](#)
55. Dipasquale, L.; d'Ippolito, G.; Fontana, A. Capnophilic lactic fermentation and hydrogen synthesis by *Thermotoga neapolitana*: An unexpected deviation from the dark fermentation model. *Int. J. Hydrogen Energy* **2014**, *39*, 4857–4862. [\[CrossRef\]](#)
56. d'Ippolito, G.; Dipasquale, L.; Fontana, A. Recycling of Carbon Dioxide and Acetate as Lactic Acid by the Hydrogen-Producing Bacterium *Thermotoga neapolitana*. *ChemSusChem* **2014**, *7*, 2678–2683. [\[CrossRef\]](#)
57. Dipasquale, L.; Adessi, A.; d'Ippolito, G.; Rossi, F.; Fontana, A.; De Philippis, R. Introducing capnophilic lactic fermentation in a combined dark-photo fermentation process: A route to unparalleled H₂ yields. *Appl. Microbiol. Biotechnol.* **2015**, *99*, 1001–1010. [\[CrossRef\]](#)
58. d'Ippolito, G.; Dipasquale, L.; Vella, F.M.; Romano, I.; Gambacorta, A.; Cutignano, A.; Fontana, A. Hydrogen metabolism in the extreme thermophile *Thermotoga neapolitana*. *Int. J. Hydrogen Energy* **2010**, *35*, 2290–2295. [\[CrossRef\]](#)

59. Nuzzo, G.; Landi, S.; Esercizio, N.; Manzo, E.; Fontana, A.; D'Ippolito, G. Capnophilic lactic fermentation from *Thermotoga neapolitana*: A resourceful pathway to obtain almost enantiopure L-lactic acid. *Fermentation* **2019**, *5*, 34. [\[CrossRef\]](#)
60. d'Ippolito, G.; Landi, S.; Esercizio, N.; Lanzilli, M.; Vastano, M.; Dipasquale, L.; Pradhan, N.; Fontana, A. CO₂-Induced Transcriptional Reorganization: Molecular Basis of Capnophilic Lactic Fermentation in *Thermotoga neapolitana*. *Front. Microbiol.* **2020**, *11*. [\[CrossRef\]](#) [\[PubMed\]](#)
61. Xu, H.; Han, D.; Xu, Z. Expression of Heterologous Cellulases in *Thermotoga* sp. Strain RQ2. *BioMed Res. Int.* **2014**, *2015*, 304523. [\[CrossRef\]](#)
62. Balk, M.; Weijma, J.; Stams, A.J.M. *Thermotoga lettingae* sp. nov., a novel thermophilic, methanol-degrading bacterium isolated from a thermophilic anaerobic reactor. *Int. J. Syst. Evol. Microbiol.* **2002**, *52*, 1361–1368. [\[CrossRef\]](#) [\[PubMed\]](#)
63. Huber, R.; Langworthy, T.A.; König, H.; Thomm, M.; Woese, C.R.; Sleytr, U.B.; Stetter, K.O. *Thermotoga maritima* sp. nov. represents a new genus of unique extremely thermophilic eubacteria growing up to 90 °C. *Arch. Microbiol.* **1986**, *144*, 324–333. [\[CrossRef\]](#)
64. Jannasch, H.W.; Huber, R.; Belkin, S.; Stetter, K.O. *Thermotoga neapolitana* sp. nov. of the extremely thermophilic, eubacterial genus *Thermotoga*. *Arch. Microbiol.* **1988**, *150*, 103–104. [\[CrossRef\]](#)
65. Windberger, E.; Huber, R.; Trincone, A.; Fricke, H.; Stetter, K.O. *Thermotoga thermarum* sp. nov. and *Thermotoga neapolitana* occurring in African continental solfataric springs. *Arch. Microbiol.* **1989**, *151*, 506–512. [\[CrossRef\]](#)
66. Jeanthon, C.; Reysenbach, A.L.; L'Haridon, S.; Gambacorta, A.; Pace, N.R.; Glénat, P.; Prieur, D. *Thermotoga subterranea* sp. nov., a new thermophilic bacterium isolated from a continental oil reservoir. *Arch. Microbiol.* **1995**, *164*, 91–97. [\[CrossRef\]](#)
67. Ravot, G.; Magot, M.; Fardeau, M.L.; Patel, B.K.C.; Prensier, G.; Egan, A.; Garcia, J.L.; Ollivier, B. *Thermotoga elfii* sp. nov., a novel thermophilic bacterium from an African oil-producing well. *Int. J. Syst. Bacteriol.* **1995**, *45*, 308–314. [\[CrossRef\]](#)
68. Fardeau, M.-L.; Ollivier, I.; Patel, B.; Magot, M.; Thomas, P.; Rimbault, A.; Rocchiccioli, F.; Garcia, J. *Thermotoga hypogea* sp. nov., a Xylanolytic, Thermophilic Bacterium from an Oil-Producing Well. *Int. J. Syst. Evol. Microbiol.* **1997**, *147*, 51–56. [\[CrossRef\]](#) [\[PubMed\]](#)
69. Takahata, Y.; Nishijima, M.; Hoaki, T.; Maruyama, T. *Thermotoga petrophila* sp. nov. and *Thermotoga naphthophila* sp. nov., two hyperthermophilic bacteria from the Kubiki oil reservoir in Niigata, Japan. *Int. J. Syst. Evol. Microbiol.* **2001**, *51*, 1901–1909. [\[CrossRef\]](#) [\[PubMed\]](#)
70. Nguyen, T.A.D.; Han, S.J.; Kim, J.P.; Kim, M.S.; Sim, S.J. Hydrogen production of the hyperthermophilic eubacterium, *Thermotoga neapolitana* under N₂ sparging condition. *Bioresour. Technol.* **2010**, *101*, S38–S41. [\[CrossRef\]](#) [\[PubMed\]](#)
71. Ngo, T.A.; Sim, S.J. Dark fermentation of hydrogen from waste glycerol using hyperthermophilic eubacterium *Thermotoga neapolitana*. *Environ. Prog. Sustain. Energy* **2012**, *31*, 466–473. [\[CrossRef\]](#)
72. Ngo, T.A.; Kim, M.S.; Sim, S.J. Thermophilic hydrogen fermentation using *Thermotoga neapolitana* DSM 4359 by fed-batch culture. *Int. J. Hydrogen Energy* **2011**, *36*, 14014–14023. [\[CrossRef\]](#)
73. Pradhan, N.; d'Ippolito, G.; Dipasquale, L.; Esposito, G.; Panico, A.; Lens, P.N.L.; Fontana, A. Simultaneous synthesis of lactic acid and hydrogen from sugars via capnophilic lactic fermentation by *Thermotoga neapolitana* cf *capnolactica*. *Biomass Bioenergy* **2019**, *125*, 17–22. [\[CrossRef\]](#)
74. Woodward, J.; Heyer, N.I.; Getty, J.P.; Neill, H.M.O.; Pinkhassik, E.; Evans, B.R. Efficient Hydrogen Production Using Enzymes of the Pentose Phosphate Pathway. In Proceedings of the 2002 U.S. DOE Hydrogen Program Review, Golden, CO, USA, 6–10 May 2002; pp. 1–12.
75. De Vrije, T.; Budde, M.A.W.; Lips, S.J.; Bakker, R.R.; Mars, A.E.; Claassen, P.A.M. Hydrogen production from carrot pulp by the extreme thermophiles *Caldicellulosiruptor saccharolyticus* and *Thermotoga neapolitana*. *Int. J. Hydrogen Energy* **2010**, *35*, 13206–13213. [\[CrossRef\]](#)
76. Frock, A.D.; Gray, S.R.; Kelly, R.M. Hyperthermophilic *Thermotoga* species differ with respect to specific carbohydrate transporters and glycoside hydrolases. *Appl. Environ. Microbiol.* **2012**. [\[CrossRef\]](#)
77. Abreu, A.A.; Tavares, F.; Alves, M.M.; Pereira, M.A. Boosting dark fermentation with co-cultures of extreme thermophiles for biohythane production from garden waste. *Bioresour. Technol.* **2016**, *219*, 132–138. [\[CrossRef\]](#)
78. Yu, X.; Drapcho, C.M.; Drapcho, C.M. Hydrogen Production by the Hyperthermophilic Bacterium *Thermotoga neapolitana* using Agricultural-Based Carbon and Nitrogen Sources. *Biol. Eng. Trans.* **2011**, *4*, 101–112. [\[CrossRef\]](#)
79. Vargas, M.; Noll, K.M. Catabolite repression in the hyperthermophilic bacterium *Thermotoga neapolitana* is independent of cAMP. *Microbiology* **1996**, *142*, 139–144. [\[CrossRef\]](#) [\[PubMed\]](#)
80. Nguyen, T.N.; Ejaz, A.D.; Brancieri, M.A.; Mikula, A.M.; Nelson, K.E.; Gill, S.R.; Noll, K.M. Whole-genome expression profiling of *Thermotoga maritima* in response to growth on sugars in a chemostat. *J. Bacteriol.* **2004**, *186*, 4824–4828. [\[CrossRef\]](#) [\[PubMed\]](#)
81. Nguyen, T.A.D.; Han, S.J.; Kim, J.P.; Kim, M.S.; Oh, Y.K.; Sim, S.J. Hydrogen production by the hyperthermophilic eubacterium, *Thermotoga neapolitana*, using cellulose pretreated by ionic liquid. *Int. J. Hydrogen Energy* **2008**, *33*, 5161–5168. [\[CrossRef\]](#)
82. Nguyen, T.A.D.; Pyo Kim, J.; Sun Kim, M.; Kwan Oh, Y.; Sim, S.J. Optimization of hydrogen production by hyperthermophilic eubacteria, *Thermotoga maritima* and *Thermotoga neapolitana* in batch fermentation. *Int. J. Hydrogen Energy* **2008**, *33*, 1483–1488. [\[CrossRef\]](#)
83. Ngo, T.A.; Nguyen, T.H.; Bui, H.T.V. Thermophilic fermentative hydrogen production from xylose by *Thermotoga neapolitana* DSM 4359. *Renew. Energy* **2012**, *37*, 174–179. [\[CrossRef\]](#)
84. Singh, R.; White, D.; Demirel, Y.; Kelly, R.; Noll, K.; Blum, P. Uncoupling fermentative synthesis of molecular hydrogen from biomass formation in *Thermotoga maritima*. *Appl. Environ. Microbiol.* **2018**, *84*. [\[CrossRef\]](#)

85. Van Niel, E.W.J.; Budde, M.A.W.; De Haas, G.; Van der Wal, F.J.; Claassen, P.A.M.; Stams, A.J.M. Distinctive properties of high hydrogen producing extreme thermophiles, *Caldicellulosiruptor saccharolyticus* and *Thermotoga elfii*. *Int. J. Hydrogen Energy* **2002**, *27*, 1391–1398. [CrossRef]
86. Benedetti, M.; Vecchi, V.; Betterle, N.; Natali, A.; Bassi, R.; Dall'Osto, L. Design of a highly thermostable hemicellulose-degrading blend from *Thermotoga neapolitana* for the treatment of lignocellulosic biomass. *J. Biotechnol.* **2019**, *296*, 42–52. [CrossRef]
87. Paritosh, K.; Kushwaha, S.K.; Yadav, M.; Pareek, N.; Chawade, A.; Vivekanand, V. Food Waste to Energy: An Overview of Sustainable Approaches for Food Waste Management and Nutrient Recycling. Available online: <https://www.hindawi.com/journals/bmri/2017/2370927/> (accessed on 15 April 2020).
88. Yun, Y.; Lee, M.; Im, S.; Marone, A.; Trably, E.; Shin, S.; Kim, M.; Cho, S.; Kim, D. Bioresource Technology Biohydrogen production from food waste: Current status, limitations, and future perspectives. *Bioresour. Technol.* **2018**, *248*, 79–87. [CrossRef]
89. Garcia-Peña, E.I.; Parameswaran, P.; Kang, D.W.; Canul-Chan, M.; Krajmalnik-Brown, R. Anaerobic digestion and co-digestion processes of vegetable and fruit residues: Process and microbial ecology. *Bioresour. Technol.* **2011**, *102*, 9447–9455. [CrossRef]
90. Bouallagui, H.; Lahdheb, H.; Ben Romdan, E.; Rachdi, B.; Hamdi, M. Improvement of fruit and vegetable waste anaerobic digestion performance and stability with co-substrates addition. *J. Environ. Manag.* **2009**, *90*, 1844–1849. [CrossRef]
91. Thanikal, J. Anaerobic Co-digestion of fruit and vegetable waste: Bio-reactor performance. *World. J. Exp. Biosci.* **2015**, *3*, 1–17.
92. Bao, B.; Chang, K.C. Carrot Pulp Chemical Composition, Color, and Water-holding Capacity as Affected by Blanching. *J. Food Sci.* **1994**, *59*, 1159–1161. [CrossRef]
93. Claassen, P.A.; Budde, M.A.; van Nooren, G.E.; Hoekema, S.; Hazewinkel, J.H.O.; van Gorenstestijn, J.W.; de Vrije, G.J. Biological hydrogen production from agro-food-by-products. In Proceedings of the Total Food: Exploiting Co-Products, Norwich, UK, 25–28 April 2004.
94. Djomo, S.N.; Humbert, S. Dagnija Blumberga Life cycle assessment of hydrogen produced from potato steam peels. *Int. J. Hydrogen Energy* **2008**, *33*, 3067–3072. [CrossRef]
95. Mars, A.E.; Veuskens, T.; Budde, M.A.W.; Van Doeveren, P.F.N.M.; Lips, S.J.; Bakker, R.R.; De Vrije, T.; Claassen, P.A.M. Biohydrogen production from untreated and hydrolyzed potato steam peels by the extreme thermophiles *Caldicellulosiruptor saccharolyticus* and *Thermotoga neapolitana*. *Int. J. Hydrogen Energy* **2010**, *35*, 7730–7737. [CrossRef]
96. Benítez, V.; Mollá, E.; Martín-Cabrejas, M.A.; Aguilera, Y.; López-Andréu, F.J.; Cools, K.; Terry, L.A.; Esteban, R.M. Characterization of Industrial Onion Wastes (*Allium cepa* L.): Dietary Fibre and Bioactive Compounds. *Plant. Foods Hum. Nutr.* **2011**, *66*, 48–57. [CrossRef] [PubMed]
97. Romano, R.T.; Zhang, R. Anaerobic digestion of onion residuals using a mesophilic Anaerobic Phased Solids Digester. *Biomass Bioenergy* **2011**, *35*, 4174–4179. [CrossRef]
98. Milquez-Sanabria, H.; Blanco-Cocom, L.; Alzate-Gaviria, L. A fast linear predictive adaptive model of packed bed coupled with UASB reactor treating onion waste to produce biofuel. *Microb. Cell Fact.* **2016**, *15*, 1–10. [CrossRef] [PubMed]
99. Sharma, K.; Mahato, N.; Nile, S.H.; Lee, E.T.; Lee, Y.R. Economical and environmentally-friendly approaches for usage of onion (*Allium cepa* L.) waste. *Food Funct.* **2016**, *7*, 3354–3369. [CrossRef] [PubMed]
100. Kadam, K.L.; Forrest, L.H.; Jacobson, W.A. Rice straw as a lignocellulosic resource: Collection, processing, transportation, and environmental aspects. *Biomass Bioenergy* **2000**, *18*, 369–389. [CrossRef]
101. Kim, S.; Dale, B.E. Global potential bioethanol production from wasted crops and crop residues. *Biomass Bioenergy* **2004**, *26*, 361–375. [CrossRef]
102. Nguyen, T.A.D.; Kim, K.R.; Kim, M.S.; Sim, S.J. Thermophilic hydrogen fermentation from Korean rice straw by *Thermotoga neapolitana*. *Int. J. Hydrogen Energy* **2010**, *35*, 13392–13398. [CrossRef]
103. Chang, A.C.C.; Tu, Y.H.; Huang, M.H.; Lay, C.H.; Lin, C.Y. Hydrogen production by the anaerobic fermentation from acid hydrolyzed rice straw hydrolysate. *Int. J. Hydrogen Energy* **2011**, *36*, 14280–14288. [CrossRef]
104. He, L.; Huang, H.; Lei, Z.; Liu, C.; Zhang, Z. Enhanced hydrogen production from anaerobic fermentation of rice straw pretreated by hydrothermal technology. *Bioresour. Technol.* **2014**, *171*, 145–151. [CrossRef]
105. Wang, D.; Ai, P.; Yu, L.; Tan, Z.; Zhang, Y. Comparing the hydrolysis and biogas production performance of alkali and acid pretreatments of rice straw using two-stage anaerobic fermentation. *Biosyst. Eng.* **2015**, *132*, 47–55. [CrossRef]
106. Kim, T.H.; Lee, Y.Y. Pretreatment of corn stover by soaking in aqueous ammonia. *Appl. Biochem. Biotechnol. Part A Enzym. Eng. Biotechnol.* **2005**, *124*, 1119–1131. [CrossRef]
107. Wyman, C.E.; Dale, B.E.; Elander, R.T.; Holtzapple, M.; Ladisch, M.R.; Lee, Y.Y. Coordinated development of leading biomass pretreatment technologies. *Bioresour. Technol.* **2005**, *96*, 1959–1966. [CrossRef]
108. Ren, N.; Li, J.; Li, B.; Wang, Y.; Liu, S. Biohydrogen production from molasses by anaerobic fermentation with a pilot-scale bioreactor system. *Int. J. Hydrogen Energy* **2006**, *31*, 2147–2157. [CrossRef]
109. Li, J.; Li, B.; Zhu, G.; Ren, N.; Bo, L.; He, J. Hydrogen production from diluted molasses by anaerobic hydrogen producing bacteria in an anaerobic baffled reactor (ABR). *Int. J. Hydrogen Energy* **2007**, *32*, 3274–3283. [CrossRef]
110. Aceves-Lara, C.A.; Latrille, E.; Bernet, N.; Buffière, P.; Steyer, J.P. A pseudo-stoichiometric dynamic model of anaerobic hydrogen production from molasses. *Water Res.* **2008**, *42*, 2539–2550. [CrossRef] [PubMed]
111. Wang, X.; Jin, B. Process optimization of biological hydrogen production from molasses by a newly isolated *Clostridium butyricum* W5. *J. Biosci. Bioeng.* **2009**, *107*, 138–144. [CrossRef] [PubMed]

112. Scoma, A.; Coma, M.; Kerckhof, F.M.; Boon, N.; Rabaey, K. Efficient molasses fermentation under high salinity by inocula of marine and terrestrial origin. *Biotechnol. Biofuels* **2017**, *10*, 1–17. [\[CrossRef\]](#) [\[PubMed\]](#)
113. Frascari, D.; Cappelletti, M.; Mendes, J.D.S.; Alberini, A.; Scimonelli, F.; Manfreda, C.; Longanesi, L.; Zannoni, D.; Pinelli, D.; Fedi, S. A kinetic study of biohydrogen production from glucose, molasses and cheese whey by suspended and attached cells of *Thermotoga neapolitana*. *Bioresour. Technol.* **2013**, *147*, 553–561. [\[CrossRef\]](#)
114. Carvalho, F.; Prazeres, A.R.; Rivas, J. Cheese whey wastewater: Characterization and treatment. *Sci. Total Environ.* **2013**, *445–446*, 385–396. [\[CrossRef\]](#)
115. Lopes, A.C.A.; Eda, S.H.; Andrade, R.P.; Amorim, J.C.; Duarte, W.F. New Alcoholic Fermented Beverages—Potentials and Challenges. *Fermented Beverages* **2019**, 577–603. [\[CrossRef\]](#)
116. Zotta, T.; Solieri, L.; Iacumin, L.; Picozzi, C.; Gullo, M. Valorization of cheese whey using microbial fermentations. *Appl. Microbiol. Biotechnol.* **2020**, *104*, 2749–2764. [\[CrossRef\]](#)
117. Ren, N.; Wang, A.; Cao, G.; Xu, J.; Gao, L. Bioconversion of lignocellulosic biomass to hydrogen: Potential and challenges. *Biotechnol. Adv.* **2009**, *27*, 1051–1060. [\[CrossRef\]](#)
118. Alvira, P.; Tomás-Pejó, E.; Ballesteros, M.; Negro, M.J. Pretreatment technologies for an efficient bioethanol production process based on enzymatic hydrolysis: A review. *Bioresour. Technol.* **2010**, *101*, 4851–4861. [\[CrossRef\]](#)
119. Isikgor, F.H.; Becer, C.R. Lignocellulosic biomass: A sustainable platform for the production of bio-based chemicals and polymers. *Polym. Chem.* **2015**, *6*, 4497–4559. [\[CrossRef\]](#)
120. Kumar, G.; Bakonyi, P.; Periyasamy, S.; Kim, S.H.; Nemestóthy, N.; Bélafi-Bakó, K. Lignocellulose biohydrogen: Practical challenges and recent progress. *Renew. Sustain. Energy Rev.* **2015**, *44*, 728–737. [\[CrossRef\]](#)
121. Sawatdeenarunat, C.; Surendra, K.C.; Takara, D.; Oechsner, H.; Khanal, S.K. Anaerobic digestion of lignocellulosic biomass: Challenges and opportunities. *Bioresour. Technol.* **2015**, *178*, 178–186. [\[CrossRef\]](#) [\[PubMed\]](#)
122. Fan, Y.; Klemes, J.J.; Lee, C.T. Pre- and post-treatment assessment for the anaerobic digestion of lignocellulosic waste: P-graph. *Chem. Eng. Trans.* **2018**, *63*, 1–6. [\[CrossRef\]](#)
123. Van Fan, Y.; Klemes, J.J.; Perry, S.; Lee, C.T. Anaerobic digestion of lignocellulosic waste: Environmental impact and economic assessment. *J. Environ. Manag.* **2019**, *231*, 352–363. [\[CrossRef\]](#) [\[PubMed\]](#)
124. Soares, J.F.; Confortin, T.C.; Todero, I.; Mayer, F.D.; Mazutti, M.A. Dark fermentative biohydrogen production from lignocellulosic biomass: Technological challenges and future prospects. *Renew. Sustain. Energy Rev.* **2020**, *117*. [\[CrossRef\]](#)
125. Wyman, V.; Henriquez, J.; Palma, C.; Carvajal, A. Lignocellulosic waste valorisation strategy through enzyme and biogas production. *Bioresour. Technol.* **2018**, *247*, 402–411. [\[CrossRef\]](#) [\[PubMed\]](#)
126. Chakraborty, D.; Shelvapulle, S.; Reddy, K.R.; Kulkarni, R.V.; Puttaiahgowda, Y.M.; Naveen, S.; Raghu, A.V. Integration of biological pre-treatment methods for increased resource replace resource with energy recovery from paper and pulp biosludge. *J. Microbiol. Methods* **2019**, *160*, 93–100. [\[CrossRef\]](#)
127. Vasco-Correa, J.; Khanal, S.; Manandhar, A.; Shah, A. Anaerobic digestion for bioenergy production: Global status, environmental and techno-economic implications, and government policies. *Bioresour. Technol.* **2018**, *247*, 1015–1026. [\[CrossRef\]](#)
128. Olsson, L.; Hahn-Hägerdal, B. Fermentation of lignocellulosic hydrolysates for ethanol production. *Enzym. Microb. Technol.* **1996**, *18*, 312–331. [\[CrossRef\]](#)
129. De Vrije, T.; De Haas, G.; Tan, G.B.; Keijsers, E.R.P.; Claassen, P.A.M. Pretreatment of *Miscanthus* for hydrogen production by *Thermotoga elfii*. *Int. J. Hydrogen Energy* **2002**, *27*, 1381–1390. [\[CrossRef\]](#)
130. De Vrije, T.; Bakker, R.R.; Budde, M.A.W.; Lai, M.H.; Mars, A.E.; Claassen, P.A.M. Efficient hydrogen production from the lignocellulosic energy crop *Miscanthus* by the extreme thermophilic bacteria *Caldicellulosiruptor saccharolyticus* and *Thermotoga neapolitana*. *Biotechnol. Biofuels* **2009**, *2*. [\[CrossRef\]](#)
131. Akyol, Ç.; Ince, O.; Bozan, M.; Ozbayram, E.G.; Ince, B. Biological pretreatment with *Trametes versicolor* to enhance methane production from lignocellulosic biomass: A metagenomic approach. *Ind. Crop. Prod.* **2019**, *140*. [\[CrossRef\]](#)
132. Amend, J.P.; Shock, E.L. Energetics of overall metabolic reactions of thermophilic and hyperthermophilic Archaea and Bacteria. *Fems Microbiol. Rev.* **2001**, *25*, 175–243. [\[CrossRef\]](#)
133. Arnoult, S.; Brancourt-Hulmel, M. A Review on *Miscanthus* Biomass Production and Composition for Bioenergy Use: Genotypic and Environmental Variability and Implications for Breeding. *BioEnergy Res.* **2014**, *8*, 502–526. [\[CrossRef\]](#)
134. Abreu, A.A.; Tavares, F.; Alves, M.M.; Cavaleiro, A.J.; Pereira, M.A. Garden and food waste co-fermentation for biohydrogen and biomethane production in a two-step hyperthermophilic-mesophilic process. *Bioresour. Technol.* **2019**, *278*, 180–186. [\[CrossRef\]](#)
135. Moretti, P.; Moraes de Araujo, J.; Borges de Castilhos, A.; Buffière, P.; Gourdon, R.; Bayard, R. Characterization of municipal biowaste categories for their capacity to be converted into a feedstock aqueous slurry to produce methane by anaerobic digestion. *Sci. Total Environ.* **2020**, *716*, 137084. [\[CrossRef\]](#) [\[PubMed\]](#)
136. Boldrin, A.; Christensen, T.H. Seasonal generation and composition of garden waste in Aarhus (Denmark). *Waste Manag.* **2010**, *30*, 551–557. [\[CrossRef\]](#)
137. Kadar, Z.; Vrije, T.; Budde, M.A.W.; Szengyel, Z.; Réczey, K.; Claassen, P.A. Hydrogen Production from Paper Sludge Hydrolysate. *Appl. Biochem. Biotechnol.* **2003**, *105–108*, 557–566. [\[CrossRef\]](#)
138. Logeswaran, V.; Ramakrishna, G. Waste Paper Sludge Ash-State of art. *Int. J. Innov. Technol. Explor. Eng.* **2019**, *8*, 2333–2338. [\[CrossRef\]](#)

139. Lin, Y.; Wu, S.; Wang, D. Hydrogen-methane production from pulp & paper sludge and food waste by mesophilic-thermophilic anaerobic co-digestion. *Int. J. Hydrogen Energy* **2013**, *38*, 15055–15062. [\[CrossRef\]](#)
140. Nguyen, T.A.D.; Kim, K.R.; Nguyen, M.T.; Kim, M.S.; Kim, D.; Sim, S.J. Enhancement of fermentative hydrogen production from green algal biomass of *Thermotoga neapolitana* by various pretreatment methods. *Int. J. Hydrogen Energy* **2010**, *35*, 13035–13040. [\[CrossRef\]](#)
141. Dipasquale, L.; D'Ippolito, G.; Gallo, C.; Vella, F.M.; Gambacorta, A.; Picariello, G.; Fontana, A. Hydrogen production by the thermophilic eubacterium *Thermotoga neapolitana* from storage polysaccharides of the CO₂-fixing diatom *Thalassiosira weissflogii*. *Int. J. Hydrogen Energy* **2012**, *37*, 12250–12257. [\[CrossRef\]](#)
142. Santibáñez, C.; Varnero, M.T.; Bustamante, M. Residual glycerol from biodiesel Manufacturing, waste or potential source of Bioenergy: A review. *Chil. J. Agric. Res.* **2011**, *71*, 469–475. [\[CrossRef\]](#)
143. Safaei, H.R.; Shekouhy, M.; Rahmanpur, S.; Shirinfeshan, A. Glycerol as a biodegradable and reusable promoting medium for the catalyst-free one-pot three component synthesis of 4H-pyrans. *Green Chem.* **2012**, *14*, 1696–1704. [\[CrossRef\]](#)
144. Yang, F.; Hanna, M.A.; Sun, R. Value-added uses for crude glycerol—A byproduct of biodiesel production. *Biotechnol. Biofuels* **2012**, *5*, 13. [\[CrossRef\]](#)
145. Pachauri, N.; He, B. Value-added Utilization of Crude Glycerol from Biodiesel Production: A Survey of Current Research Activities. In Proceedings of the 2006 ASABE Annual International Meeting, Portland, OR, USA, 9–12 July 2006; Volume 0300.
146. Thompson, J.C.; He, B.B. Characterization of Crude Glycerol From Biodiesel Production from Multiple Feedstocks. *Appl. Eng. Agric.* **2006**, *22*, 261–265. [\[CrossRef\]](#)
147. Da Silva, G.P.; Mack, M.; Contiero, J. Glycerol: A promising and abundant carbon source for industrial microbiology. *Biotechnol. Adv.* **2009**, *27*, 30–39. [\[CrossRef\]](#) [\[PubMed\]](#)
148. Pyle, D.J. Use of Biodiesel-Derived Crude Glycerol for the Production of Omega-3 Polyunsaturated Fatty Acids by the Microalga *Schizochytrium Limacinum*. Ph.D. Thesis, Virginia Polytechnic Institute and State University, Blacksburg, VA, USA, 2008.
149. Hansen, C.F.; Hernandez, A.; Mullan, B.P.; Moore, K.; Trezona-Murray, M.; King, R.H.; Pluske, J.R. A chemical analysis of samples of crude glycerol from the production of biodiesel in Australia, and the effects of feeding crude glycerol to growing-finishing pigs on performance, plasma metabolites and meat quality at slaughter. *Anim. Prod. Sci.* **2009**, *49*, 154–161. [\[CrossRef\]](#)
150. Siles López, J.Á.; de los Martín Santos, M.Á.; Chica Pérez, A.F.; Martín Martín, A. Anaerobic digestion of glycerol derived from biodiesel manufacturing. *Bioresour. Technol.* **2009**, *100*, 5609–5615. [\[CrossRef\]](#)
151. Ngo, T.A.; Kim, M.S.; Sim, S.J. High-yield biohydrogen production from biodiesel manufacturing waste by *Thermotoga neapolitana*. *Int. J. Hydrogen Energy* **2011**, *36*, 5836–5842. [\[CrossRef\]](#)
152. Dasari, M. Crude Glycerol Potential Described. *Feedstuffs*, 15 October 2007; 1–3.
153. Maru, B.T.; Bielen, A.A.M.; Kengen, S.W.M.; Constantí, M.; Medina, F. Biohydrogen Production from Glycerol using *Thermotoga* spp. *Energy Procedia* **2012**, *29*, 300–307. [\[CrossRef\]](#)
154. Maru, B.T.; Bielen, A.A.M.; Constantí, M.; Medina, F.; Kengen, S.W.M. Glycerol fermentation to hydrogen by *Thermotoga maritima*: Proposed pathway and bioenergetic considerations. *Int. J. Hydrogen Energy* **2013**, *38*, 5563–5572. [\[CrossRef\]](#)
155. Nelson, K.E.; Clayton, R.A.; Gill, S.R.; Gwinn, M.L.; Dodson, R.J.; Haft, D.H.; Hickey, E.K.; Peterson, J.D.; Nelson, W.C.; Ketchum, K.A.; et al. Evidence for lateral gene transfer between archaea and bacteria from genome sequence of *Thermotoga maritima*. *Nature* **1999**, *399*, 323–329. [\[CrossRef\]](#)
156. Van Ooteghem, S.A.; Jones, A.; Van Der Lelie, D.; Dong, B.; Mahajan, D. H₂ production and carbon utilization by *Thermotoga neapolitana* under anaerobic and microaerobic growth conditions. *Biotechnol. Lett.* **2004**, *26*, 1223–1232. [\[CrossRef\]](#) [\[PubMed\]](#)
157. Schröder, C.; Selig, M.; Schönheit, P. Glucose fermentation to acetate, CO₂ and H₂ in the anaerobic hyperthermophilic eubacterium *Thermotoga maritima*: Involvement of the Embden-Meyerhof pathway. *Arch. Microbiol.* **1994**, *161*, 460–470. [\[CrossRef\]](#)
158. Schut, G.J.; Adams, M.W.W. The iron-hydrogenase of *Thermotoga maritima* utilizes ferredoxin and NADH synergistically: A new perspective on anaerobic hydrogen production. *J. Bacteriol.* **2009**, *191*, 4451–4457. [\[CrossRef\]](#) [\[PubMed\]](#)
159. Khan, M.I.; Shin, J.H.; Kim, J.D. The promising future of microalgae: Current status, challenges, and optimization of a sustainable and renewable industry for biofuels, feed, and other products. *Microb. Cell Fact.* **2018**, *17*, 36. [\[CrossRef\]](#) [\[PubMed\]](#)
160. Miao, X.; Wu, Q. Biodiesel production from heterotrophic microalgal oil. *Bioresour. Technol.* **2006**, *97*, 841–846. [\[CrossRef\]](#)
161. Ramachandra, T.V.; Mahapatra, D.M.; Karthick, B.; Gordon, R. Milking diatoms for sustainable energy: Biochemical engineering versus gasoline-secreting diatom solar panels. *Ind. Eng. Chem. Res.* **2009**, *48*, 8769–8788. [\[CrossRef\]](#)
162. Latif, H.; Lerman, J.A.; Portnoy, V.A.; Tarasova, Y.; Nagarajan, H.; Schrimpe-Rutledge, A.C.; Smith, R.D.; Adkins, J.N.; Lee, D.-H.; Qiu, Y.; et al. The Genome Organization of *Thermotoga maritima* Reflects Its Lifestyle. *Plos Genet.* **2013**, *9*, e1003485. [\[CrossRef\]](#)
163. Rodionov, D.A.; Rodionova, I.A.; Li, X.; Ravcheev, D.A.; Tarasova, Y.; Portnoy, V.A.; Zengler, K.; Osterman, A.L. Transcriptional regulation of the carbohydrate utilization network in *Thermotoga maritima*. *Front. Microbiol.* **2013**, *4*, 244. [\[CrossRef\]](#) [\[PubMed\]](#)
164. Göker, M.; Spring, S.; Scheuner, C.; Anderson, I.; Zeytun, A.; Nolan, M.; Lucas, S.; Tice, H.; Del Rio, T.G.; Cheng, J.F.; et al. Genome sequence of the *Thermotoga thermarum* type strain (LA3T) from an African solfataric spring. *Stand. Genom. Sci.* **2015**, *9*, 1105–1117. [\[CrossRef\]](#) [\[PubMed\]](#)
165. Ravcheev, D.A.; Khoroshkin, M.S.; Laikova, O.N.; Tsoy, O.V.; Sernova, N.V.; Petrova, S.A.; Rakhmaninova, A.B.; Novichkov, P.S.; Gelfand, M.S.; Rodionov, D.A. Comparative genomics and evolution of regulons of the LacI-family transcription factors. *Front. Microbiol.* **2014**, *5*, 294. [\[CrossRef\]](#) [\[PubMed\]](#)

166. Xu, Z.; Puranik, R.; Hu, J.; Xu, H.; Han, D. Complete genome sequence of *Thermotoga* sp. strain RQ7. *Stand. Genom. Sci.* **2017**, *12*, 62. [[CrossRef](#)]
167. Beaucamp, N.; Hofmann, A.; Kellerer, B.; Jaenicke, R. Dissection of the gene of the bifunctional PGK-TIM fusion protein from the hyperthermophilic bacterium *Thermotoga maritima*: Design and characterization of the separate triosephosphate isomerase. *Protein Sci.* **1997**, *6*, 2159–2165. [[CrossRef](#)]
168. Shi, H.; Huang, Y.; Zhang, Y.; Li, W.; Li, X.; Wang, F. High-level expression of a novel thermostable and mannose-tolerant β -mannosidase from *Thermotoga thermarum* DSM 5069 in *Escherichia coli*. *Bmc Biotechnol.* **2013**, *13*. [[CrossRef](#)]
169. Martín Del Campo, J.S.; Chun, Y.; Kim, J.E.; Patiño, R.; Zhang, Y.H.P. Discovery and characterization of a novel ATP/polyphosphate xylulokinase from a hyperthermophilic bacterium *Thermotoga maritima*. *J. Ind. Microbiol. Biotechnol.* **2013**, *40*, 661–669. [[CrossRef](#)]
170. Fatima, B.; Aftab, M.N.; Haq, I.U. Cloning, purification, and characterization of xylose isomerase from *Thermotoga naphthophila* RKU-10. *J. Basic Microbiol.* **2016**, *56*, 949–962. [[CrossRef](#)]
171. Latif, H.; Sahin, M.; Tarasova, J.; Tarasova, Y.; Portnoy, V.A.; Nogales, J.; Zengler, K. Adaptive evolution of *Thermotoga maritima* reveals plasticity of the ABC transporter network. *Appl. Environ. Microbiol.* **2015**, *81*, 5477–5485. [[CrossRef](#)]
172. Xu, W.; Zhang, W.; Zhang, T.; Jiang, B.; Mu, W. l-Rhamnose isomerase and its use for biotechnological production of rare sugars. *Appl. Microbiol. Biotechnol.* **2016**, *100*, 2985–2992. [[CrossRef](#)] [[PubMed](#)]
173. Bertoldo, C.; Antranikian, G. Starch-hydrolyzing enzymes from thermophilic archaea and bacteria. *Curr. Opin. Chem. Biol.* **2002**, *6*, 151–160. [[CrossRef](#)]
174. Botha, J.; Mizrachi, E.; Myburg, A.A.; Cowan, D.A. Carbohydrate active enzyme domains from extreme thermophiles: Components of a modular toolbox for lignocellulose degradation. *Extremophiles* **2018**, *22*, 1–12. [[CrossRef](#)] [[PubMed](#)]
175. Jung, S.; Lee, D.S.; Kim, Y.O.; Joshi, C.P.; Bae, H.J. Improved recombinant cellulase expression in chloroplast of tobacco through promoter engineering and 5' amplification promoting sequence. *Plant. Mol. Biol.* **2013**, *83*, 317–328. [[CrossRef](#)] [[PubMed](#)]

3. Effect of Cultivation Parameters on Fermentation and Hydrogen Production in the Phylum Thermotogae

Mariamichela Lanzilli ¹, **Nunzia Esercizio**¹, Marco Vastano¹, Zhaohui Xu², Genoveffa Nuzzo¹, Carmela Gallo¹, Emiliano Manzo¹, Angelo Fontana ^{1,2} and Giuliana d'Ippolito ^{1,*}

¹ Institute of Biomolecular Chemistry (ICB), Consiglio Nazionale delle Ricerche (CNR), Via Campi Flegrei 34, 80078 Pozzuoli, Italy

² Department of Biological Sciences, Bowling Green State University, Bowling Green, OH 43403, USA

* Correspondence: gdippolito@icb.cnr.it; Tel.: +39-0818675096

Citation:

Lanzilli, M.; **Esercizio, N.**; Vastano, M.; Xu, Z.; Nuzzo, G.; Gallo, C.; Manzo, E.; Fontana, A.; d'Ippolito, G. Effect of Cultivation Parameters on Fermentation and Hydrogen Production in the Phylum *Thermotogae*. *Int. J. Mol. Sci.* **2021**, *22*, 341.



Review

Effect of Cultivation Parameters on Fermentation and Hydrogen Production in the Phylum *Thermotogae*

Mariamichela Lanzilli ¹, Nunzia Esercizio ¹, Marco Vastano ¹, Zhaohui Xu ², Genoveffa Nuzzo ¹, Carmela Gallo ¹, Emiliano Manzo ¹, Angelo Fontana ¹ and Giuliana d'Ippolito ^{1,*}

¹ Istituto di Chimica Biomolecolare (ICB), CNR, Via Campi Flegrei 34, 80078 Pozzuoli, Napoli, Italy; mariamichelanzilli@gmail.com (M.L.); esercizionunzia@gmail.com (N.E.); marco.vastano@gmail.com (M.V.); nuzzo.genoveffa@icb.cnr.it (G.N.); carmen.gallo@icb.cnr.it (C.G.); emanzo@icb.cnr.it (E.M.); afontana@icb.cnr.it (A.F.)

² Department of Biological Sciences, Bowling Green State University, Bowling Green, OH 43403, USA; zxu@bgsu.edu

* Correspondence: gdippolito@icb.cnr.it; Tel.: +39-081-8675096

Abstract: The phylum *Thermotogae* is composed of a single class (*Thermotogae*), 4 orders (*Thermotogales*, *Kosmotogales*, *Petrotogales*, *Mesoaciditogales*), 5 families (*Thermatogaceae*, *Fervidobacteriaceae*, *Kosmotogaceae*, *Petrotogaceae*, *Mesoaciditogaceae*), and 13 genera. They have been isolated from extremely hot environments whose characteristics are reflected in the metabolic and phenotypic properties of the *Thermotogae* species. The metabolic versatility of *Thermotogae* members leads to a pool of high value-added products with application potentials in many industry fields. The low risk of contamination associated with their extreme culture conditions has made most species of the phylum attractive candidates in biotechnological processes. Almost all members of the phylum, especially those in the order *Thermotogales*, can produce bio-hydrogen from a variety of simple and complex sugars with yields close to the theoretical Thauer limit of 4 mol H₂/mol consumed glucose. Acetate, lactate, and L-alanine are the major organic end products. *Thermotogae* fermentation processes are influenced by various factors, such as hydrogen partial pressure, agitation, gas sparging, culture/headspace ratio, inoculum, pH, temperature, nitrogen sources, sulfur sources, inorganic compounds, metal ions, etc. Optimization of these parameters will help to fully unleash the biotechnological potentials of *Thermotogae* and promote their applications in industry. This article gives an overview of how these operational parameters could impact *Thermotogae* fermentation in terms of sugar consumption, hydrogen yields, and organic acids production.

Keywords: anaerobic bacteria; hydrogen yields; fermentation rate; organic acids; nitrogen; carbon dioxide



Citation: Lanzilli, M.; Esercizio, N.; Vastano, M.; Xu, Z.; Nuzzo, G.; Gallo, C.; Manzo, E.; Fontana, A.; d'Ippolito, G. Effect of Cultivation Parameters on Fermentation and Hydrogen Production in the Phylum *Thermotogae*. *Int. J. Mol. Sci.* **2021**, *22*, 341. <https://doi.org/10.3390/ijms22010341>

Received: 12 October 2020

Accepted: 23 December 2020

Published: 30 December 2020

Publisher's Note: MDPI stays neutral with regard to jurisdictional claims in published maps and institutional affiliations.



Copyright: © 2020 by the authors. Licensee MDPI, Basel, Switzerland. This article is an open access article distributed under the terms and conditions of the Creative Commons Attribution (CC BY) license (<https://creativecommons.org/licenses/by/4.0/>).

1. Introduction

The phylum *Thermotogae* is comprised of thermophilic, hyperthermophilic, mesophilic, and thermo-acidophilic anaerobic bacteria that originated from geothermally heated environments (Table 1) [1,2]. Recent phylogenetic analyses based on gene markers/core genome inferences, comparative genomics, and whole-genome relatedness have led to a taxonomic revision of the phylum, with a single class (*Thermotogae*), 4 orders (*Thermotogales*, *Kosmotogales*, *Petrotogales*, *Mesoaciditogales*), 5 families (*Thermatogaceae*, *Fervidobacteriaceae*, *Kosmotogaceae*, *Petrotogaceae*, *Mesoaciditogaceae*), and 13 genera, i.e., *Thermotoga* (T.) [3], *Pseudothermotoga* (Pseudot.) [2,4], *Fervidobacterium* (F.) [5], *Thermosiphon* (Ts.) [6], *Kosmotoga* (K.) [7], *Mesotoga* (Ms.) [8], *DeFluviitoga* (D.) [9], *Geotoga* (G.) and *Petrotoga* (P.) [10], *Marinitoga* (Mn.) [11], *Oceanotoga* (O.) [12], *Mesoaciditoga* (M.) [13], and *Athalassatoga* (A.) (Table 1) [2,4,14]. *Thermotogae* are able to grow under mesophilic (*Kosmotogales*; *Mesoaciditogales*, *Petrotogales*) and thermophilic conditions (*Thermotogales*), but most species have optimal growth temperatures in the range of 45–80 °C (Table 1). They are Gram-negative

bacteria, except for *D. tunisiensis*, which shows a positive result in Gram staining [9]. Apart from *K. shengliensis*, whose cells are in a coccoid form, *Thermotogae* cells are rod-shaped and encapsulated by a unique outer membrane, named “toga” [1,8,15]. Usually, the cells grow singly or in pairs, but it is also possible to observe chains surrounded by a unique toga [1,2]. Cell length is typically less than 20 µm, except for *F. gondwanense* and some members of the *Petrotoga* genus, whose cells can reach to 50 µm long (Table 1) [2,10]. Almost all species grow at neutral pH, and NaCl tolerances are high among *Geotoga*, *Oceanotoga*, and *Petrotoga* species (Table 1). Numerous studies have reported that members of the phylum can grow on both simple (e.g., glucose, galactose, fructose, lactose, maltose, mannose, sucrose) and complex carbohydrates (e.g., starch, glycogen, cellulose, keratin) (Table 1). Genes, transcriptional factors, and regulatory mechanisms driving the carbohydrates utilization have been identified for multiple members of the phylum [16–18]. ABC transporters for the uptake of a broad list of sugars have also been characterized [19–23].

All species of the phylum, except for *Mesotoga spp.*, have tremendous potentials in biotechnological production of H₂, especially the order *Thermotogales*, as their hydrogen yields are close to the theoretical maximum value (Thauer limit) of 4 mol H₂/mol glucose [1,4,24]. Acetate, lactate, and L-alanine are the major organic products of the sugar fermentation [1]. *Ms. prima* and *Ms. infera* produce mainly/only acetate from sugar utilization without H₂ formation [8,25–27]. Lactate is produced by *T. maritima*, *T. neapolitana*, and *Mn. camini* in variable quantities depending on growth conditions [11,28–31]. Other significant products include ethanol (has been measured in *Geotoga*, *Petrotoga*, *Kosmotoga*, and *Oceanotoga spp.*); isovalerate, isobutyrate, and/or propionate (have been measured in *Mn. camini* and *K. olearia*); L-glutamate, alpha-aminobutyrate, hydroxyphenyl-acetate, or phenylacetate (have been measured in *F. pennavorans*) [1,32] (Table 1). Among these fermentation end-products, lactic acid has been widely used in various industries such as food, cosmetic, pharmaceutical, and chemical industries, although its primary application is serving as the building block for the production of biodegradable polylactic acid (PLA) [33]. Ethanol is an important industrial commodity; it is used as a food additive and a renewable biofuel; it is also contained in many cosmetics, households, and sanitizer products [34]. Moreover, a plethora of thermostable enzymes, harbored by most of these bacteria, are valuable components for many industrial and biotechnological applications [17,35–44].

Hydrogen (H₂) is considered a green and sustainable alternative to traditional fossil fuels and is capable of mitigating greenhouse gas emissions. Using hydrogen in fuel cells or combustion engines produces heat and electricity with water as the only waste. As the current abiotic hydrogen production method is energy-consuming and still causes pollution, emphasis must be given to biological production of the energy from renewable sources [45,46]. Biological synthesis of H₂ can use a wide range of organic substrates as feedstocks, including agro-industrial wastes and algal biomass, and may operate under various environmental conditions [1,46–54]. In addition, high temperatures help to improve the solubilization of substrates, reduce fermentation time, and lower contamination risks [55]. Although hydrogen production by *Thermotoga* species is considered one of the most challenging biological systems, no application using pure *Thermotoga* cultures has been reported at the industrial scale.

Releasing hydrogen is an efficient way to dissipate excessive reductants generated during the fermentative conversion of organic substrates. The process is generally referred to as dark fermentation (DF) and is typically influenced by environmental conditions such as pH, cell growth rate, and hydrogen partial pressure [24,56,57].

According to the classical model of dark fermentation, theoretically up to 4 mol of hydrogen may be produced from each mole of glucose, which is converted to acetate and CO₂ (Thauer limit Figure 1) [24]. When hydrogen accumulates, pyruvate is diverted away from acetate production. In this case, excessive NADH from glycolysis is not used in the energetically favorable manner to synthesize acetate and H₂ but dissipated via synthesizing other metabolic products such as lactic acid, L-alanine, ethanol, butyrate, and valerate (Figure 1) [24]. Synthesis of hydrogen in *Thermotogae* species is performed

by the heterotrimeric [FeFe]-hydrogenase, an electron-bifurcating enzyme that couples the endergonic reduction of H^+ to hydrogen by NADH to the exergonic reduction of H^+ to hydrogen by reduced ferredoxin (Figure 1) [58]. Because the hydrogenase uses both NADH and reduced ferredoxin as electron donors, hydrogen yield is influenced by factors that affect both reductants.

The value of these bacteria in biotechnological processes is rising sharply since the discovery of the bifurcating hydrogenase and will probably be enhanced with a full elucidation of the molecular and biochemical properties of the processes. Despite decades of efforts in the development of genetic tools to engineer these species, only a few of thermostable selectable markers and genetic modifications with low stability are reported, which makes it still difficult to perform genetic modifications of these organisms [59–61]. However, these difficulties could be offset by their well-known susceptibility to mutations under environmental pressures [62,63].

In recent years, many researchers have been focusing on the optimization of fermentation performance towards the production of hydrogen and other target end-products [30,43,64–71].

Anaerobic fermentation in *Thermotogae* depends on many cultivation parameters such as hydrogen partial pressure, agitation, gas sparging, culture/headspace ratio, inoculum, pH, temperature, nitrogen sources, sulfur sources, inorganic compounds, and metal ions. The effect of each factor on H_2 yield, sugar consumption rate, and formation of biotechnologically interesting end-products are discussed here. Main data are also summarized in extensive tables, citing the most important studies, with the information on their cultivation systems (e.g., reactor type, incubation periods, batch vs. continuous modality).

Table 1. Physiological and metabolic properties of *Thermotoga* species. **YE:** Yeast extract; **BHI:** Brain heart infusion; **CMC:** Carboxymethylcellulose; **S⁰** = Elemental sulfur; **Thio:** Thiosulfate; **Cys:** Cysteine; **AA:** Acetic acid; **LA:** Lactic acid; **ALA:** Alanine; **EPS:** Exopolysaccharide; **AABA:** α -aminobutyrate; **EtOH:** Ethanol; **AQDS:** Anthraquinone-2,6-disulfonate; **But:** Butyrate; **Val:** Valerate; **Glu:** Glutamate; **BuOH:** Butanol; **iBut:** isobutyrate; **iVal:** isovalerate; **PPA:** Propionic Acid; **Gly:** Glycine; **Pro:** Proline; **Fo:** Formate; **HPA:** Hydroxyphenylacetate; **PA:** Phenylacetate; **3-IAA:** Indole-3-acetate; **2-MeBu:** 2-Methylbutyrate.

Genus	Species	Isolation	Temp. Range/ Optimal (°C)	pH Range/ Optimal	Cell Dimension (Long by Wide) (μ m)	Growth Substrates	NaCl Range/ Optimal (%)	Electron Acceptor	End Products	Ref.
<i>Thermotoga</i>	<i>Thermotoga petrophila</i>	Oil reservoir, Japan	47–88/ 80	5.2–9.0/ 7.0	2.0–7.0 by 0.7–1.0	YE, peptone, glucose, fructose, ribose, arabinose, sucrose, lactose, maltose, starch, cellulose	0.1–5.5/ 1.0	S ⁰ ; Thio	AA, LA, CO ₂ , H ₂	[72]
	<i>Thermotoga naphthophila</i>	Oil reservoir, Japan	48–86/ 80	5.4–9.0/ 7.0	2.0–7.0 by 0.8–1.2	YE, peptone, glucose, galactose, fructose, mannitol, ribose, arabinose, sucrose, lactose, maltose, starch	0.1–6.0/ 1.0	S ⁰ ; Thio	AA, LA, CO ₂ , H ₂	[72]
	<i>Thermotoga maritima</i>	Geothermal vent	55–90/ 80	5.5–9.0/ 6.5	1.5–11.0 by 0.6	ribose, xylose, glucose, sucrose, maltose, lactose, galactose, starch, glycogen	0.2–3.8/ 2.7	Fe (III) S ⁰ ; Thio	AA, LA, CO ₂ , H ₂ , ALA, EPS, AABA	[3]
	<i>Thermotoga profunda</i>	Hot spring, Japan	50–72/ 60	6.0–8.6/ 7.4	0.8–2.1 by 0.4	glucose, trehalose, cellobiose, arabinose, xylose, ribose, pyruvate	n. d	S ⁰ ; Thio	n. d	[73]
	<i>Thermotoga caldifontis</i>	Hot spring, Japan	55–85/ 70	6.0–8.6/ 7.4	1.2–3.5 by 0.5	glucose, maltose, trehalose, cellobiose, arabinose, xylose, ribose, pyruvate, starch	n. d	Thio	n. d	[73]
	<i>Thermotoga neapolitana</i>	Submarine thermal vent	55–95/ 77	6.0–9.0/ 7.5	1.5–11.0 by 0.6	fructose, fucose, galactose, mannose, rhamnose, pyruvate, glucosamine, lactulose, turanose, glycerol, dextrin, ribose, xylose, glucose, sucrose, maltose, lactose, starch, glycogen	0.2–6.0/ 2.0	S ⁰	AA, ALA, CO ₂ , H ₂	[74]
<i>Pseudothermotoga</i>	<i>Pseudothermotoga lettingae</i>	Thermophilic bioreactor	50–75/ 65	6.0–8.5/ 7.0	2.0–3.0 by 0.5–1.0	glucose, EtOH, acetate, formate	0.0–2.8/ 1.0	S ⁰ ; Thio; AQDS; Fe(III)	AA, ALA, LA, EtOH, AA, BA, CO ₂ , H ₂	[75]
	<i>Pseudothermotoga elfii</i>	Oil reservoir	50–72/ 66	5.5–7.5/ 7.5	2.0–3.0 by 0.5–1.0	glucose, arabinose, fructose, lactose, maltose, mannose, ribose, sucrose, xylose	0.0–2.8/ 1.0	Thio	AA, CO ₂ , H ₂	[76]
	<i>Pseudothermotoga hypogea</i>	Oil reservoir, Africa	56–90/ 70	6.1–9.1/ 7.3–7.4	2.0–3.0 by 0.5–1.0	fructose, galactose, glucose, lactose, maltose, mannose, sucrose, xylose, xylan	0.0–1.5/ 0.2	Thio	AA, ALA, CO ₂ , H ₂ , EtOH	[77]
<i>Pseudothermotoga</i>	<i>Pseudothermotoga subterranea</i>	Oil reservoir, Paris	50–75/ 70	6.0–8.5/ 7.0	3.0–10.0 by 0.5	YE, peptone, tryptone, casein	0.0–2.4/ 1.2	Cys, Thio	n.d.	[78]
	<i>Pseudothermotoga thermarum</i>	Hot spring, Africa	55–84/ 70	6.0–9.0/ 7.0	1.5–11.0 by 0.6	starch, glucose, maltose	0.2–0.5/ 0.35	S ⁰	n.d.	[6]

Table 1. Cont.

Genus	Species	Isolation	Temp. Range/ Optimal (°C)	pH Range/ Optimal	Cell Dimension (Long by Wide) (µm)	Growth Substrates	NaCl Range/ Optimal (%)	Electron Acceptor	End Products	Ref.
<i>Ferroidobacterium</i>	<i>Ferroidobacterium nodosum</i>	Hot spring, New Zealand	40–80/ 65–70	6.0–8.0/ 7.0	1.0–2.5 by 0.5–0.55	glucose, sucrose, starch and lactose	n.d./<1.0	S ⁰	AA, LA, CO ₂ , H ₂ , EtOH, But, Val	[5]
	<i>Ferroidobacterium pennavorans</i>	Hot spring, Portugal	50–80/ 70	5.5–8.0/ 6.5	2.0–20.0 by 0.5	cellobiose, starch, glycogen, pullulan, glucose, fructose, maltose, xylose, native feathers	0.0–4.0/ 0.4	S ⁰ ; Thio	AA, CO ₂ , ALA, Glu, EtOH, But, H ₂ , BuOH	[79]
	<i>Ferroidobacterium islandicum</i>	Icelandic Hot spring	50–80/ 65	6.0–8.0/ 7.2	1.0–4.0 by 0.6	pyruvate, ribose, glucose, maltose, raffinose, starch, cellulose	0.0–1.0/ 0.2	S ⁰ ; Thio	LA, AA, H ₂ , EtOH, CO ₂ , iBut, iVal	[80]
	<i>Ferroidobacterium riparium</i>	Hot spring, Russia	46–80/ 65	5.7–7.9/ 7.8	1.0–3.0 by 0.4–0.5	peptone, YE, pyruvate, glucose, xylose, fructose, maltose, sucrose, cellobiose, starch, xylan, CMC, cellulose, filter paper	0.0–1.0/ 0.0	S ⁰	H ₂ , AA, CO ₂ , PPA, iBut, But	[81]
	<i>Ferroidobacterium gondwanense</i>	Hot spring, Australia	45–80/ 65–68	5.5–8.5/ 7.0	4.0–40.0 by 0.5–0.6	cellobiose, amylopectin, maltose, starch, dextrin, xylose, glucose, pyruvate, lactose, fructose, mannose, CMC, galactose	0.0–0.6/ 0.1	S ⁰	EtOH, AA, LA, CO ₂ , H ₂	[82]
	<i>Ferroidobacterium thailandese</i>	Hot spring, Thailand	60–88/ 78–80	6.5–8.5/ 7.5	1.1–2.5 by 0.5–0.6	glucose, maltose, sucrose, fructose, cellobiose, CMC, cellulose, starch	<0.5/0.5	S ⁰	n.d.	[83]
	<i>Ferroidobacterium changbaicum</i>	Hot spring, China	55–90/ 75–80	6.3–8.5/ 7.5	1.0–8.0 by 0.5–0.6	glucose, lactose, fructose, sucrose, maltose, starch, sorbitol, cellobiose, trehalose, galactose, melibiose, pyruvate, glycerin	0.0–1.0/ 0.0	S ⁰	n.d.	[84]
<i>Thermosipho</i>	<i>Thermosipho africanus</i>	Hot spring, Africa	53–77/ 75	6.0–8.0/ 7.2	3.0–4.0 by 0.5	glucose, ribose, maltose, starch, galactose, fructose, sucrose	0.11–3.6	S ⁰ ; Thio	AA, H ₂ , CO ₂ , LA	[85]
	<i>Thermosipho japonicus</i>	Hydrothermal vent, Japan	45–80/ 72	5.3–9.3/ 7.2–7.6	3.0–4.0 by 0.5	YE, peptone, and tryptone, maltose, glucose, galactose, starch, sacharose, ribose, casein	0.7–7.9/ 4.0	S ⁰ ; Thio	n.d.	[86]
	<i>Thermosipho geolei</i>	Oil reservoir, Russia	45–75/ 70	6.0–9.4/ 7.5	2.0–3.0 by 0.4–0.6	Glucose, peptone, beef extract, YE	0.5–7.0/ 2.0–3.0	S ⁰	H ₂ , AA, ALA, CO ₂ , iVal	[87]
<i>Thermosipho</i>	<i>Thermosipho affectus</i>	Hydrothermal vent, Atlantic Ocean	37–75/ 70	5.6–8.2/ 6.6	1.2–6.0 by 0.4–0.9	YE, beef extract, glucose, maltose, sucrose, starch, dextrin, CMC, cellulose	1.0–5.5/ 2.0	S ⁰	AA, H ₂ , CO ₂ , EtOH	[88]
	<i>Thermosipho globiformans</i>	Hydrothermal vent	40–75/ 68	5.0–8.2/ 6.8	2.0–4.0 by 0.5	YE, tryptone, starch	0.2–5.2/ 2.5	S ⁰ ; Fe ₂ O ₃	n.d.	[89]

Table 1. Cont.

Genus	Species	Isolation	Temp. Range/ Optimal (°C)	pH Range/ Optimal	Cell Dimension (Long by Wide) (µm)	Growth Substrates	NaCl Range/ Optimal (%)	Electron Acceptor	End Products	Ref.
	<i>Thermosipho melanesiensis</i>	Hydrothermal vent, Pacific Ocean	50–75/ 70	4.5–8.5/ 6.5–7.5	1.0–3.5 by 0.4–0.6	BHI, malt extract, tryptone, sucrose, starch, glucose, maltose, lactose, cellobiose, galactose	1.0–6.0/ 3.0	S ⁰	H ₂ , AA, ALA, CO ₂	[90]
	<i>Thermosipho activus</i>	Riftia sheath, Guaymas Basin	44–75/ 65	5.5–8.0/ 6.0	1.5–10.0 by 0.3–0.8	glucose, maltose, cellobiose, cellulose, filter paper, chitin, xylan, pectin, xanthan gum, YE, beef extract, tryptone, casein, keratin, arabinose, xylose, gelatin	0.3–6.0/ 2.5	S ⁰ , Fe (III)	AA, H ₂ , CO ₂	[91]
	<i>Thermosipho atlanticus</i>	Hydrothermal vent, Atlantic Ocean	45–80/ 65	5.0–9.0/ 6.0	1.0–2.6 by 0.2–0.6	cellobiose, xylose, starch, LA, maltose, mannose, trehalose, lactose, arabinose, galactose, mannitol, peptone, casamino acids, gelatin, BHI, YE, glucose	1.5–4.6/ 2.3	S ⁰ , Thio, Cys	AA, iVal, H ₂ , Gly, ALA, Pro	[92]
Geotoga	<i>Geotoga subterranea</i>	Oilfields, USA	30–60/ 45	5.5–9.0/ 6.5	4.0–7.5 by 0.5	mannose, starch, maltodextrins, glucose, lactose, sucrose, galactose, maltose	0.5–10/ 4.0	S ⁰	H ₂ , CO ₂ , AA, EtOH	[10]
	<i>Geotoga petraea</i>	Oilfields, USA	30–55/ 50	5.5–9.0/ 6.5	3.0–20.0 by 0.6	mannose, starch, maltodextrins, glucose, lactose, sucrose, galactose, maltose	0.5–10/ 3.0	S ⁰	H ₂ , CO ₂ , AA, EtOH	[10]
Petrotoga	<i>Petrotoga miotherma</i>	Oilfields, USA	35–65/ 55	5.5–9.0/ 6.5	2.0–7.5 by 0.6	mannose, starch, maltodextrins, glucose, lactose, sucrose, galactose, maltose, maltodextrins, xylose	0.5–10/ 2.0	S ⁰	H ₂ , CO ₂ , AA, EtOH	[10]
	<i>Petrotoga olearia</i>	Oil reservoir, Russia	37–60/ 55	6.5–8.5/ 7.5	0.9–2.5 by 0.3–0.6	arabinose, xylose, cellobiose, dextrin, sucrose, glucose, fructose, maltose, ribose, trehalose, xylan, pyruvate, peptone, starch	0.5–8.0/ 2.0	S ⁰	H ₂ , AA, LA, ALA, EtOH	[93]
	<i>Petrotoga sibirica</i>	Oil reservoir, Russia	37–55/ 55	6.5–9.4/ 8.0	0.9–2.5 by 0.3–0.6	sucrose, glucose, fructose, maltose, ribose, trehalose, xylan, pyruvate, peptone, galactose	0.5–7.0/ 1.0	S ⁰	H ₂ , AA, LA, ALA, EtOH	[93]
Petrotoga	<i>Petrotoga mobilis</i>	Oilfield, North Sea	40–65/ 58–60	5.5–8.5/ 6.5–7.0	1.0–50.0 by 0.5–1.5	starch, xylan, maltodextrin, maltose, cellobiose, sucrose, lactose, glucose, galactose, fructose, arabinose, xylose, ribose, rhamnose	0.5–9.0/ 3.0–4.0	S ⁰ , Thio	H ₂ , CO ₂ , AA, EtOH	[94]
	<i>Petrotoga halophila</i>	Offshore oil, Africa	45–65/ 60	5.6–7.8/ 6.7–7.2	2.0–45.0 by 0.5–0.7	arabinose, cellobiose, fructose, galactose, glucose, lactose, maltose, rhamnose, ribose, starch, sucrose, xylose, xylan, pyruvate	0.5–9.0/ 4.0–6.0	S ⁰	AA, LA, ALA, H ₂ , CO ₂	[95]

Table 1. Cont.

Genus	Species	Isolation	Temp. Range/ Optimal (°C)	pH Range/ Optimal	Cell Dimension (Long by Wide) (µm)	Growth Substrates	NaCl Range/ Optimal (%)	Electron Acceptor	End Products	Ref.
	<i>Petrotoga mexicana</i>	Offshore oil, Africa	25–65/ 55	5.8–8.5/ 6.6	1.0–30.0 by 0.5–0.7	arabinose, cellobiose, fructose, galactose, glucose, lactose, maltose, mannose, raffinose, rhamnose, ribose, starch, sucrose, xylose, xylan, pyruvate.	1.0–20.0/ 3.0	S ⁰ , Thio, Sulfite	AA, LA, H ₂ , CO ₂ , ALA	[96]
	<i>Petrotoga japonica</i>	Oil reservoir, Japan	40–65/ 60	6.0–9.0/ 7.5	2.5–7.0 by 0.25–0.75	starch, xylan, maltose, cellobiose, sucrose, lactose, glucose, galactose, fructose, casamino acids, mannose, arabinose, xylose, ribose	0.5–9.0/ 0.5–1.0	S ⁰ , Thio	AA, H ₂ , CO ₂ , ALA	[97]
	<i>Marinitoga piezophila</i>	Hydrothermal chimney, Pacific Ocean	45–70/ 65	5.0–8.0/ 6.0	1.0–1.5 by 0.5	starch, fructose, glucose, galactose, maltose, cellobiose, ribose, acetate	1.0–5.0/ 3.0	S ⁰ , Thio, Cys	n.d.	[98]
	<i>Marinitoga litoralis</i>	Hot spring, Indian Ocean	45–70/ 65	5.5–7.5/ 6.0	1.0–7.0 by 0.8–1.0	cellobiose, galactose, glucose, glycogen, lactose, maltose, ribose, starch, BHI, casamino acids, casein, peptone, pyruvate, tryptone, YE	0.8–4.6/ 2.6	S ⁰	n.d.	[99]
Marinitoga	<i>Marinitoga okinawensis</i>	Hydrothermal field, Okinawa	30–70/ 55–60	5.5–7.4/ 5.5–5.8	1.5–5.0 by 0.5–0.8	YE, tryptone, peptone, starch, glucose, glycerol	1.0–5.5/ 3.0–3.5	S ⁰ , Cys	n.d.	[100]
	<i>Marinitoga hydrogenitolerans</i>	Hydrothermal chimney, Atlantic Ocean	35–65/ 60	4.5–8.5/ 6.0	1.5–5.0 by 0.5–0.8	glucose, starch, glycogen, chitin, YE, BHI, peptone, casein, pyruvate, maltose	1.0–6.5/ 3.0–4.0	S ⁰ , Thio, Cys	AA, EtOH, Fo, H ₂ , CO ₂	[101]
	<i>Marinitoga artica</i>	Hydrothermal chimney, Norwegian	45–70/ 65	5.0–7.5/ 5.5	1.0–5.0 by 0.5–0.8	glucose, trehalose, maltose, sucrose, maltodextrin, starch, pectin, meat extract, tryptone, YE, pyruvate, fructose, mannose, cellobiose, cellulose, peptone	1.5–5.5/ 2.5	S ⁰ , Cys	n.d.	[102]
	<i>Marinitoga camini</i>	Hydrothermal chimney, Atlantic Ridge	25–65/ 55	5.0–9.0/ 7.0	2.0–3.0 by 0.5–1.0	BHI, gluten, peptone, tryptone, pyruvate, glucose, fructose, maltose, cellobiose, sucrose, starch, cellulose, CMC, pectin, chitin	1.0–4.5/ 2.0	S ⁰ , Cys	AA, iBut, iVal, H ₂ , 3-IAA, LA CO ₂ , HPA, PA	[11]
Oceanotoga	<i>Oceanotoga teriensis</i>	Offshore oil, India	25–70/ 55–58	5.5–9.0/ 7.5	1.5–1.7 by 0.5–0.7	glucose, fructose, cellobiose, arabinose, raffinose, rhamnose, sucrose, xylose, ribose, starch, EtOH, formate, acetate, BHI, YE, bio-tryptidase	0.0–12/ 4.3	S ⁰ , Thio	AA, H ₂ , CO ₂ , EtOH	[12]
Defluviitoga	<i>Defluviitoga tunisiensis</i>	Mesothermic digester	37–65/ 55	6.7–7.9/ 6.9	3.0–30.0 by 1.0	arabinose, cellobiose, fructose, galactose, glucose, lactose, maltose, mannose, raffinose, ribose, sucrose, xylose, cellulose, xylan	0.2–3.0/ 0.5	S ⁰ , Thio	AA, H ₂ , CO ₂	[9]

Table 1. Cont.

Genus	Species	Isolation	Temp. Range/ Optimal (°C)	pH Range/ Optimal	Cell Dimension (Long by Wide) (µm)	Growth Substrates	NaCl Range/ Optimal (%)	Electron Acceptor	End Products	Ref.
<i>Mesotoga</i>	<i>Mesotoga infera</i>	Deep aquifer, France	30–50/ 45	6.2–7.9/ 7.4	2.0–4.0 by 1.0–2.0	arabinose, cellobiose, fructose, galactose, glucose, lactose, LA, mannose, maltose, raffinose, ribose, sucrose, xylose	0.0–1.5/ 0.2	S ⁰	AA, CO ₂	[26]
	<i>Mesotoga prima</i>	Sediment, USA	20–50/ 37	6.5–8.0/ 7.5	1.0 by 0.2	xylose, fructose, ribose, sucrose, mannose, galactose, maltose, lactose, peptone, tryptone, casamino acids, glucose, arabinose, cellobiose, casein, pyruvate	2.0–6.0/ 4.0	S ⁰ , Thio, Sulfite	AA, But, iBut, iVal, 2–MeBu	[8]
<i>Kosmotoga</i>	<i>Kosmotoga arenicorallina</i>	Hot spring, Japan	50–65/ 60	6.2–8.0/ 7.1	1.1–2.7 by 1.1–1.9	xylose, maltose, glycerol	1.0–6.0/ 3.0	S ⁰ , Cys	n.d.	[103]
	<i>Kosmotoga pacifica</i>	Hydrothermal field, Pacific Ocean	33–78/ 70	6.2–8.0/ 7.1	1.0 by 0.6	maltose, YE, peptone, BHI, glycerol, tryptone, xylose, glucose, fructose, cellobiose, trehalose, LA, propionate, glutamate	0.5–6.0/ n.d.	S ⁰ , Cys	n.d.	[104]
	<i>Kosmotoga olearia</i>	Fluid, North Sea	20–80/ 65	5.5–8.0/ 6.8	0.8–1.2 by 0.4–0.7	maltose, ribose, sucrose, starch, casamino acids, tryptone, pyruvate	1.0–6.0/ 2.5–3.0	Thio	H ₂ , CO ₂ , AA, EtOH, PPA	[7]
	<i>Kosmotoga shengliensis</i>	Oilfield, China	45–75/ 65	6.0–8.0/ 7.0	0.7–0.9	glucose, acetate, mEtOH, galactose, fructose, xylose, sucrose, maltose, sorbitol, lactose, xylan, arabinose, formate, rhamnose, glycerol, pyruvate, starch, LA	0.0–4.0/ 1.5	S ⁰ , Thio, Sulfate	AA, LA, ALA, CO ₂ , H ₂	[15]
<i>Athalassatoga</i>	<i>Athalassatoga saccharophila</i>	Hot spring, Japan	30–60/ 55	4.5–7.5/ 5.5–6.0	0.8–2.0 by 0.7–0.8	arabinose, fructose, glucose, lactose, maltose, mannose, ribose, sucrose, xylose, starch, glycogen, peptone, YE	<1/0.0	Fe (III), Thio, Cys	AA, iBut, iVal	[14]
<i>Mesoaciditoga</i>	<i>Mesoaciditoga lauensis</i>	Hydrothermal vent, Pacific Ocean	45–65/ 57–60	4.1–6.0/ 5.5–5.7	0.8–1.0 by 0.4	YE, peptone, maltose, sucrose, glucose, xylose, ribose, starch, tryptone	0.5–6.0/ 3.0	S ⁰ , Thio, Cys	n.d.	[13]

2. Operating Conditions

2.1. H_2 Partial Pressure (P_{H_2})

Since *Thermotogae* members are hydrogen producers, tolerance to hydrogen produced by the bacteria on its own gaseous production, known as the “hydrogen partial pressure (P_{H_2})” effect, is one of the primary parameters being extensively investigated [51,70,105]. The highest hydrogen tolerance has been observed in the genus *Marinotoga*. *Mn. camini* and *Mn. piezophila* were able to grow with H_2 concentrations up to 40% and 60%, respectively. *Mn. hydrogenitolerans* and *Mn. okinawensis* can grow under 100% H_2 atmosphere with only minor inhibition on growth and fermentation [100,101]. Their remarkable resistance to high H_2 levels is probably related to the typical habitats in which *Marinotoga* species thrive [100]. However, the growth of *Thermotogae* species is often inhibited by H_2 accumulation, and the metabolism of these organisms undergoes a series of rearrangements to suit P_{H_2} levels in the bioreactor headspace. The majority of literature data refers to H_2 percentages in gaseous phase, although some studies have been reporting values of P_{H_2} . Partial pressure around 607 mbar led to decreased levels of biomass production, glucose consumption rate, and H_2 production in both *T. neapolitana* and *T. maritima* [106,107]. Boileau et al. [107] highlighted a shift of *T. maritima* glucose catabolism from acetic acid towards lactic acid when P_{H_2} increased from 7 to 607 mbar (Table 2) [106,107]. In contrast, low P_{H_2} (less than 80 mbar) promoted acetic acid accumulation. Biomass production and glucose consumption rate are unaffected when P_{H_2} is maintained within the range of 7.1–178.5 mbar (Table 2) [105,106]. In fact, P_{H_2} lower than 200 mbar is required for optimal growth in reactors, and P_{H_2} around 2900 mbar completely inhibits growth in *T. maritima* [1,45,49,108,109].

Hydrogen evolution is driven by a bifurcating hydrogenase (H_2 ase) that couples the oxidation of reduced ferredoxin (Fd) and NADH with the reduction of protons to H_2 (Figure 1) [58]. In dark fermentation, pyruvate is converted to acetate and ATP, which thermodynamically drives the H_2 -acetate pathway. Under high H_2 partial pressure, hydrogenase activity is inhibited, NADH consumption stops, pyruvate is diverted away from acetic acid production, and lactic acid synthesis becomes the only mechanism for recycling reduced electron carriers (Figure 1) [28–30,57,64,106,110]. Synthesis of lactic acid by the lactate dehydrogenase (LDH) catalyzes the conversion of pyruvate to lactate with the concomitant conversion of NADH to NAD^+ (Figure 1). The depletion of the pyruvate pool, as occurs with the synthesis of lactic acid, negatively affects hydrogen yield, preventing it from reaching the theoretical maximal value (Figure 1) [24]. This problem can be overcome by enhancing the liquid-to-gas mass transfer and keeping H_2 concentrations low in experimental conditions (See Section 2.2) or by using mixed cultures with microbial species that are able to oxidize H_2 [27,111].

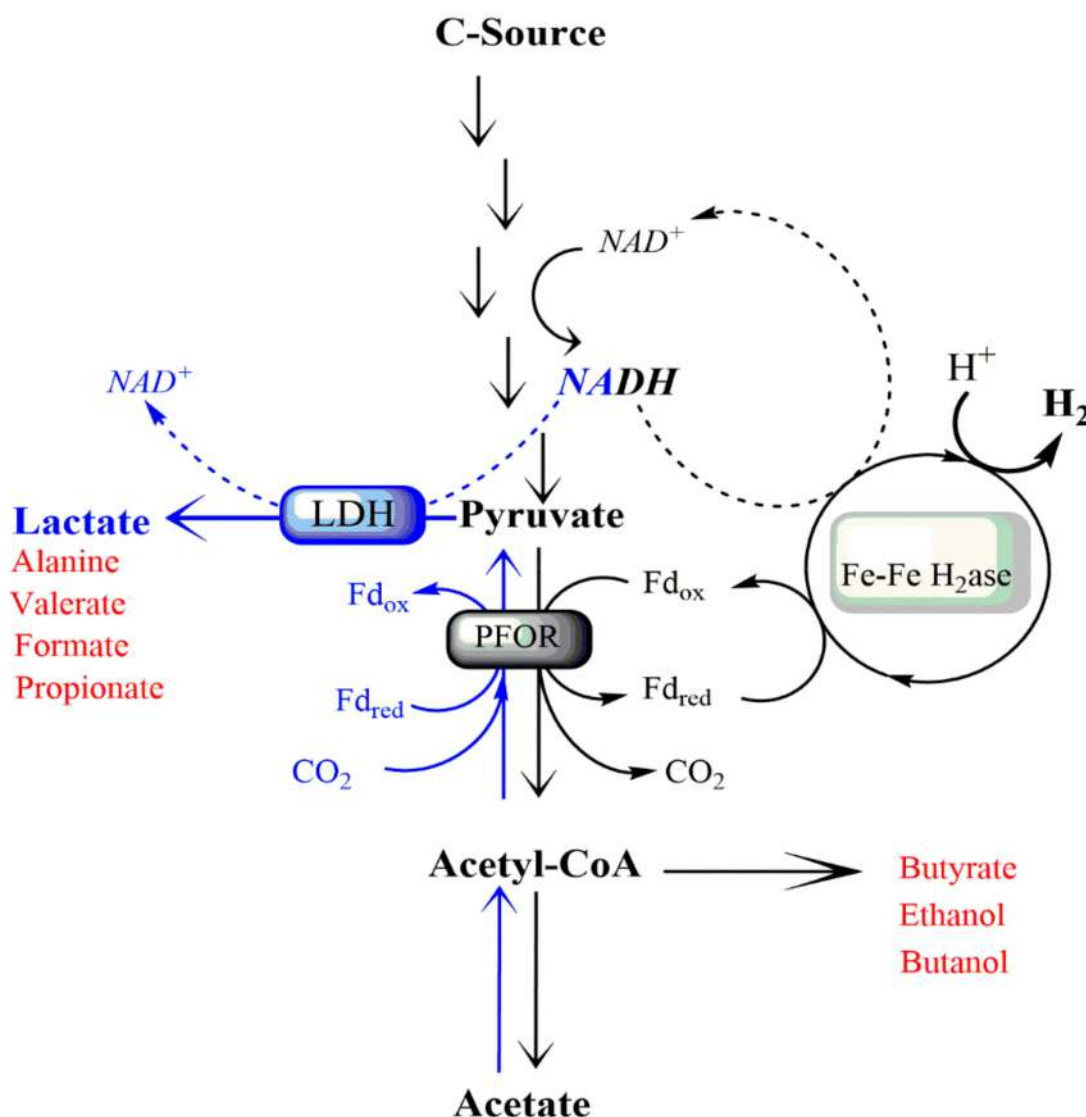


Figure 1. Schematic representation of *Thermotogae* metabolic fermentation. Dark fermentation (black arrows) of glucose leads to the production of H_2 and acetate. An increase in CO_2 concentration in the reactor headspace induces the recycling of Ac-CoA and CO_2 into lactate without impairing the synthesis of biogas (blue arrows). This process is named “Capnophilic lactic fermentation (CLF)” [30,31,56,70]. The main end-products of *Thermotogae* fermentation are H_2 , lactate, and acetate. Other fermentation products are reported in red. Fe-Fe H_2 ase = [Fe-Fe] hydrogenase; PFOR = Pyruvate ferredoxin oxidoreductase; LDH = Lactate dehydrogenase; Fd = Ferredoxin.

2.2. Shaking Speed, Culture/Headspace Volume Ratio, Gas Sparging, and Inoculum

Growth and metabolism of thermophilic bacteria are reported to be strongly affected by an increase in the hydrogen level, which makes the metabolic reactions thermodynamically unfavorable [112]. Many effective strategies have been developed to overcome the H_2 feedback inhibition, such as gas sparging, vigorous stirring, or simply increasing the gas/liquid volume ratio in the reactor. H_2 saturation is dependent on the partial pressure of hydrogen in the culture medium and its mass transfer from liquid to gas phase. As a matter of fact, the mass transfer of H_2 from liquid to gas can be improved by applying vigorous agitation in bioreactors [69,106]. Increased H_2 production rate, glucose consumption rate, and lactic acid synthesis have been observed in *T. neapolitana* cultures with agitation at 200 rpm, compared to static cultures, although the final H_2 yields were similar [106]. Comparable hydrogen yields were also observed when the agitation speed was 300 and 500 rpm, e.g.,

3.0 ± 0.0 mol H₂/mol glucose at 300 rpm vs. 3.2 ± 0.1 mol H₂/mol glucose at 500 rpm, with a mild improvement in fermentation rate (Table 2) [69]. In xylose fermentation, the highest hydrogen and organic acid yields have been reported at 400 rpm when tested in the range of 300–600 rpm [113].

To improve hydrogen liquid-gas mass transfer, Dreschke et al. [69] designed a new method that recirculated the H₂-rich biogas (GaR) into the *T. neapolitana* subs. *capnolactica* broth with agitation (300, 500 rpm). This combination accelerated the H₂ evolution rate and glucose consumption rate during glucose fermentation, compared to the treatments including agitation but excluding GaR. Nonetheless, levels of the end-products, except for H₂ yield, were not significantly altered by the combined parameters (Table 2) [69].

Since P_{H_2} depends on the culture/headspace volume ratio in the bioreactors, its impacts on the performance of fermentation have also been investigated, mainly in batch reactors. Nguyen et al. [64] have experimented various culture/headspace volume ratio from 8.3% (10 mL/120 mL) up to 50% (60 mL/120 mL) in *T. neapolitana* and *T. maritima* cultures [64]. At 8.3%, the H₂ production is the highest for both species (890 mL H₂/L medium in *T. neapolitana* and 883 mL H₂/L medium in *T. maritima*). H₂ production gradually diminished, and lactic acid production was promoted with increasing culture volumes [30,64,110]. d'Ippolito et al. [30] found 1:3 culture/headspace volume was the most suitable ratio for high hydrogen yields [30]. When these conditions were optimized, *T. neapolitana* resulted in H₂ yields between 3.46–3.85 mol H₂/mol glucose [30,114].

Gas sparging, mainly with N₂, is the most common method to reduce hydrogen partial pressure by removing H₂ and CO₂ produced from sugar fermentation in closed bioreactors [56,108,115,116]. Under nitrogen sparging conditions, the overall yield of H₂ in *T. neapolitana* fermentation was about two-fold of the non-sparged cultures, e.g., 1.82 vs. 3.24 mol H₂/mol glucose or 1.14 vs. 2.20 mol H₂/mol xylose (Table 2). The levels of acetic acid and butyrate also increased [110]. Moreover, the fermentation performance was remarkably improved when N₂-sparging was coupled with pH control in *T. neapolitana* using pure glycerol as the sole carbon source (Table 2) [116]. Keeping pH close to neutral improved the glucose utilization and H₂-acetate production rates. In contrast, lactic acid production was lowered under these conditions (0.255 mmol/L with pH control and sparging vs. 0.36 mmol/L with pH control but no sparging) (Table 2) [116]. The use of a CO₂-enriched atmosphere significantly increased both glucose consumption rate and hydrogen production rate, even though the molar yield was comparable to that of N₂-sparging (Table 2) [31]. Surprisingly, supplementation of CO₂ to *T. neapolitana* cultures induced an unexpected metabolic shift from acetic to lactic fermentation without any significant change in hydrogen production (3.6 mol/mol glucose) (Table 2) [31]. Experiments with labeled precursors revealed that part of the exogenous CO₂ was biologically coupled with acetyl-CoA to give lactic acid when the cultures were sparged with CO₂ gas or enriched in sodium bicarbonate (Figure 1) [117]. This process, named Capnophilic Lactic Fermentation (CLF), has the surprising feature to produce more lactic acid than expected from the classical dark fermentation model where H₂ production is impaired by the onset of by-passing pathways (Figure 1) [31,56,117–119]. In dark fermentation, hydrogen and lactic acid levels competed for a common pool of reducing power. Whereas, in CLF, the H₂ level remained high, probably due to additional sources of reductants to sustain NADH-dependent pathways (Figure 1) [118–120]. Recently, an additional increase in lactic acid production occurred in a *T. neapolitana* mutant that was isolated from a culture adapted to continuous exposure to CO₂ [62]. Sparging with CO₂ was also performed on the culture of other *Thermotogales* species, whose metabolic response was qualitatively and quantitatively diverse (Table 2) [70]. CO₂-enriched conditions promoted glucose consumption rate and lowered biogas production in almost all tested species [70]. *T. caldifontis*, *Pseudot. elfii*, *Pseudot. thermarum*, *Pseudot. lettingae*, and *Pseudot. subterranea* did not show substantial variations in the levels of the fermentation products compared to cultures in an N₂-enriched atmosphere [70]. *T. neapolitana*, *T. maritima*, *T. profunda*, and *Pseudot. hypogaea* species responded to CO₂ by reducing the fermentation rate. *T. neapolitana* subsp. *capno-*

lactica was the only species to increase lactic acid and H₂ yield moving from N₂-sparging to CO₂-sparging [70]. Generally speaking, the supplementation of external gas (N₂ or CO₂) successfully improves the fermentation performance in most species and lowers the inhibitory effect of H₂ accumulation, but it inevitably causes an undesired dilution of hydrogen in evolved gases. In this context, the recirculation of the H₂-rich biogas method prevents hydrogen saturation in the bioreactor without negatively affecting the content of the produced biogas [69].

The initial biomass concentration (size of inoculum) also has an unexpected impact on the fermentation of thermophilic bacteria. Using various initial biomass concentrations of *T. neapolitana* subs. *capnolactica* (in the range of 0.46–1.74 g CDW/L) under CO₂ atmosphere, hydrogen yield and the distribution of end-products were unaffected (Table 2) [68]. However, increasing inoculum size from 0.46 to 1.74 g/L reduced the fermentation time from 7 h to 3 h [68]. Moreover, the hydrogen production rate, glucose consumption rate, and biomass growth rate were increased [49,50,68]. It is worth pointing out that Ngo et al. [116] reported a reverse correlation between hydrogen production rate and inoculum size, stating that high initial biomass corresponded to a mild reduction of hydrogen production rate [116].

2.3. pH

As the fermentation of sugars leads to the production and accumulation of organic acids, the pH is decreasing during the process, which may inhibit bacterial growth before the substrates are completely consumed [30,106,113]. Two factors impose a strong inhibition on bacterial growth and H₂ production: rapid decrease in pH due to the accumulation of byproducts and feedback inhibition caused by H₂ accumulated in the headspace [65,105–108,113,121].

Thus, pH is a critical factor to control sugar consumption and direct end-products formation [65,67,117,119,122]. Gradual pH drop causes enzyme activity loss [123]. To overcome pH-induced limitations on *Thermotogae* fermentation, several studies were performed with pH adjustments [51,67,121]. In pH-controlled cultures (~6.5–7.0), H₂ and acetic acid production predominated over lactic acid and peaked around 20 h [113]. In contrast, lactic acid production only started when pH declined to around 5.0 [113].

The addition of NaOH at regular intervals and the use of buffering reagents have been regarded as the best-performing methods with serum bottles [56,66,67,113]. The optimum pH for growth and hydrogen production is 6.5–7.0 in *T. maritima* and 6.5–7.5 in *T. neapolitana* depending on substrates and growth conditions [64,113,122]. Moreover, pH 7.0 provides the most promising results in terms of H₂ and organic acids production in *T. neapolitana* [113,122]. A pH shift from 5.5 to 7.0 improved H₂ yield from 125 to 198 mL H₂/L medium in *T. neapolitana* [61]. With *T. neapolitana* cells immobilized on ceramic surfaces using glucose as the carbon source, the highest hydrogen production was observed in the pH range of 7.7–8.5 [51]. Further increase in the range of pH to 8.0–9.0 led to a dramatic decrease in the biogas evolution [64].

Different organic and inorganic buffers have been examined for their effect on anaerobic fermentation under various growth conditions and buffer concentrations [51]. According to Cappelletti et al. [51], 0.1 M HEPES resulted in the best performance, compared to MOPS, PIPES, HPO₄[−]/H₂PO₄[−], or Tris-HCl buffer in *T. neapolitana* batch cultures growing on glucose under N₂ atmosphere [51]. The good buffering properties of HEPES, whose pK (7.55) is near the optimal pH of *T. neapolitana*, was also demonstrated for *T. neapolitana* cultures growing on different complex carbon sources (cheese whey, molasses, or waste glycerol) [51,122]. In another study, 0.05 M HEPES was found to be sufficient under N₂ sparging atmosphere (Table 2) [113]. Under CLF conditions, 0.01 M MOPS, TRIS, or HEPES buffers provided satisfactory results for both H₂ and lactic acid synthesis in *T. neapolitana* subs. *capnolactica* (Table 2) [67]. More specifically, H₂ synthesis was found to be the highest in MOPS, while TRIS promoted acetic acid formation (Table 2) [67]. The highest value of

lactic acid synthesis was 14.9 ± 0.3 mM in phosphate buffer compared to 11.3 ± 0.6 mM in the standard condition (Table 2) [67].

The buffering capacity of HCO_3^- is sufficient to maintain near to optimal pH for growth (~6.5), facilitating the complete substrate degradation and desired by-product formation (Table 2) [31,56,67].

In other studies, itaconic acid was successfully used as a physiological buffer to enhance hydrogen production in *T. neapolitana* growing on glucose or glycerol [121,122]. During the cultivation with 1.5 g/L itaconic acid, the pH slowly dropped from 7.5 to 6.8 over 99 h, while the same pH change was reached within 48 h in cultures not buffered [122]. Although itaconic acid is only poorly catabolized, it affected the overall metabolism of *T. neapolitana* because H_2 and acetic acid production were almost 1.4-fold higher than the control, while lactic acid production was reduced by nearly 100% compared to the control (Table 2) [122]. In addition, Ngo and Sim [122] found that the performance of *T. neapolitana* fermentation growing on waste glycerol was improved by almost 40% by adding itaconic acid into the culture medium [122].

2.4. Temperature

Due to their origin from hot habitats, bacterial species of the phylum *Thermotogae* can live and grow at temperatures in the range of 40–90 °C (Table 1). Some species such as *K. olearia*, *O. teriensis*, *Ms. prima*, and *P. mexicana* can thrive at mesophilic temperatures (Table 1) [7,8,96,100], and other species such as *F. changbaicum*, *F. thailandese*, *T. maritima*, *Pseudot. hypogea*, and *T. neapolitana* share the ability of growing at temperatures close to 90 °C (Table 1) [3,74,77,83,94]. For a long time, researchers have selected an operating temperature of 70 °C [104,117] or 80 °C [105] to cultivate *T. neapolitana* and *T. maritima* without careful investigation of the impacts on fermentation. Nguyen et al. [64] explored changes of H_2 production with temperatures ranging from 55 to 90 °C for *T. neapolitana* and *T. maritima*. Both cultures showed approximately 100 mL H_2 /L medium at 55 °C and a maximum of 200 mL H_2 /L medium at 75–80 °C, with a decrease to 150 H_2 /L medium at 90 °C [64]. In *T. neapolitana*, high temperatures (77–85 °C) enhanced glucose uptake (2.2 mmol/L at 60 °C and 11.0 mmol/L at 77–85 °C) and boosted hydrogen yields (2.04 mol H_2 /mol consumed glucose at 60 °C and 3.85 mol H_2 /mol at 77 °C) [65]. This positive effect was also found for acetic acid (2.0 mmol/L at 60 °C and 18.0 mmol/L at 85 °C) and lactic acid production (no production at 60 °C and 1.25 mmol/L at 85 °C) (Table 2) [65]. Studies conducted on *T. maritima* hydrogenase demonstrated that this enzyme is unstable at the ambient temperature and its activity increased considerably with rising temperature (an activity of 25 units/mg at 20 °C and 110 units/mg at 90 °C [123]).

2.5. Oxygen (O_2)

Thermotogae members occur in various hot ecosystems, including hot springs, deep-sea, and shallow hydrothermal vents, and may also be exposed to O_2 in these ecological niches [1254]. Indeed, despite their anaerobic nature, O_2 tolerance is variable in the phylum; for example, *Thermotoga*, *Fervidobacterium*, and *Geotoga* genera can grow only under strictly anaerobic conditions, while *K. olearia* can survive in up to 15% O_2 [10]. With elemental sulfur, *Ts. atlanticus* can grow with up to 8% O_2 in the headspace [92]. Geochemical and microbial analyses demonstrated the wide distribution of *Thermotogae* species in ecosystems that are not only anaerobic but also partially oxygenated [124]. For this reason, the question of O_2 tolerance and microaerophilic metabolism of *Thermotogae* has been addressed by several studies [65,105,106,125–129]. Some researchers have demonstrated that low concentrations of O_2 are tolerated by *T. neapolitana* and *T. maritima* [127,128]. An O_2 insensitive hydrogenase has been described in *T. neapolitana*, explaining why microaerobic H_2 production and O_2 tolerance could take place in this bacterium [130]. Additionally, *Pseudot. hypogea* and *T. maritima* contain an NADH oxidase that may serve as an O_2 detoxification system [131,132]. Lakhal et al. [129] demonstrated O_2 consumption over 12 h during the stationary phase of *T. maritima* in a batch reactor without reducing agent [129]. O_2 presence

reduced glucose fermentation rate and significantly shifted metabolism towards lactic acid production in *T. maritima* (Table 2). This change can probably be explained by O₂ sensitivity of the hydrogenase [129]. Furthermore, *T. maritima* overproduced enzymes involved in reactive oxygen species (ROS) detoxification, iron-sulfur cluster synthesis/repair, cysteine biosynthesis, and a flavoprotein homologous to the rubredoxin of *Desulfovibrio* species that exhibited an oxygen reductase activity [127].

Van Ooteghem et al. [121] reported that O₂ concentration decreased during the growth of *F. pennavorans*, *P. miotherma*, *Ts. africanus*, *Pseudot. elfii*, and *T. neapolitana*. In these experiments, the H₂ yield greatly exceeded the theoretical limit of 4 mol H₂/mol glucose in *F. pennavorans*, *Pseudot. elfii*, and *T. neapolitana* fermentation [121]. These surprisingly high H₂ yield have led to the hypothesis of an unidentified aerobic pathway using O₂ as a terminal electron acceptor in these bacteria which may not be obligate anaerobes [121]. However, aerobic metabolism is not supported by the genomic sequence of *T. maritima*, although the enzymes involved in the pentose phosphate pathway and an NADPH-reducing hydrogenase have been identified in the genome [16]. To explain the increased yield of H₂ by *T. neapolitana* in microaerobic conditions and the existence of a catabolic process requiring O₂, van Ooteghem et al. [121] used malonic acid as an inhibitor of succinate dehydrogenase and thus the O₂-dependent metabolism. Even if the coding sequence for succinate dehydrogenase has not been identified in the *T. maritima* genome, hydrogen generation was completely inhibited for >40 h in the presence of malonate, postulating that malonate in the medium was no longer available to block catabolism [121]. Then, Eriksen et al. [106] demonstrated that malonic acid was not metabolized by *T. neapolitana* cultures but the exposure to malonic acid clearly affected the metabolism as reduced production of lactic acid and increased H₂ yield were observed [106]. Against these findings, other researchers reported a reduction of H₂ rate and production in *T. neapolitana* cultures after the injection of 6% O₂ [65,106]. The reduction of O₂ consumes reducing equivalents that are then unavailable to produce H₂. The total duration of *T. maritima* fermentation in the batch reactor was delayed about 67 h under O₂-induced stress [129]. In addition, the consumption rate of glucose was drastically reduced and the metabolism of *T. maritima* shifted towards lactic acid production due to inhibition of the O₂-sensitive hydrogenase [129].

From a technical point of view, several strategies were adopted to remove dissolved O₂ in the bioreactor: [I] sparging the culture with N₂, CO₂ or a mixture of both gases; [II] heating the medium; [III] adding a reducing agent such as sodium sulfide or cysteine-HCl in the medium; [IV] maintaining a positive pressure in the bioreactor headspace [31,56,62,67,70,105,106,113,121].

Table 2. Effects of operating conditions on *Thermotoga* fermentation. MOPS: Morpholinopropane-1-sulfonic acid; **HEPES**: 2-[4-(2-hydroxyethyl) piperazin-1-yl] ethanesulfonic acid; **TRIS**: tris(idrossimetil)amminometano cloridrato; **CDW**: Cellular dry weight; **AA**: Acetic acid; **LA**: Lactic acid; **ALA**: Alanine; **But**: Butyrate; **IA**: Itaconic acid; GaR: recirculation of H₂-rich biogas. Experiments were performed in different bioreactor configurations: **B** = Batch; **CSTR** = Continuous-flow Stirred-Tank Reactor; **CSABR**: Continuously Stirred Anaerobic Bioreactor; **SB** = Serum bottles. **H₂ column**: ^a H₂ yield = mol H₂/mol consumed substrate; ^b mL/L culture. * Values extrapolated from the graphical representation of data.

Parameter	Organism	T (°C)	Culture Type	Mixing Speed (rpm)	Reactor/Working Volume (L)	Substrate Loaded (mmol/L)	Operational Parameter	Substrate Consumed (mmol/L)	Products					Ref.
									H ₂ yield ^a	AA (mmol/L)	LA (mmol/L)	ALA (mmol/L)	But (mmol/L)	
<i>P_{H2}</i> (mbar)	<i>T. maritima</i>	80	B	350	1.4/0.1	Glucose (28)	<i>P_{H2}</i> = 7.1 ± 0.4	19.8 ± 1.1	2.34	25.0 ± 1.4	10.5 ± 0.5			[107]
							<i>P_{H2}</i> = 71.4 ± 2.1	19.7 ± 1.4	2.44	24.6 ± 2.4	11.0 ± 0.6			
							<i>P_{H2}</i> = 178.5 ± 3.5	17.2 ± 0.9	2.32	20.1 ± 1.0	9.4 ± 0.5			
							<i>P_{H2}</i> = 606.9 ± 18.7	13.4 ± 0.7	n. d.	13.0 ± 0.7	11.0 ± 0.6			
Stirring Speed (rpm)	<i>T. neapolitana</i>	75	CSABR	300	3.0/1.0	Xylose (33.3)	300	31.43	2.13 ± 0.11	41.8 ± 2.16	1.78 ± 0.11			[113]
				400			400	32.56	2.94 ± 0.15	50.12 ± 2.5	4.0 ± 0.22			
				500			500	32.03	2.31 ± 0.12	44.62 ± 2.16	4.84 ± 0.22			
				600			600	31.87	2.24 ± 0.11	41.12 ± 2.0	1.89 ± 0.11			
	<i>T. neapolitana</i> subsp. <i>capnolactica</i>	80	CSTR	300	3.0/2.0	Glucose (28)	300	22.9 ± 2.7	3.0 ± 0.0	32.3 ± 4.3	10.0 ± 1.0	1.1 ± 0.1		[69]
				500			500	24.8 ± 0.4	3.2 ± 0.1	37.7 ± 2.7	8.1 ± 0.2	1.0 ± 0.1		
				300			300 + GaR	24.7 ± 0.2	3.5 ± 0.2	39.2 ± 1.2	4.4 ± 0.1	0.9 ± 0.0		
				500			500 + GaR	24.9 ± 0.2	3.3 ± 0.1	38.7 ± 2.2	5.1 ± 0.5	0.8 ± 0.0		
Gas sparging	<i>T. neapolitana</i>	80	B	250	3.8/1.0	Glucose (28)	N ₂	25.9 ± 1.3	2.8	44.8 ± 5.4	12.5 ± 2.9	1.3 ± 0.4		[31]
							CO ₂	26.1 ± 1.2	2.8	35.6 ± 5.8	20.0 ± 6.1	2.7 ± 0.5		
		75	SB	no	0.12/0.04	Glycerol (108.6)	w/o	13 ± 0.6	1.24 ± 0.06	8.71 ± 0.35	0.36 ± 0.02			[115]
							N ₂	14 ± 0.7	2.06 ± 0.09	10.04 ± 0.5	0.34 ± 0.02			
Gas sparging	<i>T. neapolitana</i>	77	SB	150	0.12/0.04	Glucose (39)	w/o	-	1.82 ± 0.09	64.28 ± 2.83			33.48 ± 1.47	[110]
							N ₂	-	3.24 ± 0.14	81.42 ± 3.49			36.77 ± 2.04	
						Xylose (27)	w/o	-	1.14 ± 0.07	40.30 ± 3.5			37.68 ± 1.7	
							N ₂	-	2.20 ± 0.13	71.94 ± 3.66			50.62 ± 2.38	
	<i>T. neapolitana</i> subsp. <i>capnolactica</i>	80	SB	no	0.12/0.03	Glucose (28)	N ₂	25.7 ± 0.1	2.5 ± 0.06	27.3 ± 0.8	8.6 ± 0.2	2.5 ± 0.2		[70]
							CO ₂	28.3 ± 1.0	2.9 ± 0.1	22.1 ± 0.9	11.3 ± 0.1	3.0 ± 0.3		

Table 2. Cont.

Parameter	Organism	T (°C)	Culture Type	Mixing Speed (rpm)	Reactor/Working Volume (L)	Substrate Loaded (mmol/L)	Operational Parameter	Substrate Consumed (mmol/L)	Products					Ref.
									H ₂ yield ^a	AA (mmol/L)	LA (mmol/L)	ALA (mmol/L)	But (mmol/L)	
	<i>T. neapolitana</i>	80	SB	no	0.12/0.03	Glucose (28)	N ₂	21.7 ± 0.6	2.5 ± 0.03	30.2 ± 0.4	2.2 ± 0.02	1.9 ± 0.3		[70]
							CO ₂	20.8 ± 2.3	1.9 ± 0.1	20.8 ± 0.1	1.2 ± 0.06	2.4 ± 0.3		
	<i>T. maritima</i>	80	SB	no	0.12/0.03	Glucose (28)	N ₂	23.2 ± 1.0	1.9 ± 0.06	25.5 ± 0.5	5.3 ± 0.8	2.4 ± 0.06		
							CO ₂	19.9 ± 0.6	2.0 ± 0.1	18.3 ± 0.3	1.6 ± 0.2	2.3 ± 0.3		
	<i>T. naphthophila</i>	80	SB	no	0.12/0.04	Glucose (28)	N ₂	13.30 ± 1.10	2.20 ± 0.20	15.70 ± 0.10	1.40 ± 0.06	0.80 ± 0.10		
							CO ₂	20.80 ± 1.70	1.60 ± 0.20	19.20 ± 0.10	5.00 ± 0.02	1.80 ± 0.05		
	<i>T. petrophila</i>	80	SB	no	0.12/0.05	Glucose (28)	N ₂	9.20 ± 1.30	3.00 ± 0.40	13.10 ± 0.05	2.00 ± 0.01	0.00		
							CO ₂	14.20 ± 0.60	1.90 ± 0.10	12.60 ± 0.10	3.80 ± 0.02	0.30 ± 0.10		
	<i>T. caldifontis</i>	70	SB	no	0.12/0.05	Glucose (28)	N ₂	10.90 ± 1.10	2.60 ± 0.10	16.70 ± 3.60	2.20 ± 0.50	3.20 ± 0.90		
							CO ₂	15.20 ± 0.90	1.80 ± 0.03	15.60 ± 1.50	2.30 ± 0.40	6.60 ± 0.70		
	<i>T. profunda</i>	60	SB	no	0.12/0.05	Glucose (28)	N ₂	18.10 ± 0.40	1.50 ± 0.20	15.90 ± 0.40	5.70 ± 0.10	1.40 ± 0.06		
							CO ₂	22.60 ± 1.70	0.70 ± 0.04	5.60 ± 0.20	2.3 ± 0.04	2.60 ± 0.30		
	<i>Pseudot. hypogea</i>	70	SB	no	0.12/0.05	Glucose (28)	N ₂	8.80 ± 1.10	1.10 ± 0.30	6.40 ± 0.10	0.10 ± 0.00	2.90 ± 0.10		
							CO ₂	4.30 ± 0.10	0.50 ± 0.10	3.10 ± 0.20	0.10 ± 0.00	3.40 ± 0.30		
	<i>Pseudot. elfii</i>	70	SB	no	0.12/0.05	Glucose (28)	N ₂	7.00 ± 0.90	2.00 ± 0.20	8.30 ± 0.06	0.20 ± 0.03	4.20 ± 0.30		
							CO ₂	6.70 ± 0.20	2.10 ± 0.10	7.80 ± 0.30	0.10 ± 0.01	10.0 ± 0.30		
	<i>Pseudot. lettingae</i>	70	SB	no	0.12/0.05	Glucose (28)	N ₂	9.30 ± 0.50	1.20 ± 0.10	5.10 ± 0.05	0.20 ± 0.00	2.70 ± 0.05		
							CO ₂	8.10 ± 0.70	1.30 ± 0.30	4.40 ± 0.10	0.05 ± 0.01	3.70 ± 0.20		
Gas sparging	<i>Pseudot. subterranea</i>	70	SB	no	0.12/0.05	Glucose (28)	N ₂	23.10 ± 2.10	1.80 ± 0.20	30.60 ± 6.90	16.20 ± 4.60	9.50 ± 0.40		[68]
							CO ₂	27.00 ± 1.40	1.40 ± 0.10	31.90 ± 7.90	10.70 ± 4.0	20.0 ± 8.0		
	<i>Pseudot. thermarum</i>	80	SB	no	0.12/0.05	Glucose (28)	N ₂	Complete	1.8 ± 0.02	30.00 ± 2.20	6.50 ± 0.20	1.10 ± 0.07		
							CO ₂	Complete	1.50 ± 0.10	24.80 ± 0.70	5.60 ± 0.60	2.20 ± 0.20		
Biomass (g CDW/L)	<i>T. neapolitana</i>	80	Flask	300	0.25/0.2	Glucose (28)	0.46	3.2 ± 0.04	2.39	34.3 ± 0.6	10.9 ± 0.4			[68]
							0.91	2.9 ± 0.06	2.44	32.9 ± 0.8	12.2 ± 0.8			
							1.33	3.4 ± 0.01	2.58	32.3 ± 0.2	11.5 ± 0.5			
							1.74	3.0 ± 0.04	2.37	31.4 ± 1.1	14.7 ± 0.7			

Table 2. Cont.

Parameter	Organism	T (°C)	Culture Type	Mixing Speed (rpm)	Reactor/Working Volume (L)	Substrate Loaded (mmol/L)	Operational Parameter	Substrate Consumed (mmol/L)	Products					Ref.
									H ₂ yield ^a	AA (mmol/L)	LA (mmol/L)	ALA (mmol/L)	But (mmol/L)	
pH	<i>T. neapolitana</i> subsp. <i>capnolactica</i>	80	SB	no	0.12/0.03	Glucose (28)	w/o	18.54 ± 0.15	1.78 ± 0.29	22.76 ± 0.40	11.35 ± 0.62			[67]
							0.01M MOPS	26.42 ± 0.05	3.27 ± 0.18	26.65 ± 0.87	14.23 ± 0.22			
							0.01M TRIS	25.55 ± 0.06	3.10 ± 0.10	26.77 ± 0.29	12.08 ± 0.89			
							0.01M HEPES	25.99 ± 0.03	2.85 ± 0.40	25.56 ± 0.49	13.58 ± 0.88			
							0.01M HCO ₃ [−]	25.62 ± 0.10	2.20 ± 0.30	22.82 ± 0.84	14.63 ± 3.23			
							0.01M phosphate	26.17 ± 0.26	2.78 ± 0.40	24.70 ± 0.59	14.92 ± 0.25			
	<i>T. neapolitana</i>	75	CSABR	300	3.0/1.0	Glucose (28)	w/o pH control	21.98 ± 1.11	2.05 ± 0.1	30.81 ± 1.5	3.33 ± 0.22			[113]
							plus pH control	27.47 ± 1.39	3.2 ± 0.16	38.3 ± 2.0	1.77 ± 0.11			
						Xylose (33.3)	w/o pH control	29.77 ± 1.46	1.84 ± 0.09	34.47 ± 1.66	3.77 ± 0.22			
							plus pH control	31.83 ± 1.6	2.22 ± 0.11	41.8 ± 2.0	1.66 ± 0.11			
pH	<i>T. neapolitana</i>	75	CSABR	300	3.0/1.0	Sucrose (14.6)	w/o pH control	13.78 ± 0.7	3.52 ± 0.18	33.13 ± 1.65	3.11 ± 0.11			[113]
							plus pH control	14.69 ± 0.06	4.95 ± 0.25	35.47 ± 1.83	2.11 ± 0.11			
						Xylose (33.3)	w/o pH control	29.44	1.85 ± 0.09	34.97 ± 1.66	3.88 ± 0.22			
							pH = 6.5	32.57	2.71 ± 0.14	49.62 ± 2.50	3.44 ± 0.11			
							pH = 7.0	32.9	2.84 ± 0.14	50.29 ± 2.50	4.00 ± 0.22			
							pH = 7.5	31.77	2.23 ± 0.11	41.96 ± 2.16	1.89 ± 0.11			
		75	SB	no	0.04/ 0.12	Glycerol (108.6)	w/o HEPES	16.96 ± 0.8	1.23 ± 0.06	9.14 ± 0.45				[116]
							0.05 M HEPES	28.26 ± 1.4	2.73 ± 0.14	22.35 ± 1.05				
pH	<i>T. neapolitana</i>	80	B	250	3.8/1.0	Glucose (28)	w/o NaHCO ₃	25.9 ± 1.3	2.8	44.5 ± 5.4	12.5 ± 2.69			[31]
							NaHCO ₃ 14 mM	25.4 ± 2.1	1.7	30.5 ± 4.9	18.0 ± 0.6			
							NaHCO ₃ 20 mM	23.2 ± 1.9	1.0	44.4 ± 8.2	9.2 ± 2.7			
							NaHCO ₃ 40 mM	6.2 ± 0.8	2.7	18.0 ± 4.3	0.7 ± 1.5			
		75	B	no	0.12/0.04	Glycerol (108.6)	w/o IA	-	438 ± 22 ^b	7.49 ± 0.33	3.55 ± 0.22 *			[122]
							1.5 g/L IA	-	619 ± 30 ^b	11.49 ± 0.5	1.66 ± 0.0 *			

Table 2. Cont.

Parameter	Organism	T (°C)	Culture Type	Mixing Speed (rpm)	Reactor/ Working Volume (L)	Substrate Loaded (mmol/L)	Operational Parameter	Substrate Consumed (mmol/L)	Products					Ref.
									H ₂ yield ^a	AA (mmol/L)	LA (mmol/L)	ALA (mmol/L)	But (mmol/L)	
Temp. (°C)	<i>T. neapolitana</i>	60	SB	75	0.26/0.05	Glucose (14)	60	2.2 *	2.04 ± 0.05	2.0	n. d			[65]
		65					65	5.0 *	3.09 ± 0.3	7.0	0.05			
		70					70	8.5 *	3.18 ± 0.02	11.5	0.45			
		77					77	11.0 ± 0.5 *	3.85 ± 0.28	16.5	0.85 ± 0.1			
		85					85	11.0 ± 0.5 *	3.75 ± 0.49	18.0 ± 1.0	1.25 ± 0.05			
Oxygen	<i>T. maritima</i>	80	B	150	2.30/1.53	Glucose (20)	w/o O ₂	17.41	38.09 ^b	18.05	4.36	1.60 ± 0.2		[129]
							with O ₂	19.30	31.75 ^b	18.27	5.45	1.30 ± 0.2		

3. Nitrogen Containing-Compounds

Nitrogen sources (N-sources) are essential for bacterial life for the synthesis of cellular components like nucleic acids, proteins, and enzymes [133,134]. Yeast extract (YE), tryptone, and ammonium chloride (NH_4Cl) have been identified as highly efficient and versatile organic N-sources in laboratory practices. It is widely demonstrated that most of the *Thermotogae* members can use yeast extract and tryptone to grow and metabolize carbohydrates [1,10,77,108,135,136].

Numerous efforts were made to replace YE by combining casamino acids and amino acids, but *Pseudot. elfii* failed to grow on these alternative substrates. The biogas yields of cultures grown with other N-sources were about 4–14% of those with YE (Table 3) [108].

Experiments with different concentrations of YE and tryptone were performed to identify their optimal and minimal concentrations in growth media [64,108,122,137,138]. YE and tryptone are sufficient to ensure growth and hydrogen production without additional carbon sources in *Pseudot. elfii* (Table 3) [108]. van Niel et al. [108] used media with various concentrations of YE and tryptone to ferment glucose by *Pseudot. elfii* [108]. They discovered that increasing the contents of both YE and tryptone from 2 g/L to 5 g/L improved H_2 production (14.8 vs. 28.8 mmol/L) but higher contents did not further improve hydrogen and acetic acid production; high levels of both YE and tryptone only increased acetic acid production in medium lacking other C-sources [108].

When there was a low level of YE (2 g/L) but no tryptone, productions of H_2 and acetic acid remained low, suggesting that tryptone served as an energy source like YE (Table 3) [108]. Although the amino acid compositions of the two N-sources are fairly similar, tryptone contains abundant peptides, a preferred form of amino acids by many bacteria [138]. In another study [122], *T. neapolitana* biomass increased along with the increase of YE concentrations in the range of 1.0–4.0 g/L but not with higher YE concentrations (5.0–6.0 g/L) [122]. The H_2 production plateaued at 420 mL/L in *T. neapolitana* growing on glycerol with 1.0–4.0 g/L YE [122]. Experiments in *T. maritima* and *T. neapolitana* revealed that with over 2 g/L YE, there was a clear increase of acetic acid production, and hydrogen counted up to 30–33% of the total gas in the headspace, even though a mild reduction in glucose consumption occurred (Table 3) [64,138].

Nevertheless, low concentrations (2–4 g/L) of YE are still able to support productivity and bacterial growth [64,108,122,138]. d'Ippolito et al. [30] reported that 2 g/L of both tryptone and YE contributed to 10–15% of the total fermentation products in *T. neapolitana* [30]. Balk et al. [75] demonstrated that *Pseudot. lettingae* was able to degrade methanol in around 30 days in the presence of 0.5 g/L YE, whereas the substrate degradation did not occur when YE was omitted [75]. In contrast, the fermentation of *T. neapolitana* with glucose occurred in a medium without YE, even though the total glucose consumption without YE was attained in 30 h rather than 12 h. H_2 and acetate amounts were half in the medium without YE, (Table 3) [135].

The impact of an inorganic N-source on *Thermotogae* fermentation, such as NH_4Cl , has not been extensively studied, but the presence of NH_4Cl has often been associated with either exopolysaccharide (EPS) formation in *T. maritima* or alanine production in *T. neapolitana* [62,129,136,139]. It is not clear how NH_4Cl stimulates EPS production, but it might involve processing the surplus of reducing equivalents. For example, some organisms produce EPS as a mechanism to transport reducing equivalents out of the cell [140].

Han and Xu [61] demonstrated that a surplus of NH_4Cl could partially substitute YE and tryptone in an optimized medium for auxotrophic *Thermotoga* sp. RQ7 strain [61].

4. Sodium Chloride and Phosphate

All members of the phylum *Thermotogae* showed great adaptability to a wide range of salinity levels (Table 1), although the optimal concentrations of NaCl vary among the members. *Geotoga*, *Oceanotoga*, and *Petrotoga* species can survive in environments comprised of 10% NaCl, while *P. mexicana* can live in up to 20% NaCl (Table 1) [10,12,95].

In contrast, species of the genus *Fervidobacterium* can tolerate salt concentrations up to 1% [5,79–81,83]. Among the species of the genus *Mesotoga*, *Ms. infera* exhibited the lowest tolerance of NaCl (Table 1).

NaCl at 20 g/L was reported to be optimal for *T. neapolitana* growing on either glucose or glycerol when hydrogen production is concerned [64,105,106,108,110,116]. Recently, the effect of different NaCl concentrations (0–35 g/L) on the CLF process was explored in *T. neapolitana* subs. *capnolactica* using glucose as the carbon source [67]. H₂ synthesis and biomass growth were reduced by 15% and 25%, respectively, when NaCl was increased to 35 g/L (Table 3). Similarly, acetic acid production decreased from 26.1 ± 4.7 mM with 10 g/L NaCl to 23.2 ± 0.8 mM with 35 g/L NaCl. In contrast, high NaCl levels had a positive impact on lactic acid production, which increased 7.5-fold (2.8 ± 0.3 mM at 0 g/L NaCl vs. 21.6 ± 6.2 mM at 35 g/L NaCl), without affecting the overall H₂ yields (Table 3) [67]. Pradhan and coworkers [67] suggested a possible involvement of NaCl in a sodium ion gradient that potentially fuels ATP synthesis and transport processes [67]. This creates a bioenergetic balance and supplies necessary reducing equivalents to convert acetic acid into lactic acid under CLF conditions (Figure 1) [67,118,119]. Similarly, another study [141] on H₂-producing *Vibrionaceae* showed that increasing NaCl levels from 9 to 75 g/L enhanced lactic acid synthesis [141].

Regarding phosphate species, they have a strong buffering ability to mitigate pH fluctuation caused by the accumulation of volatile fatty acids [142]. Phosphate deficiency induced an increase in lactic acid production and a small decrease in H₂ formation, suggesting a slight shift of the *T. maritima* metabolism towards lactic acid production. Besides its role as a macro-element, phosphate can also interact with calcium, favoring H₂ production [141,143]. Saidi and co-workers [52] showed that *T. maritima* struggled to produce H₂ at the same rate when there was an oversupply of calcium but an undersupply of phosphate in the medium [52]. For unknown reasons, phosphate exceeding 50 mM has been suggested to inhibit *Pseudot. elfii* growth [108].

Table 3. Effect of organic nitrogen source and NaCl on *Thermotoga* fermentation. **AA:** Acetic acid; **LA:** Lactic acid; **ALA:** Alanine; **YE:** Yeast extract; **Tryp:** Tryptone; **CA:** Casamino acids; **V:** Vitamins solution [108]; **aa:** Amino acids (cysteine, alanine, asparagine, proline, glutamine, serine, and tryptophan, added at 0.2 g/L each). Experiments were performed in different bioreactor configurations: **B** = Batch; **SB** = Serum bottles. **H₂ column:** ^a % H₂ = calculated setting hydrogen production yield on medium with yeast extract to 100%; ^b mmol H₂/L medium; ^c mL H₂/L culture; ^d mol H₂/mol glucose. * Values extrapolated from the graphical representation of data.

Parameter	Organism	T (°C)	Culture Type	Mixing Speed (rpm)	Reactor/Working Volume (L)	Substrate Loaded (mmol/L)	Operational Parameter	Substrate Consumed (mmol/L)	Products				Ref.
									H ₂	AA (mmol/L)	LA (mmol/L)	ALA (mmol/L)	
Nitrogen sources (g/L)	<i>Pseudot. elfii</i>	65	B	100	3.0/1.0	no	w/o YE	-	40 ^a				[108]
							CA + V	-	4 ^a				
							CA + V + aa	-	6 ^a				
		65	B	100	3.0/1.0	Glucose (22.4)	YE (5)	n.d.	100 ^a				
							CA + V	n.d.	14 ^a				
							CA + V + aa	n.d.	14 ^a				
		65	B	100	3.0/1.0	no	YE (2) -Tryp (0)	-	13.9 ^b	3.5			
							YE (2) -Tryp (2)	-	14.8 ^b	3.4			
							YE (5) -Tryp (0)	-	14.0 ^b	0.0			
							YE (5) -Tryp (5)	-	28.8 ^b	4.9			
							YE (2) -Tryp (0)	10.3	25.8 ^b	10.7			
	<i>T. neapolitana</i>	65	B	100	3.0/1.0	Glucose (56)	YE (2) -Tryp (2)	18.3	78.5 ^b	19.7			[64]
							YE (5) -Tryp (0)	13.1	84.9 ^b	26.3			
							YE (5) -Tryp (5)	17.9	82.5 ^b	21.2			
							YE (0.5)	26.6 *	260 ^{ac}	15 *			
							YE (1.0)	26 *	320 ^{ac}	22.5 *			
Nitrogen sources (g/L)	<i>T. neapolitana</i>	80	SB	no	0.12/0.05	Glucose (28)	YE (2.0)	25.5 *	360 ^{ac}	26.6 *			[64]
							YE (4.0)	25 *	430 ^{ac}	30 *			
							YE (6.0)	25 *	430 ^{ac}	33.3 *			
	<i>T. maritima</i>	80	SB	no	0.12/0.05	Glucose (28.00)	YE (0.5)	25.5 *	190 ^{ac}	0.0 *			
							YE (1.0)	25 *	260 ^{ac}	20.8 *			
							YE (2.0)	25 *	270 ^{ac}	23 *			
	<i>T. maritima</i>	80	SB	no	0.12/0.05	Glucose (28.00)	YE (4.0)	25 *	335 ^{ac}	27.5 *			[64]
							YE (6.0)	24 *	390 ^{ac}	28 *			
	<i>T. neapolitana</i>	77	B	75	0.12/0.05	Glucose (28)	no YE	23 *	9 ^{ab}	4.2 *			[136]
							YE (0.5)	Completed *	16 ^{ab}	7.2 *			

Table 3. Cont.

Parameter	Organism	T (°C)	Culture Type	Mixing Speed (rpm)	Reactor/Working Volume (L)	Substrate Loaded (mmol/L)	Operational Parameter	Substrate Consumed (mmol/L)	Products				Ref.
									H ₂	AA (mmol/L)	LA (mmol/L)	ALA (mmol/L)	
NaCl (g/L)	<i>T. neapolitana</i> subsp. <i>capnolactica</i>	80	SB	no	0.12/0.03	Glucose (28)	w/o	25.62 ± 0.07	2.30 ± 0.50 ^d	20.66 ± 0.27	2.80 ± 0.26	1.28 ± 0.9	[67]
							NaCl (5)	26.00 ± 0.14	2.50 ± 1.20 ^d	24.59 ± 0.95	6.23 ± 3.26	1.61 ± 0.58	
							NaCl (10)	26.12 ± 0.16	3.10 ± 0.80 ^d	26.05 ± 4.69	11.61 ± 2.42	2.46 ± 0.24	
							NaCl (20)	25.96 ± 0.11	3.30 ± 0.20 ^d	25.58 ± 1.03	13.44 ± 0.94	2.41 ± 0.09	
							NaCl (30)	25.68 ± 0.25	2.91 ± 0.37 ^d	23.22 ± 0.81	21.63 ± 6.15	2.38 ± 0.10	

5. Sulfur-Containing Compounds

All members of the phylum *Thermotogae* reduced sulfur-containing compounds such as elemental sulfur (S^0), thiosulfate (Thio), and polysulfide to hydrogen sulfide (H_2S), which is produced at the expense of H_2 (Table 1) [1,4,29,76,144,145]. Sufficient supply of sulfur-containing compounds seems to be critically important; due to a large requirement for Fe-S clusters by the hydrogenase (containing 20 atoms of Fe and 18 atoms of S), PFOR, and other enzymes (Figure 1) [123,146]. In the literature, the effect of sulfur sources has been widely explored. The reduction of S-sources is considered an electron-sink reaction to deplete the surplus of electron power [3,98,107,147]. It is well known that the growth of most anaerobic bacteria of the phylum *Thermotogae* is stimulated by S-sources, but not dependent on them [1,29,52,53,75,107,125,126,144]. Generally speaking, the substrate consumption rate is benefited from a sulfur supply in the medium, except for the methanol fermentation in *Pseudot. lettingae*, which is reduced by S-containing compounds (19.7 mmol/L w/o S-source, 18.7 mmol/L with Thio and 10.6 mmol/L with S^0) (Table 4). Members of the *Mesotoga* genus are able to oxidize sugars, although with low efficiency, only when S^0 is used as the terminal electron acceptor [26,27,66,148,149]. This process gives acetic acid, CO_2 , and sulfide (2 mol of acetate and 4 mol of sulfide per mol of glucose), with no or trace amounts of H_2 (Table 4) [27]. After 250 days of *Ms. prima* cultivation, 9.21 ± 0.13 mmol/L of acetate was measured in the presence of S^0 rather than 1.67 ± 0.21 mM obtained in its absence (Table 4) [27]. Fadhlou and collaborators [27] argued that the metabolic differences between *Thermotoga* spp. and *Ms. prima* strains are related to the absence of a bifurcating [FeFe]-hydrogenase and the accumulation of NADH in *Ms. prima*, leading to growth inhibition in the absence of an external electron acceptor [27]. However, *Ms. prima* and *Ms. infera* strains grew more efficiently in a syntrophic association with a hydrogenotrophic microbial partner that serves as a biological electron acceptor compared to growing *Mesotoga* in a pure culture with sulfur as electron acceptor [26,27]. Boileau et al. [107] investigated the different responses of fermentation performance to different S-sources (Table 4) [107]. Among these compounds (Table 4), thiosulfate, cysteine, and Na_2S were the most efficient ones to optimize *T. maritima* glucose fermentation (Table 4) [107]. Biogas production and glucose utilization increased in the order of no S-source < DMSO < S^0 < Thio < Methionine (Met) < Na_2S < Cysteine (Cys) (Table 4) [107]. Moreover, Na_2S and Cys increased acetic acid production 3-fold and H_2 production 2-fold (Table 4). Thiosulfate seemed to promote lactic acid formation (0.8 ± 0.1 mM w/o S-source and 6.3 ± 0.6 mM with Thio) without affecting other products [107]. Surprisingly, lactic acid was dependent on thiosulfate concentration (0.3 mol/mol glucose w/o Thio and 0.6 mol/mol glucose with 0.24 mmol Thio), even though the proportion between lactic and acetic acid yields remained constant (Table 4). DMSO had no significant impact on *T. maritima* fermentation parameters (Table 4) [107].

In the presence of thiosulfate, the growth and glutamate production of *Fervidobacterium* is stimulated; however, S^0 does not seem to help overcoming the H_2 -feedback inhibition (Table 4) [32,80,88,144]. *P. olearia*, *P. sibirica*, and *Ts. africanus* produced small amounts of ethanol (0.17 mM for both *Petrotoga* species and 0.79 mM for *Ts. africanus*) only in the absence of S-sources (Table 4) [93,145]. *Pseudot. lettingae* produced L-alanine, at the expense of acetic acid, only when thiosulfate or S^0 was present in the medium using methanol as the substrate (Table 4) [75]. Meanwhile, the presence of thiosulfate or S^0 resulted in increased production of acetic acid and decreased production of alanine in *Pseudot. hypogea*, *Ts. melaniensis*, *Ts. geolei*, *P. olearia*, and *P. sibirica* cultures, using glucose or xylose as the carbon source (Table 4) [77,87,90,93]. When S^0 is available, no hydrogen could be detected in *Mn. hydrogenitolerans* growing on glucose [101].

Thermotogae members have been widely employed to degrade different organic wastes, and their degradation significantly benefited from the presence of a reducing agent [51–54,113,116,138]. It is noteworthy to mention that high concentrations of thiosulfinate, a volatile organo-sulfur compound found in organic wastes, has an inhibitory effect on *T. maritima* growth [54]. Similarly, Tao et al. [150] demonstrated that thiosulfinate inhibited the H_2 production by mesophilic seed sludge when co-fermenting food wastes [150].

Table 4. : Effect of sulfur compounds on *Thermotogae* fermentation. **AA**: Acetic acid; **LA**: Lactic acid; **ALA**: Alanine; **EtOH**: Ethanol; **iVal**: isovalerate; **H₂S**: Hydrogen sulfide; **Glu**: Glutamate; **DMSO**: Dimethyl Sulfoxide; **S⁰**: Elemental sulfur; **Met**: Methionine; **Thio**: Thiosulfate; **Cys**: Cysteine; **Na₂S**: Sodium sulfide. * Values extrapolated from the graphical representation of data. ** Concentrations of Sulfur compounds are 0.03 mol equivalent of sulfur. ^a H₂ produced millimolar equivalent; ^b mmol; ^c μM.

Organism	Carbon Source (mM)	Sulfur Source (mM)	Substrate Consumed (mmol/L)	Products mmol/L Culture							Ref.	
				H ₂	AA	LA	ALA	EtOH	iVal	H ₂ S		Glu
<i>T. maritima</i>	Glucose (25)	w/o	7.1 ± 0.4	21.3 ± 2.1	10.1 ± 0.8	0.8 ± 0.1	-					[107]
		DMSO **	9.2 ± 0.5	28.7 ± 2.9	13.3 ± 1.1	0.8 ± 0.1	-					
		S ⁰ **	16.6 ± 0.8	46.1 ± 4.6	23.8 ± 1.9	3.4 ± 0.3	-					
		Met **	18.3 ± 0.9	53.3 ± 5.3	26.5 ± 2.1	3.1 ± 0.3	-					
		Thio **	17.5 ± 0.9	47.3 ± 4.7	24.1 ± 1.9	6.3 ± 0.6	-					
		Cys **	20.4 ± 1.0	58.5 ± 5.8	30.5 ± 2.4	4.1 ± 0.4	-					
		Na ₂ S **	20.4 ± 1.0	54.9 ± 5.5	30.7 ± 2.5	4.7 ± 0.5	-					
	Glucose (60)	w/o Thio	17.7 ± 1.9	25.0 ± 2.2	12.8 ± 1.0	5.4 ± 0.6	1.39 ± 0.2					
		Thio (0.01)	20.0 ± 1.1	31.0 ± 2.3	16.0 ± 0.8	10.2 ± 1.1	-					
		Thio (0.03)	28.0 ± 1.5	57.9 ± 4.8	30.6 ± 1.9	8.2 ± 0.7	-					
		Thio (0.06)	38.5 ± 2.0	73.3 ± 5.9	38.2 ± 2.4	18.1 ± 1.8	-					
		Thio (0.12)	45.7 ± 2.5	99.7 ± 8.3	52.4 ± 3.3	15.4 ± 1.6	3.8 ± 0.3					
		Thio (0.18)	45.4 ± 2.2	86.9 ± 8.2	45.0 ± 2.2	23.4 ± 2.3	-					
		Thio (0.24)	43.8 ± 2.2	88.6 ± 8.9	46.1 ± 3.3	26.4 ± 1.4	3.8 ± 0.2					
Glucose (20)	w/o	13.70	36.09	15.62		0.70			n.d.		[145]	
	Thio (20)	13.55	4.02	15.99		0.80			14.45			
<i>T. neapolitana</i>	Glucose (20)	w/o	14.00	31.67	18.27		0.87			n.d.		[145]
		Thio (20)	13.90	16.07	16.12		0.60			7.39		
<i>Pseudot. lettingae</i>	Methanol (20)	w/o	19.70	n. d.	13.70		-			-		[75]
		Thio (20)	18.7	n. d.	-		5.8			11.2		
		S ⁰ (2%)	10.6	n. d.	-		3.1			7.3		
<i>Pseudot. hypogea</i>	Glucose (20)	w/o	8.60	29.03	4.49		1.71			n. d.		[145]
		Thio (20)	14.39	2.29	19.7		1.06			15.08		

Table 4. Cont.

Organism	Carbon Source (mM)	Sulfur Source (mM)	Substrate Consumed (mmol/L)	Products mmol/L Culture								Ref.
				H ₂	AA	LA	ALA	EtOH	iVal	H ₂ S	Glu	
<i>Pseudot. hypogea</i>	Glucose (20)	w/o	7.0	9.4 ^a	5.0		1.7	1.0		0.2		[77]
		Thio (20)	13.0	0.9 ^a	19.8		1.0	1.6		15.1		
<i>Pseudot. hypogea</i>	Xylose (20)	w/o	12.9	19.0 ^a	8.9		2.4	1.0		0.2		[77]
		Thio (20)	12.0	1.8 ^a	13.7		1.3	1.0		7.5		
<i>Pseudot. elfii</i>	Glucose (20)	w/o	3.1	8.8	4.0					0.0		[77]
		Thio (20)	10.4	2.0	17.9					23.00		
	Glucose (20)	w/o	2.75	7.70	3.49		1.05			n. d.		[145]
		Thio (20)	8.15	n. d.	12.63		0.41			14.55		
<i>Ts. geolei</i>	Glucose (0.28)	w/o	7.0 ^b	9.3 ^a	8.5 ^b		1.2 ^b			0.5 ^b		[87]
		S ⁰ (2%)	6.0 ^b	0.0 ^a	7.5 ^b		0.5 ^b			12.5 ^b		
<i>Ms. Prima Phos Ac3</i>	Glucose (20)	w/o	1.50 ± 0.20	<1 ^c	1.67 ± 0.21					1.05 ± 0.25		[27]
		S ⁰	6.57 ± 0.19	<1 ^c	9.21 ± 0.13					24.40 ± 0.30		
<i>Ms. Prima MesGIAg4.2T</i>	Fructose (20)	w/o	1.00 ± 0.23	<1 ^c	0.70 ± 0.41					1.18 ± 0.41		
		S ⁰	3.27 ± 0.85	<1 ^c	8.48 ± 1.96					18.03 ± 5.16		
<i>Ts. africanus</i>	Glucose (28)	w/o	7.20	16.80	7.90	<0.2		0.79		n.d.		[145]
		Thio (20)	7.70	1.00	12.40	-		-		14.60		
<i>Ts. atlanticus</i>	Glucose (28)	w/o	5.6	12.5	1.7				0.14	-		[92]
		S ⁰ (1%)	6.0	7.5	1.9				0.15	1.3		
<i>F. islandicum</i>	Glucose (20)	w/o	14.20	21.58	6.25		3.98			n.d.		[145]
		Thio (20)	16.20	n. d.	20.25		1.22			34.02		
<i>F. pennavorans</i>	Glucose (11)	w/o	-	0.25 *	6.7 *		4.0 ± 0.5 *				1.3 *	[32]
		Thio (20)	-	0.2 *	6.7 *		4.50 *				No *	

6. Metal Ions

Typically, hydrothermal ecosystems are enriched with essential micronutrients and trace metals such as soluble and insoluble iron, manganese, cobalt, and molybdenum. Some terrestrial hydrothermal waters are also characterized by chromium and uranium contents of several micrograms per liter [151]. The physiological roles that most of these metals play in microbial metabolism are still largely unknown. It is believed that their functions include energy generation and biosynthesis [151]. In addition, Mn, Fe, Zn, and Co metals are vitally important micro-elements for growth, essential for cellular transport processes, and serve as cofactors for many enzymes [152]. Understanding the physicochemical properties of extreme habitats can help to determine the metal toxicity limits on microbial growth in laboratory settings. Indeed, metal susceptibility tests have been carried out on *T. neapolitana*, *T. maritima*, and *Ts. africanus*, and have identified the following toxicity order: cadmium (1.0–10.0 μ M) > zinc (0.01–0.1 mM) > nickel (1.0–5.0 mM) > cobalt (1.0–10.0 mM) [153].

Attention has also been paid to Fe (III) reduction by thermophilic bacteria, since Fe (III) may work as an external electron acceptor in microbial metabolism [154]. Members of the phylum *Thermotogae* are capable of coupling the reduction of iron with the oxidation of a wide range of organic and inorganic compounds. *T. maritima* reduced Fe (III) into Fe (II) exclusively with molecular hydrogen as an electron donor [154]. Fe (III) reduction has also been reported to stimulate growth and mitigate H₂ inhibition in *Pseudot. lettingae*, *Pseudot. subterranea*, *Pseudot. elfii*, *Ts. affectus*, *Ts. globiformans*, and *Ts. activus* [75,76,88,89,91]. The recently characterized member of the order *Mesoaciditogales*, *A. saccharophila*, changed fermentation end-products when growing with Fe (III), favoring the production of small amounts of acetate, isobutyrate, and isovalerate [14].

Ions and metals are generally supplied in *Thermotogae* growth media through Balch's oligo-elements solution [155]. The removal of oligo-elements from *T. maritima* cultures resulted in a minor increase in lactic acid production (1.2 vs. 4.3 mmol/L) and a decrease in H₂ productivity (12.4 vs. 8.8 mmol/h/L) [52]. Limitation in iron lowered H₂ production by deviating the fermentation pathway towards the production of more reduced end-products such as lactic acid in mixed cultures [156,157]. Another study [139] highlighted how the supplementation of Fe ions to mixed cultures had pronounced effect on hydrogen activity [139]. Similarly, Fe²⁺ (as well as Co, Ni and Mn) stimulated *Pseudot. hypogea* alcohol dehydrogenase activity (ADH), an iron-containing enzyme involved in alcohol fermentation, by 10–15%, while Zn²⁺ completely inhibited the enzyme activity [158]. On the same base, the inclusion of tungsten in the growth medium of *T. maritima* increased the specific activity of both hydrogenase (by up to 10-fold) and PFOR in cell-free extracts, although the function of tungsten in the metabolism of *T. maritima* is not clear [123,126].

As for magnesium, potassium, and calcium ions, they not only play critical roles in bacterial growth, but also act as enzyme cofactors and ensure the survival of microorganisms in their hot ecosystems, by protecting double-stranded DNA from degradation [159]. The best cell yields were obtained with a low concentration of Mg²⁺ and a high concentration of Ca²⁺ [126]. It would be worthwhile to dig further into the metal ions repercussions on *Thermotogae* metabolism in future research.

7. Conclusions

Steam reforming of methane (CH₄) is currently used to produce hydrogen in the industry, as it is the most economic technology available so far. Producing hydrogen by biological means at an industrial scale remains as a challenge. Within the race to find the best way to generate hydrogen via microbes (e.g., choice of strains, substrates, fermentation conditions), *Thermotogae* seem to have many unique advantages. Optimization of their cultivation conditions is fundamental to improve the overall productivity of the fermentation system and its profitability, which determine the feasibility of replacing the current methods of hydrogen production.

The phylum *Thermotogae* comprises a wide collection of species with astonishing and unique features associated to their original habitats. Extensive research has shown tremen-

dous potentials of using these bacteria in biological production of hydrogen, degradation of wastes, and isolation of thermostable enzymes.

Many factors affect the anaerobic metabolism of *Thermotogae* species, including operating conditions (shaking, inoculum, gas sparging, and culture/headspace volume ratio), temperature, pH, nitrogen, sulfur-containing compounds, sodium chloride, phosphate, and metal ions. Optimization of these fermentation parameters has been intensively pursued with *Thermotoga* and *Pseudothermotoga* species, which are the best hydrogen producers in the phylum. In contrast, little is known regarding other species of the phylum, especially their ability to synthesize desirable biological products.

In general, *Thermotogae* fermentation is affected by the accumulation of produced biogas and organic acids because they increase hydrogen partial pressure inside of the bioreactor and drastically reduce the pH of the cultivation medium. Consequently, the metabolic process stops before the substrate is completely consumed. Gas sparging, stirring, and adjusting culture/headspace volume ratio can help to overcome the inhibition on growth caused by hydrogen accumulation. Implementing these strategies and adjusting pH during the fermentation process can result in high hydrogen yields and efficient consumption of substrates. A reduction of fermentation time by starting with the right inoculum size could cast favorable great perspectives on the economics of the industrial processes.

This review highlights the importance of nitrogen-containing compounds that need to be supplied to the medium to stimulate bacterial growth. Overall, yeast extract and tryptone are the preferred forms of nitrogen. Sulfur-containing compounds not only play a critical role in bacterial growth but also divert reducing power to selectively produce certain end-products in *Thermotogae* metabolism.

Until now, the impact of metal ions and salts on the fermentation process has not been well investigated even though it has been demonstrated that they could stimulate many key enzymes involved in various metabolic pathways.

In summary, the extensive data collection of this review offers a great reference for the optimization and development of sustainable bioprocesses based on *Thermotogae* species and helps to generate insightful perspectives for the exploitation of these anaerobic bacteria in biotechnological processes.

Funding: This research was funded by BioRECO₂VER Project, through the European Union's Horizon 2020 Research and Innovation Programme under Grant Agreement No. 760431.

Acknowledgments: The authors would like to thank Lucio Caso (CNR-ICB) for the technical support in preparing the manuscript.

Conflicts of Interest: The authors declare no conflict of interest. The funding agencies gave their permissions to the publication of manuscript.

References

1. Huber, R.H.M. *Thermotogales*; Dworkin, M., Falkow, S., Rosenberg, E., Schleifer, K.H., Stackebrandt, E., Eds.; Springer: New York, NY, USA, 2006; pp. 899–922.
2. Bhandari, V.; Gupta, R.S. The Phylum Thermotogae. In *The Prokaryotes*; Rosenberg, E., DeLong, E.F., Lory, S., Stackebrandt, E., Thompson, F., Eds.; Springer: Berlin/Heidelberg, Germany, 2014.
3. Huber, R.; Langworthy, T.A.; König, H.; Thomm, M.; Woese, C.R.; Sleytr, U.B.; Stetter, K.O. *Thermotoga maritima* Sp. Nov. Represents a New Genus of Unique Extremely Thermophilic Eubacteria Growing up to 90 °C. *Arch. Microbiol.* **1986**, *144*, 324–333. [[CrossRef](#)]
4. Belahbib, H.; Summers, Z.M.; Fardeau, M.; Joseph, M.; Tamburini, C.; Dolla, A.; Ollivier, B.; Armougom, F. Towards a Congruent Reclassification and Nomenclature of the Thermophilic Species of the Genus *Pseudothermotoga* within the Order Thermotogales. *Syst. Appl. Microbiol.* **2018**, *41*, 555–563. [[CrossRef](#)] [[PubMed](#)]
5. Patel, B.K.C.; Morgan, H.W.; Daniel, R.M. *Fervidobacterium nodosum* Gen. Nov. and Spec. Nov., a New Chemoorganotrophic, Caldoactive, Anaerobic Bacterium. *Arch. Microbiol.* **1985**, *141*, 63–69. [[CrossRef](#)]
6. Windberger, E.; Huber, R.; Trincone, A.; Fricke, H.; Stetter, K.O. *Thermotoga thermarum* Sp. Nov. and *Thermotoga Neapolitana* Occurring in African Continental Solfataric Springs. *Arch. Microbiol.* **1989**, *151*, 506–512. [[CrossRef](#)]

7. DiPippo, J.L.; Nesbø, C.L.; Dahle, H.; Doolittle, W.F.; Birkland, N.K.; Noll, K.M. *Kosmotoga olearia* Gen. Nov., Sp. Nov., a Thermophilic, Anaerobic Heterotroph Isolated from an Oil Production Fluid. *Int. J. Syst. Evol. Microbiol.* **2009**, *59*, 2991–3000. [[CrossRef](#)] [[PubMed](#)]
8. Nesbø, C.L.; Bradnan, D.M.; Adebuseyi, A.; Dłutek, M.; Petrus, A.K.; Foght, J.; Doolittle, W.F.; Noll, K.M. *Mesotoga prima* Gen. Nov., Sp. Nov., the First Described Mesophilic Species of the Thermotogales. *Extremophiles* **2012**, *16*, 387–393. [[CrossRef](#)]
9. Ben Hania, W.; Godbane, R.; Postec, A.; Hamdi, M.; Ollivier, B.; Fardeau, M.L. *Defluviitoga tunisiensis* Gen. Nov., Sp. Nov., a Thermophilic Bacterium Isolated from a Mesothermic and Anaerobic Whey Digester. *Int. J. Syst. Evol. Microbiol.* **2012**, *62*, 1377–1382. [[CrossRef](#)]
10. Davey, M.E.; Wood, W.A.; Key, R.; Nakamura, K.; Stahl, D.A. Isolation of Three Species of Geotoga and Petrotoga: Two New Genera, Representing a New Lineage in the Bacterial Line of Descent Distantly Related to the “Thermotogales”. *Syst. Appl. Microbiol.* **1993**, *16*, 191–200. [[CrossRef](#)]
11. Wery, N.; Lesongeur, F.; Pignet, P.; Derennes, V.; Cambon-Bonavita, M.A.; Godfroy, A.; Barbier, G. *Marinitoga camini* Gen. Nov., Sp. Nov., a Rod-Shaped Bacterium Belonging to the Order Thermotogales, Isolated from a Deep-Sea Hydrothermal Vent. *Int. J. Syst. Evol. Microbiol.* **2001**, *51*, 495–504. [[CrossRef](#)]
12. Jayasinghearachchi, H.S.; Lal, B. *Oceanotoga Teriensis* Gen. Nov., Sp. Nov., a Thermophilic Bacterium Isolated from Offshore Oil-Producing Wells. *Int. J. Syst. Evol. Microbiol.* **2011**, *61*, 554–560. [[CrossRef](#)]
13. Reysenbach, A.L.; Liu, Y.; Lindgren, A.R.; Wagner, I.D.; Sislak, C.D.; Mets, A.; Schouten, S. *Mesoaciditoga lauensis* Gen. Nov., Sp. Nov., a Moderately Thermoacidophilic Member of the Order Thermotogales from a Deep-Sea Hydrothermal Vent. *Int. J. Syst. Evol. Microbiol.* **2013**, *63*, 4724–4729. [[CrossRef](#)] [[PubMed](#)]
14. Itoh, T.; Onishi, M.; Kato, S.; Iino, T.; Sakamoto, M.; Kudo, T.; Takashina, T.; Ohkuma, M. *Athalassotoga saccharophila* Gen. Nov., Sp. Nov., Isolated from an Acidic Terrestrial Hot Spring, and Proposal of Mesoaciditogales Ord. Nov. and Mesoaciditogaceae Fam. Nov. in the Phylum Thermotogae. *Int. J. Syst. Evol. Microbiol.* **2016**, *66*, 1045–1051. [[CrossRef](#)] [[PubMed](#)]
15. Feng, Y.; Cheng, L.; Zhang, X.; Li, X.; Deng, Y.; Zhang, H. *Thermococcoides shengliensis* Gen. Nov., Sp. Nov., a New Member of the Order Thermotogales Isolated from Oil-Production Fluid. *Int. J. Syst. Evol. Microbiol.* **2010**, *60*, 932–937. [[CrossRef](#)] [[PubMed](#)]
16. Nelson, K.; Clayton, R.; Gill, S.; Gwinn, M.; Dodson, R.; Haft, D.; Hickey, E.; Peterson, J.; Nelson, W.; Ketchum, K.; et al. Evidence for Lateral Gene Transfer between Archae and Bacteria from Genome Sequence of *Thermotoga maritima*. *Nature* **1999**, *399*, 323–329. [[CrossRef](#)] [[PubMed](#)]
17. Connors, S.B.; Mongodin, E.F.; Johnson, M.R.; Montero, C.I.; Nelson, K.E.; Kelly, R.M. Microbial Biochemistry, Physiology, and Biotechnology of Hyperthermophilic Thermotoga Species. *FEMS Microbiol. Rev.* **2006**, *30*, 872–905. [[CrossRef](#)]
18. Rodionov, D.A.; Rodionova, I.A.; Li, X.; Ravcheev, I.; Tarasova, Y.; Portnoy, V.A.; Zengler, K.; Osterman, A.L. Transcriptional Regulation of the Carbohydrate Utilization Network in *Thermotoga maritima*. *Front. Microbiol.* **2013**, *4*, 244. [[CrossRef](#)]
19. Galperin, M.Y.; Noll, K.M.; Romano, A.H. The Glucose Transport System of the Hyperthermophilic Anaerobic Bacterium *Thermotoga neapolitana*. *Appl. Environ. Microbiol.* **1996**, *62*, 2915–2918. [[CrossRef](#)] [[PubMed](#)]
20. Paulsen, I.T.; Nguyen, L.; Sliwinski, M.K.; Rabus, R.; Jr, M.H.S. Microbial Genome Analyses: Comparative Transport Capabilities in Eighteen Prokaryotes. *J. Mol. Biol.* **2000**, *301*, 75–100. [[CrossRef](#)]
21. Nanavati, D.; Thirangoon, K.; Noll, K.M. Several Archaeal Homologs of Putative Oligopeptide-Binding Proteins Encoded by *Thermotoga maritima* Bind Sugars. *Appl. Environ. Microbiol.* **2006**, *72*, 1336–1345. [[CrossRef](#)]
22. Latif, H.; Sahin, M.; Tarasova, J.; Tarasova, Y.; Portnoy, V.A.; Nogales, J.; Zengler, K. Adaptive Evolution of *Thermotoga maritima* Reveals Plasticity of the ABC Transporter Network. *Appl. Environ. Microbiol.* **2015**, *81*, 5477–5485. [[CrossRef](#)]
23. Boucher, N.; Noll, K.M. Substrate Adaptabilities of Thermotogae Mannan Binding Proteins as a Function of Their Evolutionary Histories. *Extremophiles* **2016**, *20*, 771–783. [[CrossRef](#)] [[PubMed](#)]
24. Thauer, R.K.; Jungermann, K.; Decker, K. Energy Conservation in Chemotrophic Anaerobic Bacteria. *Bacteriol. Rev.* **1977**, *41*, 100–180. [[CrossRef](#)] [[PubMed](#)]
25. Ben Hania, W.; Ghodbane, R.; Postec, A.; Brochier-Armanet, C.; Hamdi, M.; Fardeau, M.L.; Ollivier, B. Cultivation of the First Mesophilic Representative (“Mesotoga”) within the Order Thermotogales. *Syst. Appl. Microbiol.* **2011**, *34*, 581–585. [[CrossRef](#)] [[PubMed](#)]
26. Hania, W.B.; Postec, A.; Aüllo, T.; Ranchou-Peyruse, A.; Erauso, G.; Brochier-Armanet, C.; Hamdi, M.; Ollivier, B.; Saint-Laurent, S.; Magot, M.; et al. *Mesotoga infera* Sp. Nov., a Mesophilic Member of the Order Thermotogales, Isolated from an Underground Gas Storage Aquifer. *Int. J. Syst. Evol. Microbiol.* **2013**, *63*, 3003–3008. [[CrossRef](#)] [[PubMed](#)]
27. Fadhlou, K.; Hania, W.B.; Armougom, F.; Bartoli, M.; Fardeau, M.L.; Erauso, G.; Brasseur, G.; Aubert, C.; Hamdi, M.; Brochier-Armanet, C.; et al. Obligate Sugar Oxidation in Mesotoga Spp., Phylum Thermotogae, in the Presence of Either Elemental Sulfur or Hydrogenotrophic Sulfate-Reducers as Electron Acceptor. *Environ. Microbiol.* **2017**, *20*, 281–292. [[CrossRef](#)] [[PubMed](#)]
28. Janssen, P.H.; Morgan, H.W. Heterotrophic Sulfur Reduction by Thermotoga Sp. Strain FjSS3.B1. *FEMS Microbiol. Lett.* **1992**, *96*, 213–218. [[CrossRef](#)] [[PubMed](#)]
29. Schröder, C.; Selig, M.; Schönheit, P. Glucose Fermentation to Acetate, CO₂ and H₂ in the Anaerobic Hyperthermophilic Eubacterium *Thermotoga maritima*: Involvement of the Embden-Meyerhof Pathway. *Arch. Microbiol.* **1994**, *161*, 460–470. [[CrossRef](#)]
30. D’Ippolito, G.; Dipasquale, L.; Vella, F.M.; Romano, I.; Gambacorta, A.; Cutignano, A.; Fontana, A. Hydrogen Metabolism in the Extreme Thermophile *Thermotoga neapolitana*. *Int. J. Hydrogen Energy* **2010**, *35*, 2290–2295. [[CrossRef](#)]

31. Dipasquale, L.; d'Ippolito, G.; Fontana, A. Capnophilic Lactic Fermentation and Hydrogen Synthesis by *Thermotoga neapolitana*: An Unexpected Deviation from the Dark Fermentation Model. *Int. J. Hydrogen Energy* **2014**, *39*, 4857–4862. [\[CrossRef\]](#)
32. Wushke, S.; Fristensky, B.; Zhang, X.L.; Spicer, V.; Krokhin, O.V.; Levin, D.B.; Stott, M.B.; Sparling, R. A Metabolic and Genomic Assessment of Sugar Fermentation Profiles of the Thermophilic Thermotogales, *Fervidobacterium pennivorans*. *Extremophiles* **2018**, *22*, 965–974. [\[CrossRef\]](#)
33. Vijayakumar, J.; Aravindan, R.; Viruthagiri, T. Lactic Acid and Its Potential Applications in Industries. *Bioprod. Biosyst. Eng.* **2007**, *42*, 101–103.
34. Roehr, M.; Kosaric, N.; Vardar-Sukan, F.; Pieper, H.J.; Senn, T. *The Biotechnology of Ethanol. Classical and Future Applications*; Wiley: Hoboken, NJ, USA, 2005; p. 245. ISBN 978-3-527-60234-6.
35. Vieille, C.; Zeikus, G.J. Hyperthermophilic Enzymes: Sources, Uses, and Molecular Mechanisms for Thermostability. *Microbiol. Mol. Biol. Rev.* **2001**, *65*, 1–43. [\[CrossRef\]](#) [\[PubMed\]](#)
36. Ul Haq, I.; Hussain, Z.; Khan, M.; Muneer, B.; Afzal, S.; Majeed, S.; Akram, F. Kinetic and Thermodynamic Study of Cloned Thermostable Endo-1, 4- β -Xylanase from *Thermotoga petrophila* in Mesophilic Host. *Mol. Biol. Rep.* **2012**, *39*, 7251–7261. [\[CrossRef\]](#) [\[PubMed\]](#)
37. Ul Haq, I.; Tahir, S.F.; Aftab, M.N.; Akram, F.; ur Rehman, A.; Nawaz, A.; Mukhtar, H. Purification and Characterization of a Thermostable Cellobiohydrolase from *Thermotoga petrophila*. *Protein Pept. Lett.* **2018**, *25*, 1003–1014. [\[CrossRef\]](#) [\[PubMed\]](#)
38. Colussi, F.; Viviam, M.; Ian, S.; Junio, M. Oligomeric State and Structural Stability of Two Hyperthermophilic β -Glucosidases from *Thermotoga petrophila*. *Amino Acids* **2015**, *47*, 937–948. [\[CrossRef\]](#) [\[PubMed\]](#)
39. Pollo, S.M.J.; Zhaxybayeva, O.; Nesbø, C.L. Insights into Thermoadaptation and the Evolution of Mesophily from the Bacterial Phylum Thermotogae. *Can. J. Microbiol.* **2015**, *61*, 655–670. [\[CrossRef\]](#) [\[PubMed\]](#)
40. Fatima, B.; Aftab, M.; Ul Haq, I. Cloning, Purification, and Characterization of Xylose Isomerase from *Thermotoga naphthophila* RKU-10. *J. Basic Microbiol.* **2016**, *56*, 949–962. [\[CrossRef\]](#)
41. Lopes, J.L.S.; Yoneda, J.S.; Martins, J.M.; Demarco, R. Environmental Factors Modulating the Stability and Enzymatic Activity of the *Petrotoga mobilis* Esterase (PmEst). *PLoS ONE* **2016**, *11*, e0158146. [\[CrossRef\]](#)
42. Intagun, W.; Kanoksilapatham, W. A Review: Biodegradation and Applications of Keratin Degrading Microorganisms and Keratinolytic Enzymes, Focusing on Thermophiles and Thermostable Serine Proteases. *Am. J. Appl. Sci. Rev.* **2017**, *14*, 1016–1023. [\[CrossRef\]](#)
43. Hamid, A.; Aftab, M.N. Cloning, Purification, and Characterization of Recombinant Thermostable β -Xylanase Tnap_0700 from *Thermotoga naphthophila*. *Appl. Biochem. Biotechnol.* **2019**, *189*, 1274–1290. [\[CrossRef\]](#)
44. Kang, E.; Jin, H.; La, J.W.; Park, S.; Kim, W.; Lee, W. Identification of Keratinases from *Fervidobacterium islandicum* AW-1 Using Dynamic Gene Expression pro Fi Ling. *Microb. Biotechnol.* **2019**, *13*, 442–457. [\[CrossRef\]](#) [\[PubMed\]](#)
45. European Commission. *Communication from the Commission to the European Parliament, the Council, the European Economic and Social Committee and the Committee of the Regions*; A Hydrogen Strategy for a Climate-Neutral Europe; 8.7.2020 COM 301 Final; European Commission: Brussels, Belgium, 2020.
46. Dipasquale, L.; d'Ippolito, G.; Gallo, C.; Vella, F.M.; Gambacorta, A.; Picariello, G.; Fontana, A. Hydrogen Production by the Thermophilic Eubacterium *Thermotoga neapolitana* from Storage Polysaccharides of the CO₂-Fixing Diatom *Thalassiosira weissflogii*. *Int. J. Hydrogen Energy* **2012**, *37*, 12250–12257. [\[CrossRef\]](#)
47. Angenent, L.; Karim, K.; Al-Dahhan, M.; Wrenn, B.; Domiguez-Espinosa, R. Production of Bioenergy and Biochemicals from Industrial and Agricultural Wastewater. *Trends Biotechnol.* **2004**, *22*, 477–485. [\[CrossRef\]](#) [\[PubMed\]](#)
48. De Vrije, T.; de Haas, G.G.; Tan, G.B.; Keijsers, E.R.P.; Claassen, P.A.M. Pretreatment of Miscanthus for Hydrogen Production by *Thermotoga elfii*. *Hydrog. Energy* **2002**, *27*, 1381–1390. [\[CrossRef\]](#)
49. De Vrije, T.; Budde, M.A.W.; Lips, S.J.; Bakker, R.R.; Mars, A.E.; Claassen, P.A.M. Hydrogen Production from Carrot Pulp by the Extreme Thermophiles *Caldicellulosiruptor saccharolyticus* and *Thermotoga neapolitana*. *Int. J. Hydrogen Energy* **2010**, *35*, 13206–13213. [\[CrossRef\]](#)
50. Mars, A.E.; Veuskens, T.; Budde, M.A.W.; Van Doeveren, P.F.; Lips, S.J.; Bakker, R.R.; De Vrije, T.; Claassen, P.A.M. Biohydrogen Production from Untreated and Hydrolyzed Potato Steam Peels by the Extreme Thermophiles *Caldicellulosiruptor saccharolyticus* and *Thermotoga neapolitana*. *Int. J. Hydrogen Energy* **2010**, *35*, 7730–7737. [\[CrossRef\]](#)
51. Cappelletti, M.; Bucchi, G.; De Sousa Mendes, J.; Alberini, A.; Fedi, S.; Bertin, L.; Frascari, D. Biohydrogen Production from Glucose, Molasses and Cheese Whey by Suspended and Attached Cells of Four Hyperthermophilic Thermotoga Strains. *J. Chem. Technol. Biotechnol.* **2012**, *87*, 1291–1301. [\[CrossRef\]](#)
52. Saidi, R.; Liebgott, P.P.; Gannoun, H.; Ben Gaida, L.; Miladi, B.; Hamdi, M.; Bouallagui, H.; Auria, R. Biohydrogen Production from Hyperthermophilic Anaerobic Digestion of Fruit and Vegetable Wastes in Seawater: Simplification of the Culture Medium of *Thermotoga maritima*. *Waste Manag.* **2018**, *71*, 474–484. [\[CrossRef\]](#)
53. Saidi, R.; Liebgott, P.P.; Hamdi, M.; Auria, R.; Bouallagui, H. Enhancement of Fermentative Hydrogen Production by *Thermotoga maritima* through Hyperthermophilic Anaerobic Co-Digestion of Fruit-Vegetable and Fish Wastes. *Int. J. Hydrogen Energy* **2018**, *43*, 23168–23177. [\[CrossRef\]](#)
54. Saidi, R.; Hamdi, M.; Bouallagui, H. Hyperthermophilic Hydrogen Production in a Simplified Reaction Medium Containing Onion Wastes as a Source of Carbon and Sulfur. *Environ. Sci. Pollut. Res.* **2020**, *27*, 17382–17392. [\[CrossRef\]](#)

55. Amend, J.P.; Shock, E.L. Energetics of Overall Metabolic Reactions of Thermophilic and Hyperthermophilic Archaea and Bacteria. *FEMS Microbiol. Rev.* **2001**, *25*, 175–243. [\[CrossRef\]](#) [\[PubMed\]](#)
56. Pradhan, N.; Dipasquale, L.; d'Ippolito, G.; Panico, A.; Lens, P.N.L.; Esposito, G.; Fontana, A. Hydrogen Production by the Thermophilic Bacterium *Thermotoga neapolitana*. *Int. J. Mol. Sci.* **2015**, *16*, 12578–12600. [\[CrossRef\]](#) [\[PubMed\]](#)
57. Levin, D.B.; Pitt, L.; Love, M. Biohydrogen Production: Prospects and Limitations to Practical Application. *Int. J. Hydrogen Energy* **2004**, *29*, 173–185. [\[CrossRef\]](#)
58. Schut, G.J.; Adams, M.W.W. The Iron-Hydrogenase of *Thermotoga maritima* Utilizes Ferredoxin and NADH Synergistically: A New Perspective on Anaerobic Hydrogen Production. *J. Bacteriol.* **2009**, *191*, 4451–4457. [\[CrossRef\]](#)
59. Yu, J.; Varga, M.; Mityas, C.; Noll, K.M. Liposome-Mediated DNA Uptake and Transient Expression in *Thermotoga*. *Extremophiles* **2001**, *5*, 53–60. [\[CrossRef\]](#)
60. Xu, H.; Han, D.; Xu, Z. Expression of Heterologous Cellulases in *Thermotoga* Sp. Strain RQ2. *BioMed Res. Int.* **2015**, *2015*, 304523. [\[CrossRef\]](#)
61. Han, D.; Xu, Z. Development of a PyrE—Based Selective System for *Thermotoga* sp. *Extremophiles* **2017**, *21*, 297–306. [\[CrossRef\]](#)
62. Pradhan, N.; Dipasquale, L.; Panico, A.; Lens, P.N.L.; Esposito, G.; d'Ippolito, G.; Fontana, A. Hydrogen and Lactic Acid Synthesis by the Wild-Type and a Laboratory Strain of the Hyperthermophilic Bacterium *Thermotoga neapolitana* DSMZ 4359 under Capnophilic Lactic Fermentation Conditions. *Int. J. Hydrogen Energy* **2017**, *42*, 16023–16030. [\[CrossRef\]](#)
63. Grogan, D.W.; Carver, G.T.; Drake, J.W. Genetic fidelity under harsh conditions: Analysis of spontaneous mutation in the thermoacidophilic archaeon *Sulfolobus acidocaldarius*. *Proc. Natl. Acad. Sci. USA* **2001**, *98*, 7928–7933. [\[CrossRef\]](#)
64. Nguyen, T.A.D.; Pyo Kim, J.; Sun Kim, M.; Kwan Oh, Y.; Sim, S.J. Optimization of Hydrogen Production by Hyperthermophilic Eubacteria, *Thermotoga maritima* and *Thermotoga neapolitana* in Batch Fermentation. *Int. J. Hydrogen Energy* **2008**, *33*, 1483–1488. [\[CrossRef\]](#)
65. Munro, S.A.; Zinder, S.H.; Walker, L.P. The Fermentation Stoichiometry of *Thermotoga neapolitana* and Influence of Temperature, Oxygen, and PH on Hydrogen Production. *Biotechnol. Prog.* **2009**, *25*, 1035–1042. [\[CrossRef\]](#) [\[PubMed\]](#)
66. Cappelletti, M.; Zannoni, D.; Postec, A.; Ollivier, B. Members of the Order Thermotogales: From Microbiology to Hydrogen Production. In *Microbial BioEnergy: Hydrogen Production, Advances in Photosynthesis and Respiration*; Springer: Dordrecht, The Netherlands, 2014; Volume 38, pp. 197–224.
67. Pradhan, N.; d'Ippolito, G.; Dipasquale, L.; Esposito, G.; Panico, A.; Lens, P.N.L.; Fontana, A. Simultaneous Synthesis of Lactic Acid and Hydrogen from Sugars via Capnophilic Lactic Fermentation by *Thermotoga neapolitana* Cf *Capnolactica*. *Biomass Bioenergy* **2019**, *125*, 17–22. [\[CrossRef\]](#)
68. Dreschke, G.; d'Ippolito, G.; Panico, A.; Lens, P.N.L.; Esposito, G.; Fontana, A. Enhancement of Hydrogen Production Rate by High Biomass Concentrations of *Thermotoga Neapolitana*. *Int. J. Hydrogen Energy* **2018**, *43*, 13072–13080. [\[CrossRef\]](#)
69. Dreschke, G.; Papirio, S.; Panico, A.; Lens, P.N.L.; Esposito, G.; d'Ippolito, G.; Fontana, A. H₂-Rich Biogas Recirculation Prevents Hydrogen Supersaturation and Enhances Hydrogen Production by *Thermotoga neapolitana* Cf. *Capnolactica*. *Int. J. Hydrogen Energy* **2019**, *44*, 19698–19708. [\[CrossRef\]](#)
70. Dipasquale, L.; Pradhan, N.; d'Ippolito, G.; Fontana, A. Potential of Hydrogen Fermentative Pathways in Marine Thermophilic Bacteria: Dark Fermentation and Capnophilic Lactic Fermentation in *Thermotoga* and *Pseudothermotoga* Species. In *Grand Challenges in Marine Biotechnology*; Springer: Dordrecht, The Netherlands, 2018; pp. 217–235.
71. Nuzzo, G.; Landi, S.; Esercizio, N.; Manzo, E.; Fontana, A.; d'Ippolito, G. Capnophilic Lactic Fermentation from *Thermotoga neapolitana*: A Resourceful Pathway to Obtain Almost Enantiopure L-Lactic Acid. *Fermentation* **2019**, *5*, 34. [\[CrossRef\]](#)
72. Takahata, Y.; Nishijima, M.; Hoaki, T.; Maruyama, T. *Thermotoga petrophila* sp. Nov. and *Thermotoga naphthophila* sp. Nov., Two Hyperthermophilic Bacteria from the Kubiki Oil Reservoir in Niigata, Japan. *Int. J. Syst. Evol. Microbiol.* **2001**, *51*, 1901–1909. [\[CrossRef\]](#) [\[PubMed\]](#)
73. Mori, K.; Yamazoe, A.; Hosoyama, A.; Ohji, S.; Fujita, N.; Ishibashi, J.I.; Kimura, H.; Suzuki, K.I. *Thermotoga profunda* sp. Nov. and *Thermotoga caldifontis* sp. Nov., Anaerobic Thermophilic Bacteria Isolated from Terrestrial Hot Springs. *Int. J. Syst. Evol. Microbiol.* **2014**, *64*, 2128–2136. [\[CrossRef\]](#) [\[PubMed\]](#)
74. Jannasch, H.W.; Huber, R.; Belkin, S.; Stetter, K.O. *Thermotoga neapolitana* sp. Nov. of the Extremely Thermophilic, Eubacterial Genus *Thermotoga*. *Arch. Microbiol.* **1988**, *150*, 103–104. [\[CrossRef\]](#)
75. Balk, M.; Weijma, J.; Stams, A.J.M. *Thermotoga Lettingae* sp. Nov., a Novel Thermophilic, Methanol-Degrading Bacterium Isolated from a Thermophilic Anaerobic Reactor. *Int. J. Syst. Evol. Microbiol.* **2002**, *52*, 1361–1368. [\[CrossRef\]](#) [\[PubMed\]](#)
76. Ravot, G.; Magot, M.; Fardeau, M.L.; Patel, B.K.C.; Prensier, G.; Egan, A.; Garcia, J.L.; Ollivier, B. *Thermotoga elfii* sp. Nov., a Novel Thermophilic Bacterium from an African Oil-Producing Well. *Int. J. Syst. Bacteriol.* **1995**, *45*, 308–314. [\[CrossRef\]](#)
77. Fardeau, M.L.; Ollivier, B.C.; Patel, B.K.; Magot, M.; Thomas, P.; Rimbault, A.; Rocchiccioli, F.; Garcia, J.L. *Thermotoga hypogea* sp. Nov., a Xylanolytic, Thermophilic Bacterium from an Oil-Producing Well. *Int. J. Syst. Bacteriol.* **1997**, *147*, 51–56. [\[CrossRef\]](#) [\[PubMed\]](#)
78. Jeanthon, C.; Reysenbach, A.L.; L'Haridon, S.; Gambacorta, A.; Pace, N.R.; Glénat, P.; Prieur, D. *Thermotoga subterranea* sp. Nov., a New Thermophilic Bacterium Isolated from a Continental Oil Reservoir. *Arch. Microbiol.* **1995**, *164*, 91–97. [\[CrossRef\]](#) [\[PubMed\]](#)
79. Friedrich, A.B.; Antranikian, G. Keratin Degradation by *Fervidobacterium pennavorans*, a Novel Thermophilic Anaerobic Species of the Order Thermotogales. *Appl. Environ. Microbiol.* **1996**, *62*, 2875–2882. [\[CrossRef\]](#) [\[PubMed\]](#)

80. Huber, R.; Woese, C.R.; Langworthy, T.A.; Kristjansson, J.K.; Stetter, K.O. *Fervidobacterium islandicum* Sp. Nov., a New Extremely Thermophilic Eubacterium Belonging to the “Thermotogales”. *Arch. Microbiol.* **1990**, *154*, 105–111. [\[CrossRef\]](#)
81. Podosokorskaya, O.A.; Merkel, Y.A.; Kolganova, T.V.; Chernyh, N.A.; Miroshnichenko, M.L.; Bonch-Osmolovskaya, E.A.; Kublanov, I.V. *Fervidobacterium riparium* Sp. Nov., a Thermophilic Anaerobic Cellulolytic Bacterium Isolated from a Hot Spring. *Int. J. Syst. Evol. Microbiol.* **2011**, *61*, 2697–2701. [\[CrossRef\]](#)
82. Andrews, K.T.; Patel, B.K.C. *Fervidobacterium gondwanense* Sp. Nov., a New Thermophilic Anaerobic Bacterium Isolated from Nonvolcanically Heated Geothermal Waters of the Great Artesian Basin of Australia. *Int. J. Syst. Bacteriol.* **1996**, *46*, 265–269. [\[CrossRef\]](#)
83. Kanoksilapatham, W.; Pasomsup, P.; Keawram, P.; Cuecas, A.; Portillo, M.C.; Gonzalez, J.M. *Fervidobacterium thailandense* Sp. Nov., an Extremely Thermophilic Bacterium Isolated from a Hot Spring. *Int. J. Syst. Evol. Microbiol.* **2016**, *66*, 5023–5027. [\[CrossRef\]](#)
84. Cai, J.; Wang, Y.; Liu, D.; Zeng, Y.; Xue, Y.; Ma, Y.; Feng, Y. *Fervidobacterium changbaicum* Sp. Nov., a Novel Thermophilic Anaerobic Bacterium Isolated from a Hot Spring of the Changbai Mountains, China. *Int. J. Syst. Evol. Microbiol.* **2007**, *57*, 2333–2336. [\[CrossRef\]](#)
85. Huber, R.; Woese, C.R.; Langworthy, T.A.; Fricke, H.; Stetter, K.O. *Thermosipho africanus* Gen. Nov., Represents a New Genus of Thermophilic Eubacteria within the “Thermotogales”. *Syst. Appl. Microbiol.* **1989**, *12*, 32–37. [\[CrossRef\]](#)
86. Takai, K.; Horikoshi, K. *Thermosipho japonicus* Sp. Nov., an Extremely Thermophilic Bacterium Isolated from a Deep-Sea Hydrothermal Vent in Japan. *Extremophiles* **2000**, *4*, 9–17. [\[CrossRef\]](#)
87. L’Haridon, S.; Miroshnichenko, M.L.; Hippe, H.; Fardeau, M.L.; Bonch-Osmolovskaya, E.; Stackebrandt, E.; Jeanthon, C. *Thermosipho geolei* Sp. Nov., a Thermophilic Bacterium Isolated from a Continental Petroleum Reservoir in Western Siberia. *Int. J. Syst. Evol. Microbiol.* **2001**, *51*, 1327–1334. [\[CrossRef\]](#) [\[PubMed\]](#)
88. Podosokorskaya, O.A.; Kublanov, I.V.; Reysenbach, A.L.; Kolganova, T.V.; Bonch-Osmolovskaya, E.A. *Thermosipho affectus* Sp. Nov., a Thermophilic, Anaerobic, Cellulolytic Bacterium Isolated from a Mid-Atlantic Ridge Hydrothermal Vent. *Int. J. Syst. Evol. Microbiol.* **2011**, *61*, 1160–1164. [\[CrossRef\]](#) [\[PubMed\]](#)
89. Kuwabara, T.; Kawasaki, A.; Uda, I.; Sugai, A. *Thermosipho globiformans* Sp. Nov., an Anaerobic Thermophilic Bacterium That Transforms into Multicellular Spheroids with a Defect in Peptidoglycan Formation. *Int. J. Syst. Evol. Microbiol.* **2011**, *61*, 1622–1627. [\[CrossRef\]](#) [\[PubMed\]](#)
90. Antoine, E.; Cilia, V.; Meunier, J.R.; Guezennec, J.; Lesongeur, F.; Barbier, G. *Thermosipho melanesiensis* Sp. Nov., a New Thermophilic Anaerobic Bacterium Belonging to the Order Thermotogales, Isolated from Deep-Sea Hydrothermal Vents in the Southwestern Pacific Ocean. *Int. J. Syst. Bacteriol.* **1997**, *47*, 1118–1123. [\[CrossRef\]](#) [\[PubMed\]](#)
91. Podosokorskaya, O.A.; Bonch-Osmolovskaya, E.A.; Godfroy, A.; Gavrillov, S.N.; Beskorovaynaya, D.A.; Sokolova, T.G.; Kolganova, T.V.; Toshchakov, S.V.; Kublanov, I.V. *Thermosipho activus* Sp. Nov., a Thermophilic, Anaerobic, Hydrolytic Bacterium Isolated from a Deep-Sea Sample. *Int. J. Syst. Evol. Microbiol.* **2014**, *64*, 3307–3313. [\[CrossRef\]](#) [\[PubMed\]](#)
92. Urios, L.; Cueff-Gauchard, V.; Pignet, P.; Postec, A.; Fardeau, M.L.; Ollivier, B.; Barbier, G. *Thermosipho atlanticus* Sp. Nov., a Novel Member of the Thermotogales Isolated from a Mid-Atlantic Ridge Hydrothermal Vent. *Int. J. Syst. Evol. Microbiol.* **2004**, *54*, 1953–1957. [\[CrossRef\]](#)
93. L’Haridon, S.; Miroshnichenko, M.L.; Hippe, H.; Fardeau, M.L.; Stackebrandt, E.; Jeanthon, C. *Petrotoga olearia* Sp. Nov. and *Petrotoga sibirica* Sp. Nov., Two Thermophilic Bacteria Isolated from a Continental Petroleum Reservoir in Western Siberia. *Int. J. Syst. Evol. Microbiol.* **2002**, *52*, 1715–1722. [\[CrossRef\]](#)
94. Lien, T.; Madsen, M.; Rainey, F.A.; Birkeland, N.K. *Petrotoga mobilis* Sp. Nov., from a North Sea Oil-Production Well. *Int. J. Syst. Bacteriol.* **1998**, *48*, 1007–1013. [\[CrossRef\]](#)
95. Miranda-Tello, E.; Fardeau, M.L.; Joulian, C.; Magot, M.; Thomas, P.; Tholozan, J.L.; Olivier, B. *Petrotoga halophila* Sp. Nov., a Thermophilic, Moderately Halophilic, Fermentative Bacterium Isolated from an Offshore Oil Well in Congo. *Int. J. Syst. Evol. Microbiol.* **2007**, *57*, 40–44. [\[CrossRef\]](#)
96. Miranda-Tello, E.; Fardeau, M.L.; Thomas, P.; Ramirez, F.; Casalot, L.; Cayol, J.L.; Garcia, J.L.; Ollivier, B. *Petrotoga mexicana* Sp. Nov., a Novel Thermophilic, Anaerobic and Xylanolytic Bacterium Isolated from an Oil-Producing Well in the Gulf of Mexico. *Int. J. Syst. Evol. Microbiol.* **2004**, *54*, 169–174. [\[CrossRef\]](#)
97. Purwasena, I.A.; Sugai, Y.; Sasaki, K. *Petrotoga japonica* Sp. Nov., a Thermophilic, Fermentative Bacterium Isolated from Yabase Oilfield in Japan. *Arch. Microbiol.* **2014**, *196*, 313–321. [\[CrossRef\]](#) [\[PubMed\]](#)
98. Alain, K.; Marteinsson, V.T.; Miroshnichenko, M.L.; Bonch-Osmolovskaya, E.A.; Prieur, D.; Birrien, J.-L. *Marinitoga piezophila* Sp. Nov., a Rod-Shaped, Thermo-Piezophilic Bacterium Isolated under High Hydrostatic Pressure from a Deep-Sea Hydrothermal Vent. *Int. J. Syst. Evol. Microbiol.* **2002**, *52*, 1331–1339. [\[CrossRef\]](#) [\[PubMed\]](#)
99. Postec, A.; Ciobanu, M.; Birrien, J.L.; Bienvenu, N.; Prieur, D.; Le Romancer, M. *Marinitoga litoralis* Sp. Nov., a Thermophilic, Heterotrophic Bacterium Isolated from a Coastal Thermal Spring on Île Saint-Paul, Southern Indian Ocean. *Int. J. Syst. Evol. Microbiol.* **2010**, *60*, 1778–1782. [\[CrossRef\]](#) [\[PubMed\]](#)
100. Nunoura, T.; Oida, H.; Miyazaki, M.; Suzuki, Y.; Takai, K.; Horikoshi, K. *Marinitoga okinawensis* Sp. Nov., a Novel Thermophilic and Anaerobic Heterotroph Isolated from a Deep-Sea Hydrothermal Field, Southern Okinawa Trough. *Int. J. Syst. Evol. Microbiol.* **2007**, *57*, 467–471. [\[CrossRef\]](#) [\[PubMed\]](#)

101. Postec, A.; Le Breton, C.; Fardeau, M.L.; Lesongeur, F.; Pignet, P.; Querellou, J.; Ollivier, B.; Godfroy, A. *Marinitoga hydrogenitolerans* Sp. Nov., a Novel Member of the Order Thermotogales Isolated from a Black Smoker Chimney on the Mid-Atlantic Ridge. *Int. J. Syst. Evol. Microbiol.* **2005**, *55*, 1217–1221. [[CrossRef](#)] [[PubMed](#)]
102. Steinsbu, B.O.; Røyseth, V.; Thorseth, I.H.; Steen, I.H. *Marinitoga arctica* Sp. Nov., a Thermophilic, Anaerobic Heterotroph Isolated from a Mid-Ocean Ridge Vent Field. *Int. J. Syst. Evol. Microbiol.* **2016**, *66*, 5070–5076. [[CrossRef](#)]
103. Nunoura, T.; Hirai, M.; Imachi, H.; Miyazaki, M.; Makita, H.; Hirayama, H.; Furushima, Y.; Yamamoto, H.; Takai, K. *Kosmotoga arenicorallina* Sp. Nov. a Thermophilic and Obligately Anaerobic Heterotroph Isolated from a Shallow Hydrothermal System Occurring within a Coral Reef, Southern Part of the Yaeyama Archipelago, Japan, Reclassification of *Thermococcoides shengliensis*. *Arch. Microbiol.* **2010**, *192*, 811–819. [[CrossRef](#)] [[PubMed](#)]
104. L'Haridon, S.; Jiang, L.; Alain, K.; Chalopin, M.; Rouxel, O.; Beauverger, M.; Xu, H.; Shao, Z.; Jebbar, M. *Kosmotoga pacifica* Sp. Nov., a Thermophilic Chemoorganoheterotrophic Bacterium Isolated from an East Pacific Hydrothermal Sediment. *Extremophiles* **2014**, *18*, 81–88. [[CrossRef](#)]
105. Van Ooteghem, S.A.; Beer, S.K.; Yue, P.C. Hydrogen Production by the Thermophilic Bacterium *Thermotoga neapolitana*. *Appl. Biochem. Biotechnol.* **2002**, *98–100*, 177–189. [[CrossRef](#)]
106. Eriksen, N.T.; Nielsen, T.M.; Iversen, N. Hydrogen Production in Anaerobic and Microaerobic *Thermotoga neapolitana*. *Biotechnol. Lett.* **2008**, *30*, 103–109. [[CrossRef](#)]
107. Boileau, C.; Auria, R.; Davidson, S.; Casalot, L.; Christen, P.; Liebgott, P.P.; Combet-Blanc, Y. Hydrogen Production by the Hyperthermophilic Bacterium *Thermotoga maritima* Part I: Effects of Sulfured Nutriments, with Thiosulfate as Model, on Hydrogen Production and Growth. *Biotechnol. Biofuels* **2016**, *9*, 1–17. [[CrossRef](#)] [[PubMed](#)]
108. Van Niel, E.W.J.; Budde, M.A.W.; De Haas, G.; van der Wal, F.J.; Claassen, P.A.M.; Stams, A.J.M. Distinctive Properties of High Hydrogen Producing Extreme Thermophiles, *Caldicellulosiruptor saccharolyticus* and *Thermotoga elfii*. *Int. J. Hydrogen Energy* **2002**, *27*, 1391–1398. [[CrossRef](#)]
109. Hawkes, F.; Hussy, I.; Kyazze, G.; Dinsdale, R.; Hawkes, D. Continuous Dark Fermentative Hydrogen Production by Mesophilic Microflora: Principles and Progress. *Int. J. Hydrogen Energy* **2007**, *32*, 172–184. [[CrossRef](#)]
110. Nguyen, T.A.D.; Han, S.J.; Kim, J.P.; Kim, M.S.; Sim, S.J. Hydrogen Production of the Hyperthermophilic Eubacterium, *Thermotoga neapolitana* under N₂ Sparging Condition. *Bioresour. Technol.* **2010**, *101*, S38–S41. [[CrossRef](#)]
111. Karadagli, F.; Marcus, A.K.; Rittmann, B.E. Role of Hydrogen (H₂) Mass Transfer in Microbiological H₂-Threshold Studies. *Biodegradation* **2019**, *30*, 113–125. [[CrossRef](#)]
112. Nath, K.; Das, D. Improvement of Fermentative Hydrogen Production: Various Approaches. *Appl. Microbiol. Biotechnol.* **2004**, *65*, 520–529. [[CrossRef](#)]
113. Ngo, T.A.; Mi-sun, K.; Sim, S.J. Thermophilic Hydrogen Fermentation Using *Thermotoga neapolitana* DSM 4359 by Fed-Batch Culture. *Int. J. Hydrogen Energy* **2011**, *36*, 14014–14023. [[CrossRef](#)]
114. Pradhan, N.; Dipasquale, L.; d'Ippolito, G.; Fontana, A.; Panico, A.; Lens, P.N.L.; Pirozzi, F.; Esposito, G. Kinetic modeling of fermentative hydrogen production by *Thermotoga neapolitana*. *Int. J. Hydrogen Energy* **2016**, *41*, 1–10. [[CrossRef](#)]
115. Mizuno, O.; Dinsdale, R.; Hawkes, F.R.; Hawkes, D.L. Enhancement of Hydrogen Production from Glucose by Nitrogen Gas Sparging. *Bioresour. Technol.* **2000**, *73*, 59–65. [[CrossRef](#)]
116. Ngo, T.A.; Kim, M.S.; Sim, S.J. High-Yield Biohydrogen Production from Biodiesel Manufacturing Waste by *Thermotoga neapolitana*. *Int. J. Hydrogen Energy* **2011**, *36*, 5836–5842. [[CrossRef](#)]
117. D'Ippolito, G.; Dipasquale, L.; Fontana, A. Recycling of Carbon Dioxide and Acetate as Lactic Acid by the Hydrogen-Producing Bacterium *Thermotoga neapolitana*. *ChemSuschem* **2014**, *7*, 2678–2683. [[CrossRef](#)] [[PubMed](#)]
118. Pradhan, N.; Dipasquale, L.; d'Ippolito, G.; Fontana, A.; Panico, A.; Pirozzi, F.; Lens, P.N.L.; Esposito, G. Model Development and Experimental Validation of Capnophilic Lactic Fermentation and Hydrogen Synthesis by *Thermotoga neapolitana*. *Water Res.* **2016**, *99*, 225–234. [[CrossRef](#)] [[PubMed](#)]
119. Dipasquale, L.; Adessi, A.; d'Ippolito, G.; Rossi, F.; Fontana, A.; De Philippis, R. Introducing Capnophilic Lactic Fermentation in a Combined Dark-Photo Fermentation Process: A Route to Unparalleled H₂ Yields. *Appl. Microbiol. Biotechnol.* **2015**, *99*, 1001–1010. [[CrossRef](#)] [[PubMed](#)]
120. D'Ippolito, G.; Landi, S.; Esercizio, N.; Lanzilli, M.; Vastano, M.; Dipasquale, L.; Pradhan, N.; Fontana, A. CO₂-Induced Transcriptional Reorganization: Molecular Basis of Capnophilic Lactic Fermentation in *Thermotoga neapolitana*. *Front. Microbiol.* **2020**, *11*, 171. [[CrossRef](#)] [[PubMed](#)]
121. Van Ooteghem, S.A.; Jones, A.; Van Der Lelie, D.; Dong, B.; Mahajan, D. H₂ Production and Carbon Utilization by *Thermotoga neapolitana* under Anaerobic and Microaerobic Growth Conditions. *Biotechnol. Lett.* **2004**, *26*, 1223–1232. [[CrossRef](#)] [[PubMed](#)]
122. Ngo, T.A.; Sim, S.J. Dark Fermentation of Hydrogen from Waste Glycerol Using Hyperthermophilic Eubacterium *Thermotoga neapolitana*. *Environ. Prog. Sustain. Energy* **2011**, *31*, 466–473. [[CrossRef](#)]
123. Juszczak, A.; Aono, S.; Adams, M.W.W. The Extremely Thermophilic Eubacterium, *Thermotoga maritima* Contains a Novel Iron-Hydrogenase Whose Cellular Activity Is Dependent Upon Tungsten. *J. Bacteriol. Chem.* **1991**, *226*, 13834–13841. [[PubMed](#)]
124. Rusch, A.; Walpersdorf, E.; DeBeer, D.; Gurrier, S.; Amend, P.J. Microbial Communities near the Oxidic/Anoxic Interface in the Hydrothermal System of Vulcano Island, Italy. *Chem. Geol.* **2005**, *224*, 169–182. [[CrossRef](#)]
125. Belkin, S.; Wirsén, C.O.; Jannasch, H.W. A New Sulfur-Reducing, Extremely Thermophilic Eubacterium from a Submarine Thermal Vent. *Appl. Environ. Microbiol.* **1986**, *51*, 1180–1185. [[CrossRef](#)]

126. Childers, S.E.; Vargas, M.; Noll, K.M. Improved Methods for Cultivation of the Extremely Thermophilic Bacterium *Thermotoga neapolitana*. *Appl. Environ. Microbiol.* **1992**, *58*, 3949–3953. [[CrossRef](#)]
127. Le Fourn, C.; Fardeau, M.L.; Ollivier, B.; Lojou, E.; Dolla, A. The Hyperthermophilic Anaerobe *Thermotoga maritima* Is Able to Cope with Limited Amount of Oxygen: Insights into Its Defence Strategies. *Environ. Microbiol.* **2008**, *10*, 1877–1887. [[CrossRef](#)] [[PubMed](#)]
128. Tosatto, S.C.E.; Toppo, S.; Carbonera, D.; Giacometti, G.M.; Costantini, P. Comparative Analysis of [FeFe] Hydrogenase from *Thermotogales* Indicates the Molecular Basis of Resistance to Oxygen Inactivation. *Int. J. Hydrogen Energy* **2008**, *33*, 570–578. [[CrossRef](#)]
129. Lakhal, R.; Auria, R.; Davidson, S.; Ollivier, B.; Dolla, A.; Hamdi, M.; Combet-Blanc, Y. Effect of Oxygen and Redox Potential on Glucose Fermentation in *Thermotoga maritima* under Controlled Physicochemical Conditions. *Int. J. Microbiol.* **2010**, *2010*, 896510. [[CrossRef](#)] [[PubMed](#)]
130. Kaslin, S.A.; Childers, S.E.; Noll, K.M. Membrane-Associated Redox Activities in *Thermotoga neapolitana*. *Arch. Microbiol.* **1998**, *170*, 297–303. [[CrossRef](#)] [[PubMed](#)]
131. Yang, X.; Ma, K. Purification and Characterization of an NADH Oxidase from Extremely Thermophilic Anaerobic Bacterium *Thermotoga hypogea*. *Arch. Microbiol.* **2005**, *183*, 331–337. [[CrossRef](#)] [[PubMed](#)]
132. Yang, X.; Ma, K. Characterization of an Exceedingly Active NADH Oxidase from the Anaerobic Hyperthermophilic Bacterium *Thermotoga maritima*. *J. Bacteriol.* **2007**, *189*, 3312–3317. [[CrossRef](#)]
133. Mangayil, R.; Aho, T.; Karp, M.; Santala, V. Improved Bioconversion of Crude Glycerol to Hydrogen by Statistical Optimization of Media Components. *Renew. Energy* **2015**, *75*, 583–589. [[CrossRef](#)]
134. Abdullah, M.F.; Md Jahim, J.; Abdul, P.M.; Mahmod, S.S. Effect of Carbon/Nitrogen Ratio and Ferric Ion on the Production of Biohydrogen from Palm Oil Mill Effluent (POME). *Biocatal. Agric. Biotechnol.* **2020**, *23*, 101445. [[CrossRef](#)]
135. Munro, S.A.; Choe, L.; Zinder, S.H.; Lee, K.H.; Walker, L.P. Proteomic and Physiological Experiments to Test *Thermotoga neapolitana* Constraint-Based Model Hypotheses of Carbon Source Utilization. *Biotechnol. Prog.* **2012**, *28*, 312–318. [[CrossRef](#)]
136. Rinker, K.D.; Kelly, R.M. Effect of Carbon and Nitrogen Sources on Growth Dynamics and Exopolysaccharide Production for the Hyperthermophilic Archaeon *Thermococcus litoralis* and Bacterium *Thermotoga maritima*. *Biotechnol. Bioeng.* **2000**, *69*, 537–547. [[CrossRef](#)]
137. Van Niel, E.W.J.; Hahn-Hägerdal, B. Nutrient Requirements of Lactococci in Defined Growth Media. *Appl. Microbiol. Biotechnol.* **1999**, *52*, 617–627. [[CrossRef](#)]
138. Maru, B.T.; Bielen, A.A.M.; Kengen, S.W.M.; Constantí, M.; Medinaa, F. Biohydrogen Production from Glycerol Using *Thermotoga* Spp. *Energy Procedia* **2012**, *29*, 300–307. [[CrossRef](#)]
139. Kengen, S.W.M.; Stams, A.J.M. Formation of L-Alanine as a Reduced End Product in Carbohydrate Fermentation by the Hyperthermophilic Archaeon *Pyrococcus furiosus*. *Arch. Microbiol.* **1994**, *161*, 168–175. [[CrossRef](#)]
140. Weiner, R.; Langille, S.; Quintero, E. Structure, Function, and Immu- Nochemistry of Bacterial Exopolysaccharides. *J. Ind. Microbiol.* **1995**, *15*, 339–346. [[CrossRef](#)] [[PubMed](#)]
141. Pierra, M.; Trably, E.; Godon, J.J.; Bernet, N. Fermentative Hydrogen Production under Moderate Halophilic Conditions. *Int. J. Hydrogen Energy* **2014**, *39*, 7508–7517. [[CrossRef](#)]
142. Liu, Q.; Chen, W.; Zhang, X.; Yu, L.; Zhou, J.; Xu, Y.; Qian, G. Phosphate Enhancing Fermentative Hydrogen Production from Substrate with Municipal Solid Waste Composting Leachate as a Nutrient. *Bioresour. Technol.* **2015**, *190*, 431–437. [[CrossRef](#)] [[PubMed](#)]
143. Chang, F.; Lin, C. Calcium Effect on Fermentative Hydrogen Production in an Anaerobic Up-Flow Sludge Blanket System. *Water Sci. Technol.* **2006**, *54*, 105–112. [[CrossRef](#)]
144. Ravot, G.; Ollivier, B.; Magot, M.; Patel, B.K.C.; Crolet, J.L.; Fardeau, M.L.; Garcia, J.L. Thiosulfate Reduction, an Important Physiological Feature Shared by Members of the Order Thermotogales. *Appl. Environ. Microbiol.* **1995**, *61*, 2053–2055. [[CrossRef](#)]
145. Ravot, G.; Ollivier, B.; Fardeau, M.L.; Patel, B.K.C.; Andrews, K.T.; Magot, M.; Garcia, J.L. L-Alanine Production from Glucose Fermentation by Hyperthermophilic Members of the Domains Bacteria and Archaea: A Remnant of an Ancestral Metabolism? *Appl. Environ. Microbiol.* **1996**, *62*, 2657–2659. [[CrossRef](#)]
146. Ainala, S.K.; Seol, E.; Kim, J.R.; Park, S. Effect of Culture Medium on Fermentative and CO-Dependent H₂ Production Activity in *Citrobacter amalonaticus* Y19. *Int. J. Hydrogen Energy* **2016**, *41*, 6734–6742. [[CrossRef](#)]
147. Huber, R.; Stetter, K.O. The Order Thermotogales. In *The Prokaryotes*; Springer: New York, NY, USA, 1992; pp. 93809–93815.
148. Hania, W.B.; Fadhlou, K.; Brochier-Armanet, C.; Persillon, C.; Postec, A.; Hamdi, M.; Dolla, A.; Ollivier, B.; Fardeau, M.L.; Le Mer, J.; et al. Draft Genome Sequence of Mesotoga Strain PhosAC3, a Mesophilic Member of the Bacterial Order Thermotogales, Isolated from a Digestor Treating Phosphogypsum in Tunisia. *Stand. Genom. Sci.* **2015**, *10*, 1–7. [[CrossRef](#)] [[PubMed](#)]
149. Nesbø, C.L.; Charchuk, R.; Pollo, S.M.J.; Budwill, K.; Kublanov, I.V.; Haverkamp, T.H.A.; Foght, J. Genomic Analysis of the Mesophilic Thermotogae Genus *Mesotoga* Reveals Phylogeographic Structure and Genomic Determinants of Its Distinct Metabolism. *Environ. Microbiol.* **2019**, *21*, 456–470. [[CrossRef](#)] [[PubMed](#)]
150. Tao, Z.; Yang, Q.; Yao, F.; Huang, X.; Wu, Y.; Du, M.; Chen, S.; Liu, X.; Li, X.; Wang, D. The Inhibitory Effect of Thiosulfate on Volatile Fatty Acid and Hydrogen Production from Anaerobic Co-Fermentation of Food Waste and Waste Activated Sludge. *Bioresour. Technol.* **2020**, *297*, 122428. [[CrossRef](#)] [[PubMed](#)]
151. Slobodkin, A.I. Thermophilic Microbial Metal Reduction. *Microbiologia* **2005**, *74*, 581–595. [[CrossRef](#)]

152. Gomez-Romero, J.; Gonzalez-Garcia, A.; Chairez, I.; Torres, L.; García-Peña, E.I. Selective Adaptation of an Anaerobic Microbial Community: Biohydrogen Production by Co-Digestion of Cheese Whey and Vegetables Fruit Waste. *Int. J. Hydrogen Energy* **2014**, *39*, 12541–12550. [[CrossRef](#)]
153. Llanos, J.; Capasso, C.; Parisi, E.; Prieur, D.; Jeanthon, C. Susceptibility to Heavy Metals and Cadmium Accumulation in Aerobic and Anaerobic Thermophilic Microorganisms Isolated from Deep-Sea Hydrothermal Vents. *Curr. Microbiol.* **2000**, *41*, 0201–0205. [[CrossRef](#)]
154. Vargas, M.; Kashefi, K.; Blunt-harris, E.L.; Lovley, D.R. Fe (III) Reduction on Early Earth. *Nature* **1998**, *395*, 65–67. [[CrossRef](#)]
155. Balch, W.E.; Fox, G.E.; Magrum, L.J.; Woese, C.R.; Wolfe, R.S. Methanogens: Reevaluation of a Unique Biological Group. *Microbiol. Rev.* **1979**, *43*, 260–296. [[CrossRef](#)]
156. Lee, Y.J.; Miyahara, T.; Noike, T. Effect of Iron Concentration on Hydrogen Fermentation. *Bioresour. Technol.* **2001**, *80*, 227–231. [[CrossRef](#)]
157. Zhang, Y.; Shen, J. Effect of Temperature and Iron Concentration on the Growth and Hydrogen Production of Mixed Bacteria. *Int. J. Hydrogen Energy* **2006**, *31*, 441–446. [[CrossRef](#)]
158. Ying, X.; Wang, Y.; Badiei, H.R.; Karanassios, V.; Ma, K. Purification and Characterization of an Iron-Containing Alcohol Dehydrogenase in Extremely Thermophilic Bacterium *Thermotoga hypogea*. *Arch. Microbiol.* **2007**, *187*, 499–510. [[CrossRef](#)] [[PubMed](#)]
159. Trivedi, S.; Rao, S.R.; Gehlot, H.S. Nucleic Acid Stability in Thermophilic Prokaryotes: A Review Nucleic Acid Stability in Thermophilic Prokaryotes: A Review. *J. Cell Mol. Biol.* **2005**, *4*, 61–69.

4. CO₂-Induced Transcriptional Reorganization: Molecular Basis of Capnophilic Lactic Fermentation in *Thermotoga neapolitana*

Giuliana d'Ippolito*†, Simone Landi*†, **Nunzia Esercizio**, Mariamichela Lanzilli, Marco Vastano, Laura Dipasquale, Nirakar Pradhan and Angelo Fontana

Bio-Organic Chemistry Unit, Institute of Biomolecular Chemistry, Italian National Research Council (CNR),
Pozzuoli, Italy

Citation:

d'Ippolito G, Landi S, **Esercizio N**, Lanzilli M, Vastano M, Dipasquale L, Pradhan N and Fontana A (2020) CO₂-Induced Transcriptional Reorganization: Molecular Basis of Capnophilic Lactic Fermentation in *Thermotoga neapolitana*. *Front. Microbiol.* 11:171.



CO₂-Induced Transcriptional Reorganization: Molecular Basis of Capnophilic Lactic Fermentation in *Thermotoga neapolitana*

Giuliana d'Ippolito^{*†}, Simone Landi^{*†}, Nunzia Esercizio, Mariamichella Lanzilli, Marco Vastano, Laura Dipasquale, Nirakar Pradhan and Angelo Fontana

Bio-Organic Chemistry Unit, Institute of Biomolecular Chemistry, Italian National Research Council (CNR), Pozzuoli, Italy

OPEN ACCESS

Edited by:

Masahiro Ito,
Toyo University, Japan

Reviewed by:

Tamotsu Kanai,
Kyoto University, Japan
Shuning Wang,
Shandong University, China

*Correspondence:

Giuliana d'Ippolito
gdippolito@icb.cnr.it
Simone Landi
s.landi@icb.cnr.it;
s.landi87@gmail.com

[†]These authors have contributed
equally to this work and share first
authorship

Specialty section:

This article was submitted to
Extreme Microbiology,
a section of the journal
Frontiers in Microbiology

Received: 31 July 2019

Accepted: 24 January 2020

Published: 18 February 2020

Citation:

d'Ippolito G, Landi S, Esercizio N,
Lanzilli M, Vastano M, Dipasquale L,
Pradhan N and Fontana A (2020)
CO₂-Induced Transcriptional
Reorganization: Molecular Basis
of Capnophilic Lactic Fermentation
in *Thermotoga neapolitana*.
Front. Microbiol. 11:171.
doi: 10.3389/fmicb.2020.00171

Capnophilic lactic fermentation (CLF) is a novel anaplerotic pathway able to convert sugars to lactic acid (LA) and hydrogen using CO₂ as carbon enhancer in the hyperthermophilic bacterium *Thermotoga neapolitana*. In order to give further insights into CLF metabolic networks, we investigated the transcriptional modification induced by CO₂ using a RNA-seq approach. Transcriptomic analysis revealed 1601 differentially expressed genes (DEGs) in an enriched CO₂ atmosphere over a total of 1938 genes of the *T. neapolitana* genome. Transcription of PFOR and LDH genes belonging to the CLF pathway was up-regulated by CO₂ together with 6-phosphogluconolactonase (6PGL) and 6-phosphogluconate dehydratase (EDD) of the Entner–Doudoroff (ED) pathway. The transcriptomic study also revealed up-regulation of genes coding for the flavin-based enzymes NADH-dependent reduced ferredoxin:NADP oxidoreductase (NFN) and NAD-ferredoxin oxidoreductase (RNF) that control supply of reduced ferredoxin and NADH and allow energy conservation-based sodium translocation through the cell membrane. These results support the hypothesis that CO₂ induces rearrangement of the central carbon metabolism together with activation of mechanisms that increase availability of the reducing equivalents that are necessary to sustain CLF. In this view, this study reports a first rationale of the molecular basis of CLF in *T. neapolitana* and provides a list of target genes for the biotechnological implementation of this process.

Keywords: lactic acid, pyruvate, glycolysis, hydrogenase, thermophilic, RNA-seq

INTRODUCTION

Thermotoga neapolitana is a hyperthermophilic anaerobic bacterium of the order Thermotogales (Belkin et al., 1986). The taxonomic group shares a rod shape and complex outer envelope called toga that surrounds the bacterial cell and forms a periplasmic space around the poles (Angel et al., 1993). *T. neapolitana* and other sister species are good candidates for the sustainable and efficient conversion of food and agriculture residues to hydrogen (H₂) by Dark Fermentation (Connors et al., 2006; Manish and Banerjee, 2008; Hallenbeck and Ghosh, 2009; Guo et al., 2010; d'Ippolito et al., 2010; Elleuche et al., 2014; Pradhan et al., 2015, 2016a).

In the last years, we reported that *T. neapolitana* also operates a novel, anaplerotic process named capnophilic lactic fermentation (CLF) for the synthesis of almost enantiopure L-lactic acid

(LA) without affecting H₂ production (Dipasquale et al., 2014; d'Ippolito et al., 2014; Pradhan et al., 2016b, 2019; Nuzzo et al., 2019). The metabolic process is activated by CO₂ (capnophilic means “requiring CO₂”) and, nominally, is dependent on a Janus pathway including a catabolic branch leading to acetyl-CoA (AcCoA) from sugars by glycolysis, and an anabolic branch that combines AcCoA and CO₂ to give LA through reduction of newly synthesized pyruvate (PYR) by a NADH-dependent lactic dehydrogenase (LDH) (Figure 1).

This second part of the pathway requires an additional burden of reducing equivalents and determines an unconceivable deviation from Dark Fermentation model for carbon and hydrogen balance (Dipasquale et al., 2014). We showed that CLF is not equally active in all members of the order Thermotogales (Dipasquale et al., 2018) but the almost complete absence of molecular and biochemical studies on metabolism of this group of bacteria has been an insurmountable barrier to explore this process that presumably involves crosstalk of several pathways. The aim of the present work was to investigate the role of CO₂ as biochemical trigger in *T. neapolitana* and to correlate metabolic change with or without CO₂ to hydrogen and LA production. We based our analysis on a differential RNA-sequencing of the strain *T. neapolitana* subsp. *capnolactica*, a mutant that shows an incremented operation of CLF (Pradhan et al., 2017). Transcriptome studies were associated to the experimental

response of the bacterium to CO₂. Under our experimental conditions, CO₂ sparging generates a complex equilibrium between carbon dioxide as a gas or dissolved in the aqueous phase, and its hydrated derivatives H₂CO₃, HCO₃⁻, CO₃⁼. For simplicity we refer to all these chemical forms as CO₂ throughout the manuscript.

MATERIALS AND METHODS

Biological Material

Thermotoga neapolitana subsp. *capnolactica* (DSM 33003) derives from the DSMZ 4359T strain that was stimulated in our laboratory under saturating concentration of CO₂ (Pradhan et al., 2017). Bacterial cells were grown in a modified ATCC 1977 culture medium containing 10 ml/L of filter-sterilized vitamins and trace element solution (DSM medium 141) together with 10 g/L NaCl, 0.1 g/L KCl, 0.2 g/L MgCl₂·6H₂O, 1 g/L NH₄Cl, 0.3 g/L K₂HPO₄, 0.3 g/L KH₂PO₄, 0.1 g/L CaCl₂·2H₂O, 1 g/L cysteine-HCl, 2 g/L yeast extract, 2 g/L tryptone, 5 g/L glucose, and 0.001 g/L resazurin (d'Ippolito et al., 2010).

Bacterial Growth

Bacterial precultures (30 mL) were incubated overnight at 80°C without shaking and used to inoculate (6% v/v) cultures in 120 ml serum bottles with a final culture volume of 30 mL. Oxygen was removed by heating until solution was colorless. Cultures were sparged with CO₂ gas (CLF condition, three bottles) or N₂ gas (control, three bottles) for 5 min at 30 mL/min. pH was monitored and adjusted to approximately 7.5 by 1 M NaOH. Sparging followed by pH adjustment was repeated every 24 h. Inoculated bottles were maintained in a heater (Binder ED720) at 80°C. Cell growth was determined by optical density (OD) at 540 nm (UV/Vis Spectrophotometer DU 730, Beckman Coulter). Samples (2 ml of medium) were collected from each bottle after 0, 24, and 48 h. After centrifugation at 16,000 × g for 15 min (Hermle Z3236K), residues and supernatants were kept at -20°C until analysis. Cell morphology was monitored by microscope observation (Axio VertA1, Carl Zeiss, magnification of 100×).

Gas Analysis

Gas (H₂ and CO₂) measurements were performed by gas chromatography (GC) on an instrument (Focus GC, Thermo Scientific) equipped with a thermoconductivity detector (TCD) and fitted with a 3 m molecular sieve column (Hayesep Q). N₂ was used as carrier gas. Gas sampling was carried out at 24 and 48 h.

Chemical Analysis

Glucose concentration was determined by the dinitrosalicylic acid method calibrated on a standard solution of 2 g/L glucose (Bernfeld, 1995). Organic acids were measured by ERETIC ¹H NMR as described by Nuzzo et al. (2019). All experiments were performed on a Bruker DRX 600 spectrometer equipped with an inverse TCI CryoProbe. Peak integration, ERETIC

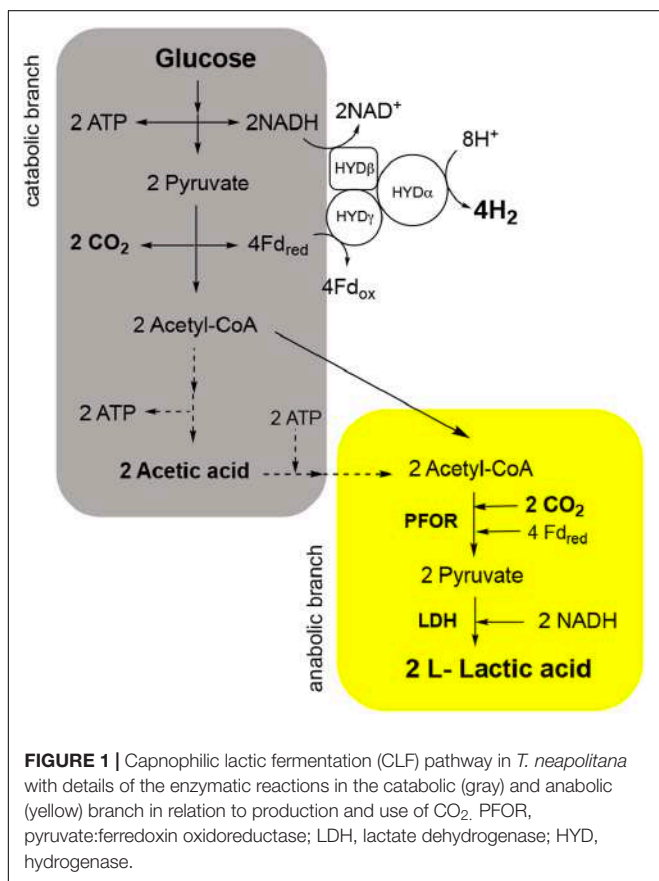
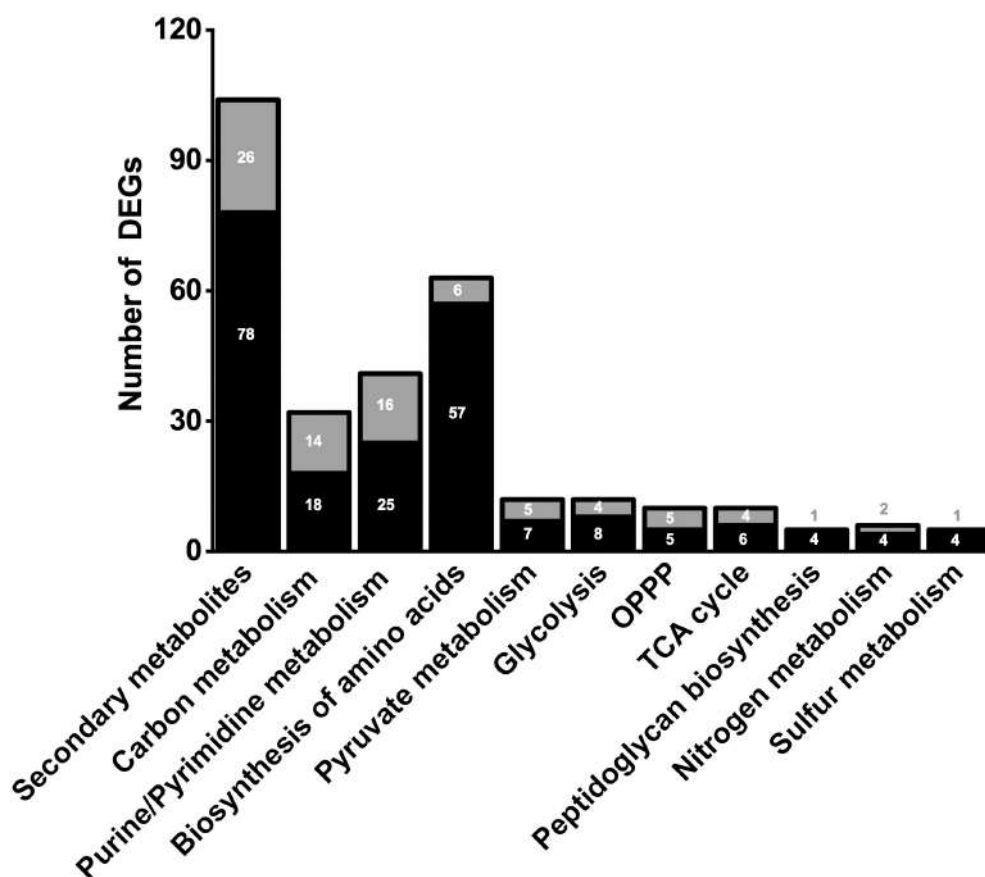


TABLE 1 | Growth parameters (OD₅₄₀ and percentage of glucose consumption) and product yields (H₂, acetic acid, and lactic acid – LA) in *T. neapolitana* cultures sparged with N₂ and CO₂ after 24 and 48 h.

	N ₂						CO ₂					
	Growth parameters		Yields (mol/mol glucose)				Growth parameters		Yields (mol/mol glucose)			
	OD ₅₄₀	Glucose (%)	H ₂	AA	LA	LA/AA	OD ₅₄₀	Glucose (%)	H ₂	AA	LA	LA/AA
24 h	1.03 ± 0.01	37 ± 1.6	2.44 ± 0.1	1.16 ± 0.01	0.29 ± 0.01	0.25	1.02 ± 0.01	44 ± 1.6*	2.83 ± 0.2*	1.25 ± 0.06*	0.38 ± 0.02*	0.31
48 h	1.17 ± 0.03	68 ± 5	2.28 ± 0.2	1.11 ± 0.01	0.26 ± 0.01	0.23	1.06 ± 0.05	88 ± 6*	2.70 ± 0.4	1.09 ± 0.02	0.42 ± 0.04*	0.39

Asterisks (*) indicate significant variation between CO₂ and N₂ samples at *p*-value ≤ 0.05. AA, acetic acid; LA, lactic acid.

**FIGURE 2** | Number of significant (≤0.05 FDR) up-regulated (black) and down-regulated (gray) DEGs of selected metabolic pathways. Number of genes in correlated pathways were identified using KEGG categories.

measurements, and spectrum calibration were obtained by the specific subroutines of Bruker Top-Spin 3.1 program. Spectra were acquired with the following parameters: flip angle = 90°, recycle delay = 20 s, SW = 3000 Hz, SI = 16K, NS = 16, RG = 1. An exponential multiplication (EM) function was applied to the FID for line broadening of 1 Hz. No baseline correction was used.

RNA Extraction and Sequencing

RNA (three replicates for CLF and three replicates for control) was extracted by standard method with TRIzol (Invitrogen, Carlsbad, CA, United States). Concentration in each sample was determined by a ND-1000 Spectrophotometer

(NanoDrop) and quality assessed by Agilent 2100 Bioanalyzer and Agilent RNA 6000 nano kit (Agilent Technologies, Santa Clara, CA, United States). Hi-quality RNA samples were used for high-throughput sequencing. Indexed libraries were prepared from 4 µg/ea purified RNA with TruSeq Stranded mRNA Sample Prep Kit (Illumina) according to the manufacturer's instructions. Libraries were quantified using the Agilent 2100 Bioanalyzer (Agilent Technologies) and pooled such that each index-tagged sample was present in equimolar amounts, with final concentration of the pooled samples of 2 nM. The pooled samples were subject to cluster generation and sequencing using an Illumina HiSeq

2500 System (Illumina) in a 2 × 100 paired-end format at a final concentration of 8 pmol. RNA extraction and the sequencing service was provided by Genomix4life SRL (Baronissi, Salerno, Italy).

RNA-Seq Bioinformatic Analysis

Quality check of the sequenced reads was performed using the FAST QC software¹. The obtained high-quality reads were used for mapping by the Bowtie software (Langmead and Salzberg, 2012). Genome of *T. neapolitana* DSM_4359 at GenBank database (assembly accession: GCA_000018945.1) was used as

¹<http://www.bioinformatics.babraham.ac.uk/projects/fastqc/>

TABLE 2 | List of DEGs related to carbon metabolism.

Locus	Fold change	Description
Glycolysis – Embden–Meyerhof–Parnas		
CTN_RS05065	2.18	Glucokinase
CTN_RS01845	1.84	Glucose-6-phosphate isomerase
CTN_RS02345	−1.79	6-Phosphofructokinase
CTN_RS01945	−1.39	6-Phosphofructokinase, pyrophosphate-dependent
CTN_RS01890	−1.66	Fructose-bisphosphate aldolase
CTN_RS09450	−1.40	Glyceraldehyde-3-phosphate dehydrogenase
CTN_RS05810	−1.98	Glycerate kinase
CTN_RS06075	1.88	Phosphoglycerate mutase
CTN_RS08475	−2.40	Phosphopyruvate hydratase aka Enolase
CTN_RS02350	−1.80	Pyruvate kinase
OPP and Entner–Doudoroff common enzymes		
CTN_RS07110	4.84	Glucose-6-phosphate 1-dehydrogenase
CTN_RS07115	5.50	6-Phosphogluconolactonase
Entner–Doudoroff		
CTN_RS00550	5.83	6-Phosphogluconate dehydratase ^a
CTN_RS03140	1.26	2-Dehydro-3-deoxyphosphogluconate aldolase
OPP		
CTN_RS01150	−1.40	6-Phosphogluconate dehydrogenase, Decarboxylating
CTN_RS04470	1.64	Ribulose-phosphate-epimerase
CTN_RS07445	NDE	Ribose-5-phosphate isomerase
CTN_RS04700	1.81	Transketolase
CTN_RS08090	−1.60	Transketolase, C-terminal subunit
CTN_RS08085	−2.66	Transketolase, N-terminal subunit
CTN_RS07710	−5.74	Fructose-6-phosphate aldolase
CTN_RS01915	NDE	Fructose-6-phosphate aldolase
Other genes		
CTN_RS01940	6.16	Citrate synthase
CTN_RS07145	6.35	Isocitrate dehydrogenase
CTN_RS09470	2.92	Fumarate hydratase class I
CTN_RS00600	−1.81	Fumarate hydratase, C-terminal subunit
CTN_RS00605	−2.54	Fumarate hydratase, N-terminal subunit
CTN_RS01300	−2.01	2-Oxoglutarate ferredoxin oxidoreductase, beta subunit
CTN_RS00595	1.26	Malate oxidoreductase

^a6-Phosphogluconate dehydratase was previously annotated as dihydroxy-acid dehydratase. The correct annotation was performed using a BlastP approach on the Ensembl bacteria database.

reference. The quality statistics of the mapping process is showed in the **Supplementary Table 1**. The counting of the mapped reads was performed by the software HTScount. In order to define the set of expressed genes, raw read counts were normalized using the TMM method (Trimmed mean). Differentially expressed genes (DEGs) were obtained by the DESeq2 package of R language at a false discovery rate (FDR) ≤ 0.05 (Love et al., 2014). Expression values were reported as “Fold Change” (ratio of the normalized expression value in sample over control). Values <1 are shown as (−1/FC) to display negative regulation. Cluster analysis was performed using the MeV software based on the respective normalized reads count values (Howe et al., 2011). The number of clusters was determined by Figure of Merit (FOM) analysis. Clusters were generated by employing *k*-means clustering with Euclidian distances. In gene ontology enrichment analysis (GOEA), categories with a number of entries lower than 4 were excluded in the final output.

Real-Time PCR

RNAseq results were validated by real-time PCR. Triplicate quantitative assays were performed using a Platinum SYBR Green qPCR SuperMix (Life Technologies, Carlsbad, CA, United States). Cells from control cultures (N₂ sparging) were used as calibrators and RNA 16S served as endogenous reference gene (Okonkwo et al., 2017). Calculation of gene expression was carried out using the 2^{−ΔΔCt} method as in Livak and Schmittgen (2001). For each sample, mRNA amount was calculated relatively to the calibrator sample for the corresponding genes. Primers used for genes expression analysis are listed in **Supplementary Table 2**.

Western Blotting

Bacterial cells were grown under CLF condition and control as described above. Samples were collected after 12, 15, 36, 39, 42, and 45 h. Proteins extraction was performed on 1.5 ml of culture. After centrifugation at 10,000 × *g* for 20 min at 4°C, the pellets were suspended in cracking buffer (100 mM Tris-HCl pH 7.5, 30% glycerol, 2% SDS, 4 mM EDTA, 28 mM β-mercaptoethanol) and incubated at 100°C for 10 min. After centrifugation at 10,000 × *g* at 4°C for 1 h, the supernatants were recovered and protein content was measured by Bradford reagent (Bio-Rad, Hercules, CA, United States). Protein fractionation was performed on SDS polyacrylamide gel using a precast 4–15% Mini-PROTEAN TGX Stain Free (Bio-Rad, Hercules, CA, United States) and electro-transferred on polyvinylidene difluoride membrane (PVDF) using the Trans-Blot Turbo Transfer System (Bio-Rad, Hercules, CA, United States) following the manufacturer's instructions. The detection of protein was performed by primary antibody raised in rabbit (1:1000; PRIMM Srl, Milan, Italy) against peptide 149–359 of *T. neapolitana* PYR synthase subunit A (PFOR-A) (NCBI database protein accession number YP_002534223.1) and against peptide 1–192 of *T. neapolitana* Fe–Fe hydrogenase subunit β (β-HYD) (NCBI database protein accession number AAC02685.1). Horseradish peroxidase (HRP)-conjugated anti-rabbit secondary antibody was used for staining (Sigma; 1:7000).

Western blot filters were visualized by Clarity™ Western ECL substrate (Bio-Rad, Hercules, CA, United States) and subjected to analysis using Image Lab 6.0 Software (Bio-Rad, Hercules, CA, United States). Analysis included the determination of intensity of total Stain-Free fluorescence and intensity of PFOR-A and β-HYD blots for each lane by the “Lane and Bands” tool. Results were expressed as relative percentage of antibody blot intensity respect to intensity of total proteins.

Data Availability

The raw sequencing data from this study are stored in the NCBI SRA database² and are retrievable under the accession code PRJNA574556.

²<http://www.ncbi.nlm.nih.gov>

Statistics

Each experiment was performed at least in triplicate. Values were expressed as mean ± standard deviation (SD). The statistical significance of OD₅₄₀, qRT-PCR, sugar consumption, organic acid, and H₂ yields was evaluated through Student's *t*-test ($p \leq 0.05$). The differentially expressed data from the RNA-seq approach were filtered using an FDR ≤ 0.05.

RESULTS

Differential Response of Bacterial Cell to CO₂ and N₂

Sparging of CO₂ did not affect cell growth (OD₅₄₀) in comparison to control under N₂ but increased significantly glucose consumption rate. In agreement with previous reports

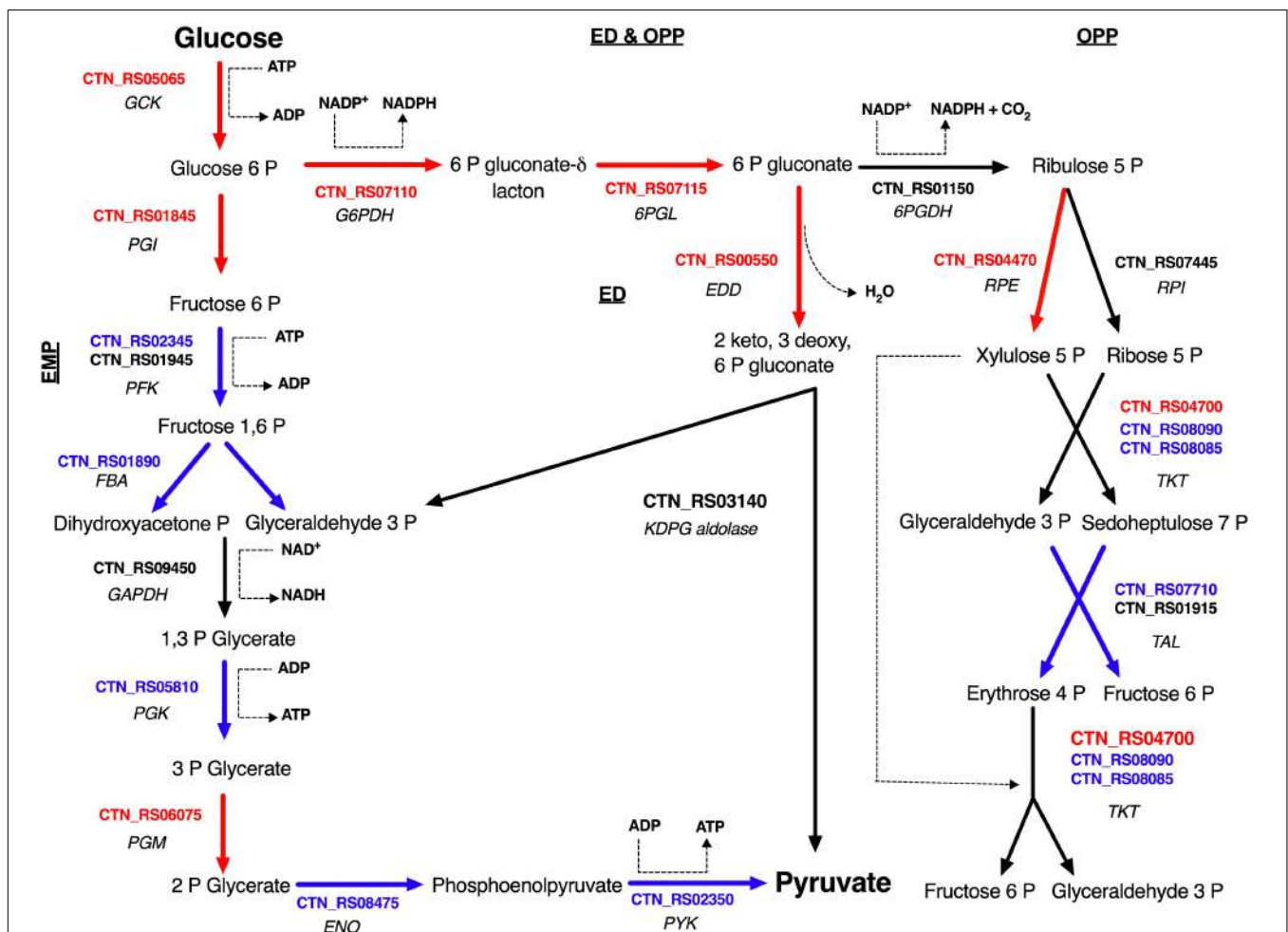


FIGURE 3 | Glucose utilization model in *T. neapolitana* cells under CO₂. Genes up- and down-regulated are highlighted in red and blue, respectively; NDE genes with $1.5 < fc < -1.5$ are in black. GCK, glucokinase; PGI, glucose-6-phosphate isomerase; PFK, 6-phosphofructokinase; FBA, fructose-bisphosphate aldolase; GAPDH, glyceraldehyde-3-phosphate dehydrogenase; PGK, glyceraldehyde kinase; PGM, phosphoglycerate mutase; ENO, enolase (Aka phosphoenolpyruvate hydratase); PYK, pyruvate kinase; G6PDH, glucose-6-phosphate dehydrogenase; 6PGL, 6-phosphogluconolactonase; EDD, 6-phosphogluconate dehydratase; KDPG aldolase, 2-dehydro-3-deoxyphosphogluconate aldolase; 6PGDH, 6-phosphogluconate dehydrogenase; RPE, ribulose 5 phosphate epimerase; RPI, ribulose 5 phosphate isomerase; TKT, transketolase; TAL, transaldolase.

(Dipasquale et al., 2014; Pradhan et al., 2017), the overall effect of CO₂ on the fermentation process was the increase of LA production without changing H₂ yield (except for a slight increase at 24 h) in comparison to N₂-treated cells. This outcome was more evident at 48 h when lactic/acetic acid ratio was 0.23 under N₂ and 0.39 under CO₂ (Table 1).

TABLE 3 | List of DEGs related to CLF pathway.

Locus	Fold change	Descriptions
CFL core enzymes		
CTN_RS03385	3.07	Pyruvate synthase subunit <i>porA</i> (aka <i>PFORα</i>)
CTN_RS03380	1.70	Pyruvate synthase subunit <i>porB</i> (aka <i>PFORβ</i>)
CTN_RS03395	2.61	Pyruvate synthase subunit <i>porC</i> (aka <i>PFORγ</i>)
CTN_RS03390	2.99	Pyruvate synthase subunit <i>porD</i> (aka <i>PFORδ</i>)
CTN_RS03950	2.74	L-lactate dehydrogenase
CTN_RS05285	1.78	Fe-hydrogenase alpha subunit
CTN_RS05290	1.27	Fe-hydrogenase beta subunit
CTN_RS05295	NDE	Fe-hydrogenase gamma subunit
CTN_RS02020	1.16	Acetate kinase
CTN_RS07210	1.78	Phosphate acetyltransferase
Putative energy sustaining enzymes		
CTN_RS04025	1.50	NFN (NADH-dependent Reduced Ferredoxin:NADP Oxidoreductase) ^a
CTN_RS04020	1.77	NFN(NADH-dependent Reduced Ferredoxin:NADP Oxidoreductase) ^a
CTN_RS02150	1.39	Electron transport complex, <i>RnfABCDGE</i> type, A subunit
CTN_RS02165	2.67	Electron transport complex, <i>RnfABCDGE</i> type, D subunit precursor
CTN_RS02155	1.93	Electron transport complex, <i>RnfABCDGE</i> type, E subunit
CTN_RS02160	2.52	Electron transport complex, <i>RnfABCDGE</i> type, G subunit precursor
CTN_RS05860	5.96	Thioredoxin
CTN_RS08515	3.09	Thioredoxin reductase
Hydrogenase maturation enzymes		
CTN_RS06540	5.98	Iron-only hydrogenase system regulator
CTN_RS06525	7.52	FeFe hydrogenase H-cluster radical SAM maturase HYDE*
CTN_RS01115	1.28	FeFe hydrogenase H-cluster radical SAM maturase HYDF*
CTN_RS06535	6.39	FeFe hydrogenase H-cluster radical SAM maturase HYDG
CoA-related enzyme		
CTN_RS08445	2.27	Pantothenate kinase
PFOR cofactors		
CTN_RS08225	5.96	Ferredoxin
CTN_RS07010	1.96	Ferredoxin
CTN_RS03680	2.55	Ferredoxin family protein

^aNADH-dependent reduced ferredoxin:NADP oxidoreductase were previously and uncorrected annotated as dihydroorotate dehydrogenase (CTN_RS04025) and glutamate synthase, beta subunit (CTN_RS04020). The correct annotations were performed using the structures and the sequencing of the *Thermotoga maritima* orthologs (Demmer et al., 2015). *FeFe hydrogenase H-cluster radical SAM maturase HYDEF were previously and uncorrected annotated as biotin synthetase and small GTP binding protein. The correct annotations were performed using a BLASTp approach.

Massive Molecular Rearrangement Induced by CO₂ in *T. neapolitana* subsp. *capnolactica*

In order to clarify the molecular effects of CO₂, an RNA-sequencing approach was performed by using N₂-treated cells as control. The transcriptomic analysis gave from 19,390,095 to 31,800,340 reads with a percentage of alignment rate >98.59% (Supplementary Table 1). We identified 1601 DEGs between experiments under CO₂ (CLF samples) and N₂ (control) (see Supplementary Information). In particular, 612 DEGs showed a significant fold change up to ≥1.5 whereas 593 DEGs were down-regulated (fold change below −1.5) (Figure 2). Considering the whole genome of *T. neapolitana*, CO₂-dependent DEGs accounted for 83% of the bacterial genes. GOEA of DEGs highlighted change of 45 metabolic networks under CLF conditions, with 26 related to up-regulation and 19 to down-regulation (Supplementary Figure 1). The analysis indicated increased expression of genes related to RNA translation (GO:0006412), ribosome organization (GO:0015934, GO:0015935), transcription factor (TF) (GO:0003700), and amino acids biosynthesis (GO:0009089, GO:0009088, GO:0006526, GO:0009097, GO:0009098, GO:0009073, GO:0006541). Expression and regulation of proteins related to active transport, including major facilitator proteins, and various membrane channels and antiporters, put forward a general down-regulation of sugar transport and vice versa an increased mobilization of phosphate, polyamine, and amino acids. The GOEA also suggested a significant impact of CO₂ on organization of the cell-wall (GO:0071555) with a marked down-regulation of the degradation of polysaccharides of the outer membrane (xylan catabolic process, GO:0045493; endoglucanase activity, GO:0004519). Interestingly, two of the three genes encoding for the outer membrane proteins that form the structure of toga (Petrus et al., 2012), namely CTN_RS01400 and CTN_RS01395, showed a similar decrease of expression. A number of TFs were also regulated by CO₂ treatment, including a number of TFs involved in the regulation of sugar catabolism (AraC and LacI). As expected by the simultaneous production of LA and H₂, we found the enrichment of metabolic categories related to redox reactions (Cell redox homeostasis – GO:0045454; Electron carrier activity – GO:0009055; and Oxidoreductase activity – GO:0016491) and carbon metabolism.

Central Carbon Metabolism Under CLF Conditions

Sparging by CO₂ induced up-regulation of glucokinase (GCK – CTN_RS05065) and glucose 6-phosphate isomerase (PGI – CTN_RS01845) that catalyze the starting steps of Embden–Meyerhof–Parnas glycolysis (EMP) (Table 2). On the other hand, we found that other enzymes of EMP were significantly down-regulated. Inspection of other genes related to central carbon metabolism revealed a significant transcription of glucose-6-phosphate dehydrogenase (G6PDH – CTN_RS07110) and 6-phosphogluconolactonase (6PGL – CTN_RS07115). These enzymes preside over the synthesis of 6-phospho gluconate that is the first metabolite of the main alternative pathways

of glucose catabolism, namely ED and oxidative pentose phosphate (OPP) pathway. On the whole, these data suggest a diversion of carbon flux from EMP to ED or OPP pathways (Figure 3). This evidence was further validated by RT-PCR that showed up-regulation of 6-phosphogluconate dehydratase (EDD – CTN_RS00550) that control the key step of ED and down-regulation of 6-phosphofructokinase (PFK – CTN_RS02345) that is the regulator enzyme of EMP (Supplementary Figure 2). Analysis of the genes of Krebs cycle reveals that *T. neapolitana* apparently lacks the whole pathway. However, we found a significant upregulation of the expression of citrate synthase (CTN_RS01940) and isocitrate dehydrogenase (CTN_RS07145) (Table 2).

Regulation of CLF Pathway

Genes encoding key enzymes of the anabolic branch of CLF pathway were differential expressed by CO₂ (Table 3). Pyruvate:ferredoxin oxidoreductase (PFOR, E.C. 1.2.7.1) is a heterotetramer enzyme that operates the reversible coupling of AcCoA and CO₂ to PYR under CLF conditions (d'Ippolito et al., 2014). Each subunit of this enzyme (CTN_RS03380, CTN_RS03385, CTN_RS03390, and CTN_RS03395) showed a significant increase of expression. In consideration of the double function of PFOR as catabolic (from PYR to AcCoA) and anabolic (from AcCoA and CO₂ to PYR) enzyme, the up-regulation is in good agreement with both the general acceleration of metabolism induced by CO₂ and the enhanced demand of PYR to feed the downfield synthesis of LA. According to this view, LDH (E.C. 1.1.1.27 – CTN_RS03950) was also up-regulated under the experimental conditions. A specific biochemical character of CLF is the increase of the rate of H₂ synthesis during the fermentation process (Dipasquale et al., 2014). The molecular analysis revealed a significant up-regulation of the expression of the α -subunit of the bacterial hydrogenase (CTN_RS05285) together with two of the three proteins (CTN_RS06525, HYD E; CTN_RS06535, HYD G) that are necessary to the complex process of maturation of this enzyme. The α -subunit (HYD α) contains the catalytic H-cluster (Schut and Adams, 2009) that is committed to reduction of H⁺ to hydrogen gas. In their model of the hydrogenase of *Thermotoga maritima*, Schut and Adams (2009) have discussed a trimeric bifurcating enzyme that catalyzes multiple electron transfer events simultaneously. HYD α is the final collector of this transfer of electrons from NADH and reduced ferredoxin; thus, it is plausible that the experimentally observed boost of the H₂ production rate requires an accelerated turnover of this protein under CLF conditions. The CO₂-induced upregulation of PFOR and HYD was further confirmed by western blotting analysis carried out on PFOR α and the β -subunit of hydrogenase (HYD β) (Figure 4).

Redox Re-organization Under CLF Conditions

Enhancement of cell reductants, e.g., NAD(P)H or ferredoxin (Fd), represents a major requirement to sustain the simultaneous production of H₂ and LA during CLF (Dipasquale et al.,

2014; d'Ippolito et al., 2014). RNA-seq approach revealed up-regulation of several genes involved in redox reactions and electron transport. Intriguingly, among up-regulated DEGs we found a significant expression of genes coding for enzymes related to the flavin-based oxidoreductase enzymes NADH-dependent reduced ferredoxin:NADP oxidoreductase (NFN) (CTN_RS04025 and CTN_RS04020) and NAD-Ferredoxin oxidoreductase (RNF) (CTN_RS02165, CTN_RS02160, and CTN_RS02155). Both these proteins are energy conservation systems. NFN controls supply of reduced ferredoxin and NADH by oxidation of NADPH while RNF couples reversible consumption of NADH with synthesis of reduced Fd and trans-membrane transport of Na⁺ or H⁺ (Hess et al., 2013). K-means cluster analysis of DEGs identified five different groups of genes with similar expression profile (not shown). One of the up-regulated cluster (Supplementary Figure 3) included genes coding for PFOR (CTN_RS03385, CTN_RS03390, and CTN_RS03395), flavin-based protein complexes (RNF and NFN – CTN_RS02160, CTN_RS02165, CTN_RS04020, and CTN_RS04025), thioredoxin (CTN_RS05860 and CTN_RS08515), ferredoxin (CTN_RS08225), Na/P cotransporter family protein (CTN_RS07190), and G6PDH (CTN_RS07110). The clustering was coherent with the fermentation results and suggested a CO₂-stimulated rearrangement of the bacterial metabolism that links NAD(P)H from ED/OPP, PYR synthesis by PFOR, and production of NADH by flavin-based energy conservation systems. According to the experimental results, up-regulation of these pathways could be consistent with increase of the availability of redox potential for the synthesis of LA and H₂ during CLF.

DISCUSSION

Thermophilic bacteria, such as *Thermotogales*, have been acquiring an emerging attention in biotechnology for hydrogen production by digestion of organic residues (Connors et al., 2006; Elleuche et al., 2014; Pradhan et al., 2015). Among thermophilic bacteria, *T. neapolitana* shows an interesting potential for the simultaneous production of hydrogen and LA by CLF (Dipasquale et al., 2014; d'Ippolito et al., 2014; Pradhan et al., 2017). In the present study, a selected strain of this bacterium, namely *T. neapolitana* subsp. *capnolactica* (Pradhan et al., 2017) was characterized by comparative analysis of gene expression profiling under CO₂ (CLF conditions) and N₂ (control). The study showed transcriptional changes that well correlate with the promoting effect of CO₂ on both the synthesis of LA and the rate of hydrogen production and glucose consumption. The appearance of this bacterial phenotype was accompanied by variation in the expression of 1601 genes related to central biochemical pathways including glycolysis, TCA, cell wall construction, and protein synthesis. Under light microscopy, the cells showed a typical rod shape with a more homogeneous length than the control bacteria under N₂ that vice versa were round-shaped (Supplementary Figure 4). In agreement with the acceleration of the fermentation

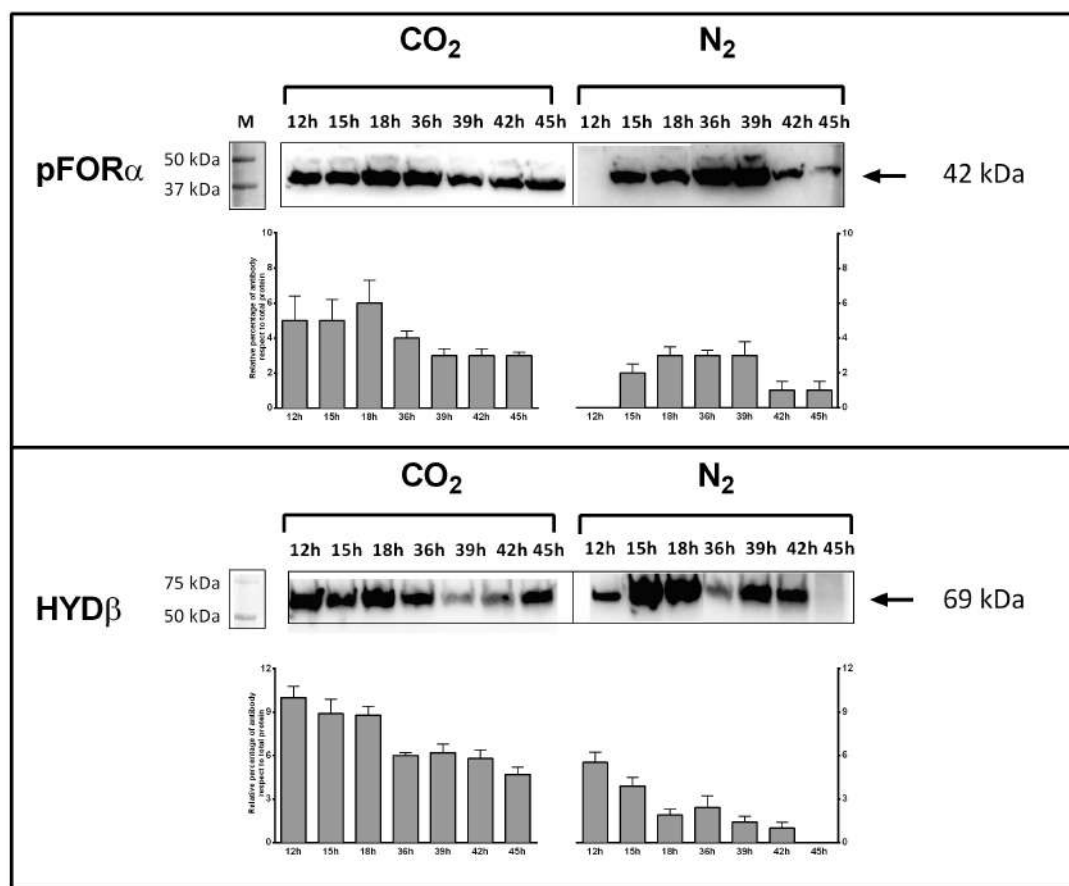


FIGURE 4 | Expression of pyruvate:ferredoxin oxidoreductase (PFOR) and Fe-Fe hydrogenase (HYD) in *T. neapolitana* subsp. *capnolactica*. Bacterial cultures were grown under N₂ or CO₂, and collected at 12, 15, 18, 36, 39, 42, and 45 h. PFOR levels were detected by using a polyclonal antibody raised in rabbits against peptide 149–359 of subunit α. HYD levels were detected by using a polyclonal antibody raised in rabbits against peptide 1–192 of subunit β. Western blot filters were subjected to analysis using Image Lab 6.0 Software (Bio-Rad, Hercules, CA, United States). Analysis included the intensity determination of total Stain-Free fluorescence and intensity of PFOR-α and β-HYD blots for each lane. Results were expressed as relative percentage of antibody blot intensity respect intensity of total proteins.

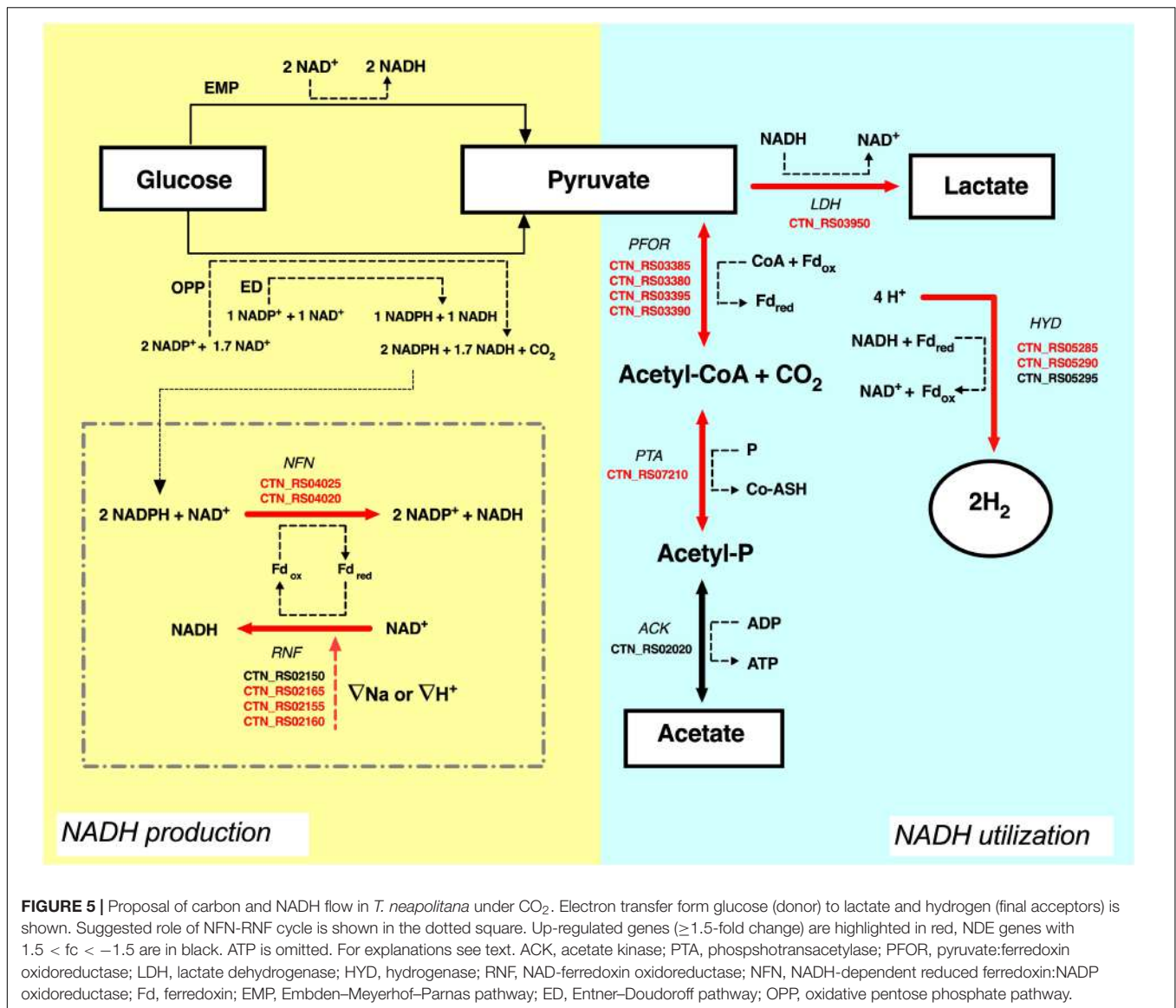
rate, CO₂ also triggered modification of the expression of 105 genes related to control of extracellular transport. Latif et al. (2015) have recently underlined that adaptation of *Thermotoga maritima* to achieve improved growth fitness requires plasticity of the ABC transporters. We found that expression of several ABC transporters of *T. neapolitana* was differently regulated (Supplementary Information), which is consistent with the modulation of these proteins in response to the different environmental conditions.

These molecular changes were driven by a number of key TFs that were differentially expressed under CO₂. In particular, we observed different regulation of genes of the LacI family, such as LacI, AraC, and XylR, that are tightly linked to distinct regulons of carbohydrate catabolism (Ravcheev et al., 2014). These proteins have been also identified as regulators of sugar metabolism in Thermotogales, including *T. neapolitana* and *T. maritima* (Rodionov et al., 2013). Thus, control of their expression seems to corroborate the observation that the metabolic acceleration triggered by CO₂ is sustained by a

change of sugar catabolism in association with a more effective import/export of substrates.

According to this view, under CLF conditions, the bacterial cells showed an interesting shift of glucose utilization through down-regulation of EMP and activation of the alternative ED and/or OPP (Figure 3). EMP is energetically more effective than other glycolytic pathways because of the higher ATP yields per glucose unit. However, the energetic cost for the synthesis of the proteins carrying out the 10 reactions of this pathway may represent a growth-limiting factor (Molenaar et al., 2009; Flamholz et al., 2013). Recently, Singh et al. (2018) have discussed the role of OPP in providing additional reductants for H₂ production in *T. maritima*. ED and OPP show a number of energetic advantages per glucose unit [reduced protein cost or increased amount of NAD(P)H, respectively] in comparison to EMP, thus switch from EMP to ED or OPP can be functional to the increased demand of reducing equivalents during CLF.

The analysis of the transcripts suggested that another pool of NADH could derive from the flavin-based oxido-reductase



enzymes NFN and RNF that are both up-regulated by CO₂. In *T. maritima*, NFN is a bifurcating enzyme that couples the oxidation of NADPH to the exergonic reduction of NAD⁺ and the endergonic reduction of Fd (Demmer et al., 2015). Electron bifurcation is one of the mechanisms of energy conservation that biological organisms use to minimize free-energy loss in redox reactions. Bifurcating enzymes catalyze endoergonic and exoergonic electron transfer reactions to circumvent thermodynamic barriers and to carry out reactions that have unfavorable free energy variations (Buckel and Thauer, 2018). Deletion of the NFN complex (Tsac_2085 NfnA and Tsac_2086 NfnB) genes led to the total loss of NADPH-dependent activity and reduces ethanol fermentation in the thermophilic anaerobe *Thermoanaerobacterium saccharolyticum* (Lo et al., 2015). On the other hand, the RNF complex couples the reversible flow of electrons from reduced ferredoxin to NAD⁺. The process is associated with the transport of Na⁺ across the cell membrane

and the direction of the electron flow is dependent on the sodium gradient (Biegel et al., 2011; Buckel and Thauer, 2013; Hess et al., 2013). The high production of hydrogen in *T. neapolitana* is associated to consumption of hydrogen ions (H⁺). RNF activity could be related to Na⁺ or H⁺ transport to balance the loss of H⁺ and to maintain the ionic homeostasis in the cell. As suggested in **Figure 5**, the combination of RNF with NFN may generate a cyclic process leading to production of NADH. In this view, synthesis of LA could be another mechanism to get rid of the excess of reducing equivalents. A similar cycle has been postulated between RNF and ferredoxin-dependent NADH oxidoreductase (FNOR) in *T. saccharolyticum* in order to operate a net transfer of protons across the cell membrane and eliminate the proton gradient that could be lethal for the cells (Tian et al., 2016).

As already reported by Krebs (1941), CO₂ affects carboxylation reactions also in heterotrophs. In *T. neapolitana*,

in addition to the indirect effect on the bacterial metabolism by gene regulation, CO₂ plays a direct role as chemical reagent in the reaction to give PYR from acetate by PFOR. Thus, increase of the concentration of CO₂ is very likely the driven force to reverse the oxidative decarboxylation of PYR and to yield carbon fixation. The occurrence of this reaction could explain the experimentally observed presence of PFOR even after the end of sugar consumption by glycolysis (d'Ippolito et al., 2014). At the moment we do not know whether this occurs for inversion of the functionality of PFOR or it is due to a newly synthesized pool of the enzyme (**Figure 1**). Synthetic PFOR is the key enzyme of the autotrophic fixation by the Wood–Ljungdahl pathway in acetogens (Furdui and Ragsdale, 2000). After our publication of the synthetic activity of PFOR in *T. neapolitana* (d'Ippolito et al., 2014), Xiong et al. (2016) have reported a similar mechanism in *Clostridium thermocellum*. In this work, the authors report assimilation of CO₂ during cellobiose metabolism with fixation of over 40% of labeled carbon in PYR that derives from PFOR-dependent synthesis. This process is very similar to that of *T. neapolitana* thus suggesting that the activation of the anaplerotic reductive C1 pathway dependent on PFOR can be more common than it is generally believed. It is obvious that the energy requirements of this process need to be considered within a comprehensive organization of the cellular redox pathways.

CONCLUSION

In conclusion, the present work showed a correlation between the gene expression, the metabolic adaptation and the biochemical phenotype of the bacterium *T. neapolitana* under conditions that promote CLF. In accordance with acceleration of H₂ synthesis, the CO₂-induced effects clearly indicated an increased energetic metabolism of *T. neapolitana* that is sustained by a concerted reorganization of the cell metabolism including at least variation of central carbon metabolism, activation of anaplerotic oxidoreductase processes and increase of the exchange across the membrane. Similar effects on enhancement of the energetic metabolism or cell growth upon exposure to CO₂ have been reported in other anaerobic bacteria, such as *Streptococcus thermophilus* (Arioli et al., 2009) and *C. thermocellum* (Xiong et al., 2016). The most significant trait of the molecular adaptation induced by CO₂ in *T. neapolitana* is related to additional

production of reductants by the EMP/ED-OPP switch and the bifurcating mechanisms based on the overexpression of the flavin-based complexes, such as NFN and RFN.

DATA AVAILABILITY STATEMENT

The raw sequencing data from this study are stored in the NCBI SRA database (<http://www.ncbi.nlm.nih.gov>) and are retrievable under the accession code PRJNA574556.

AUTHOR CONTRIBUTIONS

Gd'I conceived the whole research project, and wrote and amended the manuscript. SL conceived the idea of writing the manuscript, bioinformatic analysis, and wrote and amended the manuscript. NE performed the microbiology and western blot analysis. ML and MV performed the western blot. LD and NP performed the microbiology and sequencing analysis. AF planned and coordinated the whole research project and the experiments along with Gd'I, and wrote and amended the manuscript.

FUNDING

This research was funded by the BioRECO2VER Project, through the European Union's Horizon 2020 Research and Innovation Programme under Grant Agreement No. 760431.

ACKNOWLEDGMENTS

The authors would like to thank Dr. Lucio Caso (CNR-ICB) for the technical support in microbiological activities.

SUPPLEMENTARY MATERIAL

The Supplementary Material for this article can be found online at: <https://www.frontiersin.org/articles/10.3389/fmicb.2020.00171/full#supplementary-material>

REFERENCES

- Angel, A. M., Brunene, M., and Baumeister, W. (1993). The functional properties of OmpB, the regularly arrayed porin of the hyperthermophilic bacterium *Thermotoga neapolitana*. *FEMS Microbiol.* 109, 231–236. doi: 10.1016/0378-1097(93)90025-w
- Arioli, S., Roncada, P., Salzano, A. M., Deriu, F., Corona, S., Guglielmetti, S., et al. (2009). The relevance of carbon dioxide metabolism in *Streptococcus thermophilus*. *Microbiol.* 155, 1953–1965. doi: 10.1099/mic.0.024737-24730
- Belkin, S., Wirsén, C. O., and Jannasch, H. W. (1986). A new sulfur-reducing, extremely thermophilic eubacterium from a submarine thermal vent. *Appl. Environ. Microbiol.* 51, 1180–1185. doi: 10.1128/aem.51.6.1180-1185.1986
- Bernfeld, P. (1995). Amylases a and b. *Methods Enzymol.* 1, 149–158.
- Biegel, E., Schmidt, S., González, J. M., and Müller, V. (2011). Biochemistry, evolution and physiological function of the Rnf complex, a novel ion-motive electron transport complex in prokaryotes. *Cell. Mol. Life Sci.* 68, 613–634. doi: 10.1007/s00018-010-0555-558
- Buckel, W., and Thauer, R. K. (2013). Energy conservation via electron bifurcating ferredoxin reduction and proton/Na⁺ translocating ferredoxin oxidation. *Biochim. Biophys. Acta* 1827, 94–113. doi: 10.1016/j.bbabi.2012.07.002
- Buckel, W., and Thauer, R. K. (2018). Flavin-based electron bifurcation, ferredoxin, flavodoxin, and anaerobic respiration with protons (Ech) or NAD⁺ (Rnf) as electron acceptors: a historical review. *Front. Microbiol.* 14:401. doi: 10.3389/fmicb.2018.00401
- Connors, S. B., Mongodin, E. F., Johnson, M. R., Montero, C. I., Nelson, K. E., and Kelly, R. M. (2006). Microbial biochemistry, physiology, and biotechnology of hyperthermophilic *Thermotoga* species. *FEMS Microbiol. Rev.* 30, 872–905. doi: 10.1111/j.1574-6976.2006.00039.x
- Demmer, J. K., Huang, H., Wang, S., Demmer, U., Thauer, R. K., and Ermler, U. (2015). Insights into flavin-based electron bifurcation via the NADH-dependent

- reduced ferredoxin:NADP oxidoreductase structure. *J. Biol. Chem.* 290, 21985–21995. doi: 10.1074/jbc.M115.656520
- Dipasquale, L., d'Ippolito, G., and Fontana, A. (2014). Capnophilic lactic fermentation and hydrogen synthesis by *Thermotoga neapolitana*: an unexpected deviation from the dark fermentation model. *Int. J. Hydrogen Energ.* 39, 4857–4862. doi: 10.1016/j.ijhydene.2013.12.183
- Dipasquale, L., Pradhan, N., d'Ippolito, G., and Fontana, A. (2018). "Potential of hydrogen fermentative pathways in marine thermophilic bacteria: dark fermentation and capnophilic lactic fermentation in thermotoga and pseudothermotoga species," in *Grand Challenges in Marine Biotechnology*, eds P. H. Rampelotto, and A. Trincon, (Berlin: Springer), 217–235. doi: 10.1007/978-3-319-69075-9_6
- d'Ippolito, G., Dipasquale, L., and Fontana, A. (2014). Recycling of carbon dioxide and acetate as lactic acid by the hydrogen-producing bacterium *Thermotoga neapolitana*. *ChemSusChem* 7, 2678–2683. doi: 10.1002/cssc.201402155
- d'Ippolito, G., Dipasquale, L., Vella, F. M., Romano, I., Gambacorta, A., Cutignano, A., et al. (2010). Hydrogen metabolism in the extreme thermophile *Thermotoga neapolitana*. *Int. J. Hydrogen Energ.* 35, 2290–2295. doi: 10.1016/j.ijhydene.2009.12.044
- Elleuche, S., Schröder, C., Sahm, K., and Antranikian, G. (2014). Extremozymes-biocatalysts with unique properties from extremophilic microorganisms. *Curr. Opin. Biotechnol.* 29, 116–123. doi: 10.1016/j.copbio.2014.04.003
- Flamholz, A., Noor, E., Bar-Even, A., Liebermeister, W., and Milo, R. (2013). Glycolytic strategy as a tradeoff between energy yield and protein cost. *PNAS* 110, 10039–10044. doi: 10.1073/pnas.1215283110
- Furdui, C., and Ragsdale, S. W. (2000). The role of pyruvate ferredoxin oxidoreductase in pyruvate synthesis during autotrophic growth by the Wood-Ljungdahl pathway. *J. Biol. Chem.* 275, 28494–28499. doi: 10.1074/jbc.M003291200
- Guo, X. M., Trably, E., Latrille, E., Carrère, H., and Steyer, J. P. (2010). Hydrogen production from agricultural waste by dark fermentation: a review. *Int. J. Hydrogen Energ.* 35, 10660–10673. doi: 10.1016/j.ijhydene.2010.03.008
- Hallenbeck, P. C., and Ghosh, D. (2009). Advances in fermentative biohydrogen production: the way forward? *Trends Biotechnol.* 27, 287–297. doi: 10.1016/j.tibtech.2009.02.004
- Hess, V., Schuchmann, K., and Müller, V. (2013). The ferredoxin:NAD⁺ oxidoreductase (Rnf) from the acetogen *Acetobacterium woodii* requires Na⁺ and is reversibly coupled to the membrane potential. *J. Biol. Chem.* 288, 31496–31502. doi: 10.1074/jbc.M113.510255
- Howe, E. A., Sinha, R., Schlauch, D., and Quackenbush, J. (2011). RNA-Seq analysis in MeV. *Bioinformatics* 27, 3209–3210. doi: 10.1093/bioinformatics/btr490
- Krebs, H. A. (1941). Carbon dioxide assimilation in heterotrophic organisms. *Nature* 147, 560–563. doi: 10.1038/147560a0
- Langmead, B., and Salzberg, S. L. (2012). Fast gapped-read alignment with Bowtie 2. *Nat. Methods* 9, 357–359. doi: 10.1038/nmeth.1923
- Latif, H., Sahin, M., Tarasova, J., Tarasova, Y., Portnoy, V. A., Nogales, J., et al. (2015). Adaptive evolution of *Thermotoga maritima* reveals plasticity of the ABC transporter network. *Appl. Environ. Microbiol.* 81, 5477–5485. doi: 10.1128/AEM.01365-1315
- Livak, K. J., and Schmittgen, T. D. (2001). Analysis of relative gene expression data using real-time quantitative PCR and the 2- $\Delta\Delta$ CT method. *Methods* 25, 402–408. doi: 10.1006/meth.2001.1262
- Lo, J., Zheng, T., Olson, D. G., Ruppertsberger, N., Tripathi, S. A., Tian, L., et al. (2015). Deletion of nfnAB in *Thermoanaerobacterium saccharolyticum* and its effect on metabolism. *J. Bacteriol.* 197, 2920–2929. doi: 10.1128/JB.00347-15
- Love, M. I., Huber, W., and Anders, S. (2014). Moderated estimation of fold change and dispersion for RNA-seq data with DESeq2. *Genome Biol.* 15, 1–21. doi: 10.1186/s13059-014-0550-8
- Manish, S., and Banerjee, R. (2008). Comparison of biohydrogen production processes. *Int. J. Hydrogen Energ.* 33, 279–286. doi: 10.1016/j.ijhydene.2007.07.026
- Molenaar, D., Van Berlo, R., De Ridder, D., and Teusink, B. (2009). Shifts in growth strategies reflect tradeoffs in cellular economics. *Mol. Syst. Biol.* 5, 1–10. doi: 10.1038/msb.2009.82
- Nuzzo, G., Landi, S., Esercizio, N., Manzo, E., Fontana, A., and d'Ippolito, G. (2019). Capnophilic lactic fermentation from *Thermotoga neapolitana*: a resourceful pathway to obtain almost enantiopure L-lactic acid. *Fermentation* 5:34. doi: 10.3390/fermentation5020034
- Okonkwo, O., Lakaniemi, A. M., Santala, V., Karp, M., and Mangayil, R. (2017). Quantitative real-time PCR monitoring dynamics of *Thermotoga neapolitana* in synthetic co-culture for biohydrogen production. *Int. J. Hydrogen Energ.* 43, 3133–3141. doi: 10.1016/j.ijhydene.2017.12.002
- Petrus, A. K., Swithers, K. S., Ranjit, C., Wu, S., Brewer, H. M., Gogarten, J. P., et al. (2012). Genes for the major structural components of *Thermotogales* species' togas revealed by proteomic and evolutionary analyses of OmpA and OmpB homologs. *PLoS One* 7:e40236. doi: 10.1371/journal.pone.0040236
- Pradhan, N., Dipasquale, L., d'Ippolito, G., Fontana, A., Panico, A., Lens, P. N. L., et al. (2016a). Kinetic modeling of fermentative hydrogen production by *Thermotoga neapolitana*. *Int. J. Hydrogen Energ.* 41, 4931–4940. doi: 10.1016/j.ijhydene.2016.01.107
- Pradhan, N., Dipasquale, L., d'Ippolito, G., Fontana, A., Panico, A., Pirozzi, F., et al. (2016b). Model development and experimental validation of capnophilic lactic fermentation and hydrogen synthesis by *Thermotoga neapolitana*. *Water Res.* 99, 225–234. doi: 10.1016/j.watres.2016.04.063
- Pradhan, N., Dipasquale, L., d'Ippolito, G., Panico, A., Lens, P. N. L., Esposito, G., et al. (2015). Hydrogen production by the thermophilic bacterium *Thermotoga neapolitana*. *Int. J. Hydrogen Energ.* 16, 12578–12600. doi: 10.3390/ijms160612578
- Pradhan, N., Dipasquale, L., d'Ippolito, G., Panico, A., Lens, P. N. L., Esposito, G., et al. (2017). Hydrogen and lactic acid synthesis by the wild-type and a laboratory strain of the hyperthermophilic bacterium *Thermotoga neapolitana* DSMZ 4359T under capnophilic lactic fermentation conditions. *Int. J. Hydrogen Energ.* 42, 16023–16030. doi: 10.1016/j.ijhydene.2017.05.052
- Pradhan, N., d'Ippolito, G., Dipasquale, L., Esposito, G., Panico, A., Lens, P. N. L., et al. (2019). Simultaneous synthesis of lactic acid and hydrogen from sugars via capnophilic lactic fermentation by *Thermotoga neapolitana* cf *capnolactica*. *Biomass Bioenerg.* 125, 17–22. doi: 10.1016/j.biombioe.2019.04.007
- Ravcheev, D. A., Khoroshkin, M. S., Laikova, O. N., Tsou, O. V., Sernova, N. V., Petrova, S. A., et al. (2014). Comparative genomics and evolution of regulons of the LacI-family transcription factors. *Front. Microbiol.* 5:294. doi: 10.3389/fmicb.2014.00294
- Rodionov, D. A., Rodionova, I. A., Li, X., Ravcheev, D. A., Tarasova, Y., Portnoy, V. A., et al. (2013). Transcriptional regulation of the carbohydrate utilization network in *Thermotoga maritima*. *Front. Microbiol.* 4:244. doi: 10.3389/fmicb.2013.00244
- Schut, G. J., and Adams, M. W. (2009). The iron-hydrogenase of *Thermotoga maritima* utilizes ferredoxin and NADH synergistically: a new perspective on anaerobic hydrogen production. *J. Bacteriol.* 191, 4451–4457. doi: 10.1128/JB.01582-08
- Singh, R., White, D., Demirel, Y., Kelly, R., Noll, K., and Blum, P. (2018). Uncoupling Fermentative Synthesis of Molecular Hydrogen from Biomass Formation in *Thermotoga maritima*. *Appl. Environ. Microbiol.* 84:e00557-15..
- Tian, L., Lo, J., Shao, X., Zheng, T., Olson, D. G., and Lynd, L. R. (2016). Ferredoxin:NAD oxidoreductase of *Thermoanaerobacterium saccharolyticum* and its role in ethanol formation. *Appl. Environ. Microbiol.* 82, 7134–7141. doi: 10.1128/aem.02130-16
- Xiong, W., Lin, P. P., Magnusson, L., Warner, L., Liao, J. C., and Maness, P. (2016). CO₂-fixing one-carbon metabolism in a cellulose-degrading bacterium *Clostridium thermocellum*. *PNAS* 113, 13180–13185. doi: 10.1073/pnas.1605482113

Conflict of Interest: The authors declare that the research was conducted in the absence of any commercial or financial relationships that could be construed as a potential conflict of interest.

Copyright © 2020 d'Ippolito, Landi, Esercizio, Lanzilli, Vastano, Dipasquale, Pradhan and Fontana. This is an open-access article distributed under the terms of the Creative Commons Attribution License (CC BY). The use, distribution or reproduction in other forums is permitted, provided the original author(s) and the copyright owner(s) are credited and that the original publication in this journal is cited, in accordance with accepted academic practice. No use, distribution or reproduction is permitted which does not comply with these terms.

5 Improvement of CO₂ and Acetate Coupling into Lactic Acid by Genetic Manipulation of the Hyperthermophilic Bacterium *Thermotoga neapolitana*

Nunzia Esercizio^{1,†}, Mariamichela Lanzilli^{1,†}, Marco Vastano^{1,†}, Zhaohui Xu², Simone Landi³, Lucio Caso¹, Carmela Gallo¹, Genoveffa Nuzzo¹, Emiliano Manzo¹, Angelo Fontana^{1,3} and Giuliana d'Ippolito^{1,*}

¹ Institute of Biomolecular Chemistry (ICB), Consiglio Nazionale delle Ricerche (CNR), Via Campi Flegrei 34, 80078 Pozzuoli, Italy; n.esercizio@icb.cnr.it (N.E.); m.lanzilli@icb.cnr.it (M.L.); marco.vastano@gmail.com (M.V.); l.caso@icb.cnr.it (L.C.); carmen.gallo@icb.cnr.it (C.G.); nuzzo.genoveffa@icb.cnr.it (G.N.); emanzo@icb.cnr.it (E.M.); afontana@icb.cnr.it (A.F.)

² Department of Biological Sciences, Bowling Green State University, Bowling Green, OH 43403, USA; zxu@bgsu.edu

³ Laboratory of Bio-Organic Chemistry and Chemical Biology, Department of Biology, University of Naples "Federico II", Via Cinthia, 80126 Napoli, Italy; simone.landi@unina.it

* Correspondence: gdippolito@icb.cnr.it; Tel.: +39-0818675096

† These authors contributed equally to this work.

Citation:

Esercizio, N.; Lanzilli, M.; Vastano, M.; Xu, Z.; Landi, S.; Caso, L.; Gallo, C.; Nuzzo, G.; Manzo, E.; Fontana, A.; et al. Improvement of CO₂ and Acetate Coupling into Lactic Acid by Genetic Manipulation of the hyperthermophilic Bacterium *Thermotoga neapolitana*. *Microorganisms* **2021**, *9*, 1688.



Article

Improvement of CO₂ and Acetate Coupling into Lactic Acid by Genetic Manipulation of the Hyperthermophilic Bacterium *Thermotoga neapolitana*

Nunzia Esercizio ^{1,†}, Mariamichela Lanzilli ^{1,†}, Marco Vastano ^{1,†}, Zhaohui Xu ², Simone Landi ³, Lucio Caso ¹, Carmela Gallo ¹, Genoveffa Nuzzo ¹, Emiliano Manzo ¹, Angelo Fontana ^{1,3} and Giuliana d'Ippolito ^{1,*}

¹ Institute of Biomolecular Chemistry (ICB), Consiglio Nazionale delle Ricerche (CNR), Via Campi Flegrei 34, 80078 Pozzuoli, Italy; n.esercizio@icb.cnr.it (N.E.); m.lanzilli@icb.cnr.it (M.L.); marco.vastano@gmail.com (M.V.); l.caso@icb.cnr.it (L.C.); carmen.gallo@icb.cnr.it (C.G.); nuzzo.genoveffa@icb.cnr.it (G.N.); emanzo@icb.cnr.it (E.M.); afontana@icb.cnr.it (A.F.)

² Department of Biological Sciences, Bowling Green State University, Bowling Green, OH 43403, USA; zxu@bgsu.edu

³ Laboratory of Bio-Organic Chemistry and Chemical Biology, Department of Biology, University of Naples "Federico II", Via Cinthia, 80126 Napoli, Italy; simone.landi@unina.it

* Correspondence: gdippolito@icb.cnr.it; Tel.: +39-0818675096

† These authors contributed equally to this work.



Citation: Esercizio, N.; Lanzilli, M.; Vastano, M.; Xu, Z.; Landi, S.; Caso, L.; Gallo, C.; Nuzzo, G.; Manzo, E.; Fontana, A.; et al. Improvement of CO₂ and Acetate Coupling into Lactic Acid by Genetic Manipulation of the Hyperthermophilic Bacterium *Thermotoga neapolitana*. *Microorganisms* **2021**, *9*, 1688. <https://doi.org/10.3390/microorganisms9081688>

Academic Editor: David W. Reed

Received: 22 June 2021

Accepted: 30 July 2021

Published: 9 August 2021

Publisher's Note: MDPI stays neutral with regard to jurisdictional claims in published maps and institutional affiliations.



Copyright: © 2021 by the authors. Licensee MDPI, Basel, Switzerland. This article is an open access article distributed under the terms and conditions of the Creative Commons Attribution (CC BY) license (<https://creativecommons.org/licenses/by/4.0/>).

Abstract: Capnophilic lactic fermentation (CLF) represents an attractive biotechnological process for biohydrogen production and synthesis of L-lactic acid from acetate and CO₂. The present study focuses on a genetic manipulation approach of the *Thermotoga neapolitana* DSM33003 strain to enhance lactic acid synthesis by the heterologous expression of a thermostable acetyl-CoA synthetase that catalyses the irreversible acetate assimilation. Because of the scarcity of available genetic tools, each transformation step was optimized for *T. neapolitana* DSM33003 to cope with the specific needs of the host strain. Batch fermentations with and without an external source of acetate revealed a strongly increased lactate production (up to 2.5 g/L) for the recombinant strain compared to wild type. In the engineered bacterium, the assimilation of CO₂ into lactic acid was increased 1.7 times but the hydrogen yield was impaired in comparison to the wild type strain. Analysis of fermentation yields revealed an impaired metabolism of hydrogen in the recombinant strain that should be addressed in future studies. These results offer an important prospective for the development of a sustainable approach that combines carbon capture, energy production from renewable source, and the synthesis of high value-added products, which will be addressed in future studies.

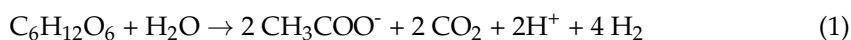
Keywords: L-lactic acid; hydrogen; acetate assimilation; CO₂ absorption; hyperthermophile engineering

1. Introduction

Thermophilic and hyperthermophilic bacteria represent attractive and still poorly explored candidates in designing efficient microbial cell factories for target bioprocesses. High temperature biotransformation, in fact, provides numerous technological advantages, including (i) reduced contamination risks, (ii) increased solubility of renewable substrates such as lignocellulosic biomasses, (iii) continuous recovery of volatile chemical products directly from reactor headspace, and (iv) decreased cooling costs [1,2]. Moreover, for biohydrogen production, the process becomes thermodynamically more favourable at high temperatures, thus increasing the overall productivity [3].

Among hyperthermophilic bacteria (over 80 °C), microorganisms belonging to the order *Thermotogales* have the ability to convert several types of carbohydrate-rich biomasses

into H_2 by dark fermentation (DF) with yields close to the Thauer limit of 4 moles of hydrogen per mole of glucose, according to the following reaction [4–10]:



The ΔG° of this reaction is $-206.3 \text{ kJ mol}^{-1}$ [4]. Few species can approach this limit due to thermodynamic limitations and metabolic requirements such as maintaining a supply of NADH that can be met by lactate production.

Thermotoga neapolitana is a rod-shaped bacterium of approximately $1.0\text{--}10.0 \mu\text{m}$ in length and $0.4\text{--}1.0 \mu\text{m}$ in diameter. The bacteria are wrapped by an external membrane named “toga” [5,6] that forms an outer sheath ballooning over the ends [11]. A few years ago, we reported a novel anaerobic process, named capnophilic lactic fermentation (CLF) (capnophilic means “requiring CO_2 ”), that enables a non-competitive synthesis of L-lactic acid (LA) and hydrogen in *T. neapolitana* [12–15]. As shown in Figure 1, the fermentation process is activated by CO_2 and, nominally, is dependent on a Janus pathway, which includes a catabolic branch leading to acetyl-CoA (Ac-CoA) from sugars by glycolysis as well as an anabolic branch converting Ac-CoA and CO_2 to pyruvate by PFOR (pyruvate:ferredoxin oxidoreductase; EC 1.2.7.1) and synthesizing LA by lactate dehydrogenase (LDH; EC 1.1.1.27) [12,14–17]. In addition to energetic flow derived from glycolysis, analysis of the transcripts suggested that flavin-based oxido-reductase enzymes such as NADH-dependent reduced ferredoxin: NADP oxidoreductase (NFN) and NAD ferredoxin oxidoreductase (RNF) supply reduced ferredoxin and NADH to support concomitant synthesis of lactic acid and hydrogen [17].

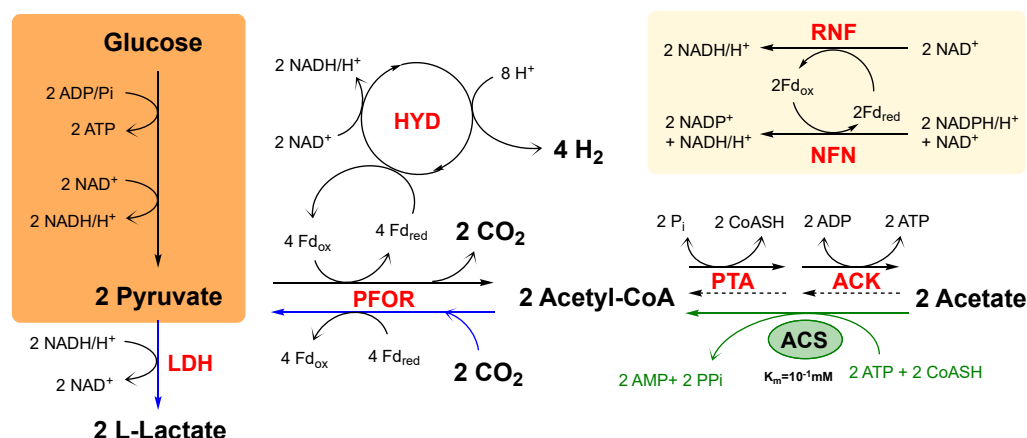


Figure 1. Schematic representation of the biochemical pathway underlying the CLF process. Plain black arrows indicate the catabolic branch; blue arrows indicate the anabolic branch; green arrow indicates the ACS heterologous insertion. Boxes indicate glycolysis (orange) and putative NADH production by flavin-based oxido-reductase enzymes (pale yellow). ACK, acetate kinase; PTA, phosphotransacetylase; ACS, acetyl-CoA synthetase; PFOR, pyruvate:ferredoxin oxidoreductase; LDH, lactate dehydrogenase; HYD, hydrogenase; RNF, NAD-ferredoxin oxidoreductase; NFN, NADH-dependent reduced ferredoxin:NADP oxidoreductase; Fd, ferredoxin. Green arrow indicates the ACS heterologous insertion.

In *T. neapolitana*, the acetate (AA) dissimilation pathway is supported by the reversible enzyme phosphate acetyltransferase (PTA; EC 2.3.1.8) and acetate kinase (ACK; EC 2.7.2.1). PTA converts acetyl-CoA and inorganic phosphate to acetyl-P and CoASH, while ACK converts acetyl-P and ADP to acetate and ATP [18]. AMP-AcetylCoA synthetase (ACS; EC 6.2.1.1) is considered a key enzyme involved in the irreversible acetate assimilation but not found in the *T. neapolitana* genome. In contrast to the ACK-PTA system, ACS first converts acetate and ATP to the enzyme-bound intermediate acetyl-adenylate (acetyl-AMP) while producing pyrophosphate. It then reacts acetyl-AMP with CoASH to form acetyl-CoA,

releasing AMP [19,20]. Metabolic engineering targeting the intracellular acetyl-CoA pool is typically conducted to enhance the acetyl-CoA supply for producing high-value added chemicals using acetyl-CoA as a precursor [21]. Heterologous expression of ACS has been described as a good strategy to increase acetate assimilation pathway [22].

The aim of the present study was to boost the flow from CO₂ and acetyl-CoA to LA (Figure 1—blue arrows) in order to increase the fixation rate of environmental CO₂ into LA and overtake the production of CO₂ from glycolysis (Figure 1—black arrows). Considering the upregulation of PFOR and LDH under CO₂ [17], an increase of the upstream acetate uptake could improve the acetate and CO₂ coupling. Although disruption of ACK and/or PTA may represent a valid approach to increase acetyl-CoA availability, methodology for knock-out of specific gene in *T. neapolitana* has not been reported. The strategy of this work was to increase acetate uptake in *T. neapolitana* by heterologous expressing a *Thermus thermophilus* ACS (Figure 1—green arrow). To achieve this, we adopted genetic manipulation techniques that were developed for other *Thermotoga* strains and optimized them for *T. neapolitana* DSM 33003, which is a strain adapted to saturating CO₂ concentration [23].

2. Materials and Methods

2.1. Strains and Growth Conditions

Thermotoga neapolitana subsp. *capnolactica* (DSM 33003) derives from the DSMZ 4359T strain that was isolated in our laboratory under saturating concentrations of CO₂ [23]. Bacterial cells were grown in a modified ATCC 1977 culture medium containing 10 mL/L of filter-sterilized vitamins and trace element solution (DSM medium 141) together with 10 g/L NaCl, 0.1 g/L KCl, 0.2 g/L MgCl₂ × 6H₂O, 1 g/L NH₄Cl, 0.3 g/L K₂HPO₄, 0.3 g/L KH₂PO₄, 0.1 g/L CaCl₂ × 2H₂O, 1 g/L cysteine-HCl, 2 g/L yeast extract, 2 g/L tryptone, 5 g/L glucose, and 0.001 g/L resazurin [17]. Resazurin was used as redox-sensitive indicator of oxygen levels in the medium. Media was aliquoted in 120 mL serum bottles, with 30 mL of culture. Anaerobic conditions were obtained by heating the medium until the solution became colourless. Serum bottles were sealed, capped, and autoclaved for 10 min at 110 °C. When needed, 2-¹³C-sodium acetate 20 mM was added into medium from a 60× stock solution, after filtration at 0.22 µm. Kanamycin and chloramphenicol were tested at 80 °C at different concentrations to test strain sensitivity (kanamycin: 200, 350, 400, and 500 µg/mL; chloramphenicol: 30, 50, 100, 150, and 300 µg/mL). Chloramphenicol at 200 µg/mL was used for selection of transformed strains. For routine experiment, bacterial precultures were incubated overnight at 80 °C without shaking and used to inoculate (6% v/v) cultures in 120 mL serum bottles with a final culture volume of 30 mL. Cultures were sparged with CO₂ gas for 5 min at 30 mL/min. Inoculated bottles were maintained in a heater (Binder ED720) at 80 °C. Every 24 h, 2 mL of samples were collected from each bottle, using a syringe through the rubber septum without altering the anaerobic atmosphere. The aliquots were centrifuged at 16,000× g for 15 min (Hermle Z3236K, Wehingen, Germany), and supernatants were stored at −20 °C until analyses. Every 24 h, pH was monitored, CO₂ was sparged for 5 min, and pH was adjusted to approximately 7.5 by 1 M NaOH. Cell growth was determined by measuring optical density (OD) at 540 nm (UV/Vis Spectrophotometer DU 730, Beckman Coulter, Pasadena, CA, USA). Cell morphology and spheroplast formation were monitored by microscope observation (Axio VertA1, Carl Zeiss, Oberkochen, Germany, magnification of 100×).

2.2. Gas and Chemical Analysis

H₂ measurements were performed by gas chromatography (GC) (Focus GC, Thermo Scientific, Waltham, MA, USA) equipped with a thermoconductivity detector (TCD) and fitted with a 3 m molecular sieve column (Hayesep Q). N₂ was used as the carrier gas. Glucose concentration was determined by the dinitrosalicylic acid method calibrated on a standard solution of 1 g/L glucose (Bernfeld, 1995). Organic acids were measured by ERETIC ¹H NMR as described by Nuzzo et al. (2019). All experiments were performed

on a Bruker DRX 600 spectrometer equipped with an inverse TCI CryoProbe. Peak integration, ERETIC measurements, and spectrum calibration were obtained by the specific subroutines of Bruker Top-Spin 3.1 program. Spectra were acquired with the following parameters: flip angle = 90°, recycle delay = 20 s, SW = 3000 Hz, SI = 16K, NS = 16, and RG = 1. An exponential multiplication (EM) function was applied to the FID for line broadening of 1 Hz. No baseline correction was used. For carbon balance, CO₂ was estimated according to the amount of produced acetic acid. For the correlation between cells dry weight (CDW) measurement and OD_{540nm}, a previously determined equation was used: $CDW (g/L) = 0.347 \times OD_{540nm} + 0.016$ [24]. The chemical composition of the dry cells was estimated adapting the empirical formula C₅H₈O₃NS_{0.05} reported in literature [25]. Data were averages of eight biological replicates for culture without and three biological replicates for culture with exogenous acetate.

2.3. Construction of Vectors

Vectors were constructed by following standard cloning methods and verified by restrictive digestions. The *Thermotoga-E. coli* shuttle vector pDH10 was used as the parent vector. DNA sequences were synthesized by GeneArt™, after codon usage optimization (Figure S1). Our selective marker was the chloramphenicol acetyltransferase (*cat*) gene variant A138T from *Staphylococcus aureus*, which was evolved by Kobayashi et al. (2015) for higher thermal stability [26]. The *cat* gene was cloned between EcoNI and EcoRI in place of the *kan* gene in pDH10, resulting in plasmid pGD11. The *acs* gene from *Thermus thermophilus* H8 (TTHA1248) was inserted downstream of the promoter sequence of *T. thermophilus* H8, which was already reported by Han et al. (2012) to be active in *Thermotoga* and was cloned into XbaI-SacI pGD11 to give rise to pGD11-ACS [27].

2.4. Spheroplast Formation and Transformation

Preparation of spheroplasts was adapted from a protocol already reported for *T. neapolitana* [28]. Briefly, 50 mL of *T. neapolitana* cells in early stationary phase was harvested and washed twice with WB solution [300 mM KCl, 2 mM MgSO₄ and 40 mM K₂HPO₄ (pH 7.0)]. After centrifugation at 16,000 × *g* for 15 min, spheroplasts were prepared by resuspending the pelleted cells in 500 µL of WB containing 350 mM sucrose, 2 mg/mL EDTA and 2 mg/mL lysozyme. The cell suspension was incubated at 37 °C and spheroplast formation was monitored by optical microscope at magnification 100× and reticulated lens. Efficiency of toga removal was estimated by the ratio between round cell number and total cell number. After 90 min of treatment, an efficiency of 80% in spheroplast formation was estimated. The reaction was stopped by incubation at 77 °C for 5 min. Spheroplasts were centrifuged and resuspended in the appropriate buffer to test different transformation protocols (natural transformation, liposome-mediated transformation, and electroporation-mediated transformation). For natural transformation, as reported by Han et al. (2014), 1 mL of the overnight culture or spheroplast preparation, obtained as described above, was collected by centrifugation, resuspended in 200 µL of fresh medium, and was injected into a 100 mL serum bottle containing 10 mL of fresh medium; DNA substrate was added to a final concentration of 5 µg/mL [29]. Then, the culture-DNA mixture was incubated at 80 °C for 4 to 6 h with gentle agitation (100 rpm) and then transferred into 100 mL serum bottles containing fresh medium, with a supplement of 200 µg/mL chloramphenicol for selection. Growth was monitored for 48 h. For liposome-mediated transformation, as reported by Yu et al. (2001), spheroplasts were resuspend in 1 mL solution (pH 7.4) of 4.5 mM NH₄Cl, 0.3 mM CaCl₂, 0.34 mM K₂HPO₄, 22 mM KCl, 2 mM MgSO₄, 340 mM NaCl, and 20 mM HEPES [30]. A DNA: liposome mixture was prepared by mixing 5 µg DNA to 20 µg DOTAP in a total volume of 100 µL of 20 mM HEPES buffer (pH 7.4). After 15 min of incubation at room temperature, the mixture was added to the spheroplasts suspension and incubated for 1 h at 37 °C. A 0.5 mL portion of the spheroplasts suspension was transferred into 10 mL medium in a serum bottle and incubated at 77 °C for cell recovery (5 h) and then inoculated in medium containing the antibiotic. For electroporation-mediated transformation, spher-

plasts were resuspended in 300 µL of electroporation buffer containing 10% glycerol and 0.85 M sucrose solution (EB), which was adapted from Han [27]. Two different amounts of spheroplast preparations (10^7 and 10^8) were tested for electroporation. Plasmid DNA (5 µg) was mixed with 300 µL of freshly made competent cells and incubated on ice for 5 min prior to introduction to a pre-chilled cuvette of 1 mM gap. For all operations, the capacitance was set at 25 µF, and the exponential pulses were tested with the following resistances and voltages: 400 Ω & 1.25 kV; 200 Ω & 1.8 kV; and 200 Ω & 2 kV (Gene PulserXcell™, Bio-Rad Laboratories, Hercules, CA, USA). After electroporation, 1 mL of fresh medium was added into each cuvette, and the cell suspension was transferred to 10 mL medium in a serum bottle and incubated at 77 °C with for 3 h for recovery and then inoculated in medium containing the antibiotic. Different amounts of the transformant cultures (2 mL, 5 mL, 10 mL, and 20 mL) were treated for plasmid isolation with QIAGEN miniprep kit according to manufacturer's instructions. The same protocol was also applied to 5 mL culture of *T. sp* RQ7 strain, and cryptic plasmid pRQ7 was revealed, indicating that the extraction procedure was successful. For PCR analysis, KAPA Taq PCR kit (MERK) was used. For target amplification, following ACS primers were used: *acs_Fw*: CGCCAACGT-GCTGAAAAGACTGGG; *acs_Rev*: GGCCAAGGTCTCGTGATACACAGG. PCR protocol was validated using pGD11-ACS extracted from *E. coli* as the template.

3. Results and Discussion

3.1. Assessment of Genetic Tools and Transformation Method

Genetic methods for the study of hyperthermophilic bacteria are at early stages of development. Although some examples of transformation of *Thermotogales* strains are reported [29,31–33], engineering approaches with these bacteria remain limited due to the technological barriers posed by their thermophilic and strictly anaerobic nature. Even fewer studies have been reported about the genetic transformation of bacteria belonging to *Thermotoga* genus (Table 1), and only the most recent reports focus on the development of auxotrophic strains [32,34] and knock-out of specific genes [33,35]. Therefore, considerable efforts have been paid to the development of methods to address an efficient transformation of DSM33003 (Figure S2). This work included identification of selection markers, preparation of competent cells, assessment of transformation techniques, and vector design.

In order to define a suitable selective marker, *T. neapolitana* DSM33003 was tested for its viability against kanamycin and chloramphenicol at 80 °C, which are thermostable antibiotics used for selection in *Thermotoga* species (Table 1). Due to the inconsistent results reported for the screening of transformed *T. neapolitana* on plate, the selection was carried out only in liquid media [30]. The thermostable antibiotics were tested at different concentrations ranging from 30 to 400 µg/mL by monitoring cell growth at 24 h, 48 h, and 72 h (Figure S3). Although kanamycin is the most widely used selective agent for bacteria of the genus *Thermotoga* (Table 1), DSM33003 is not sensitive to kanamycin, in agreement with another report on *T. neapolitana* [30]. On the contrary, chloramphenicol totally inhibited cell growth at concentration above 200 µg/mL and thus was chosen as the thermostable selective agent for DSM33003 at 200 µg/mL in liquid medium.

For vector design, the plasmid pDH10 (GenBank: JN813374) was used as the starting material. Vector pGD11 was constructed by replacing the Kan^r sequence of pDH10 with the evolved variant of chloramphenicol acetyltransferase (*cat*) from *Staphylococcus aureus* with increased thermal stability [26]. In addition to Kan^r sequence, pDH10 carries ColE1 origin of replication (*ori*) and β-lactamase (Amp^r) for amplification and selection in *E. coli*. Moreover, like pJY1, pDH10 relies on the sequence of the endogenous plasmid pRQ7 to guarantee replication in *Thermotoga* [30]. The heterologous sequence of ACS and the selected promoter from *T. thermophilus* HB8 were optimized according to codon usage of *T. neapolitana*, synthesized, and cloned into XbaI-SacI in pGD11, resulting in the plasmid pGD11-ACS (Figure S4).

Table 1. Genetic manipulation reported for *Thermotoga* genus. Antibiotic (ant), auxotrophy (aux), and spheroplast (sph). All replicating plasmid used in the above-mentioned studies are based on the sequence of endogenous cryptic plasmid pRQ7.

Strain	Selection	Strategy	Transformation Technique	Target	Ref.
<i>T. maritima</i>	ant (kanamycin)	Replicating plasmid	sph-DOTAP/electroporation	<i>kan</i> heterologous expression	[27]
	ant (kanamycin)	Replicating plasmid	sph-DOTAP	<i>kan</i> heterologous expression	[30]
	aux (uracil)	Chromosomal recombination	sph-DOTAP/natural transformation	knock-out & knock-in <i>araA</i>	[34]
	aux (uracil)	Chromosomal recombination	natural transformation	knock-out <i>malkX</i> genes	[33]
	ant (kanamycin)	Chromosomal recombination	electroporation	transient inactivation of <i>ldh</i>	[33]
	aux (uracil)	Chromosomal recombination	electroporation	knock-in <i>malk3</i>	[33]
<i>T. sp. RQ7</i>	ant (kanamycin)	Replicating plasmid	sph-DOTAP/electroporation	<i>kan</i> heterologous expression	[27]
	ant (kanamycin)	Replicating plasmid	natural transformation	<i>kan</i> heterologous expression	[29]
	aux (uracil)	Replicating plasmid	natural transformation	<i>pyrE</i> heterologous expression	[32]
<i>T. sp. RQ2</i>	ant (kanamycin)	Replicating plasmid	natural transformation	<i>kan</i> + <i>amyA-celB</i> heterologous expression	[31]
	ant (kanamycin)	Replicating plasmid	natural transformation	<i>kan</i> + <i>xynB-celB</i> heterologous expression	[31]
	ant (kanamycin)	Replicating plasmid	natural transformation	<i>kan</i> + <i>xynB-celA</i> heterologous expression	[31]
<i>T. neapolitana</i>	ant (chloramphenicol)	Replicating plasmid	sph-DOTAP	<i>cat</i> heterologous expression	[30]

It has been reported that the periplasmic space between toga and plasma membrane negatively affects the transformation of *Thermotoga* spp. as the wider the space correlates to the lower permeation of DNA [29]. In 2001, Yu et al. reported acquisition of transient chloramphenicol resistance in liquid culture of *T. neapolitana* after spheroplast formation [30]. Analogously, pDH10 vector has been used to confer kanamycin resistance to *T. maritima* and *T. sp* RQ7 by liposome-mediated transformation of spheroplast [27]. Removal of toga in *T. neapolitana* DSM33003 was obtained by adapting original protocol reported in Yu et al., 2001 [30]. Cells harvested in early stationary phase were treated with 3 mg/mL lysozyme and incubated for 90 min at 37 °C. This treatment induced formation of round spheroplasts clearly distinguishable from rod-shaped cells with toga by optical microscope at 100× (Figure S5).

3.2. Generation of Recombinant Strains

Among *Thermotoga* spp., DNA uptake has been achieved by electroporation, natural transformation, and liposome-mediated electroporation (Table 1). Various conditions were investigated, including different electroporation pulses (1.25 kW–400 ω , 1.8 kW–200 ω), amount of plasmid DNA (1 μ g, 5 μ g), and spheroplast concentration (10^7 , 10^8). The most replicable condition assuring stable chloramphenicol-resistant *T. neapolitana* cells was electroporation at 1.8 kW–200 ω with 5 μ g of pGD11-ACS. Natural transformation was successful only when applied to spheroplast suspension of the bacterial cells, indicating that this strain is not naturally competent [32].

Despite several attempts to reveal ACS sequence by PCR from the plasmid and genomic DNA preparations of *T. neapolitana* transformants, no amplification was observed (primer sequences in Figure S4). The absence of amplified ACS may be caused by low copy numbers of the shuttle vectors, although a chromosomal integration cannot be excluded at the moment. It is worth to note that for all episomal transformations reported for *Thermotogales*, the whole plasmid was never revealed, and only PCR amplified fragments were used as further proof of transformation in addition to resistance acquisition [27,29–31]. Phenotypical traits of recombinant strains represent an indirect way to demonstrate DNA perturbation. For example, Xu reported the absence of PCR amplicons of a heterologous cellulase gene in a recombinant *Thermotoga* sp RQ2 strain, which clearly expressed the expected extracellular cellulase activity [31]. Recombinant strains *T. neapolitana* DSM33003/pGD11-ACS (named *Acs03*) and *T. neapolitana* DSM33003/pGD11 (the empty vector) were characterized for their capacities to couple acetate and CO₂ into LA in standard medium with antibiotic in comparison to the wild type strain (wt) in the standard condition without antibiotic (Figure 2).

Cells transformed with the empty vector showed a slowdown in growth compared to wt, probably due to a slight effect of the backbone plasmid including antibiotic resistance (Figure 2a). This influence was overcome in the *Acs03* recombinant strain, probably due to the occurrence of the heterologous gene or spontaneous mutation that improved the strain. In fact, *Acs03* accelerated growth and glucose consumption arising similar values of wt after 72 h of fermentation (Figure 2a).

Different yields of acetate (AA) and lactate (LA) were observed in *Acs03* compared to the empty vector and wt strains (Figure 2b). *Acs03* produced minor yield of AA (0.75 ± 0.02) in comparison to wt (1.15 ± 0.02) and empty vector control (1.3 ± 0.13) and doubled LA yield from 0.5 ± 0.03 (wt and empty vector control) to 1.13 ± 0.11 mM (Figure 2b). Increase of lactate in *Acs03* is partially covered by decrease of acetate yield. Significantly, ratio LA/AA in *Acs03* was about three times higher than in wt (0.44) and strain with empty vector (0.36) (Table 2). H₂ production was greatly impacted in *Acs03*, halving from 3.04 ± 0.1 mM to 1.56 ± 0.17 mM in *Acs03*.

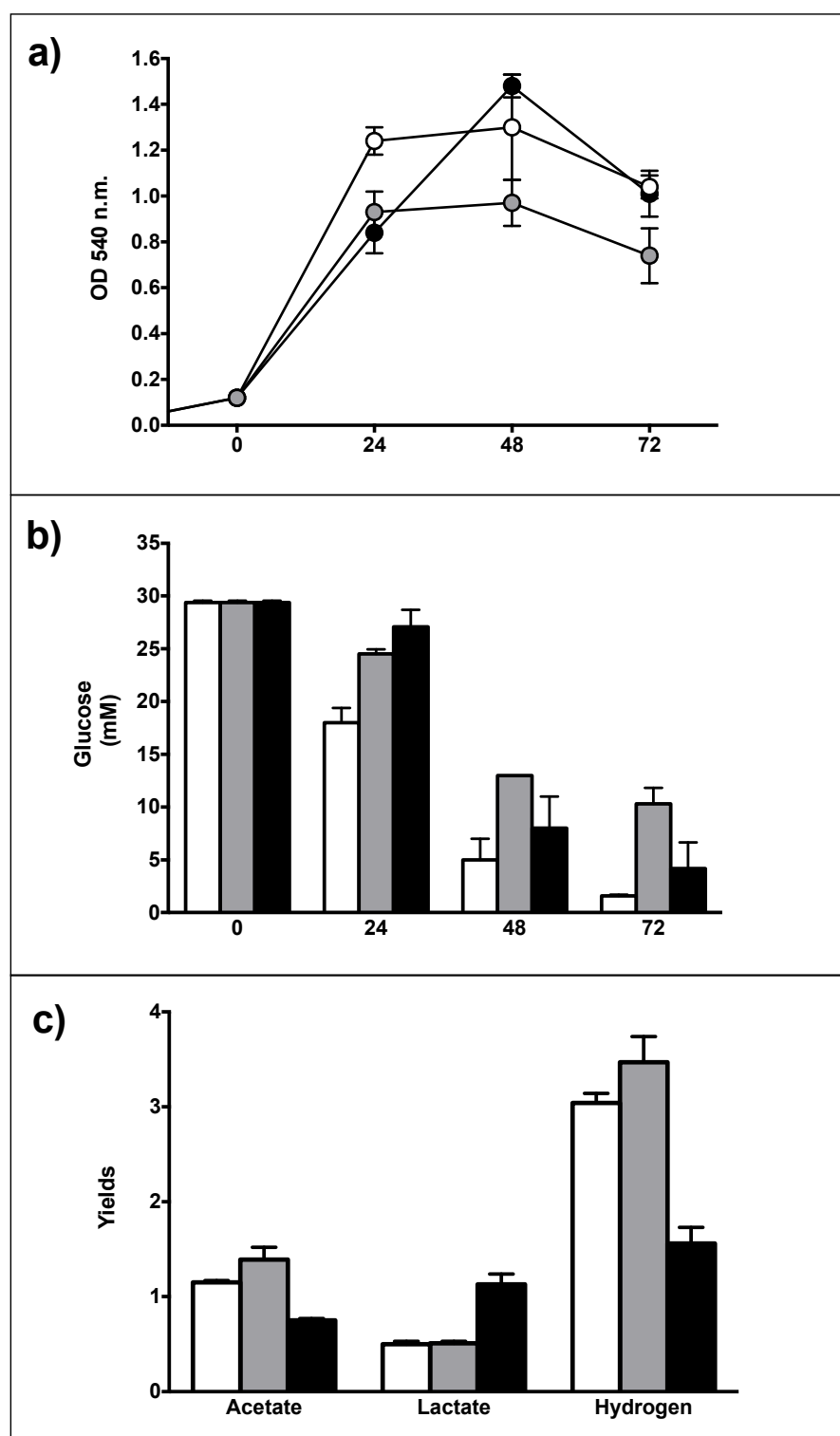


Figure 2. Batch fermentations of wild type (white circle/bars), empty vector (grey circle/bars) and ACS recombinant strain (black circle/bars) after 72 h in static condition. (a) Growth curves, expressed as OD_{540nm}; (b) Glucose consumption, expressed as mM; (c) Fermentation products, expressed as yield (mmol product/mmol consumed glucose). Chloramphenicol was used at 200 µg/mL for selection of recombinant strains. Data are expressed as mean ± SD, *n* = 3.

Table 2. Ratio of lactate (LA) and acetate (AA) yield in wild type (wt), empty vector, and ACS recombinant strain (*Acs03*).

	LA/AA
wt	0.44
Empty vector	0.36
<i>Acs03</i>	1.5

3.3. Catabolic and Anabolic Origins of Lactate

Generally, LA is formed from pyruvate reduction catalysed by LDH. Under CLF conditions, pyruvate can derive either from glycolysis (catabolic pyruvate) or enzymatic coupling of acetate and CO₂ (anabolic pyruvate) (Figure 1). To assess the origin of increased level of LA in *Acs03*, the contribution of each pathway to LA production was measured with external labelled 2-¹³C-acetate [14]. Consumption of 20 mM exogenous 2-¹³C-AA and formation of 3-¹³C-lactate (3-¹³C-LA) were monitored in ¹H-NMR spectra by integrating doublets flanking the methyl natural resonances of acetate at 1.9 ppm (methyl group of 2-¹³C-AA) and lactate at 1.33 ppm (methyl group of 3-¹³C-LA) (Figure S6). Although uptake of exogenous 2-¹³C-AA was quite similar for both strains (7.3 ± 0.4 mM for wt and 9.3 ± 1.1 mM for *Acs03*), capability to convert 2-¹³C-AA into 3-¹³C-LA was enhanced in the recombinant bacterium (Figure 3). Labelled LA was 1.7 fold higher in *Acs03* (6.67 ± 0.40 mM) in comparison to wt (3.90 ± 0.1 mM). Considering the stoichiometric reaction, we assessed that *Acs03* recycle 293.5 ± 18 mg/L of CO₂ and 547 ± 32 mg/L of acetate into 747 ± 45 mg/L of sodium lactate; in contrast, the wt recycled 172 ± 4.4 of CO₂ and 320 ± 8.2 of acetate into 437 ± 11.2 mg/L of sodium lactate. Molecular reorganization induced by pGD11-ACS in the recombinant strain *Acs03* boosted the fixation of CO₂ into lactate by 70%.

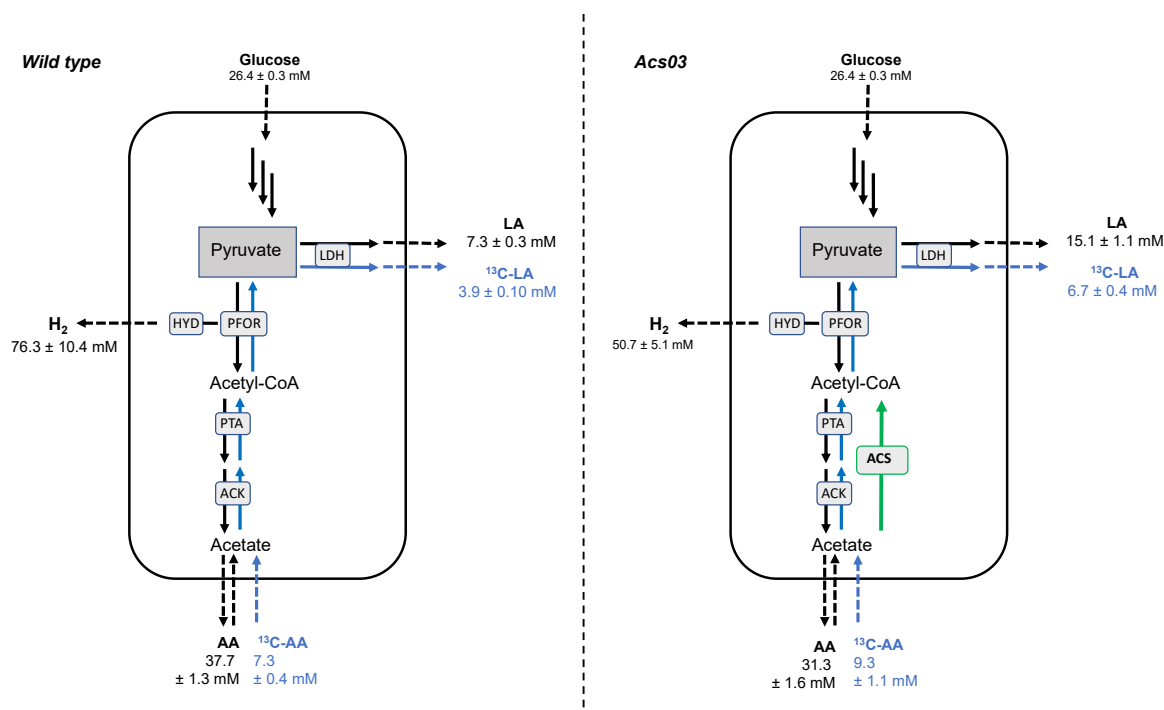


Figure 3. Capnophilic Lactic Fermentation (CLF) flow using 28 mM glucose and 20 mM 2-¹³C-acetate in the wild type and *Acs03* recombinant strain. Unlabelled lactate (LA) derived from catabolic pyruvate (glycolysis) and anabolic pyruvate produced by coupling reaction of CO₂ and unlabelled acetate (AA) produced by fermentation. 2-¹³C-acetate (¹³C-AA) is internalized and metabolized to 3-¹³C-lactate (¹³C-LA). ACK, acetate kinase; PTA, phosphotransacetylase; ACS, acetylCoA synthetase; PFOR, pyruvate:ferredoxin oxidoreductase; LDH, lactate dehydrogenase; HYD, hydrogenase. Green arrow indicates ACS heterologous insertion. Data are expressed as mean ± SD, *n* = 3.

As stated above, unlabelled-LA can be derived from pyruvate produced by glycolysis and/or from AA uptake. During the fermentation, exogenous labelled AA is diluted with unlabelled-AA produced by glucose catabolism. Although flux quantification from 1-¹³C-AA into 3-¹³C-LA is an underestimation of total LA deriving by coupling reaction of CO₂ and AA (endogenous + exogenous), it represents an unequivocal way to estimate the minimal flux, highlighting the improved performances of *AcS03* in comparison to wt.

Production of catabolic lactate identified as unlabelled-LA was also enhanced in the recombinant strain (from 7.3 ± 0.3 mM in wt to 15.1 ± 1.1 mM in *AcS03*), supporting a major flux from catabolic pyruvate to lactate. This should account for the reduction of hydrogen production from 76.3 ± 10.4 mM in wt to 50.7 ± 5.1 mM in *AcS03*. In dark fermentation, 2 mol of acetic acid and 4 mol of H₂ are theoretically produced for each mole of consumed glucose [4]. Theoretically, also in CLF, two moles of H₂ are produced for each mol of acetic acid, according to the Equation (2).

$$Y_{H_2}/Y_{AA} = 2 \quad (2)$$

On these bases, the ratio expressed in Equation (2) is about 2.0 and 1.6 for wt and *AcS03*, respectively. Hydrogen recovery was close to 100% in wt, and the experimental production (2.89 ± 0.39 mM) was very similar to expected theoretical amount (2.85 ± 0.1 mM) (Figure 3). On the other hand, in *AcS03* the H₂ recovery was around 80% and the experimental production (1.92 ± 0.19 mM) was significantly lower than the theoretical value (2.37 ± 0.12 mM). Hydrogenase in *T. neapolitana* belongs to flavin-based electron bifurcating (FBEB) Fe-Fe hydrogenases and catalyses the oxidation/reduction of NADH and ferredoxin simultaneously in a 1:1 ratio to evolve H₂ [36]. It utilizes the exergonic oxidation of Fd (*E*_m = −453 mV) to drive the unfavorable oxidation of NADH (*E*₀ = −320 mV) to produce H₂ (*E*₀ = −420 mV). The overall hydrogenase reaction can be described as follows:



Thus, loss in H₂ yield with *AcS03* is very likely related to the increased consumption of NADH for the additional synthesis of lactic acid with consequent reduction of the availability of this cofactor for the H₂ production. Under CLF, in addition to energetic flow derived from glycolysis, flavin-based enzymes NFN and RNF are suggested to be involved in the supply of reduced ferredoxin and NADH to support concomitant synthesis of lactic acid and hydrogen [17]. DNA perturbation imposed by heterologous expression of ACS probably impacted this electron balance circuit, lowering the general yield of hydrogen as electron sink. In theory, the demand of NADH might also be sustained by H₂ consumption in recombinant strain.

A metabolic reorganization in microorganism overexpressing acetate activating pathway has been reported with conflicting results [37–40]. Zhang engineered *E. coli* with ACK-PTA and ACS pathways to increase N-acetylglutamate (NAG) production from acetate. The strain overexpressing ACK-PTA pathways increased NAG production 77.9% compared to the wild type strain, while the strain expressing ACS resulted in the biomass and NAG production about 40% lower than the wild type [40]. In contrast, the ACS pathway has been reported as the best choice for itaconic acid production in *E. coli*. In conditions tested by Noh [39], ACK-PTA pathway did not affect acetate consumption and itaconic acid production and caused a significative biomass reduction (wt, 0.81 ± 0.05 g/L; ACS expressing, 1.25 ± 0.12 g/L; ACK-PTA expressing, 0.21 ± 0.01 g/L) [39]. It worth noting that, in ACS-expressing systems, a significant effect is caused by higher ATP demand of this acetate activating pathway [41].

4. Conclusions

A metabolic engineering approach has boosted acetate uptake and reductive carboxylation of acetyl coenzyme of CLF pathway in *T. neapolitana* DSM33003. The enhancement was achieved by transformation with heterologous ACS-coding gene from *T. thermophilus*.

Detailed characterization of fermentation products of the recombinant strain proved the restructuring of metabolic fluxes and resulted in a doubled production of lactic acid and a reduction of H₂ production. Batch fermentations with exogenous ¹³C-labeled acetate established that the increased lactate in recombinant strain derived both from anabolic and catabolic branch of CLF. Forthcoming studies will focus on selective approaches of strain engineering to increase CO₂ fixation into lactic acid without impairing hydrogen production.

Supplementary Materials: The following are available online at <https://www.mdpi.com/article/10.3390/microorganisms9081688/s1>.

Author Contributions: Conceptualization, G.d. and A.F.; Experimental activity, M.V., N.E., M.L., S.L. and L.C.; Data analysis, all authors; Data curation, S.L. and M.V.; Writing—original draft, M.V., N.E., M.L., S.L. and G.d.; Writing—review and editing, Z.X., C.G., G.N., E.M. and A.F.; Supervision, G.d., A.F. and Z.X.; Funding acquisition, A.F. and G.d. All authors have read and agreed to the published version of the manuscript.

Funding: This research was funded by the BioRECO2VER Project, through the European Union's Horizon 2020 Research and Innovation Programme under Grant Agreement No. 760431.

Conflicts of Interest: The authors declare that the research was conducted in the absence of any commercial or financial relationships that could be construed as a potential conflict of interest.

References

1. Zeldes, B.M.; Keller, M.W.; Loder, A.J.; Straub, C.T.; Adams, M.W.W.; Kelly, R.M. Extremely thermophilic microorganisms as metabolic engineering platforms for production of fuels and industrial chemicals. *Front. Microbiol.* **2015**, *6*, 1209. [CrossRef]
2. Frock, A.D.; Kelly, R.M. Extreme thermophiles: Moving beyond single-enzyme biocatalysis. *Curr. Opin. Chem. Eng.* **2012**, *1*, 363–372. [CrossRef]
3. Verhaart, M.R.A.; Bielen, A.A.M.; Van Der Oost, J.; Stams, A.J.M.; Kengen, S.W.M. Hydrogen production by hyperthermophilic and extremely thermophilic bacteria and archaea: Mechanisms for reductant disposal. *Environ. Technol.* **2010**, *31*, 993–1003. [CrossRef]
4. Thauer, R.K.; Jungermann, K.; Decker, K. Energy Conservation in Chemotrophic Anaerobic Bacteria. *Am. Soc. Microbiol. Vol.* **1977**, *41*, 100–180. [CrossRef]
5. Huber, R.; Hannig, M. Thermotogales. *Prokaryotes* **2006**, 899–922. [CrossRef]
6. Bhandari, V.; Gupta, R.S. *The Phylum Thermotogae*; Springer: Berlin/Heidelberg, Germany, 2014.
7. Pradhan, N.; Dipasquale, L.; D'Ippolito, G.; Panico, A.; Lens, P.N.L.; Esposito, G.; Fontana, A. Hydrogen production by the thermophilic bacterium *Thermotoga neapolitana*. *Int. J. Mol. Sci.* **2015**, *16*, 12578–12600. [CrossRef]
8. Belahbib, H.; Summers, Z.M.; Fardeau, M.L.; Joseph, M.; Tamburini, C.; Dolla, A.; Ollivier, B.; Armougom, F. Towards a congruent reclassification and nomenclature of the thermophilic species of the genus *Pseudothermotoga* within the order *Thermotogales*. *Syst. Appl. Microbiol.* **2018**, *41*, 555–563. [CrossRef] [PubMed]
9. Shao, W.; Wang, Q.; Rupani, P.F.; Krishnan, S.; Ahmad, F.; Rezaia, S.; Rashid, M.A.; Sha, C.; Md Din, M.F. Biohydrogen production via thermophilic fermentation: A prospective application of *Thermotoga* species. *Energy* **2020**, *197*, 117199. [CrossRef]
10. Lanzilli, M.; Esercizio, N.; Vastano, M.; Xu, Z.; Nuzzo, G.; Gallo, C.; Manzo, E.; Fontana, A.; D'Ippolito, G. Effect of cultivation parameters on fermentation and hydrogen production in the phylum *Thermotogae*. *Int. J. Mol. Sci.* **2021**, *22*, 341. [CrossRef]
11. Jannasch, H.W.; Huber, R.; Belkin, S.; Stetter, K.O. *Thermotoga neapolitana* sp. nov. of the extremely thermophilic, eubacterial genus *Thermotoga*. *Arch. Microbiol.* **1988**, *150*, 103–104. [CrossRef]
12. Dipasquale, L.; D'Ippolito, G.; Fontana, A. Capnophilic lactic fermentation and hydrogen synthesis by *Thermotoga neapolitana*: An unexpected deviation from the dark fermentation model. *Int. J. Hydrog. Energy* **2014**, *39*, 4857–4862. [CrossRef]
13. Dipasquale, L.; Pradhan, N.; Ippolito, G. Potential of Hydrogen Fermentative Pathways in Marine Thermophilic Bacteria: Dark Fermentation and Capnophilic Lactic Fermentation in *Thermotoga* and *Pseudothermotoga* Species. In *Grand Challenges in Marine Biotechnology, Grand Challenges in Biology and Biotechnology*; Springer: Cham, Switzerland, 2018; pp. 217–235, ISBN 9783319690759.
14. d'Ippolito, G.; Dipasquale, L.; Fontana, A. Recycling of Carbon Dioxide and Acetate as Lactic Acid by the Hydrogen-Producing Bacterium *Thermotoga neapolitana*. *ChemSusChem* **2014**, *7*, 2678–2683. [CrossRef]
15. Nuzzo, G.; Landi, S.; Esercizio, N.; Manzo, E.; Fontana, A.; D'Ippolito, G. Capnophilic lactic fermentation from *Thermotoga neapolitana*: A resourceful pathway to obtain almost enantiopure L-lactic acid. *Fermentation* **2019**, *5*, 34. [CrossRef]
16. Pradhan, N.; Dipasquale, L.; d'Ippolito, G.; Fontana, A.; Panico, A.; Pirozzi, F.; Lens, P.N.L.; Esposito, G. Model development and experimental validation of capnophilic lactic fermentation and hydrogen synthesis by *Thermotoga neapolitana*. *Water Res.* **2016**, *99*, 225–234. [CrossRef]
17. d'Ippolito, G.; Landi, S.; Esercizio, N.; Lanzilli, M.; Vastano, M.; Dipasquale, L.; Pradhan, N.; Fontana, A. CO₂-Induced Transcriptional Reorganization: Molecular Basis of Capnophilic Lactic Fermentation in *Thermotoga neapolitana*. *Front. Microbiol.* **2020**, *11*, 171. [CrossRef]

18. Wolfe, A.J. The Acetate Switch. *Microbiol. Mol. Biol. Rev.* **2005**, *69*, 12–50. [[CrossRef](#)] [[PubMed](#)]
19. Berg, P. Acyl adenylates; an enzymatic mechanism of acetate activation. *J. Biol. Chem.* **1956**, *222*, 991–1013. [[CrossRef](#)]
20. Chou, T.C.; Lipmann, F. Separation of acetyl transfer enzymes in pigeon liver extract. *J. Biol. Chem.* **1952**, *196*, 89–103. [[CrossRef](#)]
21. Krivoruchko, A.; Zhang, Y.; Siewers, V.; Chen, Y.; Nielsen, J. Microbial acetyl-CoA metabolism and metabolic engineering. *Metab. Eng.* **2015**, *28*, 28–42. [[CrossRef](#)] [[PubMed](#)]
22. Song, J.Y.; Park, J.S.; Kang, C.D.; Cho, H.Y.; Yang, D.; Lee, S.; Cho, K.M. Introduction of a bacterial acetyl-CoA synthesis pathway improves lactic acid production in *Saccharomyces cerevisiae*. *Metab. Eng.* **2016**, *35*, 38–45. [[CrossRef](#)] [[PubMed](#)]
23. Pradhan, N.; Dipasquale, L.; d'Ippolito, G.; Panico, A.; Lens, P.N.L.; Esposito, G.; Fontana, A. Hydrogen and lactic acid synthesis by the wild-type and a laboratory strain of the hyperthermophilic bacterium *Thermotoga neapolitana* DSMZ 4359T under capnophilic lactic fermentation conditions. *Int. J. Hydrog. Energy* **2017**, *42*, 16023–16030. [[CrossRef](#)]
24. Pradhan, N.; Dipasquale, L.; D'Ippolito, G.; Fontana, A.; Panico, A.; Lens, P.N.L.; Pirozzi, F.; Esposito, G. Kinetic modeling of fermentative hydrogen production by *Thermotoga neapolitana*. *Int. J. Hydrog. Energy* **2016**, *41*, 4931–4940. [[CrossRef](#)]
25. Munro, S.A.; Zinder, S.H.; Walker, L.P. The fermentation stoichiometry of *Thermotoga neapolitana* and influence of temperature, oxygen, and pH on hydrogen production. *Biotechnol. Prog.* **2009**, *25*, 1035–1042. [[CrossRef](#)]
26. Kobayashi, J.; Furukawa, M.; Ohshiro, T.; Suzuki, H. Thermoadaptation-directed evolution of chloramphenicol acetyltransferase in an error-prone thermophile using improved procedures. *Appl. Genet. Mol. Biotechnol.* **2015**, *99*, 5563–5572. [[CrossRef](#)]
27. Han, D.; Norris, S.M.; Xu, Z. Construction and transformation of a *Thermotoga-E. coli* shuttle vector. *BMC Biotechnol.* **2012**, *12*. [[CrossRef](#)]
28. Käslin, S.A.; Childers, S.E.; Noll, K.M. Membrane-associated redox activities in *Thermotoga neapolitana*. *Arch. Microbiol.* **1998**, *170*, 297–303. [[CrossRef](#)]
29. Han, D.; Xu, H.; Puranik, R.; Xu, Z. Natural transformation of *Thermotoga* sp. strain RQ7. *BMC Biotechnol.* **2014**, *14*. [[CrossRef](#)]
30. Yu, J.S.; Vargas, M.; Mityas, C.; Noll, K.M. Liposome-mediated DNA uptake and transient expression in *Thermotoga*. *Extremophiles* **2001**, *5*. [[CrossRef](#)]
31. Xu, H.; Han, D.; Xu, Z. Expression of Heterologous Cellulases in *Thermotoga* sp. Strain RQ2. *Biomed. Res. Int.* **2015**. [[CrossRef](#)]
32. Han, D.; Xu, Z. Development of a pyrE-based selective system for *Thermotoga* sp. strain RQ7. *Extremophiles* **2017**, *21*, 297–306. [[CrossRef](#)]
33. Singh, R.; White, D.; Demirel, Y.; Kelly, R.; Noll, K.; Blum, P. Uncoupling fermentative synthesis of molecular hydrogen from biomass formation in *Thermotoga maritima*. *Appl. Environ. Microbiol.* **2018**, *84*, 998–1016. [[CrossRef](#)]
34. White, D.; Singh, R.; Rudrappa, D.; Mateo, J.; Kramer, L.; Freese, L.; Blum, P. Contribution of pentose catabolism to molecular hydrogen formation by targeted disruption of arabinose isomerase (araA) in the hyperthermophilic bacterium *Thermotoga maritima*. *Appl. Environ. Microbiol.* **2017**, *83*, 2631–2647. [[CrossRef](#)]
35. Singh, R.; White, D.; Blum, P. Identification of the ATPase Subunit of the Primary Maltose Transporter in the Hyperthermophilic Anaerobe *Thermotoga maritima*. *Appl. Environ. Microbiol.* **2017**, *83*, e00930-17. [[CrossRef](#)]
36. Greening, C.; Trchounian, A.; Costa, K.; Müller, V.; Schuchmann, K.; Chowdhury, N.P. Complex Multimeric [FeFe] Hydrogenases: Biochemistry, Physiology and New Opportunities for the Hydrogen Economy. *Front. Microbiol.* **2018**, *9*. [[CrossRef](#)]
37. Xiao, Y.; Ruan, Z.; Liu, Z.; Wu, S.G.; Varman, A.M.; Liu, Y.; Tang, Y.J. Engineering *Escherichia coli* to convert acetic acid to free fatty acids. *Biochem. Eng. J.* **2013**, *76*, 60–69. [[CrossRef](#)]
38. Zhu, N.; Xia, H.; Wang, Z.; Zhao, X.; Chen, T. Engineering of Acetate Recycling and Citrate Synthase to Improve Aerobic Succinate Production in *Corynebacterium glutamicum*. *PLoS ONE* **2012**, *8*. [[CrossRef](#)]
39. Noh, M.H.; Lim, H.G.; Woo, S.H.; Song, J.; Jung, G.Y. Production of itaconic acid from acetate by engineering acid-tolerant *Escherichia coli* W. *Biotechnol. Bioeng.* **2018**, *115*, 729–738. [[CrossRef](#)]
40. Zhang, S.; Yang, W.; Chen, H.; Liu, B.; Lin, B.; Tao, Y. Metabolic engineering for efficient supply of acetyl-CoA from different carbon sources in *Escherichia coli*. *Microb. Cell Fact.* **2019**, *18*, 130. [[CrossRef](#)]
41. Shi, L.L.; Da, Y.Y.; Zheng, W.T.; Chen, G.Q.; Li, Z.J. Production of polyhydroxyalkanoate from acetate by metabolically engineered *Aeromonas hydrophila*. *J. Biosci. Bioeng.* **2020**, *130*, 290–294. [[CrossRef](#)]



Consiglio Nazionale
delle Ricerche



6. Evidence for a pentose phosphate pathway in the hyperthermophilic anaerobic bacterium *Thermotoga neapolitana*

Nunzia Esercizio¹ et al.,

¹ Institute of Biomolecular Chemistry (ICB), Consiglio Nazionale delle Ricerche (CNR), Via Campi Flegrei 34, 80078 Pozzuoli, Italy

² Department of Biology, University of Naples "Federico II", Via Cinthia, I-80126 Napoli, Italy



Article

Evidence for a pentose phosphate pathway in the hyperthermophilic anaerobic bacterium *Thermotoga neapolitana*

Nunzia Esercizio¹ et al.

¹ Institute of Biomolecular Chemistry (ICB), Consiglio Nazionale delle Ricerche (CNR), Via Campi Flegrei 34, 80078 Pozzuoli, Italy

² Department of Biology, University of Naples "Federico II", Via Cinthia, I-80126 Napoli, Italy

Abstract: The concomitant production of hydrogen and lactic acid via capnophilic lactic fermentation in the hyperthermophilic bacterium *Thermotoga neapolitana* requires additional redox potential to support these reduction reactions under CO₂. Rearrangement of the central carbon metabolism could ulteriorly boost the process. Along with the conventional Embden-Meyerhof pathway described in *T. neapolitana*, this work aims to highlight the presence and the activation of other alternative glycolytic pathways under capnophilic conditions (CO₂-induced) through experiments with ¹³C-labelled substrates, mainly 1,2-¹³C₂-glucose, 2-¹³C-glucose, 3-¹³C-glucose. The analysis of ¹³C labeling pattern by ¹H and ¹³C-NMR of the fermentation products, and the determination of the isotopic abundance of lactate isotopomers through GC-MS show the absence of the Entner-Doudoroff pathway and a possible activation of the pentose phosphate pathway. This result represents an interesting point of view, since it deviates from *T. maritima* in which ED was described. The pentose phosphate pathway could contribute to the generation of extra redox potential in form of NADH/NADPH during glucose catabolism.

Keywords: pentose phosphate pathway; redox potential; lactate; green hydrogen

Citation: Lastname, F.; Lastname, F.; Lastname, F. Title. *Int. J. Mol. Sci.* **2022**, *23*, x. <https://doi.org/10.3390/xxxxx>

Academic Editor: Firstname Lastname

Received: date

Accepted: date

Published: date

Publisher's Note: MDPI stays neutral with regard to jurisdictional claims in published maps and institutional affiliations.



Copyright: © 2022 by the authors. Submitted for possible open access publication under the terms and conditions of the Creative Commons Attribution (CC BY) license (<https://creativecommons.org/licenses/by/4.0/>).

1. Introduction

Thermotoga neapolitana is an anaerobic hyperthermophilic bacterium able to grow on different range of monosaccharides (hexoses and pentoses) and polysaccharides as carbon sources. Glucose fermentation generates the highest hydrogen yields, up to 3.5 mol H₂/mol sugar and organic acids, in particular acetic and lactic acid in different percentage (Jannasch et al., 1998; Huber and Hanning 2006; d'Ippolito et al., 2010; Eriksen et al., 2011; Cappelletti et al., 2014; Esercizio et al., 2021a). Up to now, sugar degradation in *Thermotoga neapolitana* is primarily operated by the classical EMP pathway, as described by d'Ippolito et al., 2010 with labeling experiments with 1,2-¹³C₂-glucose (d'Ippolito et al., 2010), in which a possible activation of ED pathway has excluded (d'Ippolito et al., 2010). This deviates from the results obtained in *Thermotoga maritima*, in which 15% activation of ED has been demonstrated (Schröder et al. 1994; Selig et al., 1997). In capnophilic condition, CO₂ sparging induced an up-regulation of the starting steps of the EMP (glucokinase (GCK – CTN_RS05065) and glucose 6-phosphate isomerase (PGI – CTN_RS01845)) and a significant down-regulation of subsequent enzymes. On the other hand, an up-regulation of glucose-6-phosphate dehydrogenase (G6PDH – CTN_RS07110) and 6-phosphogluconolactonase (6PGL – CTN_RS07115), recognized as the first responsible of the alternative glycolytic pathways ED and OPP suggests a metabolic switch of from EMP to ED or OPP (d'Ippolito et al., 2020). The activation of sugar degrading pathways in hyperthermophilic bacteria have been less studied, with the exception of *Thermotoga maritima* (Schröder et al. 1994; Schönheit and Schäfer 1995; Selig et al. 1997; De Vrije et al., 2007).

Several advantages are known in glucose catabolism through ED and/or OPP compared to EMP in term of reduced protein costs and amount of NAD(P)H, and the contribution of OPP in increasing hydrogen production has been elucidated in *T.maritima* (Woodward et al., 2002; Molenaar et al., 2009; Kim et al., 2011; Flamholz et al., 2013; Singh et al., 2018; d'Ippolito et al., 2020). All these evidences could justify the metabolic switch from EMP to ED or OPP in *Thermotoga neapolitana* under CLF condition as an advantageous mechanism to increase the availability of reducing equivalents required to sustain the concomitant productions of hydrogen and lactic acid. Reducing equivalents in form of NADPH are crucial in biosynthesis, and among the most important known NADPH-generating reactions there are: the oxidative pentose phosphate pathway (oxPPP), the Entner–Doudoroff (ED) pathway, and the isocitrate dehydrogenase step of the tricarboxylic acid (TCA) cycle (Spaan et al., 2005). The ED pathway is widely distributed with its variants among archaea, and is mainly present in modern prokaryotes, and even in Eukarya, representing the more primitive glycolytic pathway (Romano et al., 1996; Spaans et al., 2005; De Vrije et al., 2007). The OPP, similar to EMP, is an ancient biological process able to provide building blocks and NADPH for nucleic and amino acids syntheses. The oxidative irreversible branch is responsible for the production of NADPH, while the non-oxidative reversible branch generates metabolites also linked with the central carbohydrate metabolism, in form of glycolytic intermediates fructose-6-phosphate and glyceraldehyde-3-phosphate (Bertels et al., 2021). The reactions of the oxidative branch appear evolutionary more variables, as it is largely absent in archaea, in which a special ribulose monophosphate pathway (RMP) replaces the reactions of the oxidative PPP (Stincone et al., 2015; Bertels et al., 2021). On the other hand, the non-oxidative PPP branch results ubiquitous and provide the RNA backbone precursors ribose 5-phosphate and erythrose 4-phosphate as precursors for aromatic amino acids. These evidences might indicate that the oxidative part of the PPP pathway is evolutionarily newer than the non-oxidative branch (Stincone et al., 2015).

Since *T.neapolitana* apparently lacks the whole TCA pathway, the presence of alternative glycolytic pathways proves necessary to frame their role in feeding extra reducing equivalents and, in general, in the entire metabolism (d'Ippolito et al., 2020).

In this paper, retro-biosynthetic experiments have been conducted using different labeled ^{13}C -glucose precursors, particularly 1,2- $^{13}\text{C}_2$ -glucose, 3- ^{13}C -glucose and 2- ^{13}C -glucose, and the fermentation broth has been analyzed by NMR spectroscopy (^1H , ^{13}C and 2D-NMR) and GC-MS technique, to reconstruct the biosynthetic activated pathways through the analysis of the end-products, mainly acetate and lactate. This approach highlighted for the first time the activation of pentose phosphate pathway in *Thermotoga neapolitana* under capnophilic condition as alternative glycolytic pathway in glucose fermentation, while the activation of ED has been again excluded.

2. Results

2.1 Fermentation of 1,2- $^{13}\text{C}_2$ -glucose

The possible activation of alternative glycolytic pathways has been studied by a retro-biosynthetic approach. *T.neapolitana* cultures were incubated with 5g/L of 1,2- $^{13}\text{C}_2$ -glucose, 3- ^{13}C -glucose and 2- ^{13}C -glucose respectively, and the fermentation broth has been collected and analyzed through NMR and GC-MS analysis, to retrace labeled carbons in the end-products.

^1H NMR analysis of the fermentation broth with 1,2- $^{13}\text{C}_2$ glucose confirms the results showed in d'Ippolito et al., 2010. As reported in the expected labelled patterns in d'Ippolito et al., 2010, the presence of the major EMP products, the 2,3- $^{13}\text{C}_2$ -lactate and 1,2- $^{13}\text{C}_2$ -acetate, has been highlighted (d'Ippolito et al., 2010). The 2,3- $^{13}\text{C}_2$ -lactate is observable in

^1H NMR (Fig. 1A) as a “doublet of doublets”, that is a quartet around the unlabelled doublets of methyl group of lactate ($\delta=1.30\text{ppm}$, $^1J_{\beta\text{H}-\alpha\text{H}} = 7\text{ Hz}$), with

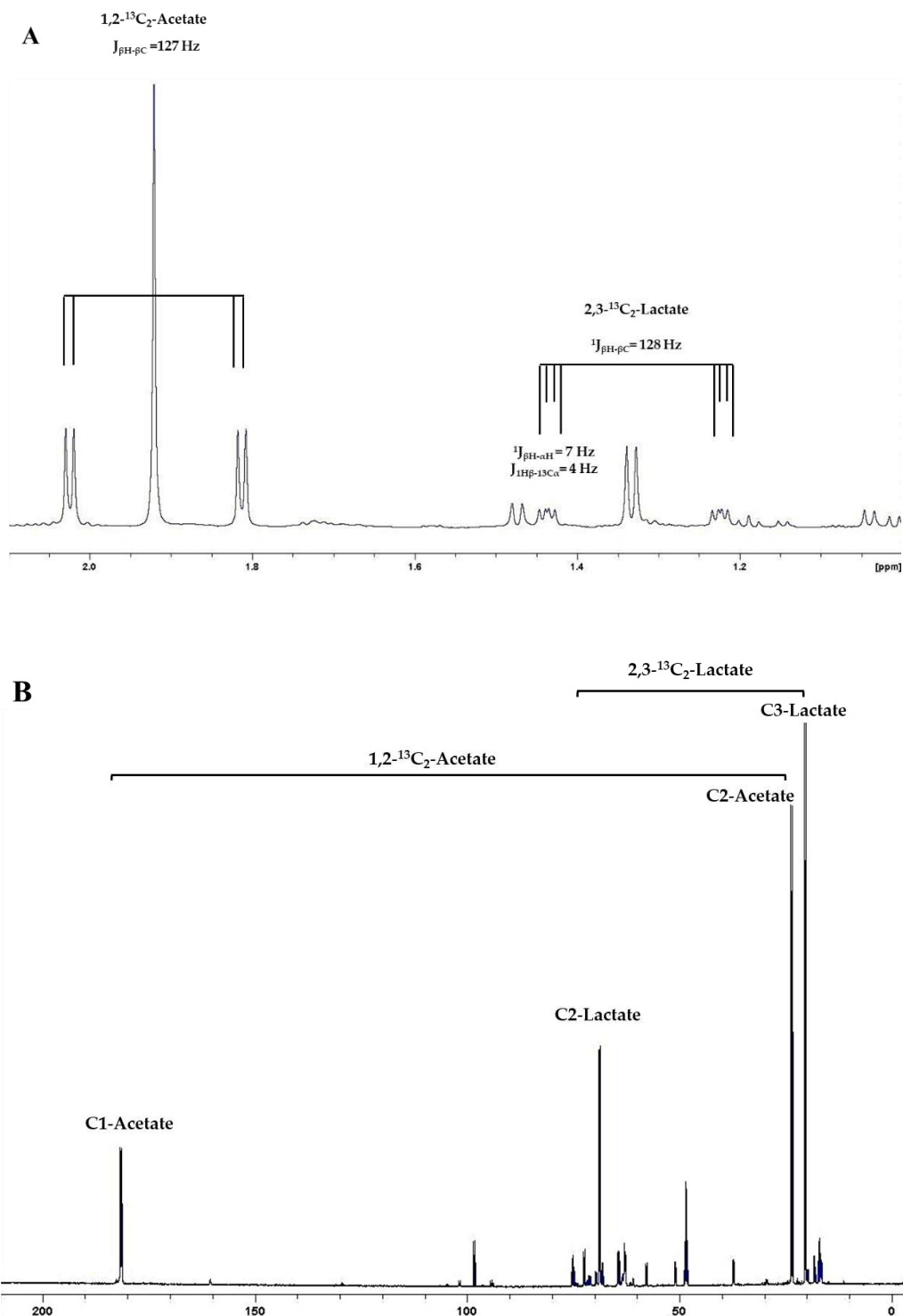


Fig.1 ^1H (A) and ^{13}C (B) NMR spectra of the fermentation broth supplied with $1,2\text{-}^{13}\text{C}_2$ glucose. $2,3\text{-}^{13}\text{C}_2\text{-lactate}$ and $1,2\text{-}^{13}\text{C}_2\text{-acetate}$ were observable in ^1H NMR by the doublet around the singlet at 1.90 ppm and the quartet around the doublet at 1.33 ppm respectively. The specific coupling constants are indicated. In ^{13}C NMR, carbon-carbon couplings are confirmed.

splitting $^1J_{\beta\text{H}-\beta\text{C}} = 128$ Hz (Lloyd et al., 2004). The first doublet describes the interaction of $^1\text{H}_\beta$ - $^1\text{H}_\alpha$ with $J = 7$ Hz, additionally splitting in another doublet with $J = 4$ Hz, representing the interaction of $^1\text{H}_\beta$ - $^{13}\text{C}_\alpha$. The presence of 1,2- $^{13}\text{C}_2$ -acetate was also revealable in ^1H NMR by the doublet around the singlet signal at 1.9 ppm, with $J_{\beta\text{H}-\beta\text{C}} = 127$ Hz, due to the coupling between the protons of the methyl group and the carboxyl function of acetate (**Fig.1A**). ^{13}C NMR analysis also confirm these evidences: the doublets at 21 ppm and 68.8 ppm with $J_{\alpha\text{C}-\beta\text{C}} = 37$ Hz are characteristic of the coupling between the methyl group and the alcoholic function of lactate, while the doublets at 24 ppm and 181 ppm with $J_{\alpha\text{C}-\beta\text{C}} = 52$ Hz indicate the coupling between the methyl group and the carboxyl function of acetate (**Fig.1B**). The EMP pathway was also confirmed in ^{13}C spectrum by the presence of labelled alanine in C_2 and C_3 (2,3- $^{13}\text{C}_2$ -alanine) as result of trans-amination from pyruvate, with doublets at 17 ppm and 51 ppm ($J = 34.7$ Hz). The 2D-NMR analysis (^{13}C - ^{13}C COSY spectrum) highlights also the correlations signals related to the presence of all the three forms of labelled 1,2- $^{13}\text{C}_2$ fructose (doublets of β -FP C1/C2, β -FF C1/C2 and α -FF C1/C2 fructose with $J = 50$ Hz at 64 ppm and 98 ppm, 62 ppm and 102 ppm and 63 ppm and 105 ppm respectively). No specific indications about the activation of the other glycolytic pathways were observed through NMR analysis.

2.2 Fermentation of 3- ^{13}C -glucose

The 3- ^{13}C -glucose is the key precursor for the evaluation of the Entner-Doudoroff pathway activation. Selig et al., 1997 showed in *T.maritima* the isotopic enrichment of the methyl groups of both acetate and lactate (2- ^{13}C -acetate and 3- ^{13}C -lactate) after incubation with 3- ^{13}C -glucose in the fermentation broth, as the results of the activation of ED (Selig et al., 1997). The analysis carried out on *T.neapolitana subsp.capnolactica* allow to exclude the presence of this pathway, since the expected labeled signals have not been found, as showed in ^1H and ^{13}C spectra. Only the unlabeled forms of acetate and lactate were detectable in ^1H spectrum of *T.neapolitana* fermentation broth (**Fig.2A**). Moreover, in ^{13}C spectrum, only the singlet signals at 182.5 and 176 ppm, corresponding to 1- ^{13}C -lactate and 1- ^{13}C -alanine respectively, derived from EMP pathway, were obtained. However, the presence of weak signals in ^{13}C spectra could be attributed to the activation of OPP pathway: first of all, the presence of a doublet around the singlet at 68.8 ppm, with $J = 55$ Hz, suggesting a possible coupling between the carboxyl group and the alcoholic function of lactate, even no signal is detectable around the singlet at 182.5 ppm (**Supplementary SX**). As showed in the expected labeling patterns published in Brekke et al., 2012, in which the activation of OPP pathway has been retraced with the same precursor, the 1,2- $^{13}\text{C}_2$ -lactate could be derived directly from OPP pathway: the synthesis of 1,2- $^{13}\text{C}_2$ fructose 6-phosphate could be the result of transketolase activity from 1- ^{13}C -erytrose 4-phosphate and 2- ^{13}C -xylulose 5-phosphate in the non-oxidative reactions of OPP pathway, and then metabolized through EMP to generate 1,2- $^{13}\text{C}_2$ -lactate, 1- ^{13}C -acetate and $^{13}\text{CO}_2$ (Brekke et al., 2012). Moreover, we can assume an additional contribution of the CLF pathway in the generation of 1,2- $^{13}\text{C}_2$ -lactate from 1- ^{13}C -acetate and the $^{13}\text{CO}_2$, the latter derived both from EMP and OPP activation. The final 2D-NMR analysis (^{13}C - ^{13}C COSY spectrum) confirms the presence of 1,2- $^{13}\text{C}_2$ -lactate with correlation signals at 180 ppm and 68 ppm (**Fig.2B**).

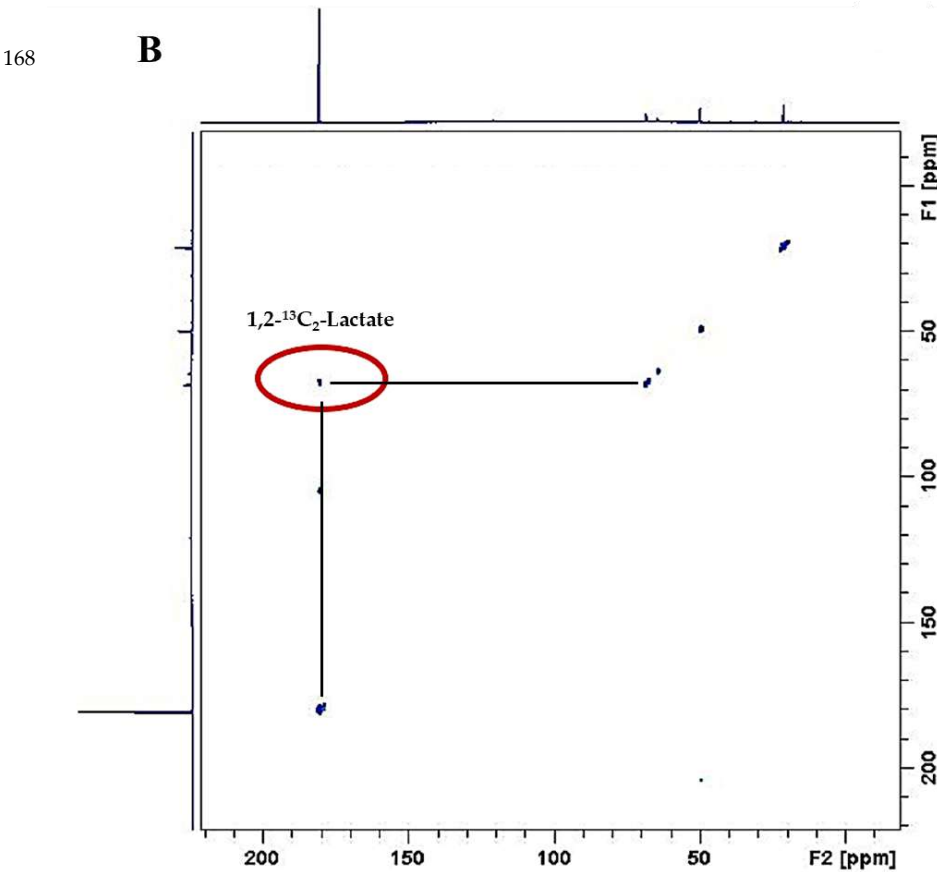
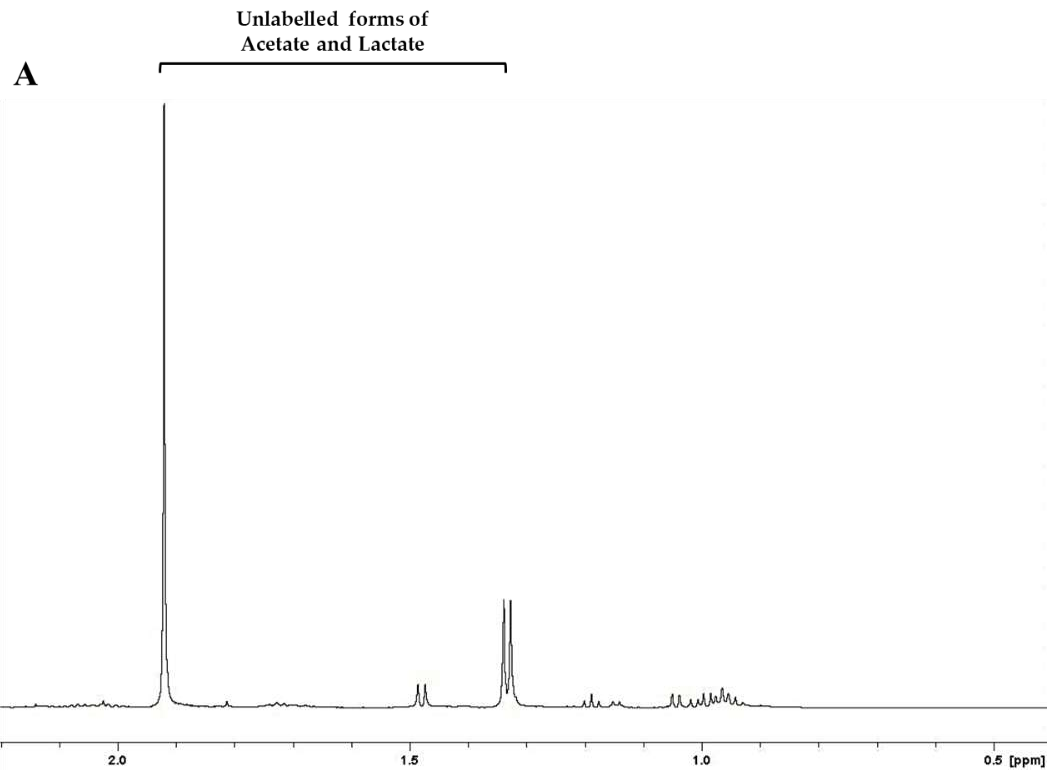


Fig.2 ^1H (A) and COSY ^{13}C - ^{13}C (B) NMR spectra of the fermentation broth of *Thermotoga neapolitana* supplied with 5 g/L of 3- ^{13}C glucose. ^1H NMR spectrum demonstrated the presence of only the unlabeled forms of acetate and lactate at 1.90 and 1.33 ppm respectively. ^{13}C - ^{13}C COSY spectrum Lines showed correlation between C1 (180 ppm) and C2 (68.8 ppm) of 1,2- $^{13}\text{C}_2$ -lactate.

As deduced from NMR analysis, the labeling pattern of lactate was precisely quantified by GC-MS analysis. The mass isotopomer distribution was evaluated in the fermentation broth with labeled glucose compared to a standard naturally labeled solution. The experimental mass distribution of the selected ion of TBDMS2-lactate (tert-butyldimethylsilyl derivate of lactate), $[\text{M}-\text{tB}]^+$, with m/z 261 showed an increase in the abundance of both $m+1$ and $m+2$ isotopomers compared to the standard, suggesting the presence of both the mono-labelled and di-labelled forms of lactate (**Table 1**). Although a qualitative analysis about the position of labeled ^{13}C is not possible with GC-MS, the increase in the $m+2$ isotopomer clearly demonstrated that lactate derived from a single labeled substrate possess two labeled ^{13}C as the results of the activation of OPP pathway.

Table 1. Mass isotopomer distribution of labeled and unlabeled lactate from 3- ^{13}C -glucose determined by GC/MS analysis.

	Unlabeled standard	Sample with 3- ^{13}C -glucose
261 m/z		
M	68.66	32.21
M+1	20.16	29.17
M+2	9.45	28.55
M+3	1.73	10.08

2.1.3 Fermentation of 2- ^{13}C -glucose

The incubation with 2- ^{13}C -glucose does not allow to discriminate between EMP and ED pathways, since the fermentation products of both via have the same labelling pattern. Either way produced, in fact, 1- ^{13}C -acetate and 2- ^{13}C -lactate. The 1- ^{13}C -acetate was evident in both ^1H and ^{13}C NMR spectra, with a splitted signal at 1.92 ppm and a singlet at 181 ppm respectively (**Fig.3A-3B**). The 2- ^{13}C -lactate was evident in ^{13}C spectrum with a singlet at 68.8 ppm (**Fig.3B**). The presence of a doublet around the carboxyl group of lactate, with $J=55\text{Hz}$ in ^{13}C spectrum could be attribute again to 1,2- $^{13}\text{C}_2$ -lactate (**Fig.3B**), and the 2D-NMR analysis (^{13}C - ^{13}C COSY spectrum) also confirm the correlation signals at 180 ppm and 68 ppm (spectrum not showed). In this context, as showed in the expected labeled pattern of fermentation in Brekke et al., 2012, the activation of OPP pathway generates $^{13}\text{CO}_2$, that could be coupled to 1- ^{13}C -acetate produced via EMP to produce 1,2- $^{13}\text{C}_2$ -lactate through CLF pathway.

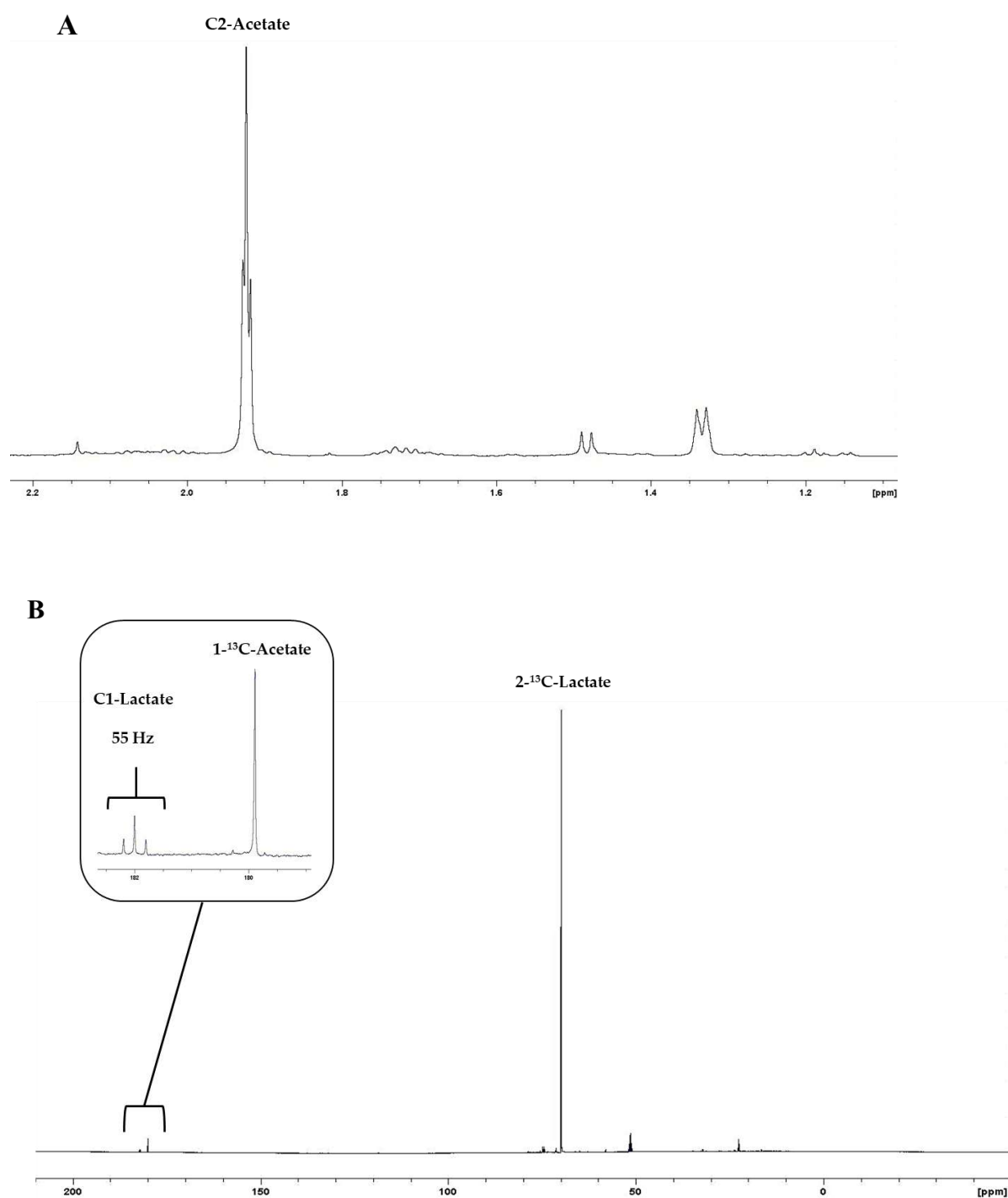


Fig.3 ^1H (A) and ^{13}C (B) NMR spectra of the supernatant with 2- ^{13}C glucose. The inset in section B shows the signals of doubly ^{13}C -labeled lactate (1,2- $^{13}\text{C}_2$ -lactate) at 180 ppm.

The mass distribution of labeled lactate was again quantified by GC-MS analysis. An increase in the $m+1$ and $m+2$ abundance of the selected ion $[\text{M-tB}]^+$, (m/z 261) suggested the presence of the mono-labelled and di-labelled forms of lactate (**Table 2**). To further confirm the presence of the 1,2- $^{13}\text{C}_2$ -lactate, the mass distribution of another selected fragment $[\text{M-COtB}]^+$ with m/z 233, as result of a molecular rearrangement and the

subsequent loss of 85 m/z relative to $[M]^+$ (due to the elimination of COtB), was evaluated. Surprisingly, the increase in the m+1 abundance in the fragment with m/z 233 demonstrated the presence of a single labeled ^{13}C , represented in this case only by the carbonylic carbon (CO) of lactate present in the fragment (Table 2), thus confirming the labeling of the C1 of lactate. Instead, the abundance of the m+2 isotopomer was comparable to the standard (Table 2).

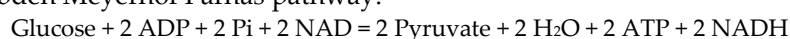
Table 2. Mass isotopomer distribution of labeled and unlabeled lactate from 2- ^{13}C -glucose determined by GC/MS analysis.

	Unlabeled standard	Sample with 2- ^{13}C -glucose
261 m/z		
M	68.66	36.70
M+1	20.16	35.46
M+2	9.45	19.34
M+3	1.73	8.50
233 m/z		
M	71.18	42.19
M+1	19.29	42.17
M+2	7.83	12.18
M+3	1.70	3.46

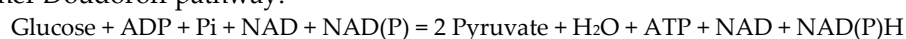
3. Discussion

Thermotoga neapolitana subsp. *capnolactica* (DSM 33003) represents an adapted strain in which CLF pathway was described for the first time (d'Ippolito et al., 2014; Dipasquale et al., 2014; Pradhan et al., 2016; d'Ippolito et al., 2020). The source of the extra reducing equivalents responsible for the concomitant production of hydrogen and lactic acid has to still been clarified to reconstruct the entire metabolic pathway. The analysis of the glycolytic pathways in *Thermotoga neapolitana* fits into this context, in order to evaluate the possibility of a metabolic switch from the classical Embden-Meyerhof pathway to an alternative via, as Entner-Doudoroff or PP pathways, thus explaining an energy advantage in term of ATP and/or reducing equivalents. The central metabolic pathways, as glycolysis, tend to be amphibolic, since they consist of a set of reactions that either generate usable energy, mainly in form of ATP (catabolism), or consume that energy to synthesize cellular components and to growth (anabolism) (Wolfe et al., 2015). Different strategies are available in nature to balance energy consumption and energy demand, includes the choice between EMP, ED and PP. A first assessment of the energy contribution of each glycolytic pathways are evident from the following equations (Folch et al., 2021):

- (1) Embden Meyerhof Parnas pathway:



- (2) Entner Doudoroff pathway:



- (3) Pentose phosphate pathway:



The Embden-Meyerhof Parnas (EMP) pathway is the most common bacterial glycolytic pathway. It invests two molecules of ATP in the first steps to phosphorylate and active the hexose sugar and to rearrange it for the cleavage into two triose phosphate (dihydroxyacetone-phosphate and D-glyceraldehyde-3-phosphate) (Wolfe et al., 2015). In the second part, each triose phosphate molecules are phosphorylated and oxidized (via NAD⁺) by glyceraldehyde dehydrogenase (GAPDH). Two subsequent substrate level phosphorylation yield 4 ATP and 2 pyruvate molecules. The net yield is of 2 ATP molecules per glucose with the concomitant reduction of 2 NAD⁺ (Equation 1) (Wolfe et al., 2015; Folch et al., 2021).

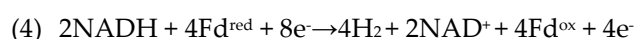
The Entner Doudoroff (ED) pathway is the second prominent glycolytic pathway, mainly known for Bacteria and few eukaryotic microorganisms, and widely distributed in Archaea with several modifications (Bräsen et al., 2014). Its general scheme is quite similar to the EMP: hexoses are phosphorylated and then the cleavage of 2-keto-3-deoxy-6-phosphogluconate into pyruvate and D-glyceraldehyde-3-phosphate generates 1 ATP per glucose and the reduction of 1 NADP⁺ and 1 NAD⁺ instead of reducing 2 NAD⁺ (see Equation 2) (Flamholz et al., 2013; Folch et al., 2021). The prominent differences are in the specific redox cofactors used (e.g., only NAD⁺ in EMP and both NAD⁺ and NADP⁺ in ED), and in ATP yields: the EMP pathway produces two ATP per glucose while the ED only one.

The Pentose-Phosphate (PP) pathway oxidizes glucose-6-phosphate to pentose phosphates, and it is an essential anabolic pathway to generate NADPH and building blocks for diverse biosynthetic processes (Wolfe et al., 2015; Folch et al., 2021). It differs from EMP since it uses a different set of reactions, different cofactors (NADP⁺ rather than NAD⁺) and produce D-ribose-5-phosphate, sedoheptulose-7-phosphate, and erythrose-4-phosphate, precursors for the biosynthesis of amino acids, nucleic acids, and other macromolecules, including ATP, coenzyme A, NADH and FADH₂ (Wolfe et al., 2015). The ribulose-5-phosphate splitting to β-D-fructose 6-phosphate and D-glyceraldehyde 3-phosphate, and the complete metabolism of both the molecules via EMP, generates 7/3 ATP per glucose, and the production of CO₂ results in more NADPH than from the other glycolytic pathways (see Equation 3) (Folch et al., 2021).

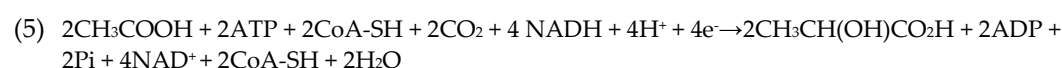
The choice of glycolytic pathway reflects the need to balance the energy consumption of ATP and cofactors, the production of ATP, and the synthesis of proteins and macromolecules. Since some intermediates and cofactors (e.g., dihydroxyacetone phosphate, glyceraldehyde-3-phosphate, pyruvate and NADH) are extracted from the glycolytic pathway to entry into the anabolic biosynthetic reactions, the yields of the metabolic pathway per glucose are always lower than theoretical. To reach the theoretical yields, all the electrons present in the substrate should be end up in the products, and then be redox-neutral (Folch et al., 2021). The presence of external electron acceptors, for example like in respiration, deviates electrons away from the products, thus reducing the net yields (Weusthuis et al., 2020).

The pyruvate generated from the EMP, ED and PP pathways is further metabolized by fermentation in absence of oxygen, and the end-products formation has to regenerate the redox cofactors used during glycolysis. To perform this partial oxidation, pathway intermediates act as electron donors and electron acceptors. The choice of the fermentation end-products determines the balance between the net ATP and the net recycled electron acceptors (Wolfe et al., 2015). *Thermotoga* spp. seems to operate a mixed acid fermentation, since pyruvate could undergo to terminal oxidation to acetate or can be diverted away for the synthesis of other organic substrates, as lactate, with NADH oxidation, or for the biosynthesis in form of acetyl-CoA. Lactate levels can vary among the *Thermotoga* species from trace amounts up to levels comparable with acetate (Schönheit, 1995; Anshuman et al., 2005; Khanna & Das, 2012; Schut & Adams, 2009). The advantage of the mixed acid fermentation is the possibility to generate additional ATP, when pyruvate is channeling through acetate, while recycling NAD⁺, when is converted to products such as lactate, ethanol or succinate (Wolfe et al., 2015).

In *Thermotoga* spp. glucose degradation and acetate production are also accompanied by hydrogen production via dark fermentation (Khanna et al., 2012). The electron-bifurcating [FeFe]-hydrogenase couples the unfavorable endoergonic reduction of H^+ to hydrogen by oxidation of NADH to the favorable exergonic oxidation of reduced ferredoxin, cyclically produced by pyruvate:ferredoxin oxidoreductase (PFOR) during the oxidation of pyruvate to acetyl coenzyme A (Schut & Adams, 2009). The overall hydrogenase reaction as summarized in the following Equation (4):



Thermodynamically, hydrogen production by reduction of H^+ with NADH is an unfavorable process in contrast with the organic acid formation, as lactate or ethanol (Cappelletti et al., 2014). However, in *Thermotoga* sp, hydrogen yields are close to 4 mol/mol of glucose oxidized, suggesting that thermodynamic constraints are overcome (Cappelletti et al., 2014). The presence of the Capnophilic lactic fermentation (CLF) in *T. neapolitana* further induces an energy rearrangement in the metabolism of this strain, since the competition for the NADH pools, required for both hydrogen and lactic acid productions, represent the main node that has to be balanced to sustain the entire process (see Equation 5):



Transcriptional analysis on *T. neapolitana* subsp. *capnolactica* under CLF condition showed an up-regulation of the alternative glycolytic pathways, suggesting that this metabolic condition pushed the cell through the activation of other mechanism to support the energy demand. In this context, the activation of the pentose phosphate pathway could be the key strategy since it provides more reducing power in form of NADH and more NADPH than the other glycolytic pathways.

Previously studies with labelled glucose fixed at 15% the contribution of the ED pathway in *Thermotoga maritima* wild type strain, and genomic analysis confirms the presence of all the gene involved in the alternative glycolytic pathways in *Thermotoga* metabolism (Selig et al., 1997; Flamholz et al., 2013; Singh et al., 2018). However, they assumed that the metabolically evolved strains of *T. mar*, able to produce more than the theoretical 4 mol of H_2 , seems to direct the carbon flux to the PP intermediates in order to generate additional reducing equivalents leading to greater levels of H_2 (Singh et al., 2017). Moreover, the NADPH generated via PP pathway could be direct to the NFN complex, catalyzing an extra pool of NADH, increasing the amount of reducing equivalents available for H_2 production (Singh et al., 2018).

Hence, our data about the activation of the pentose phosphate pathway in *T. neapolitana* opens up an interesting scenario in the metabolism of *Thermotogales* sp., since evidence of its activation has never been found in these species. NMR analysis (^1H and ^{13}C NMR) and GC-MS analysis were performed in order to retrace the metabolic flux of the fermentation products in the exhaust broth, and their relative isotopomers abundance was evaluated compared to the unlabeled form. The predominance of the Embden-Meyerhof pathway was demonstrated by the presence of all the expected labelling pattern of acetate and lactate derived from the fermentation of with 1,2- $^{13}\text{C}_2$ -glucose, 2- ^{13}C -glucose and 3- ^{13}C -glucose. In contrast, both ^1H and ^{13}C NMR results on the samples with 3- ^{13}C -glucose are significative to exclude the activation of the Entner-Doudoroff as alternative glycolytic pathway activated in *T. neapolitana* fermentation, due to the absence of labelled signals in both the methyl groups of acetate and lactate.

The clues that suggest an activation of the pentose phosphate pathway come from the ^{13}C NMR experiments and GC-MS analysis, in which a double labelled lactate together

with the single labeled form was observable, thus suggesting a substrate recycling via PP intermediates.

Based on these observations, the mechanism proposed for *T.maritima* modified strain could be clearly adapted to *T.neapolitana subsp. capnolactica*, since an up-regulation of also NFN and RNF complexes have been observed under CLF condition (d'Ippolito et al., 2020). Therefore, the pentose phosphate pathway could have a key role in CLF, since it could feed extra molecules of NADH, directly used for hydrogen production, and also NADPH molecules, that could be converted in NADH through the NFN complex, and used for the production of lactic acid via CLF simultaneously.

4. Materials and Methods

4.1 Culture conditions

Anaerobic cultures of *Thermotoga neapolitana subsp. capnolactica* (DSM 33003), derived from the DSMZ 4359T strain that was stimulated in our laboratory under saturating concentration of CO₂ for several years (Pradhan et al., 2017), were grown at 80°C in Tn medium supplemented with 28mM (5g/L) of glucose in 120 mL serum bottles with working volume of 30 mL. Fermentation batches were inoculated (6% v/v) with an overnight preculture at 80°C without shaking. Before each experiment, cultures were sparging with CO₂ or N₂ to remove oxygen for 5 min at 30 mL/min. Then pH was monitored and adjusted to 7.5 with NaOH 1M. These procedures were repeated every 24 h. Inoculated bottles were maintained in a heater (Binder ED720) at 80°C. Cell growth was determined by optical density (OD) at 540 nm (UV/Vis Spectrophotometer DU 730, Beckman Coulter). Samples (2 mL of medium) were collected from each bottle after 0, 24, and 48 h. After centrifugation at 16,000 × g for 15 min (Hermle Z3236K), residues and supernatants were kept at -20°C until analysis. Cell morphology was monitored by microscope observation (Axio VertA1, Carl Zeiss, magnification of 100×) (d'Ippolito et al., 2010; Dipasquale et al., 2014).

4.2 Chemical analysis

Hydrogen production was measured by a GC (Focus GC, Thermo Scientific) equipped with a thermoconductivity detector (TCD) and fitted with a 3 m molecular sieve column (Hayesep Q). N₂ was used as carrier gas at 20 mL/min. The headspace gas was sampled using a gas-tight syringe and equilibrated at room temperature. The glucose concentration was determined by the dinitrosalicylic acid method calibrated on a standard solution of 2 g L⁻¹ (Bernfeld et al., 1995). Fermentation products (acetic acid, lactic acid, alanine and others) were assessed by ¹H and ¹³C NMR spectroscopy. After centrifugation at 16,000 × g for 15 min (Hermle Z3236K), culture medium (0.6 mL) was diluted with D₂O/CD₃OD (2:1 v/v) and transferred to an NMR tube. Spectra were recorded on a Bruker DRX 600 spectrometer equipped with an inverse TCI CryoProbe.

4.3 ¹³C-labeling experiments

T.neapolitana subsp. capnolactica (DSM 33003) was grown as described above using a culture medium supplemented with 5 g/L of 1,2-¹³C₂-glucose, 2-¹³C-glucose and 3-¹³C-glucose (Sigma-Aldrich, Italy). Serum bottles were incubated at 80°C for 48h with pH correction and N₂ or CO₂ sparge. Gas samples from the headspace were regularly analyzed by GC, and the supernatant for NMR and MS analysis was collected by centrifugation.

4.4 NMR analysis

Organic acids concentrations were measured by ERETIC ¹H NMR applied on culture broth after dilution of supernatant (0.6 mL) with 0.1 mL of D₂O and transfer to an NMR

tube. All experiments were performed on Bruker DRX 600 spectrometer equipped with an inverse TCI CryoProbe. Peak integration, ERETIC measurements and spectrum calibration were obtained by the specific subroutines of Bruker Top-Spin program. Peak integration is based on the calibration with a standard solution of sodium lactate (20mM) in the same experimental condition. For the labelled patterns analysis and signals attribution also ^{13}C NMR and COSY NMR were performed on the same samples.

4.5 GC/MS analysis

The analysis of the ^{13}C labeling pattern of lactate and the quantification of the mass isotopomer distribution was performed by GC/MS using the method previously described in Adler et al., 2013 (Adler et al., 2013). Culture supernatant (5 μl) was dried under a nitrogen stream and then resuspended in 50 μl of dimethyl formamide (0.1% pyridine), and derivatized with 50 μl N-methyl-N-t-butyltrimethylsilyl-trifluoroacetamide (MBDSTFA) (Sigma-Aldrich, Italy). Samples were then analyzed by gas chromatography-mass spectrometry (GC/MS) using the following method: 80°C for 2 min; ramp, 15°C min $^{-1}$; final temperature, 325°C. Selected ion monitoring (SIM) was performed from m/z 261 to 264 to quantify the mass isotopomer of m+0, m+1, m+2, and m+3 ion fragments that contained all carbon atoms of lactate (M-57). The same selected ion monitoring (SIM) was performed from m/z 233 to 235 to quantify the mass isotopomer of m+0, m+1 and m+2 of ion fragments that contained only the CO of lactate (M-CO_tBu; M-85). Ion fragment intensities were calculated with the following equation 6 from Kagan et al., 2017:

$$(6) \quad \% \text{ ion intensity} = \frac{\frac{m}{z} \text{ intensity}}{\sum \text{ion fragments}}$$

In which m/z intensities of individual fragments were divided by the sum of the intensity of all identified fragments. Data were compared to a non-labeled standard solution of sodium lactate.

5. Conclusions

This work described for the first time the activation of the pentose phosphate pathway in *Thermotoga neapolitana*. This result has a significative role in the study of the central carbon metabolism in hyperthermophilic bacteria, since in literature no other similar examples of the activation of this glycolytic pathway are known in bacteria and Archaea.

The discovery of the activation of the pentose phosphate pathway adds an important element in the reconstruction of metabolic reactions that occur in the cell when the CLF pathway is active, since it could provide the additional electrons required for the production of hydrogen and lactic acid simultaneously. Moreover, these data clearly show how *Thermotoga neapolitana* rearranges its metabolism according to the metabolic needs of the cell, activating alternative pathways to support all its reactions.

Author Contributions: Conceptualization, GD and AF; Experimental activity NE, ML, LC; Data analysis, NE, LF, GN and GD; Data curation, GD; Writing, NE and GD Supervision, GD and AF; Funding acquisition, AF and GD. All authors have read and agreed to the published version of the manuscript.

Funding: This research was funded by BioRECO2VER_H2020NMBP-BIO-2017 project, grant number 760431.

Acknowledgments: All the authors acknowledge Lucio Caso for technical support.

Conflicts of Interest: The authors declare no conflict of interest.

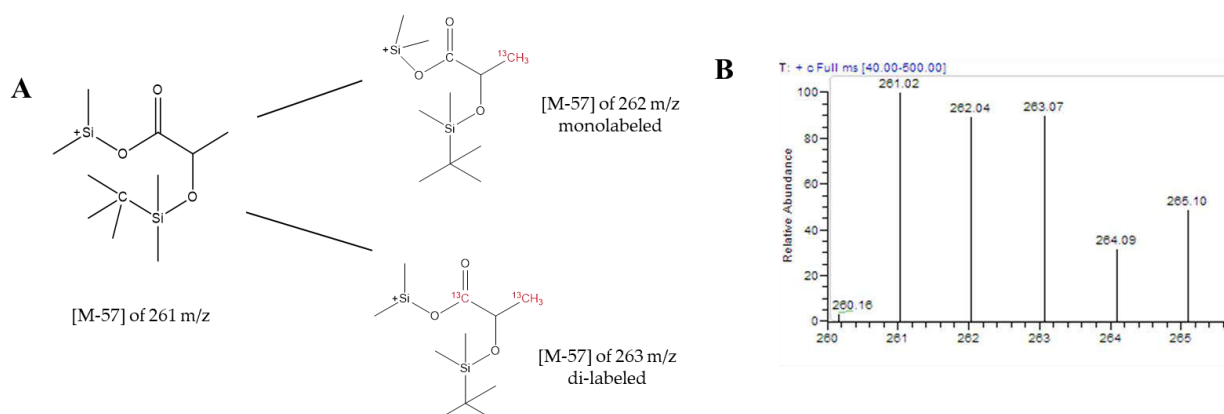
References

1. H. W. Jannasch, R. Huber, S. Belkin, and K. O. Stetter, "*Thermotoga neapolitana* sp. nov. of the extremely thermophilic, eubacterial genus *Thermotoga*," *Arch. Microbiol.*, vol. 150, no. 1, pp. 103–104, **1988**.
2. R. Huber and M. Hannig, "*Thermotogales*," *The Prokaryotes*, pp. 899–922, **2006**.
3. G. d'Ippolito et al., "Hydrogen metabolism in the extreme thermophile *Thermotoga neapolitana*," *Int. J. Hydrogen Energy*, vol. 35, no. 6, pp. 2290–2295, **2010**.
4. N. T. Eriksen, M. L. Riis, N. K. Holm, and N. Iversen, "H₂ synthesis from pentoses and biomass in *Thermotoga* spp.," *Biotechnol. Lett.*, vol. 33, no. 2, pp. 293–300, Feb. **2011**.
5. M. Cappelletti, Davide Zannoni, and B. O. Anne Postec, "Members of the Order *Thermotogales*: From Microbiology to Hydrogen Production," *Microb. BioEnergy Hydrog. Prod. Adv. Photosynth. Respir.*, vol. 38, pp. 321–347, **2014**.
6. N. Esercizio et al., "Fermentation of biodegradable organic waste by the family thermotogaceae," *Resources*, vol. 10, no. 4, **2021**.
7. C. Schröder, M. Selig, and P. Schönheit, "Glucose fermentation to acetate, CO₂ and H₂ in the anaerobic hyperthermophilic eubacterium *Thermotoga maritima*: involvement of the Embden-Meyerhof pathway," *Arch. Microbiol.*, vol. 161, no. 6, pp. 460–470, **1994**.
8. M. Selig, K. B. Xavier, H. Santos, and P. Schönheit, "Comparative analysis of Embden-Meyerhof and Entner-Doudoroff glycolytic pathways in hyperthermophilic archaea and the bacterium *Thermotoga*," *Arch. Microbiol.*, vol. 167, no. 4, pp. 217–232, **1997**.
9. G. d'Ippolito et al., "CO₂-Induced Transcriptional Reorganization: Molecular Basis of Capnophilic Lactic Fermentation in *Thermotoga neapolitana*," *Front. Microbiol.*, vol. 11, **2020**.
10. E. M. F. Brekke, A. B. Walls, A. Schousboe, H. S. Waagepetersen, and U. Sonnewald, "Quantitative importance of the pentose phosphate pathway determined by incorporation of ¹³C from 2-¹³C- and 3-¹³C-glucose into TCA cycle intermediates and neurotransmitter amino acids in functionally intact neurons," *J. Cereb. Blood Flow Metab.*, vol. 32, no. 9, pp. 1788–1799, **2012**.
11. P. Schönheit and T. Schäfer, "Metabolism of hyperthermophiles," *World J. Microbiol. Biotechnol.*, vol. 11, no. 1, pp. 26–57, Jan. **1995**.
12. T. De Vrije et al., "Glycolytic pathway and hydrogen yield studies of the extreme thermophile *Caldicellulosiruptor saccharolyticus*," *Appl. Microbiol. Biotechnol.*, vol. 74, no. 6, pp. 1358–1367, **2007**.
13. J. Woodward, N. I. Heyer, J. P. Getty, H. M. O. Neill, E. Pinkhassik, and B. R. Evans, "Efficient Hydrogen Production Using Enzymes of the Pentose Phosphate Pathway," *US DOE Hydrog. Progr. Rev.*, pp. 1–12, **2002**.
14. D. Molenaar, R. Van Berlo, D. De Ridder, and B. Teusink, "Shifts in growth strategies reflect tradeoffs in cellular economics," *Mol. Syst. Biol.*, vol. 5, no. 1, p. 323, Jan. **2009**.
15. Y. M. Kim, H. S. Cho, G. Y. Jung, and J. M. Park, "Engineering the pentose phosphate pathway to improve hydrogen yield in recombinant *Escherichia coli*," *Biotechnol. Bioeng.*, vol. 108, no. 12, pp. 2941–2946, **2011**.
16. A. Flamholz, E. Noor, A. Bar-Even, W. Liebermeister, and R. Milo, "Glycolytic strategy as a tradeoff between energy yield and protein cost," *Proc. Natl. Acad. Sci. U. S. A.*, vol. 110, no. 24, pp. 10039–10044, **2013**.
17. R. Singh, D. White, Y. Demirel, R. Kelly, K. Noll, and P. Blum, "Uncoupling fermentative synthesis of molecular hydrogen from biomass formation in *Thermotoga maritima*," *Appl. Environ. Microbiol.*, vol. 84, no. 17, pp. 998–1016, Sep. **2018**.
18. S. K. Spaans, R. A. Weusthuis, J. van der Oost, and S. W. M. Kengen, "NADPH-generating systems in bacteria and archaea," *Front. Microbiol.*, vol. 6, no. JUL, pp. 1–27, **2015**.
19. A. H. Romano and T. Conway, "Evolution of carbohydrate metabolic pathways," *Res. Microbiol.*, vol. 147, no. 6–7, pp. 448–455, **1996**.
20. L. K. Bertels, L. F. Murillo, and J. J. Heinisch, "The pentose phosphate pathway in yeasts—more than a poor cousin of glycolysis," *Biomolecules*, vol. 11, no. 5, **2021**.
21. A. Stincone et al., "The return of metabolism: Biochemistry and physiology of the pentose phosphate pathway," *Biol. Rev.*, vol. 90, no. 3, pp. 927–963, **2015**.
22. S. G. Lloyd, H. Zeng, P. P. Wang, and J. C. Chatham, "Lactate isotopomer analysis by ¹H NMR spectroscopy: Consideration of long-range nuclear spin-spin interactions," *Magn. Reson. Med.*, vol. 51, no. 6, pp. 1279–1282, **2004**.
23. N. Pradhan et al., "Model development and experimental validation of capnophilic lactic fermentation and hydrogen synthesis by *Thermotoga neapolitana*," *Water Res.*, vol. 99, no. April, pp. 225–234, **2016**.
24. A. J. Wolfe, "Glycolysis for Microbiome Generation," *Microbiol. Spectr.*, vol. 3, no. 3, **2015**.
25. P. L. Folch, M. M. M. Bisschops, and R. A. Weusthuis, "Metabolic energy conservation for fermentative product formation," *Microbial Biotechnology*, vol. 14, no. 3, pp. 829–858, **2021**.
26. C. Bräsen, D. Esser, B. Rauch, and B. Siebers, "Carbohydrate metabolism in archaea: Current insights into unusual enzymes and pathways and their regulation," *JAMA Ophthalmol.*, vol. 132, no. 3, pp. 326–331, **2014**.
27. R. A. Weusthuis, P. L. Folch, A. Pozo-Rodríguez, and C. E. Paul, "Applying Non-canonical Redox Cofactors in Fermentation Processes," *iScience*, vol. 23, no. 9, **2020**.
28. Anshuman K, Mike M, Brenda J. Hydrogen: the energy source for the 21st century. *Technovation* **2005**;25(5):569–85.

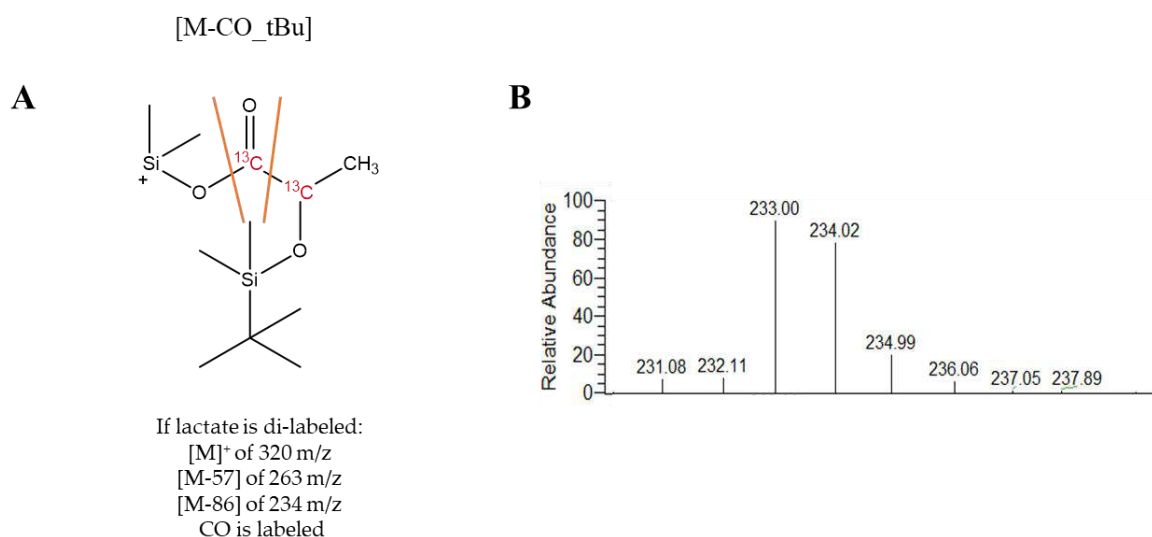
29. N. Khanna and D. Das, "Biohydrogen production by dark fermentation," *Wiley Interdiscip. Rev. Energy Environ.*, vol. 2, no. 4, pp. 401–421, **2012**. 583
584
30. G. J. Schut and M. W. W. Adams, "The iron-hydrogenase of *Thermotoga maritima* utilizes ferredoxin and NADH synergistically: A new perspective on anaerobic hydrogen production," *J. Bacteriol.*, vol. 191, no. 13, pp. 4451–4457, **2009**. 585
586
31. R. Singh, D. White, and P. Blum, "Identification of the ATPase Subunit of the Primary Maltose Transporter in the Hyperthermophilic Anaerobe *Thermotoga maritima*," *Appl. Environ. Microbiol.*, vol. 83, no. 18, **2017**. 587
588
32. N. Pradhan et al., "Hydrogen and lactic acid synthesis by the wild-type and a laboratory strain of the hyperthermophilic bacterium *Thermotoga neapolitana* DSMZ 4359T under capnophilic lactic fermentation conditions," *Int. J. Hydrogen Energy*, vol. 42, no. 25, pp. 16023–16030, **2017**. 589
590
591
33. P. Adler, C. J. Bolten, K. Dohnt, C. E. Hansen, and C. Wittmann, "Core fluxome and metafluxome of lactic acid bacteria under simulated cocoa pulp fermentation conditions," *Appl. Environ. Microbiol.*, vol. 79, no. 18, pp. 5670–5681, **2013**. 592
593
594
595
596
597
598
599
600
601
602
603
604
605
606
607
608
609
610
611
612
613
614
615
616
617
618
619
620
621
622
623
624
625
626
627
628
629
630
631
632
633
634
635
636
637
638
639
640
641
642

Supplementary Materials

643



Supplementary S2 (A) Structural representation of the fragment [M-tB]⁺ with 261 m/z and the possible labeled forms. (B). GC-MS spectrum of derivatized extract of *T. neapolitana*.



Supplementary S3 (A) Structural representation of the fragment [M-CO_tBu] and the possible fragments. (B). GC-MS spectrum of derivatized extract of *T. neapolitana*.

7. Occurrence of Capnophilic Lactic Fermentation in the Hyperthermophilic Anaerobic Bacterium *Thermotoga* sp. Strain RQ7

Nunzia Esercizio¹, Mariamichela Lanzilli ¹, Simone Landi ^{1,2, *}, Lucio Caso¹, Zhaohui Xu³, Genoveffa Nuzzo¹, Carmela Gallo ¹, Emiliano Manzo¹, Sergio Esposito², Angelo Fontana ^{1,2} and Giuliana d'Ippolito ^{1, *}

¹ Institute of Biomolecular Chemistry (ICB), Consiglio Nazionale delle Ricerche (CNR), Via Campi Flegrei 34, 80078 Pozzuoli, Italy

² Laboratory of Bio-Organic Chemistry and Chemical Biology, Department of Biology, University of Naples "Federico II", Via Cinthia, 80126 Napoli, Italy

³ Department of Biological Sciences, Bowling Green State University, Bowling Green, OH 43403, USA

* Correspondence: simone.landi@unina.it (S.L.); gdippolito@icb.cnr.it; Tel.: +39-0818675096

Citation:

Esercizio, N.; Lanzilli, M.; Landi, S.; Caso, L.; Xu, Z.; Nuzzo, G.; Gallo, C.; Manzo, E.; Esposito, S.; Fontana, A.; et al. Occurrence of Capnophilic Lactic Fermentation in the Hyperthermophilic Anaerobic Bacterium *Thermotoga* sp. Strain RQ7. *Int. J. Mol. Sci.* **2022**, *23*, 12049.



Article

Occurrence of Capnophilic Lactic Fermentation in the Hyperthermophilic Anaerobic Bacterium *Thermotoga* sp. Strain RQ7

Nunzia Esercizio ¹, Mariamichela Lanzilli ¹, Simone Landi ^{1,2,*}, Lucio Caso ¹, Zhaohui Xu ³,
Genoveffa Nuzzo ¹, Carmela Gallo ¹, Emiliano Manzo ¹, Sergio Esposito ², Angelo Fontana ^{1,2}
and Giuliana d'Ippolito ^{1,*}

¹ Institute of Biomolecular Chemistry (ICB), National Research Council (CNR), Via Campi Flegrei 34, 80078 Pozzuoli, Italy

² Department of Biology, University of Naples "Federico II", Via Cinthia, 80126 Napoli, Italy

³ Department of Biological Sciences, Bowling Green State University, Bowling Green, OH 43403, USA

* Correspondence: simone.landi@unina.it (S.L.); gdippolito@icb.cnr.it (G.d.); Tel.: +39-(081)-8675096 (G.d.)

Abstract: Capnophilic lactic fermentation (CLF) is an anaplerotic pathway exclusively identified in the anaerobic hyperthermophilic bacterium *Thermotoga neapolitana*, a member of the order Thermotogales. The CO₂-activated pathway enables non-competitive synthesis of hydrogen and L-lactic acid at high yields, making it an economically attractive process for bioenergy production. In this work, we discovered and characterized CLF in *Thermotoga* sp. strain RQ7, a naturally competent strain, opening a new avenue for molecular investigation of the pathway. Evaluation of the fermentation products and expression analyses of key CLF-genes by RT-PCR revealed similar CLF-phenotypes between *T. neapolitana* and *T. sp.* strain RQ7, which were absent in the non-CLF-performing strain *T. maritima*. Key CLF enzymes, such as PFOR, HYD, LDH, RNF, and NFN, are up-regulated in the two CLF strains. Another important finding is the up-regulation of V-ATPase, which couples ATP hydrolysis to proton transport across the membranes, in the two CLF-performing strains. The fact that V-ATPase is absent in *T. maritima* suggested that this enzyme plays a key role in maintaining the necessary proton gradient to support high demand of reducing equivalents for simultaneous hydrogen and lactic acid synthesis in CLF.

Keywords: hydrogen; lactic acid; CO₂ valorization; ATPase; bio-based process; green chemistry; *Thermotoga neapolitana*; *Thermotoga maritima*



Citation: Esercizio, N.; Lanzilli, M.; Landi, S.; Caso, L.; Xu, Z.; Nuzzo, G.; Gallo, C.; Manzo, E.; Esposito, S.; Fontana, A.; et al. Occurrence of Capnophilic Lactic Fermentation in the Hyperthermophilic Anaerobic Bacterium *Thermotoga* sp. Strain RQ7. *Int. J. Mol. Sci.* **2022**, *23*, 12049. <https://doi.org/10.3390/ijms231912049>

Academic Editors: Giuseppe Manco, Yannick J. Bomble and Elena Porzio

Received: 2 August 2022

Accepted: 6 October 2022

Published: 10 October 2022

Publisher's Note: MDPI stays neutral with regard to jurisdictional claims in published maps and institutional affiliations.

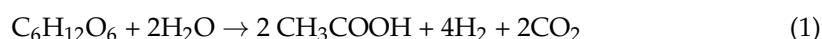


Copyright: © 2022 by the authors. Licensee MDPI, Basel, Switzerland. This article is an open access article distributed under the terms and conditions of the Creative Commons Attribution (CC BY) license (<https://creativecommons.org/licenses/by/4.0/>).

1. Introduction

The order Thermotogales represents a group of anaerobic hyperthermophilic bacteria that are recognized as promising microorganisms for bio-hydrogen production from sugars via dark fermentation [1–4]. A number of *Thermotoga* and *Pseudothermotoga* species demonstrated efficient fermentation performance using different substrates, including simple monosaccharides (hexoses and pentoses) and complex polysaccharides (e.g., starch, lactose, sucrose, and cellobiose) [1,4–7]. The ability of these microorganisms to generate green hydrogen from organic wastes, such as food scrapes, lignocellulosic biomasses and glycerol, further strengthens their values in the production of sustainable bioenergy [4].

Theoretically, up to 4 mole of hydrogen can be produced from each mole of hexose, with acetic acid and CO₂ as the byproducts [8], as shown in Equation (1).



In practice, more reduced volatile fatty acids, such as lactic acid and ethanol, accumulate during dark fermentation, which competes for reducing power and lowers the experimental yield of hydrogen [9].

Recently, we reported a new pathway named capnophilic lactic fermentation (CLF) in *Thermotoga neapolitana* (Figure 1) [10]. Under CO₂ atmosphere, CLF enables the non-competitive synthesis of L-lactic acid and hydrogen at the same time. Besides a classic catabolic branch from sugars to acetate, the pathway also has an anabolic branch from acetyl-CoA to lactate, enabled by sequential actions of pyruvate:ferredoxin oxidoreductase (PFOR) and lactate dehydrogenase (LDH) [10–14]. To support the concomitant production of hydrogen and lactic acid, the additional NADH requirement is likely satisfied by a CO₂-induced metabolic process involving NAD-Ferredoxin oxidoreductase (RNF) and NADH-dependent reduced ferredoxin:NADP oxidoreductase (NFN) [9,14–16].

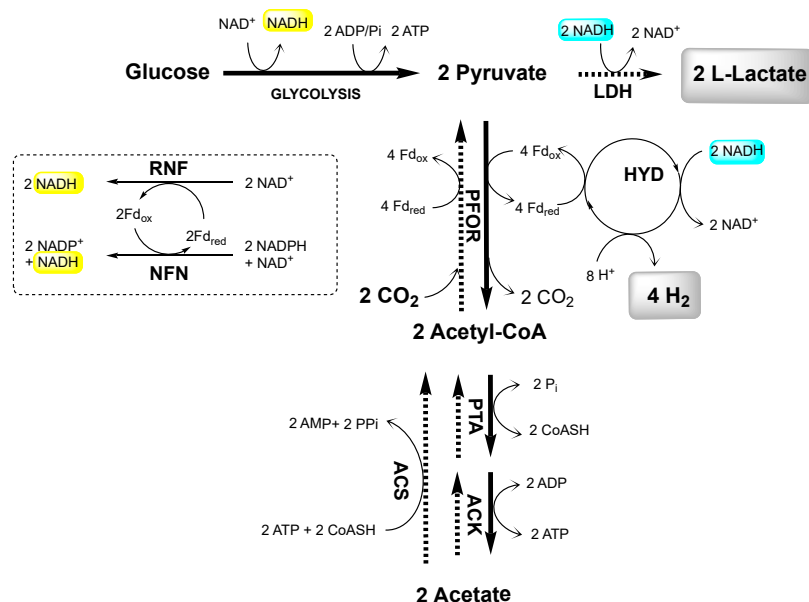


Figure 1. Schematic proposal of the CLF pathway in *T. neapolitana*. ACK, acetate kinase; PTA, phosphotransacetylase; ACS, acetyl-CoA synthetase; PFOR, pyruvate:ferredoxin oxidoreductase; LDH, lactate dehydrogenase; HYD, hydrogenase; RNF, NAD-ferredoxin oxidoreductase; NFN, NADH-dependent reduced ferredoxin:NADP oxidoreductase; Fd, ferredoxin. NADH-source reactions in yellow; NADH-consuming reactions in turquoise. Protons are omitted in the REDOX reactions.

Enzymatic reductive carboxylation of acetate to lactate offers a biological mechanism to convert CO₂ into commodity chemicals and thus has a considerable biotechnological significance [10,17]. To improve the fixation rate of CO₂ into lactate, a strategy to increase acetate uptake has been attempted in *T. neapolitana* by heterologous expression of *Thermus thermophilus* acetyl-CoA synthetase (ACS), which is involved in irreversible acetate assimilation [15]. Genetic engineering of *T. neapolitana* remains challenging, however, due to the lack of appropriate selective markers and low efficiencies of the transformation methods available to this organism, such as liposome-mediated transformation and electroporation [15,18].

T. sp. strain RQ7, isolated from marine sediments of Ribeira Quente (Azores), is the first *Thermotoga* strain to be found naturally competent, making genetic manipulation of *Thermotoga* more feasible [19,20]. The construction of *Thermotoga*-*E. coli* shuttle vectors and the development of new selective schemes based on the pyrEF system have greatly expanded the toolbox for genetic manipulation of *Thermotoga* spp. [15,19–21]. The genomes of *T. neapolitana* and *T. sp.* strain RQ7 share an average nucleotide identity of 98.49%, suggesting that *T. sp.* strain RQ7 is a strain of *T. neapolitana* [22].

The aim of the present work was to assess whether *T. sp.* strain RQ7 was able to perform CLF. Under CO₂ insufflation to induce CLF, the fermentation parameters of RQ7 were tested, including growth rate, glucose consumption, hydrogen, and organic acid production. The results were compared with the CLF-performing strain *T. neapolitana* and

non-CLF-performing strain *T. maritima*. The gene expression levels of CLF key enzymes were also investigated to highlight the molecular differences of the three strains.

2. Results

2.1. Fermentation Products under N_2 and CO_2 in *T. neapolitana*, *T. sp.* Strain RQ7, and *T. maritima*

T. neapolitana (*Tnea*), *T. sp.* strain RQ7 (*Trq7*), and *T. maritima* (*Tmar*) were grown on glucose under N_2 and CO_2 atmospheres in static batches to assess the fermentation performance after 24 and 48 h. As shown in Figure 2, in *Tnea* and *Trq7*, CO_2 accelerated the consumption of glucose, which was almost depleted within 48 h (~87%). In *Tmar*, the glucose consumption was similar under N_2 and CO_2 conditions. The consumption rates were significantly lower in *Tmar* than the other two strains.

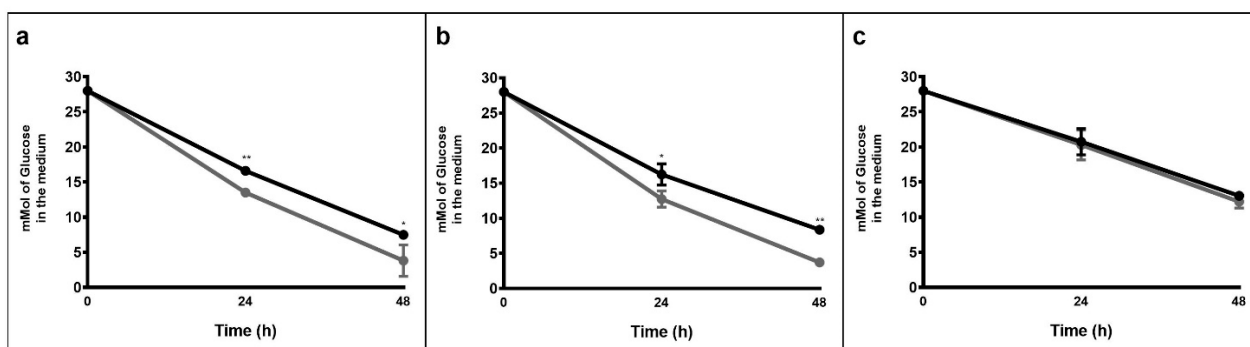


Figure 2. Glucose consumption of *Tnea* (a), *Trq7* (b), and *Tmar* (c) after 24 and 48 h, under N_2 (black bars) and CO_2 (gray bars) conditions. Asterisks indicate significant differences: *, $p \leq 0.05$; **, $p \leq 0.001$.

For hydrogen production, all strains exhibited no significant differences between N_2 and CO_2 sparging after either 24 or 48 h (Figure 3). Total hydrogen production was lower in *Tmar* compared to the other two strains, parallel to the lower consumption of glucose.

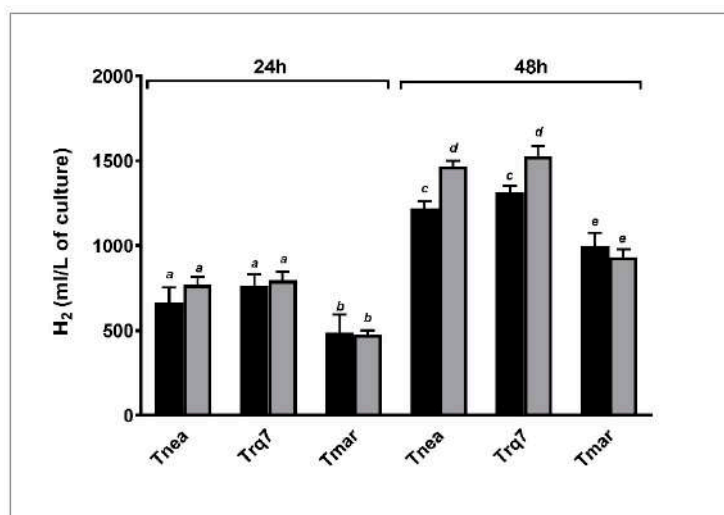


Figure 3. Hydrogen cumulative production after 24 and 48 h, with N_2 (black bars) and CO_2 (gray bars). Letters indicate ANOVA significance between treatments and species.

Acetic acid and lactic acid are the main organic end products in sugar fermentation by *Thermotogales* [3,8,23]. Interestingly, CO_2 did not affect acetate production in any strains compared to N_2 sparging, at either 24 or 48 h (Figure 4a). In *Tnea* and *Trq7*, CO_2 insufflation

doubled the lactate level at both 24 and 48 h, whereas in *Tmar*, no significant difference in lactate levels was observed at either time point (Figure 4b).

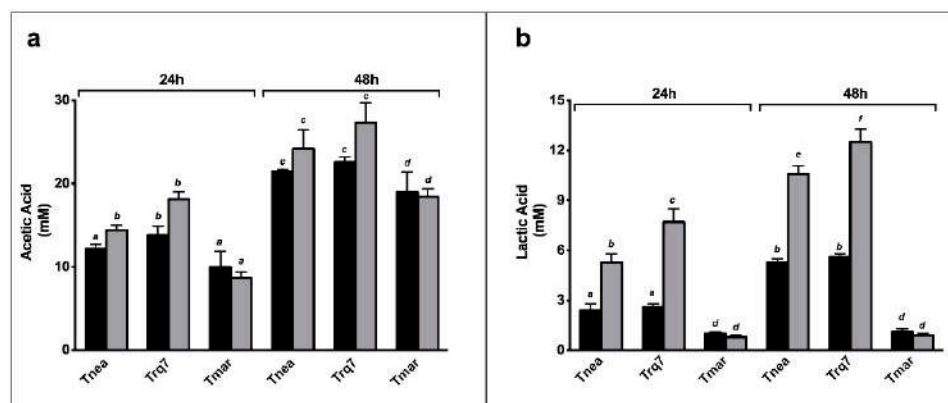


Figure 4. Acetic acid (a) and lactic acid (b) production under N₂ (black bars) and CO₂ (gray bars) conditions, at 24 and 48 h. Letters indicate ANOVA significances between treatments and species.

CLF is characterized by increased lactate synthesis without affecting hydrogen production, which was confirmed in *Tnea* and *Trq7*. Approximately 2.6 mol hydrogen/mol glucose was observed in *Tnea* and *Trq7* regardless of the sparging method, whereas the lactic acid yield roughly increased by 0.2 mol/mol glucose by replacing N₂ with CO₂ (from 0.27 to 0.47 mol/mol glucose) (Table 1). The ratio between lactic acid and acetic acid was nearly doubled in both *Tnea* and *Trq7* after sparging with CO₂. These results demonstrated the activation of the CLF pathway in *Tnea* and *Trq7*, which manifested that *Trq7* is a CLF-performing strain. No activation of CLF was observed in *Tmar* since the lactate levels remained low in both sparging cases.

Table 1. Hydrogen, acetic acid (AA), and lactic acid (LA) yields (mol/mol glucose) at 24 and 48 h. Letters indicate ANOVA significant differences between treatments, chemical products and bacterial species. Data are expressed as mean \pm SD, $n = 9$.

	24 h				48 h			
	H ₂	AA	LA	LA/AA	H ₂	AA	LA	LA/AA
<i>Tnea</i> N ₂	2.60 \pm 0.15 a	1.08 \pm 0.02 b	0.21 \pm 0.02 c	0.20 \pm 0.02	2.40 \pm 0.12 a	1.03 \pm 0.03 b	0.26 \pm 0.01 c	0.25 \pm 0.01
<i>Tnea</i> CO ₂	2.04 \pm 0.07 a	0.98 \pm 0.03 b	0.36 \pm 0.06 d	0.37 \pm 0.05	2.41 \pm 0.08 a	0.94 \pm 0.06 b	0.45 \pm 0.03 e	0.48 \pm 0.02
<i>Trq7</i> N ₂	2.31 \pm 0.04 a	1.13 \pm 0.07 b	0.22 \pm 0.01 c	0.19 \pm 0.01	2.64 \pm 0.04 a	1.09 \pm 0.06 b	0.27 \pm 0.01 c	0.25 \pm 0.01
<i>Trq7</i> CO ₂	2.17 \pm 0.26 a	0.95 \pm 0.09 b	0.46 \pm 0.05 e	0.48 \pm 0.03	2.56 \pm 0.26 a	0.96 \pm 0.08 b	0.47 \pm 0.03 e	0.49 \pm 0.05
<i>Tmar</i> N ₂	2.42 \pm 0.82 a	0.96 \pm 0.01 b	0.12 \pm 0.04 f	0.10 \pm 0.06	2.67 \pm 0.04 a	1.07 \pm 0.11 b	0.07 \pm 0.01 f	0.06 \pm 0.00
<i>Tmar</i> CO ₂	2.60 \pm 0.89 a	0.99 \pm 0.20 b	0.11 \pm 0.03 f	0.09 \pm 0.00	2.33 \pm 0.03 a	1.15 \pm 0.12 b	0.06 \pm 0.01 f	0.05 \pm 0.00

2.2. Gene Expression Level of Key CLF Enzymes

As reported in Figure 1, the CLF pathway involves glycolysis followed by at least four transformations requiring (1) PFOR, the reversible enzyme responsible for both the catabolic reaction from pyruvate to acetyl-CoA and the anabolic reaction from acetyl-CoA and CO₂ to pyruvate; (2) LDH, for the synthesis of lactic acid from pyruvate; (3) HYD, containing the H-cluster for the reduction of H⁺ to hydrogen; (4) phosphate acetyltransferase (PTA) and acetate kinase (ACK), reversible enzymes participating in the acetate dissimilation pathway from acetyl-CoA to acetate and vice-versa. In order to underline the molecular differences among the three strains, we compared the gene expression levels of these five enzymes after 24 h of fermentation under the N₂ and CO₂ sparging (Figure 5).

The qRT-PCR analysis of the selected genes showed similar transcription levels in *Tnea* and *Trq7*, with 6.2 and 3.2-fold increases in *HYDa*, 19.4 and 8.6-fold increases in *PFOR*, 19.6 and 12.4-fold increases in *LDH*, and 5.45 and 5.14-fold increases in *PTA* (Figure 5). *ACK* did not change significantly under the two sparging treatments in both strains. In *Tmar*,

CO₂ insufflation induced no significant changes in *LDH*, *ACK*, and *PTA*, and only a slight decrease in *HYDa* and a 2.7-fold increase in *PFOR*.

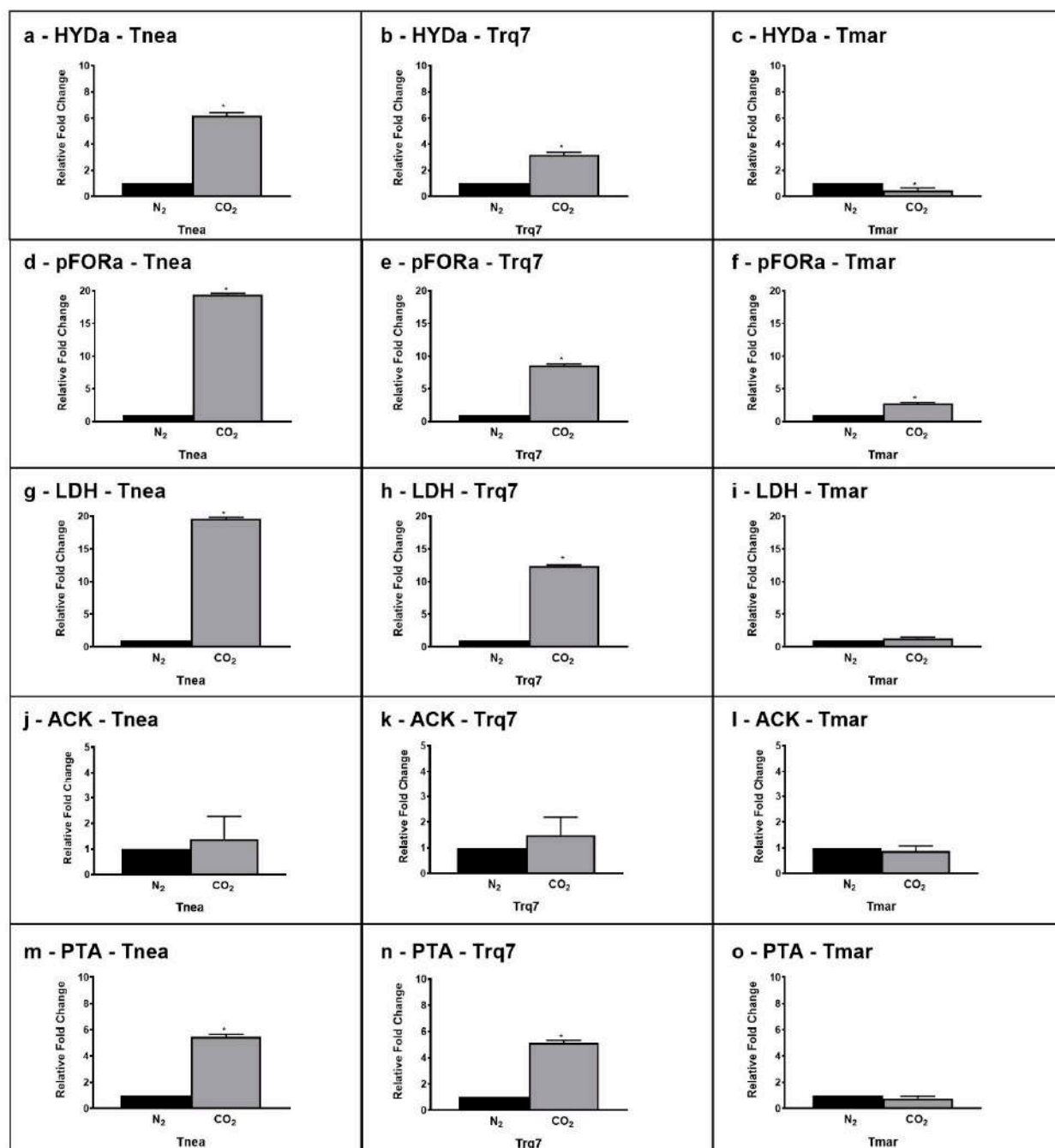


Figure 5. Gene expression levels of HYD (CTN_RS05285 (a–c)), PFOR (CTN_RS03385 (d–f)), LDH (CTN_RS03950 (g–i)), ACK (CTN_RS02020 (j–l)), and PTA (CTN_RS07210 (m–o)) after 24 h under N₂ (black bars) and CO₂ (gray bars) conditions in *Tnea*, *Trq7* and *Tmar*. Variations are indicated as relative fold changes in CO₂ with respect to N₂. mRNA levels were calculated relative to the expression of 16S RNA. Asterisks indicate significantly different values at $p \leq 0.05$ (*).

2.3. Expression of Energy-Related Enzymes

The above results of *Tnea* were in good agreement with our previous data obtained from a transcriptomic study [14], which had also revealed the effects on a number of energy-related enzymes, including flavin-based oxidoreductase enzymes such as NAD-ferredoxin oxidoreductase (*RNF*) (CTN_RS02165), NADH-dependent reduced ferredoxin:NADP oxi-

doreductase (NFN) (CTN_RS04020), and ATPases involved in ion translocation. For this reason, we also analyzed these genes in the three strains under both sparging conditions.

RFN and NFN transfer electrons between ferredoxin and NAD(P)H and generate an ion gradient across the cell membrane. Sparging with CO₂ versus N₂ increased the expression of NFN 3.2-fold in *Tnea*, 3.2-fold in *Trq7*, and 1.9-fold in *Tmar*. Meanwhile, RFN exhibited a 13.2-fold increase in *Tnea*, 7.7-fold increase in *Trq7*, and no change in *Tmar* (Figure 6).

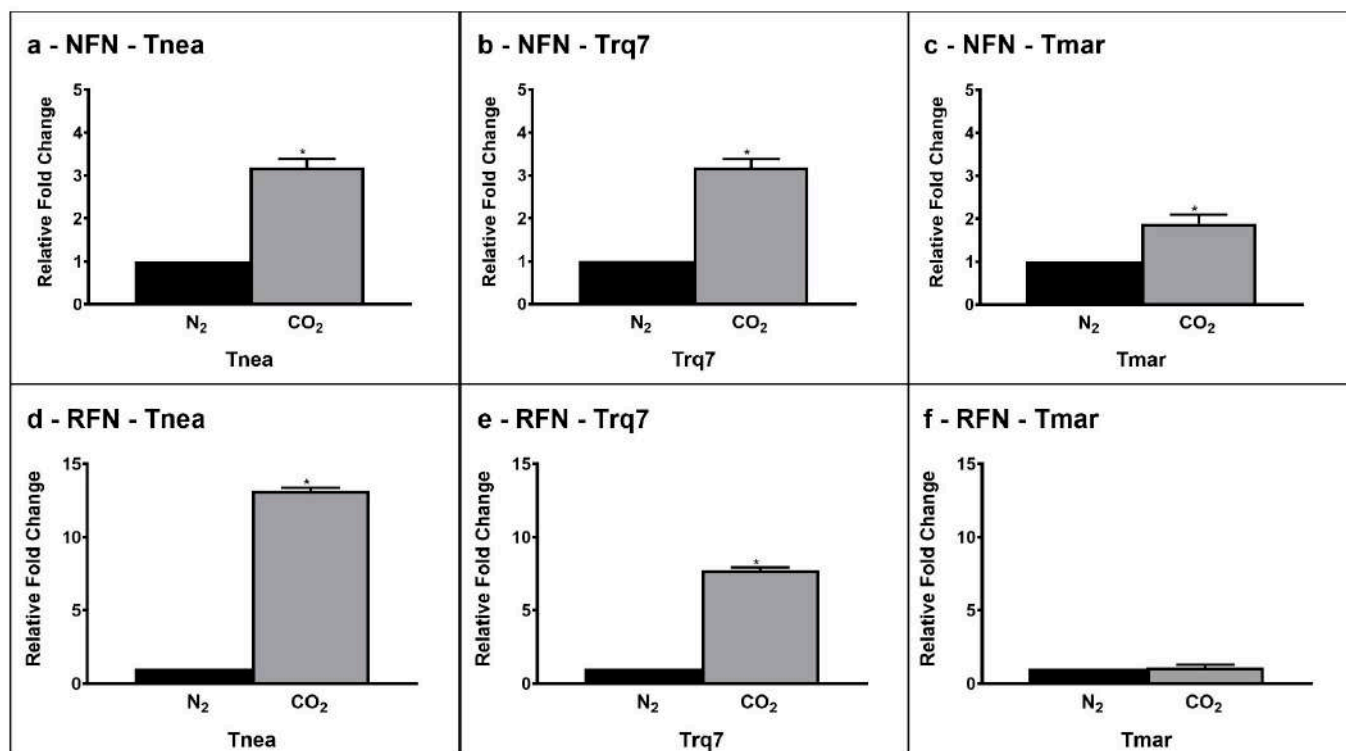


Figure 6. Gene expression levels of NFN (CTN_RS04020 (a–c)) and RFN (CTN_RS02165 (d–f)) under N₂ (black bars) and CO₂ (gray bars) conditions *Tnea*, *Trq7* and *Tmar*. Variations are indicated as relative fold changes in CO₂ with respect to N₂. mRNA levels were calculated relative to the expression of 16S RNA. Asterisks indicate significantly different values at $p \leq 0.05$ (*).

Ion-translocating ATPases are essential cellular energy converters, which transduce the chemical energy of ATP hydrolysis into transmembrane ionic electrochemical potential gradients [24–26]. Gene clusters encoding F- and V-ATPases have been described in *Tnea*, whereas *Tmar* has only F-ATPase gene clusters [27]. In order to determine occurrence of ATPases in *Trq7*, we mined its genome using the sequences of *Tnea* V-ATPase (CTN_RS04525–CTN_RS04550) and *Tnea* F-ATPase (CTN_RS04140–CTN_RS04180) (Table 2). Our results confirmed the absence of V-ATPase subunits in *Tmar* and showed the presence of both F- and V-type ATPases in *Trq7*. As expected, *Tnea* and *Trq7* demonstrated sequence similarities for both V- and F-ATPases with 98–100% of identities for any analyzed subunits.

The bioinformatic results were confirmed by PCR amplification of the catalytic subunits of the F-type (CTN_RS04145) and V-type (CTN_RS04540). *Tnea* and *Trq7* presented both subunits while *Tmar* showed the F-ATPase subunit only (Supplementary Figure S1).

A further bioinformatic analysis on other species of the Thermotogaceae family, including the genera *Thermotoga* (*T. naphthophila* and *T. petrophila*) and *Pseudothermotoga* (*P. lettingae*, *P. hypogea*, and *P. thermarum*), indicated that these species possessed the F-ATPase gene cluster but not the V-ATPase one (Supplementary Tables S1 and S2). *P. hypogea* showed the presence of an ATPase classified as the V/A-type, with a weak similarity (25–50%) to the V-ATPase complex of *Tnea*, thus representing a different enzyme. On the other hand, the F-ATPases of *Tmar*, *T. naphthophila* and *T. petrophila* showed high levels of identity in all

the subunits (around 99–100% with each other), compared to 76–86% of identities to the F-ATPase of *Tnea*.

These results suggested that the V-ATPase gene family is a specific and unique feature of the two CLF-performing strains, *Tnea* and *Trq7*, among *Thermotogales*. Therefore, we compared the expression levels of the ATPases in *Tnea*, *Trq7*, and *Tmar*, after 24 h of fermentation with N₂ and CO₂-sparing (Figure 7). For the V-ATPase, we selected the catalytic subunit α (CTN_RS04540) and the regulatory subunit β (CTN_RS04545), and for the F-ATPase, we chose the regulatory subunit α (CTN_RS04145). Both analyzed genes coding for V-ATPase were up-regulated in *Tnea* and *Trq7* under the CLF conditions. These strains, respectively, showed an increase in expression 1.73 and 2.19-fold for subunit α and 4.46 and 2.24-fold for subunit β (Figure 7). Considering the absence of the V-ATPase, *Tmar* was investigated only for the expression of the F-ATPase. In all three strains, a significant down-regulation of the F-ATPase subunit α was observed, with 1.8, 2.6, and 3.3-fold changes for *Tnea*, *Trq7*, and *Tmar*, respectively (Figure 7).

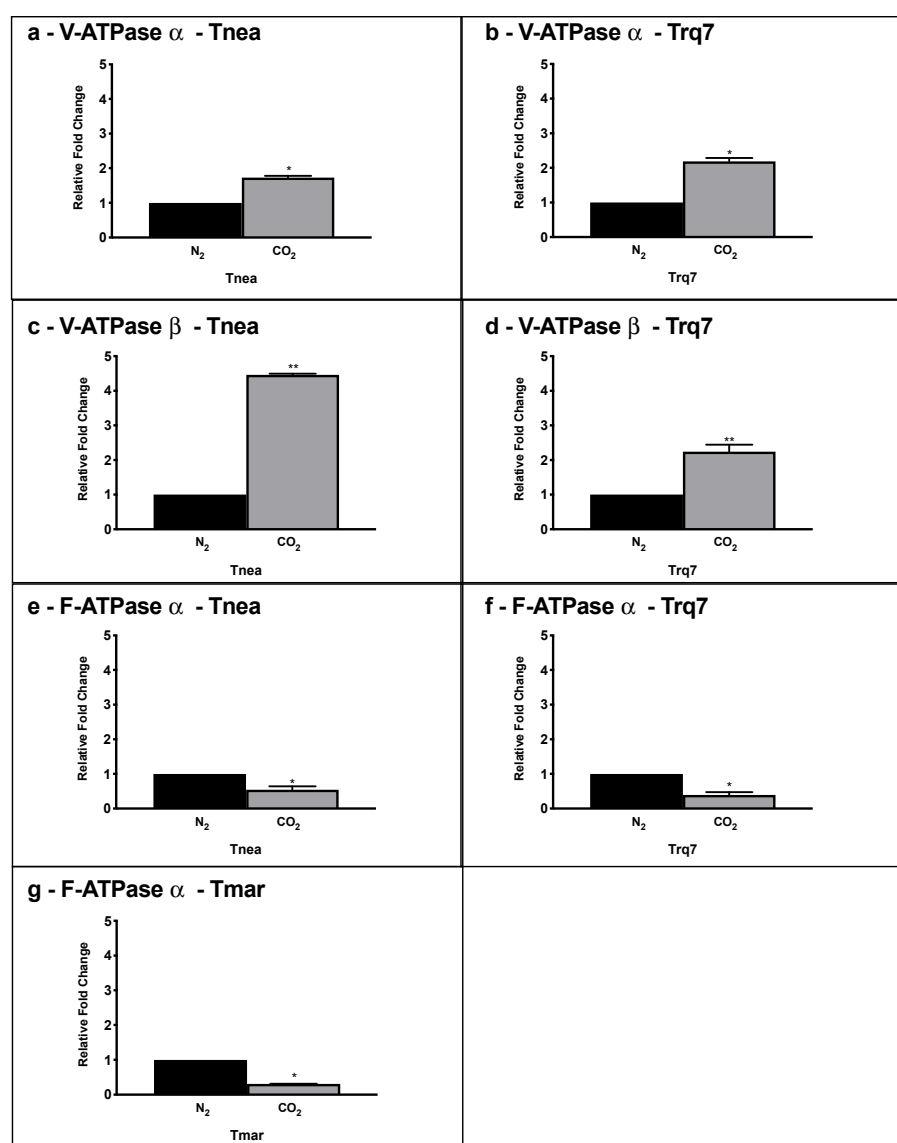


Figure 7. Gene expression levels of V-ATPase subunit α (a,b) V-ATPase subunit β (c,d), and F-ATPase subunit α (e–g), in *Tnea*, *Trq7*, and *Tmar* under N₂ (black bars) and CO₂ (gray bars) conditions, measured by qRT-PCR. Variations are indicated as relative fold changes in CO₂ with respect to N₂. mRNA levels were calculated relatively to the expression of 16S RNA. Asterisks indicate significantly different values at $p \leq 0.05$ (*) and $p \leq 0.001$ (**).

Table 2. F-type and V-type ATPases locus tags in *Tnea*, *Trq7*, and *Tmar*.

Enzymes	<i>Tnea</i>	<i>Trq7</i>	<i>Tmar</i>
V-ATPase subunit A-atpA	CTN_RS04540	TRQ7_06035	Absent
V-ATPase subunit B-atpB	CTN_RS04545	TRQ7_06040	Absent
V-ATPase subunit D-atpD	CTN_RS04550	TRQ7_06045	Absent
V-ATPase subunit E-atpE	CTN_RS04535	TRQ7_06030	Absent
V-ATPase subunit F-atpF	CTN_RS04525	TRQ7_06020	Absent
V-ATPase subunit G-atpG	CTN_RS04530	TRQ7_06025	Absent
F-ATPase subunit A-atpB	CTN_RS04145	TRQ7_05640	TM_1616
F-ATPase subunit B-atpF	CTN_RS04155	TRQ7_05650	TM_1614
F-ATPase subunit C-atpE	CTN_RS04150	TRQ7_05645	TM_1615
F-ATPase subunit Delta-atpH	CTN_RS04160	TRQ7_05655	TM_1613
F-ATPase subunit Epsilon-atpC	CTN_RS04180	TRQ7_05675	TM_1609
F-ATPase subunit Gamma-atpG	CTN_RS04170	TRQ7_05665	TM_1611
F-ATPase subunit Alpha-atpA	CTN_RS04165	TRQ7_05660	TM_1612
F-ATPase subunit I-atpI	CTN_RS04140	TRQ7_05635	-
F-ATPase subunit Beta- atpD	CTN_RS04175	TRQ7_05670	TM_1610

3. Discussion

Capnophilic lactic fermentation (CLF) is a unique pathway of *T. neapolitana*, which is triggered by CO₂ and induces an increase in lactate whereas it has no impact on the hydrogen yield [10,11,13,14]. The CLF phenotype can be readily recognized by comparing the yields of fermentation products under N₂ and CO₂ insufflation [10]. Screening of eight species of the genus *Thermotoga* (*T. neapolitana*, *T. neapolitana* subsp. *capnolactica*, *T. maritima*, *T. naphthophila*, *T. petrophila*, *T. caldifontis*, *T. hypogea*, *T. profunda*) and four species of the genus *Pseudothermotoga* (*P. elfii*, *P. lettingae*, *P. subterranea*, *P. thermarum*) revealed that CLF pathway is only retained in *T. neapolitana* [28]. Moreover, *T. neapolitana* subsp. *capnolactica*, a strain adapted in our laboratory under saturating concentrations of CO₂, showed a further improved capability of performing CLF in comparison to its parent strain [13].

The analysis of fermentation parameters in *T. sp.* strain RQ7 revealed a clear CLF-phenotype resembling *T. neapolitana* in producing the same hydrogen yield and double lactate under CO₂. Furthermore, the two strains showed a similar molecular response leading to up-regulation of the genes responsible for hydrogen and lactic acid synthesis with acetate assimilation. It is worth noting that the strong increase in PTA expression well correlated to the acetate assimilation (the ascending pathway in Figure 1), as demonstrated in *T. neapolitana* by both the incorporation of ¹³C-acetate into lactic acid [10,11,13,14] and the moderate increase in lactic acid synthesis due to expression of heterologous ACS [15]. The yields of fermentation products are very different in non-CLF-performing strain *T. maritima*, with no significant differences observed under N₂ and CO₂ insufflation. Since *T. sp.* strain RQ7 is a naturally competent strain, genetic manipulation of this organism is more feasible than other *Thermotoga* strains [19,20]. The identification of *T. sp.* strain RQ7 as a CLF-performing strain opens the door to elucidate the molecular mechanism of CLF pathway and to discover new performing strains.

The genomes of *T. neapolitana* and *T. sp.* strain RQ7 share an average nucleotide identity of 98.49%, making RQ7 a sister strain of *T. neapolitana* [22]. Both bacteria can redirect the flux of NADH and ferredoxin to sustain simultaneous NADH-dependent reactions, thus enabling the CLF pathway. Analyses with qRT-PCR suggested an up-regulation of the key enzymes involved in the anabolic pathway from acetate and CO₂ to lactic acid in *T. neapolitana* and *T. sp.* strain RQ7, particularly PFOR and LDH. In fact, considering the bi-function of PFOR as both a catabolic (from pyruvate to acetyl-CoA) and an anabolic (from acetyl-CoA and CO₂ to pyruvate) node, the up-regulation is in good agreement with both the general increase in the metabolism rate induced by CO₂ and the enhanced demand of pyruvate to feed the downstream synthesis of lactic acid by LDH. The same enzymes are not differentially expressed in *T. maritima* under CO₂, where the flux from acetyl-CoA to lactic acid remained unchanged. CO₂ possibly induced a re-organization of

cellular redox balance to sustain simultaneous reduction reactions, such as lactate formation from pyruvate and the conversion of protons to molecular hydrogen. A pool of additional reducing equivalents may derive from the flavin-based oxidoreductase enzymes NFN and RNF, which control the supply of reduced ferredoxin and NADH and allow energy conservation based on sodium translocation through the cell membrane. Both enzymes are up-regulated under CO₂ in *T. neapolitana* and *T. sp.* strain RQ7 but not in *T. maritima*, supporting the hypothesis of their involvement in CLF activation to create a cyclic process for regeneration of NADH and NADPH [14].

Another important aspect of CLF pathway is the generation of ion gradients (Na⁺ and/or H⁺) across the cell membrane. The biochemical characterization of the RNF-ATP synthase supercomplex in *T. maritima* demonstrates that RNF is a Na⁺-dependent ion-translocating respiratory enzyme and is associated with an ATP-synthase activity in the respiratory chain via electrochemical Na⁺ potential [29]. Membrane-bound ATPases are essential in energy conservation, i.e., catalyzing the synthesis or hydrolysis of ATP driven by H⁺/Na⁺ gradients [25,26,30].

ATPases couple the translocation of protons or sodium ions across the membrane to the concomitant synthesis or hydrolysis of ATP [25]. ATPases are grouped into three classes: A-type, F-type, and V-type. A- and F-types are reversible enzymes that harness the energy of an ion gradient across the membrane to synthesize ATP [30–33]. V-type ATPases can couple the free energy of ATP hydrolysis to proton or sodium translocation and thereby generate an ion-motive force, which is useful for a variety of secondary channel-mediated or active transport [30]. V-type ATPase or its genes have been reported in hyperthermophilic archaea [34,35], while most ATPases in bacteria are F-type. However, it has been documented that the thermophilic bacteria *Thermus thermophilus* [36] and *Clostridium feravidus* [37] have V-type ATPases, although F-type ATPases are found in other *Thermus* species [38]. Our bioinformatic analysis within the Thermotogaceae family revealed that all the analyzed species of *Thermotoga* and *Pseudothermotoga*, including *T. maritima*, have F-type ATPases, whereas *T. neapolitana* and *T. sp.* strain RQ7 are the only ones that possess V-type ATPase. Co-existence of V- and F-type ATPases in *T. neapolitana* and the mere presence of the F-type in *T. maritima* have been reported by Iida et al., 2002 [27]. In this context, the presence and regulation of both F- and V-ATPases in *T. neapolitana* and *T. sp.* strain RQ7 might be crucial to the CLF mechanism. Gene expression analysis of V-ATPases in *T. neapolitana* and *T. sp.* strain RQ7 revealed an up-regulation of this enzyme induced by CO₂, whereas F-ATPase showed a general down-regulation both in CLF performing and non-performing strains. H⁺/Na⁺ gradients could play an important role in this scheme. The prediction and categorization of ATPase in Na⁺ or H⁺-dependent enzymes can be obtained by sequence analysis of the membrane embedded c/K-oligomers ring which consists a common set of amino acids involved in sodium or proton binding [25]. Based on the sequence analysis of the c/K subunits, the F-ATPases in both *T. maritima* and *T. neapolitana* have been predicted to translocate Na⁺ ions, and the V-ATPase of *T. neapolitana* is supposed to be H⁺-dependent [25]. The Na⁺-dependence of F-ATPase has been demonstrated in *T. maritima* with a connection to the Na⁺-translocating RNF complex [29,39]. Under a CO₂ atmosphere, the up-regulation of RNF complex and the down-regulation of F-ATPase seem to indicate that a sodium gradient has been generated in the cell by the RNF complex to generate surplus of NADH, which is not exploited by F-ATPase to synthesize ATP. General acceleration of central carbon metabolism observed under CLF forces the cell to dissipate ATP rather than to synthesize it. In *T. neapolitana* and *T. sp.* strain RQ7, the presence and up-regulation of V-ATPase during CLF may be due to the requirement to hydrolyze ATP and “push” cytosolic H⁺ across the membrane against their electrochemical gradient. This generates an ion-motive force (IMF), useful for a variety of secondary channel-mediated or active transport to move substrates or ions over the cellular membrane [30]. V-ATPase based mechanism should be a fundamental step to construct a respiratory chain which contributes to energy conservation and supports redox reactions during CLF.

Parallel studies of the metabolism in *T. neapolitana* and *T. sp.* strain RQ7 are in progress. The preliminary results corroborate the results here presented and will be the subject of a future report on the analogies between the two bacteria.

4. Materials and Methods

4.1. Biological Materials

Three *Thermotoga* strains were used in this study: *Thermotoga sp.* strain RQ7 (*Trq7*), *Thermotoga maritima* (*Tmar*), and *Thermotoga neapolitana* (*Tnea*) subsp. *capnolactica* (DSM 33003), which were derived from the DSMZ 4359T strain after evolving in our laboratory under saturating concentration of CO₂ for several years [13]. *Trq7* was gifted by Dr. Harald Huber at the University of Regensburg, Germany. *Tmar* was obtained from DSMZ (DSM 3109). Bacterial cells were anaerobically grown in a modified ATCC 1977 culture medium containing 10 mL/L of filter-sterilized vitamins and trace element solutions (DSM medium 141) together with 10 g/L NaCl, 0.1 g/L KCl, 0.2 g/L MgCl₂·6H₂O, 1 g/L NH₄Cl, 0.3 g/L K₂HPO₄, 0.3 g/L KH₂PO₄, 0.1 g/L CaCl₂·2H₂O, 0.5 g/L cysteine-HCl, 2 g/L yeast extract, 2 g/L tryptone, 5 g/L glucose, 0.001 g/L resazurin (redox indicator) [40].

4.2. Bacterial Growth

Aliquots of medium were distributed into 120 mL serum bottles. Pre-cultures (30 mL) were incubated overnight at 80 °C without shaking and used to inoculate (6% *v/v*) the samples. Standard culture medium was distributed into 120 mL serum bottles using 30 mL working volume. Oxygen was removed by heating reactors while sparging its content with a stream of pure N₂ (control) or CO₂ (trigger of CLF) until the solution was colorless. All the experiments were conducted in triplicates. pH was monitored and adjusted to approximately 7.5 by 1 M NaOH. Sparging followed by pH adjustment was repeated every 24 h. Inoculated bottles were maintained in a heater (Binder ED720) at 80 °C. Cell growth was determined by optical density (OD) at 540 nm (UV/Vis Spectrophotometer DU 730, Beckman Coulter). Aliquots of 2 mL of medium were collected from each sample after 0 h, 24 h and 48 h, centrifuged at 16,000× *g* for 15 min (Hermle Z3236K), and kept at −20 °C until further analyses.

4.3. Gas Analyses

Gas (H₂ and CO₂) measurements were performed using gas chromatography (GC) on an instrument (Focus GC, Thermo fisher, Waltham MA, USA) equipped with a thermo-conductivity detector (TCD) and fitted with a 3 m molecular sieve column (Hayesep Q). N₂ was used as carrier gas. Analyses were carried out at 24 h and 48 h prior to each gas sparging.

4.4. Chemical Analyses

Glucose concentration was determined by the dinitrosalicylic acid method calibrated on a standard solution of 2 g/L glucose [41]. Organic acids were measured by ERETIC 1H NMR as described by Nuzzo et al. [17]. All experiments were performed on a Bruker DRX 600 spectrometer equipped with an inverse TCI CryoProbe. Peak integration, ERETIC measurements and spectrum calibration were obtained by the specific subroutines of the Bruker Top-Spin 3.1 program. Spectra were acquired with the following parameters: flip angle = 90°, recycle delay = 20 s, SW = 3000 Hz, SI = 16 K, NS = 16, and RG = 1. An exponential multiplication (EM) function was applied to the FID for line broadening of 1 Hz. No baseline correction was used.

4.5. RNA Extraction and Real-Time PCR

Aliquots of 20 mL of cultured cells were collected after 24 h from *Tnea*, *Trq7*, and *Tmar*. Additional samples were collected after 48 h for *Tmar*. Total RNA was extracted using the standard RNA extraction method with TRIzol (Invitrogen, Carlsbad, CA, USA), and cDNA synthesis were performed using the Quantitech[®] RNA reverse transcription kit

(Quiagen, Hilden, Germany). The RNA amounts were measured with a NanoDrop ND-1000 spectrophotometer (Thermo fisher, Waltham, MA, USA). Gene expression analysis was carried out by qRT-PCR. Triplicate quantitative assays were performed using a StepONE plus Real-time PCR system (Applied Biosystems, Foster City, CA, USA) and Platinum SYBR Green qPCR SuperMix (Life Technologies, Carlsbad, CA, USA), with the following program: 5 min at 95 °C, 15 s at 95 °C, 30 s at 60 °C, 40 cycles. The gene of 16S RNA served as the endogenous reference [42]. Calculation of gene expression was carried out using the $2^{-\Delta\Delta C_t}$ method as in Livak and Schmittgen [43]. For each sample, the mRNA levels of selected genes were calculated relative to the calibrator sample for corresponding genes. Primers used for genes expression analyses are listed in Supplementary Table S3.

4.6. Bioinformatic Analysis

Thermotogales genomes and the protein sequences of *Tnea* V-ATPase and F-ATPase were obtained from the Ensembl bacteria database (<https://bacteria.ensembl.org/index.html>) (accessed on January 2020). Sequence comparison was performed using the Ensembl BLASTP and NCBI BLASTP tools (<https://blast.ncbi.nlm.nih.gov/Blast.cgi>, accessed on 1 April 2022).

4.7. DNA Extraction and PCR Amplification of ATPase

Genomic DNA was extracted from 20 mL of cultures of *Tnea*, *Trq7* and *Tmar* after 24 h of growth, using a DNA extraction kit (Macherey-nagel, Oensingen, Switzerland) and following the manufacturer's instructions. For amplification of V-ATPase and F-ATPase, primers were designed on catalytic subunits coded by CTN_RS04540 and CTN_RS04145 (Supplementary Table S3). PCR was performed using the following conditions: 5 min at 95 °C, 45 s at 95 °C, 30 s at 60 °C, 72 °C 2 min, 72 °C 10 min, 40 cycles.

4.8. Statistics

Each experiment was performed with at least three replicates. Values were expressed as mean \pm standard deviation (SD). The statistical significance of comparison between the different treatments (N₂ vs CO₂) and species (*Tnea*, *Trq7* and *Tmar*) was calculated through analysis of variance (ANOVA) for hydrogen and organic acids yields ($\alpha = 0.05$). Differences between means were evaluated for significance using the Tukey–Kramer test. For OD₅₄₀, glucose consumption, and qRT-PCR, the statistical significance of comparison between the N₂ and CO₂ was calculated through Student's *t*-test ($p \leq 0.05$).

Supplementary Materials: The following supporting information can be downloaded at: <https://www.mdpi.com/article/10.3390/ijms231912049/s1>.

Author Contributions: Experimental activity and software, N.E., M.L., L.C. and S.L.; Data analysis, all authors; Data curation, S.L. and N.E.; Writing—original draft, N.E., S.L., M.L. and G.d.; Writing—review and editing, Z.X., C.G., G.N., E.M., S.E. and A.F.; Conceptualization, G.d.; Supervision, A.F. and G.d.; Funding acquisition, A.F. and G.d. All authors have read and agreed to the published version of the manuscript.

Funding: This research was funded by MISE, PNRR—Ricerca Idrogeno—Mission M2.C2—Investimento 3.5: Ricerca e sviluppo sull'idrogeno, POR ENEA-CNR-RSE, Delibera 14 luglio 2022 n. 37/2022/G.

Institutional Review Board Statement: Not applicable.

Informed Consent Statement: Not applicable.

Data Availability Statement: Not applicable.

Conflicts of Interest: The authors declare no conflict of interest.

References

1. Huber, R.; Hannig, M. Thermotogales. *Prokaryotes* **2006**, *7*, 899–922. [CrossRef]
2. Bhandari, V.; Gupta, R.S. The Phylum Thermotogae. In *The Prokaryotes*; Springer: Berlin/Heidelberg, Germany, 2014.

3. Lanzilli, M.; Esercizio, N.; Vastano, M.; Xu, Z.; Nuzzo, G.; Gallo, C.; Manzo, E.; Fontana, A.; D'Ippolito, G. Effect of cultivation parameters on fermentation and hydrogen production in the phylum thermotogae. *Int. J. Mol. Sci.* **2021**, *22*, 341. [[CrossRef](#)] [[PubMed](#)]
4. Esercizio, N.; Lanzilli, M.; Vastano, M.; Landi, S.; Xu, Z.; Gallo, C.; Nuzzo, G.; Manzo, E.; Fontana, A.; D'Ippolito, G. Fermentation of biodegradable organic waste by the family thermotogaceae. *Resources* **2021**, *10*, 34. [[CrossRef](#)]
5. Cappelletti, M.; Bucchi, G.; De Sousa Mendes, J.; Alberini, A.; Fedi, S.; Bertin, L.; Frascari, D. Biohydrogen production from glucose, molasses and cheese whey by suspended and attached cells of four hyperthermophilic Thermotoga strains. *J. Chem. Technol. Biotechnol.* **2012**, *87*, 1291–1301. [[CrossRef](#)]
6. Cappelletti, M.; Zannoni, D.; Postec, A.; Ollivier, B. Members of the Order Thermotogales: From Microbiology to Hydrogen Production. *Microb. BioEnergy Hydrog. Prod. Adv. Photosynth. Respir.* **2014**, *38*, 321–347. [[CrossRef](#)]
7. Pradhan, N.; d'Ippolito, G.; Dipasquale, L.; Esposito, G.; Panico, A.; Lens, P.N.L.; Fontana, A. Simultaneous synthesis of lactic acid and hydrogen from sugars via capnophilic lactic fermentation by *Thermotoga neapolitana* cf capnolactica. *Biomass Bioenergy* **2019**, *125*, 17–22. [[CrossRef](#)]
8. Thauer, R.K.; Jungermann, K.; Decker, K. Energy Conservation in Chemotrophic Anaerobic Bacteria. *Am. Soc. Microbiol.* **1977**, *41*, 100–180. [[CrossRef](#)]
9. Schut, G.J.; Adams, M.W.W. The iron-hydrogenase of *Thermotoga maritima* utilizes ferredoxin and NADH synergistically: A new perspective on anaerobic hydrogen production. *J. Bacteriol.* **2009**, *191*, 4451–4457. [[CrossRef](#)]
10. Dipasquale, L.; D'Ippolito, G.; Fontana, A. Capnophilic lactic fermentation and hydrogen synthesis by *Thermotoga neapolitana*: An unexpected deviation from the dark fermentation model. *Int. J. Hydrogen Energy* **2014**, *39*, 4857–4862. [[CrossRef](#)]
11. d'Ippolito, G.; Dipasquale, L.; Fontana, A. Recycling of Carbon Dioxide and Acetate as Lactic Acid by the Hydrogen-Producing Bacterium *Thermotoga neapolitana*. *ChemSusChem* **2014**, *7*, 2678–2683. [[CrossRef](#)]
12. Pradhan, N.; Dipasquale, L.; D'Ippolito, G.; Panico, A.; Lens, P.N.L.; Esposito, G.; Fontana, A. Hydrogen production by the thermophilic bacterium *Thermotoga neapolitana*. *Int. J. Mol. Sci.* **2015**, *16*, 12578–12600. [[CrossRef](#)]
13. Pradhan, N.; Dipasquale, L.; d'Ippolito, G.; Panico, A.; Lens, P.N.L.; Esposito, G.; Fontana, A. Hydrogen and lactic acid synthesis by the wild-type and a laboratory strain of the hyperthermophilic bacterium *Thermotoga neapolitana* DSMZ 4359T under capnophilic lactic fermentation conditions. *Int. J. Hydrogen Energy* **2017**, *42*, 16023–16030. [[CrossRef](#)]
14. d'Ippolito, G.; Landi, S.; Esercizio, N.; Lanzilli, M.; Vastano, M.; Dipasquale, L.; Pradhan, N.; Fontana, A. CO₂-Induced Transcriptional Reorganization: Molecular Basis of Capnophilic Lactic Fermentation in *Thermotoga neapolitana*. *Front. Microbiol.* **2020**, *11*, 171. [[CrossRef](#)]
15. Esercizio, N.; Lanzilli, M.; Vastano, M.; Xu, Z.; Landi, S.; Caso, L.; Gallo, C.; Nuzzo, G.; Manzo, E.; Fontana, A.; et al. Improvement of CO₂ and acetate coupling into lactic acid by genetic manipulation of the hyperthermophilic bacterium thermotoga neapolitana. *Microorganisms* **2021**, *9*, 1688. [[CrossRef](#)]
16. Buckel, W.; Martin, W. Energy Conservation in Fermentations of Anaerobic Bacteria. *Front. Microbiol.* **2021**, *12*, 703525. [[CrossRef](#)]
17. Nuzzo, G.; Landi, S.; Esercizio, N.; Manzo, E.; Fontana, A.; D'Ippolito, G. Capnophilic lactic fermentation from *Thermotoga neapolitana*: A resourceful pathway to obtain almost enantiopure L-lactic acid. *Fermentation* **2019**, *5*, 34. [[CrossRef](#)]
18. Yu, J.S.; Vargas, M.; Mityas, C.; Noll, K.M. Liposome-mediated DNA uptake and transient expression in Thermotoga. *Extremophiles* **2001**, *5*, 53–60. [[CrossRef](#)]
19. Han, D.; Norris, S.M.; Xu, Z. Construction and transformation of a Thermotoga-E. coli shuttle vector. *BMC Biotechnol.* **2012**, *12*, 2. [[CrossRef](#)]
20. Han, D.; Xu, H.; Puranik, R.; Xu, Z. Natural transformation of *Thermotoga* sp. strain RQ7. *BMC Biotechnol.* **2014**, *14*, 39. [[CrossRef](#)]
21. Han, D.; Xu, Z. Development of a pyrE-based selective system for *Thermotoga* sp. strain RQ7. *Extremophiles* **2017**, *21*, 297–306. [[CrossRef](#)]
22. Xu, Z.; Puranik, R.; Hu, J.; Xu, H.; Han, D. Complete genome sequence of *Thermotoga* sp. strain RQ7. *Stand. Genom. Sci.* **2017**, *12*, 62. [[CrossRef](#)] [[PubMed](#)]
23. Schönheit, P.; Schäfer, T. Metabolism of hyperthermophiles. *World J. Microbiol. Biotechnol.* **1995**, *11*, 26–57. [[CrossRef](#)] [[PubMed](#)]
24. Fillingame, R.H. Coupling H⁺ transport and atp synthesis in F₁FO-ATP synthases: Glimpses of interacting parts in a dynamic molecular machine. *J. Exp. Biol.* **1997**, *200*, 217–224. [[CrossRef](#)] [[PubMed](#)]
25. Mulkidjanian, A.Y.; Galperin, M.Y.; Makarova, K.S.; Wolf, Y.I.; Koonin, E.V. Evolutionary primacy of sodium bioenergetics. *Biol. Direct* **2008**, *3*, 13. [[CrossRef](#)]
26. Calisto, F.; Sousa, F.M.; Sena, F.V.; Refojo, P.N.; Pereira, M.M. Mechanisms of Energy Transduction by Charge Translocating Membrane Proteins. *Chem. Rev.* **2021**, *121*, 1804–1844. [[CrossRef](#)]
27. Iida, T.; Inatomi, K.I.; Kamagata, Y.; Maruyama, T. F- and V-type ATPases in the hyperthermophilic bacterium *Thermotoga neapolitana*. *Extremophiles* **2002**, *6*, 369–375. [[CrossRef](#)]
28. Dipasquale, L.; Pradhan, N.; Ippolito, G. Potential of Hydrogen Fermentative Pathways in Marine Thermophilic Bacteria: Dark Fermentation and Capnophilic Lactic Fermentation in Thermotoga and Pseudothermotoga Species. In *Grand Challenges in Marine Biotechnology, Grand Challenges in Biology and Biotechnology*; Springer: Berlin/Heidelberg, Germany, 2018; pp. 217–235. ISBN 9783319690759.
29. Kuhns, M.; Trifunović, D.; Huber, H.; Müller, V. The Rnf complex is a Na⁺ coupled respiratory enzyme in a fermenting bacterium, *Thermotoga maritima*. *Commun. Biol.* **2020**, *3*, 431. [[CrossRef](#)]

30. Grüber, G.; Wieczorek, H.; Harvey, W.R.; Müller, V. Structure-function relationships of A-, F- and V-ATPases. *J. Exp. Biol.* **2001**, *204*, 2597–2605. [[CrossRef](#)]
31. Mitchell, P. Coupling of phosphorylation to electron and hydrogen transfer by a chemi-osmotic type of mechanism. *Nature* **1961**, *191*, 144–148. [[CrossRef](#)]
32. Dimroth, P. Primary sodium ion translocating enzymes. *Biochim. Biophys. Acta (BBA)-Bioenerg.* **1997**, *1318*, 11–51. [[CrossRef](#)]
33. Müller, V.; Ruppert, C.; Lemker, T. Structure and function of the A1A0-ATPases from methanogenic archaea. *J. Bioenerg. Biomembr.* **1999**, *31*, 15–27. [[CrossRef](#)]
34. Ki, T.; Iida, T.; Hoaki, T.; Kamino, K.; Inatomi, K.; Kamagata, Y.; Maruyama, T. Vacuolar-type ATPase in a hyperthermophilic archaeum, *Thermococcus* sp. *Biochem. Biophys. Res. Commun.* **1996**, *229*, 559–564. [[CrossRef](#)]
35. Iida, T.; Kanai, S.; Inatomi, K.I.; Kamagata, Y.; Maruyama, T. Alpha- and beta-subunits of a V-type membrane ATPase in a hyperthermophilic sulfur-dependent archaeum, *Thermococcus* sp. KI. *Biochim. Biophys. Acta (BBA)-Biomembr.* **1997**, *1329*, 12–17. [[CrossRef](#)]
36. Tsutsumi, S.; Denda, K.; Yokoyama, K.; Oshima, T.; Date, T.; Yoshida, M. Molecular cloning of genes encoding major two subunits of a eubacterial V-type ATPase from *Thermus thermophilus*. *Biochim. Biophys. Acta (BBA)-Bioenerg.* **1991**, *1098*, 13–20. [[CrossRef](#)]
37. Zu Bentrup, K.H.; Ubbink-Kok, T.; Lolkema, J.S.; Konings, W.N. An Na⁺-pumping V1V0-ATPase complex in the thermophilic bacterium *Clostridium fervidus*. *J. Bacteriol.* **1997**, *179*, 1274–1279. [[CrossRef](#)]
38. Radax, C.; Sigurdsson, O.; Hreggvidsson, G.O.; Aichinger, N.; Gruber, C.; Kristjansson, J.K.; Stan-Lotter, H. F- and V-ATPases in the genus *Thermus* and related species. *Syst. Appl. Microbiol.* **1998**, *21*, 12–22. [[CrossRef](#)]
39. Nesbø, C.L.; Charchuk, R.; Pollo, S.M.J.; Budwill, K.; Kublanov, I.V.; Haverkamp, T.H.A.; Foght, J. Genomic analysis of the mesophilic *Thermotoga* genus *Mesotoga* reveals phylogeographic structure and genomic determinants of its distinct metabolism. *Environ. Microbiol.* **2019**, *21*, 456–470. [[CrossRef](#)]
40. d'Ippolito, G.; Dipasquale, L.; Vella, F.M.; Romano, I.; Gambacorta, A.; Cutignano, A.; Fontana, A. Hydrogen metabolism in the extreme thermophile *Thermotoga neapolitana*. *Int. J. Hydrogen Energy* **2010**, *35*, 2290–2295. [[CrossRef](#)]
41. Bernfeld, P. Amylases, A and B Methodology. *Enzymology* **1986**, *1*, 149–158. [[CrossRef](#)]
42. Okonkwo, O.; Lakaniemi, A.M.; Santala, V.; Karp, M.; Mangayil, R. Quantitative real-time PCR monitoring dynamics of *Thermotoga neapolitana* in synthetic co-culture for biohydrogen production. *Int. J. Hydrogen Energy* **2018**, *43*, 3133–3141. [[CrossRef](#)]
43. Livak, K.J.; Schmittgen, T.D. Analysis of Relative Gene Expression Data Using Real-Time Quantitative PCR and the 2[−]ΔΔCT Method. *Methods* **2001**, *25*, 402–408. [[CrossRef](#)]



Consiglio Nazionale
delle Ricerche



8. Effect of inorganic sulfured sources on CLF pathway in *Thermotoga neapolitana*

Nunzia Esercizio ¹ et al.,

¹ National Research Council of Italy, Institute of biomolecular chemistry, Research Division Pozzuoli, 80078 (Naples), Italy.

² Department of Biology, University of Naples "Federico II", Via Cinthia, I-80126 Napoli, Italy.



Type of the Paper (Article)

Effect of inorganic sulfured sources on CLF pathway in *Thermotoga neapolitana*

Nunzia Esercizio ¹ et al.

¹ National Research Council of Italy, Institute of biomolecular chemistry, Research Division Pozzuoli, 80078 (Naples), Italy.

² Department of Biology, University of Naples “Federico II”, Via Cinthia, I-80126 Napoli, Italy.

Received: date; Accepted: date; Published: date

Abstract:

Thermotoga neapolitana (*Tnea*) is a hyperthermophilic anaerobic bacterium of the order *Thermotogales*. These were recurrently retrieved in volcanic and geothermal sulfur-rich environments. *Tnea* is able to convert sugars to lactic acid (LA) and hydrogen (H₂) by a peculiar pathway called Capnophilic lactic fermentation (CLF). In recent years we elucidated tricky steps of CLF but some key nodes of the pathway still remain unknown. The purpose of this study was to investigate the effects on CLF of different sulfur (S) compounds with different redox state. To do this, we used different S suppliers namely cysteine (cyst), sodium sulfide (Na₂S), elemental sulfur (S₀), sodium thiosulfate (Na₂S₂O₃), sodium sulfite (Na₂SO₃) and sodium sulfate (Na₂SO₄). Our results showed that S compounds significantly affect growth, metabolism and fermentation pathways of *Tnea*. These modifications appear to be influenced by the oxidation state of the S compounds: higher oxidation state drastically modified CLF pathway, while the lowers maintain canonical H₂ and LA yields. In this view, this study reports a first role of S about the regulation of the CLF pathway, suggesting the hypothesis that S is necessary to sustain the complex metabolic reorganization induced by CO₂ in *Tnea*.

Keywords: Lactic Acid; CO₂, NFN, Hydrogenase, pFOR, MBX, Sulfide dehydrogenase.

1. Introduction

*Tne*a is a hyperthermophilic anaerobic bacterium of the order *Thermotogales* showing a rod shape and a complex outer envelope called toga that surrounds the bacterial cell forming a periplasmic space around the poles [Angel et al., 1993]. Among extreme thermophilic bacteria, members of the order *Thermotogales* have proven to be promising candidates in fermentation processes of biodegradable waste [Lanzilli et al., 2020; Esercizio et al., 2021a]. In fact, a number of *Thermotogales* species were tested for the use of different polysaccharides, food waste and lignocellulose biomass to produce H₂ and/or organic acid [Esercizio et al., 2021a]. Upon common anaerobic condition *Tne*a is able to produce H₂ through dark fermentation. Interestingly, *Tne*a is a performing producer of H₂, showing a yield very close to the theoretical Thauer limit of four moles of H₂ per mole of consumed sugar [Schut and Adams, 2009; d'ippolito et al., 2014; Pradhan et al., 2015; Pradhan et al., 2017ab; Lanzilli et al., 2020].

In recent years a novel and innovative pathway named capnophilic lactic fermentation (CLF) was identified in *Tne*a and *Trq7* [d'Ippolito et al., 2014; Dipasquale et al., 2015; Esercizio et al., 2022]. This pathway is able to perform the biosynthesis of hydrogen (H₂) and lactic acid (LA) by the CO₂ recycling [d'ippolito et al., 2011; Dipasquale et al., 2014; Dipasquale et al., 2015; Pradhan et al., 2017a, d'Ippolito et al., 2020]. Particularly, CLF is not equally reported in all different species of the order *Thermotogales* [Dipasquale et al., 2018]. The manipulation of the sparging gas by N₂/CO₂ switch, trigger the strain-peculiar pathway CLF, producing LA with no loss in term of H₂ [d'ippolito et al., 2011; Dipasquale et al., 2014; Pradhan et al., 2017a, d'Ippolito et al., 2020]. As well as H₂, LA is a marketable fermentation product, used for pharmaceutical, food and industrial applications especially as building block of bioplastics [Juturu and Wu, 2016]. Recently, the LA production using CLF has been highlighted more desirable for commercial applications considering the enantiopure L-LA produced using *Tne*a [Nuzzo et al., 2019]. Considering the attractive ability of *Thermotogales* in different biotechnological applications, the engineering manipulations of different strains were recently reported [Han and Xu, 2017; Singh et al., 2018; Esercizio et al., 2021b]. *Thermotoga maritime* cells were deprived of a functioning lactate dehydrogenase showing an increased hydrogen production and biomass [Singh et al., 2018]. Promising results were also reported by the heterologous expression of Acetyl-CoA synthetase (ACS) from *Thermus thermophilus* into *Tne*a cells inducing an increased CO₂ and acetate coupling into LA [Esercizio et al., 2021b].

The molecular mechanisms regulating CLF were recently elucidated by transcriptomic approach [d'Ippolito et al., 2020]. An increased molecular expression and/or protein occurrence were reported for key enzymes of the CLF pathway namely hydrogenase (HYD), pyruvate:ferredoxin oxidoreductase (pFOR) and lactate dehydrogenase (LDH) [d'Ippolito et al., 2014; d'Ippolito et al., 2020]. Furthermore, a reductans recovery cycle able to sustain the CLF electrons requirement was suggested. This cycle together with a glycolytic pathways switch contribute to an adequate synthesis of NAD(P)H [d'Ippolito et al., 2020]. The electronic pools administration is a critical turning point for the regulation of CLF, which required NADH and reduced ferredoxin for the reactions catalyzed by LDH, HYD and pFOR. The CLF assisting pathway is regulated by two enzymes, NFN (NADH-dependent Reduced Ferredoxin:NADP Oxidoreductase) and RNF (NAD:ferredoxin oxidoreductase). These enzymes used electron bifurcation to catalyze endo- and/or exoergonic electron transfer reactions between NADH, NADPH and ferredoxin obtaining energy conservation and the reduction of the free energy loss in redox reactions [Buckel and Thauer, 2018]. Although these suggestions clarify possible mechanisms for the recovery of the electron pools, the energetic source sustaining CLF still remain unknown. It is worth to point that *Tne*a was originally discovered as sulfur (S) reducing bacteria in the 1986 and a number of sulfur compounds were recently assayed to identify the optimal condition for *Thermotogales* growth upon classical anaerobic condition [Belkin et al., 1986; Boileau et al., 2016]. Intriguingly, hyperthermophilic anaerobic S reducing bacteria such as *Pyrococcus furiosus* and *Thermococcus kodakariensis* showed a strictly correlation between hydrogen, oxidative and S metabolisms [Santangelo et al., 2011; Wu et al., 2018]. Particularly, manipulation of genes related to

oxidative metabolism induced detrimental effects about the bacteria growth while deletion of genes related to S assimilation induced a reduction in H₂ biosynthesis [Bridger et al., 2011; Santangelo et al., 2011]. The aim of the present work was to investigate the possible role of S as key energetic source to perform CLF. To do this, we investigated six different S compounds, analyzing their effects on *Tne* fermentation productions and molecular regulation. Furthermore, a bioinformatic investigation was performed on *Thermotogales* genomes to identify genes involved in S assimilation and metabolism to identify putative actors involved in S metabolism and fermentative pathways.

2. Results

2.1 Capnophilic lactic fermentation is influenced by S source in *Thermotoga*

Tne was grown under CO₂ insufflation, using inorganic sulfured sources with different S oxidation number (ON), at concentration of 4 mmol L⁻¹ equivalent of sulfur. Experiments were performed testing sodium sulfide (Na₂S, ON = -2), elemental sulfur (S₀, ON = 0), sodium thiosulfate (Na₂S₂O₃, ON = +2), sodium sulfite (Na₂SO₃, ON = +4), sodium sulfate (Na₂SO₄, ON = +6) and in absence of S source (No S). Results were compared with standard conditions of CLF, which was reported using cysteine (cyst, ON = -2) as sulfured source (d'Ippolito et al., 2010; d'Ippolito et al., 2014; Dipasquale et al., 2014; Nuzzo et al., 2019; Pradhan et al., 2017ab, Pradhan et al., 2019). As showed in **Supplemental Figure 1**, after 24 hours no significant differences of growth parameter were reported using Na₂S, S₀ and Na₂S₂O₃ in comparison with Cyst. After 48 hours, control and S₀ showed a reduction of OD 540, whereas Na₂S and Na₂S₂O₃ maintained high absorbance values. Na₂SO₄ and No S showed unchanged absorbance levels at 24h and 48 hours. These values were significantly lower compared with Na₂S and Na₂S₂O₃. Considering glucose utilization, Na₂S, Na₂S₂O₃ and S₀ reported comparable consumption with Cyst after 24h and 48h (**Figure 1A**). Na₂SO₄ and No S showed a faster consumption of glucose compared with the other species consuming 27.6 and 28.4 mMol of glucose after 48h. Intriguingly, Na₂SO₃ is the only S source reporting detrimental effects on growth and glucose consumption. Globally, with the exception of Na₂SO₃, upon all the analyzed S species, *Tne* is able to consume the 60% of glucose in the medium, at least (> of 20 mMol of glucose). *Tne* growth in presence of Na₂SO₃ consumed the lower amount of glucose of the medium about 15.5 mMol. As showed in **Figure 1B**, Cyst showed the maximum H₂ production about of 1836 mL/L of culture. All analyzed conditions with the exception for Na₂S₂O₃, showed significant decrease of H₂ productions compared with cyst about 16%, 24%, 96%, 26% and 33% for Na₂S, S₀, Na₂SO₃, Na₂SO₄ and No S, respectively. Particularly Na₂S₂O₃ showed comparable H₂ with Cyst about 1743.03 mL/L of culture. Interestingly, S₀ showed a faster H₂ production after 24h (1344.05 mL/L of culture) but no significant differences comparing 24h and 48h. Na₂SO₃ showed a very scarce production of H₂ at both 24h and 48h reporting values about 67 and 75 mL/L.

Acetic Acid (AA) and Lactic acid (LA) are the major fermentative products of *Tne*. After 48 h of growth upon CO₂, Cyst and Na₂S showed no significant differences in term of AA production reporting 31.6 and 29.4 mM of this organic acid (**Figure 2**). With the exception of Na₂SO₃, the other S species reported significant decline of AA production compared with Cyst/Na₂S related with the corresponding oxidative. Particularly, Na₂SO₄ and No S reported a production of AA about 21.5 and 22.6 mM, respectively while Na₂SO₃ showed the lower value about 2.49 mM. Considering LA, Cyst, Na₂S, S₀ and Na₂S₂O₃ reported no significant differences after 48h of growth. These species produced LA level ranging from 9.03 mM to 10.45 mM. The most oxidant species (Na₂SO₃ and Na₂SO₄) and the absence of S condition (No S) showed instead a significant increase of LA. Particularly these conditions reached 15.23, 21.44 and 26.44 mM of LA after 48h for Na₂SO₃, Na₂SO₄ and No S, respectively.

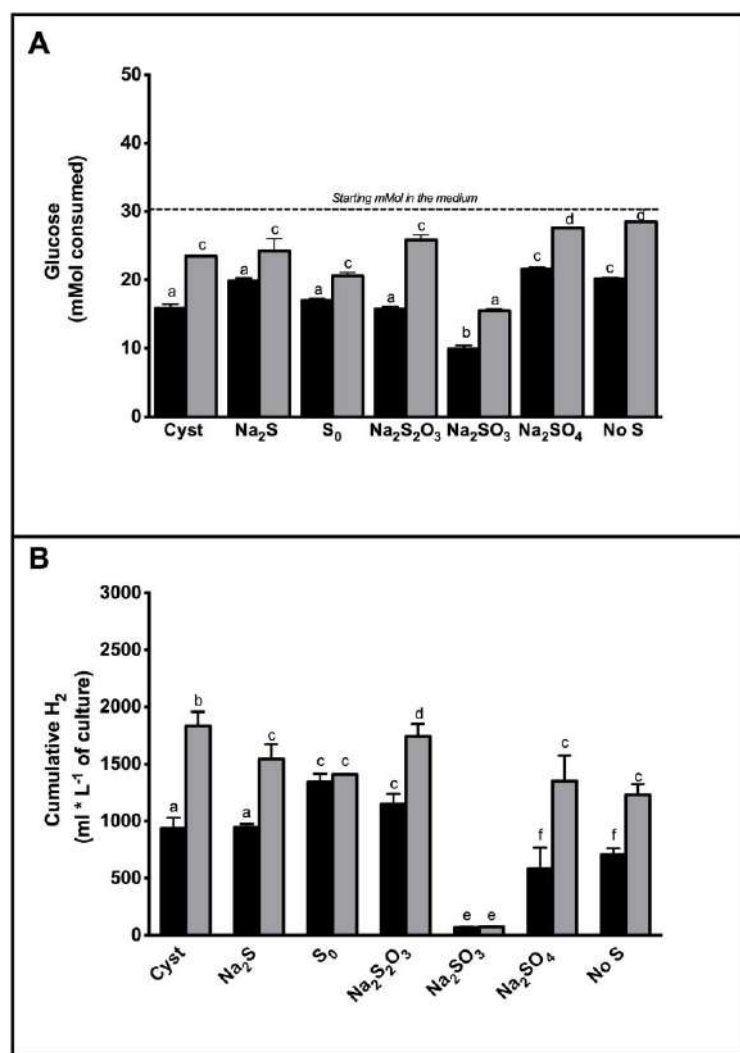


Figure 1. Glucose consumption (A) and Hydrogen production (B) of *Tneal* growth in presence of cysteine, Na₂S, S₀, Na₂S₂O₃, Na₂SO₃, Na₂SO₄ and in absence of S compounds after 24h (black bars) and 48h (grey bars). Letters indicate ANOVA significantly different values in different S compounds.

In order to evaluate the CLF effects, H₂, AA and LA yields were compared. CLF phenotype is reported as an increased LA yield and LA/AA ratio with no loss in term of H₂ yield upon CO₂ insufflations [d'Ippolito et al., 2014; d'Ippolito et al., 2020]. As showed in **Table 1**, oxidation state of S compounds clearly affects organic acids productivity (LA and AA). CLF phenotypes were reported only using Cyst and Na₂S as S sources which showing 3.20-3.16 and 0.40-0.34 yields for H₂ and LA, respectively. Intriguingly, organic acid and H₂ yields appear to be directly correlated with the oxidation state of S compounds (with the exception of Na₂SO₃). Concerning Na₂SO₄ and No S phenotype the fermentation products were probably no obtained from CLF pathway considering the increased LA yields (0.78 and 0.93, respectively) but the decreased H₂ yields (2.00 and 1.77, respectively). Unexpectedly, Na₂SO₃, showed the higher LA yield (0.98) and the lower H₂ yield (0.29).

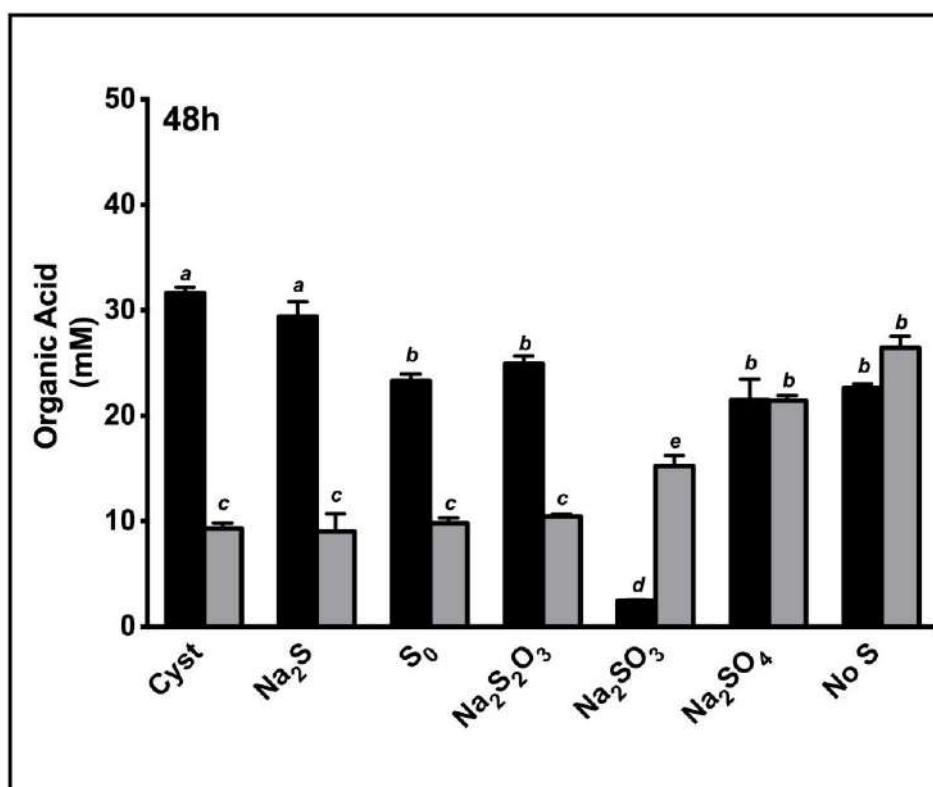


Figure 2. Acetic acid (AA – black bars) and lactic acid (LA – grey bars) production of *Tneal* growth in presence of cysteine, Na₂S, S₀, Na₂S₂O₃, Na₂SO₃, Na₂SO₄ and in absence of S compounds after 48h. Letters indicate ANOVA significantly different values in different S compounds.

Table 1. Sulfur compounds effects on H₂, acetic acid and lactic acid yields (mol/mol glucose).

Sulfur compounds	Oxidation Nr	H ₂	Acetate	Lactate	LA/AA (mM)
Cysteine	-1/-2	3.20 ± 0.18	1.35 ± 0.02	0.40 ± 0.02	0.29 ± 0.02
Na ₂ S	-2	3.16 ± 0.23	1.16 ± 0.07	0.34 ± 0.05	0.30 ± 0.09
S ₀	0	2.80 ± 0.19	1.13 ± 0.04	0.48 ± 0.03	0.42 ± 0.01
Na ₂ S ₂ O ₃	+2	1.89 ± 0.19	0.96 ± 0.06	0.40 ± 0.00	0.42 ± 0.02
Na ₂ SO ₃	+4	0.21 ± 0.01	0.16 ± 0.00	0.98 ± 0.05	6.11 ± 0.29
Na ₂ SO ₄	+6	2.00 ± 0.27	0.78 ± 0.07	0.78 ± 0.02	1.00 ± 0.10
No S	-	1.77 ± 0.11	0.79 ± 0.01	0.93 ± 0.04	1.17 ± 0.03

The key enzyme of CLF pathway is the Pyruvate:Ferredoxin Oxidoreductase (PFOR - E.C. 1.2.7.1). This enzyme catalyzes the decarboxylation of pyruvate to acetyl-CoA and the reversible reaction for the recycling of CO₂ into LA using pyruvate as intermediate [D'ippolito et al., 2014]. In order to evaluate the ability of pFOR to incorporate CO₂ into LA, labeled-sodium carbonate (Na₂CO₃) was used to perform an in-vitro CO₂ generation reaction. Using this approach, the insufflation was performed using labeled CO₂, and an estimation of the labeled LA was obtained through a mass spectrometry approach to quantify the CO₂ recycling efficiency. As reported in **Figure 3**, an increased LA synthesis was reported from the S compound with the lower ON cyst/Na₂S to the higher, Na₂SO₄. The percentage of labeled LA showed minor differences between different S compounds treatments, ranging from 22% to 33%.

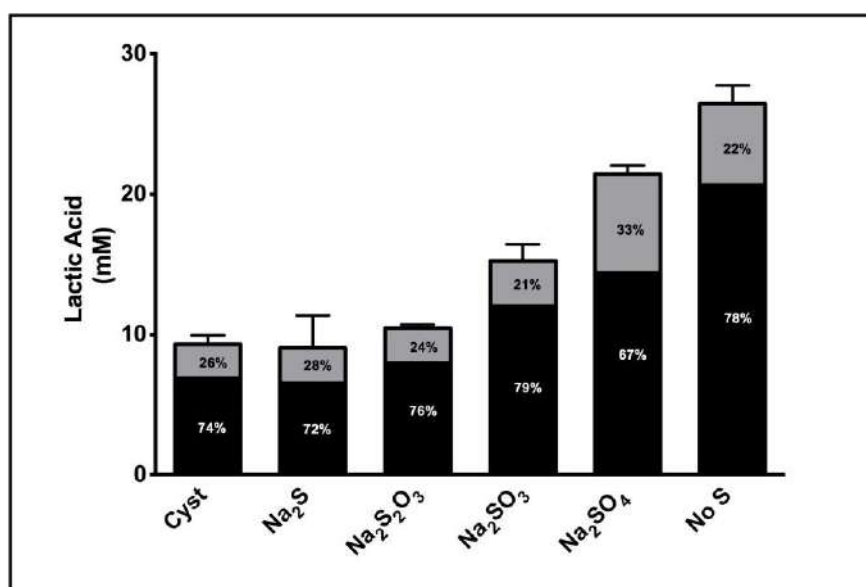


Figure 3. Percentage of labeled LA (grey bars) and non-labeled LA (black bars) produced by *Tnea* using labeled CO₂ as sparging gas in presence of cysteine, Na₂S, Na₂S₂O₃, Na₂SO₃, Na₂SO₄, and in absence of S compounds (No S).

2.2 Identification of S metabolism related genes in *Thermotoga neapolitana*

Tnea was originally identified as sulfur reducing bacteria in the 1986 [Belkin et al., 1986]. Bacterial S metabolism is composed of both assimilatory and dissimilatory S oxidoreductive pathways. Assimilatory S reduction is a critical anabolic microbial pathway necessary to assimilate S into organic compounds [Wu et al., 2021]. S oxidative bacteria mainly involved the SOX pathway. The complete set of SOX gene cluster encode for a complex composed by four proteins involved in thiosulfate-, sulfite-, sulfur- and sulfide-dependent cytochrome c reduction [Wu et al., 2021].

In order to clarify genes involved in S metabolism we mined the *Tnea* genome to identify genes related to S reductive/oxidative recognized pathways. Query sequences were selected using representing bacteria for each sulfur related pathways. As reported in **Table 2**, using a BLASTp approach no genes related to assimilatory and dissimilatory S reductive pathways were reported as well as genes related to SOX pathway. In this analysis, CTN_RS04900 and CTN_RS04005 were

181 reported as BLAST false positive hits (with poor alignment stats value) using Sulfate
182 adenylyltransferase (CysN and CysNC), and Sulfate thiol esterase (SoxB) sequences, respectively.
183 Nucleotide and amino acidic sequences analysis of CTN_RS04900 and CTN_RS04005 confirm the
184 canonical *T.nea* annotation as Elongation factor Tu and UDP-sugar hydrolase, respectively.
185



Table 2. BLASTp analysis of conventional S bacterial metabolic pathways vs *Tnea* genome. QC = Query coverage; I = Identities. Hits with QC ≤ 25% were not considered. APS= adenosine 5'-phosphosulfate; PAPS = phosphoadenosine-5'-phosphosulfate.

Enzymes	Genes	Pathways	Reactions	Query organism	Uniprot ID	Best hit in <i>Tnea</i> genome
Sulfate adenyltransferase subunit 1	CysN	Assimilatory S red.	Sulfate → APS	<i>Escherichia coli</i>	P23845	CTN_RS04900 QC=50% I=28%
Sulfate adenyltransferase subunit 2	CysD	Assimilatory S red.	Sulfate → APS	<i>Escherichia coli</i>	P21156	No hit
Adenylylsulfate kinase	CysC	Assimilatory S red.	APS → PAPS	<i>Escherichia coli</i>	P0A6J2	QC ≤ 25% Hit
Bifunctional CysN/CysC	CysNC	Assimilatory S red.	Sulfate → PAPS	<i>Clostridium pasteurianum</i>	A0A0H3JBE3	CTN_RS04900 QC=67% I=27%
P adenosinephosphosulfate reductase	CysH	Assimilatory S red.	PAPS → Sulfite	<i>Escherichia coli</i>	Q8X7U3	QC ≤ 25% Hit
Sulfite reductase	CysJ	Assimilatory S red.	Sulfite → Sulfide	<i>Escherichia coli</i>	P38038	QC ≤ 25% Hit
Sulfite reductase	CysI	Assimilatory S red.	Sulfite → Sulfide	<i>Escherichia coli</i>	P17846	No hit
Sulfate adenyltransferase	Sat	Dissimilatory S red./ox.	Sulfate ↔ APS	<i>Desulfovibrio vulgaris</i>	Q72CI8	QC ≤ 25% Hit
Adenylylsulfate reductase	Apr	Dissimilatory S red./ox.	APS ↔ Sulfite	<i>Desulfovibrio vulgaris</i>	B8DS75	QC ≤ 25% Hit
Sulfite reductase	Dsr	Dissimilatory S red./ox.	Sulfite ↔ Sulfide	<i>Desulfovibrio vulgaris</i>	P45574	No hit
L-cysteine S-thiosulfotransferase	SoxA	Sox pathway	Thiosulfate ↔ Sulfate	<i>Paracoccus pantotrophus</i>	O33434	No hit
Sulfate thiol esterase	SoxB	Sox pathway	Thiosulfate ↔ Sulfate	<i>Paracoccus pantotrophus</i>	A0A1I5INZ6	CTN_RS04005 QC=71% I=27%
Sulfite dehydrogenase	SoxC	Sox pathway	Thiosulfate ↔ Sulfate	<i>Paracoccus pantotrophus</i>	A0A1I5IPK4	No hit
Sulfur oxidation c-type cytochrome	SoxX	Sox pathway	Thiosulfate ↔ Sulfate	<i>Paracoccus pantotrophus</i>	A0A454NKG7	No hit
Thiosulfate oxidation carrier protein	SoxY	Sox pathway	Thiosulfate ↔ Sulfate	<i>Paracoccus pantotrophus</i>	A0A1I5INT1	No hit
Sulfur compound chelating protein	SoxZ	Sox pathway	Thiosulfate ↔ Sulfate	<i>Paracoccus pantotrophus</i>	A0A1I5IPZ6	No hit
Sulfide-quinone reductase	Sqr	Sulfur oxidation pathway	Sulfate → Sulfur	<i>Desulfurolobus ambivalens</i>	Q7ZAG8	No hit
Sulfur oxygenase/reductase	Sor	Sulfur oxidation pathway	Sulfur → Sulfite	<i>Desulfurolobus ambivalens</i>	P29082	No hit
Sulfide oxidase	–	Sulfur oxidation pathway	Sulfite → Sulfate	<i>Desulfovibrio</i>	A0A1Q8QN01	No hit
Sulfur response regulator	SurR	Transcription factor		<i>Thermococcus</i>	B7R559	No hit

188



Interestingly, there are a number of archaeal peculiar S reducing mechanisms [Schut et al., 2007; Santangelo et al., 2011]. In order to obtain a complete overview of possible S metabolism related mechanisms, genes from *Pyrococcus furiosus* were searched along the *Tnea* genome (Table 3). Using the NSR from *P. furiosus* (Pf1186) we identified CTN_RS01565 coding for a NADH:polysulfide oxidoreductase. This archeal enzyme is proposed to constitute a novel S reducing system and to play a key action for the re-oxidation of ferredoxin and NAD(P)H, respectively [Schut et al., 2007].

Using the sulfide dehydrogenase subunit alfa/beta (Pf1327) of *P. furiosus* we identify two genes (CTN_RS04020 and CTN_RS04025) recently identified to codifying different subunits of the bifurcating enzymes NFN (NADH-dependent Reduced Ferredoxin:NADP Oxidoreductase) [D'Ippolito et al., 2020]. This evidence is in according with Ma and Adams [1994], which reported that this enzyme is able to catalyze both the reversible ferredoxin:NADPH oxidoreductase both the reversible oxidoreduction of polysulfide to H₂S with NADPH as electron donor/acceptor. In order to confirm this assignation, we aligned CTN_RS04020 and CTN_RS04025 with sulfide dehydrogenase subunit alfa/beta of *Pyrococcus furiosus* (SudAB – Supplemental Figure S2).

In addition, when *Thermococcales* as *P. furiosus* or *T. kodakarensis* growth on elemental sulfur (S₀), the peculiar membrane-bound oxidoreductase complex (MBX) is utilized to reduce the sulfane-sulfur of polysulfide by using ferredoxin (Fd) as electron donor. Considering this alternative enzymatic function this complex was recently also named MBS (membrane-bound sulfane reductase) [Wu et al., 2018]. The entire operons of MBX (Pf1441-Pf1453) and of the similar Membrane bound hydrogenase (MBH – Pf1423-1436) from *P. furiosus* were used as queries to identify possible hits in *Tnea* genome. This analysis showed the presence of 12 genes similar to the *P. furiosus* MBX/MBH complexes (CTN_R06775; CTN_RS06780; CTN_RS06785; CTN_RS06790; CTN_RS06795; CTN_RS06800; CTN_RS06805; CTN_RS06810; CTN_RS06815; CTN_RS06820; CTN_RS06825; CTN_RS06830). Considering that MBX alignments showed higher identities and genes with consecutive positions along the genome, these 12 *Tnea* genes may be considered as a putative MBX(S) complex. With the exception of CTN_R06775 which is annotated as glutamate dehydrogenase, the other identified genes (CTN_RS06780-CTN_RS06830) showed annotations consistent with the MBX functions as NADH dehydrogenase's, cation antiporters and NADH-quinone (or ubiquinone) oxidoreductase.

Similar bioinformatic comparisons were conducted using other *thermotogales* namely *T. maritima*, *T. naphthophila*, *T. petrophila*, *T. RQ7*, *Pseudothermotoga lettingae*, and *Pseudothermotoga thermarum* (Supplemental table 1-2). Each analyzed *thermotogales* showed the absence of genes related to the common S metabolic pathways with the exception of Adenylylsulfate kinase in the RQ7 genome (TRQ7_01650; QC=99%, I=52%) and Phosphoadenosine phosphosulfate reductase in the *Petrophila* genome (Tpet_1751; QC=68%, I=25%). NSR and SudAB orthologous were identified in all *thermotogales* genomes (Supplemental table 1).

Table 3. BLASTp analysis of archel S related metabolic pathways from *P. furiosus* vs *Tnea* genome. QC = Query coverage; I = Identities.

Enzymes	Gene	Locus	<i>Tnea</i> Best hit	Alignment stats
CoA dep NAD(P)H sulfur reductase	NSR	Pf1186	CTN_RS01565	QC=98% I=35%
Sulfide dehydrogenase sub alfa	SudA	Pf1327	CTN_RS04020	QC=98% I=59%
Sulfide dehydrogenase sub beta	SudB	Pf1327	CTN_RS04025	QC=97% I=55%
Membrane bound oxidoreductase a	MBX a	Pf1453	CTN_RS06830	QC = 92%; I=45%
Membrane bound oxidoreductase b	MBX b	Pf1452	CTN_RS06825	QC = 75%; I=45%
Membrane bound oxidoreductase d	MBX d	Pf1450	CTN_RS06820	QC = 63%; I=44%
Membrane bound oxidoreductase f	MBX f	Pf1449	CTN_RS06815	QC = 89%; I=41%
Membrane bound oxidoreductase g	MBX g	Pf1448	CTN_RS06810	QC = 91%; I=44%
Membrane bound oxidoreductase h	MBX h	Pf1447	CTN_RS06800	QC = 72%; I=31%
Membrane bound oxidoreductase h	MBX h	Pf1446	CTN_RS06805	QC = 76%; I=32%
Membrane bound oxidoreductase m	MBX m	Pf1445	CTN_RS06795	QC = 97%; I=38%
Membrane bound oxidoreductase j	MBX j	Pf1444	CTN_RS06790	QC = 91%; I=58%
Membrane bound oxidoreductase k	MBX k	Pf1443	CTN_RS06785	QC = 76%; I=39%
Membrane bound oxidoreductase l	MBX l	Pf1442	CTN_RS06780	QC = 93%; I=48%
Membrane bound oxidoreductase n	MBX n	Pf1441	CTN_RS06775	QC = 48%; I=46%
Membrane bound hydrogenase a	MBH a	Pf1423	CTN_RS06835	QC = 96%; I=36%
Membrane bound hydrogenase b	MBH b	Pf1424	CTN_RS06830	QC = 96%; I=42%
Membrane bound hydrogenase c	MBH c	Pf1425	CTN_RS06825	QC = 86%; I=36%
Membrane bound hydrogenase d	MBH d	Pf1426	CTN_RS03355	QC = 19%; I=36%
Membrane bound hydrogenase e	MBH e	Pf1427	CTN_RS06815	QC = 52%; I=46%
Membrane bound hydrogenase f	MBH f	Pf1428	CTN_RS06815	QC = 87%; I=38%
Membrane bound hydrogenase g	MBH g	Pf1429	CTN_RS06810	QC = 94%; I=36%
Membrane bound hydrogenase h	MBH h	Pf1430	CTN_RS06800	QC = 70%; I=29%
Membrane bound hydrogenase i	MBH i	Pf1431	CTN_RS06645	QC = 26%; I=42%
Membrane bound hydrogenase j	MBH j	Pf1432	CTN_RS06790	QC = 88%; I=42%
Membrane bound hydrogenase k	MBH k	Pf1433	CTN_RS06785	QC = 55%; I=32%
Membrane bound hydrogenase l	MBH l	Pf1434	CTN_RS06780	QC = 87%; I=29%
Membrane bound hydrogenase m	MBH m	Pf1435	CTN_RS06795	QC = 92%; I=27%
Membrane bound hydrogenase n	MBH n	Pf1436	CTN_RS06775	QC = 69%; I=34%

Finally, as showed in **supplemental table S2**, *T. maritima* and *T.RQ7* showed the presence of MBX putative genes. These identified loci showed similarities with *Tnea*, and together these three *thermotogales* showed identical alignment stats *vs P. furiosus*. The others *thermotogales* showed poor alignment stats *vs P.furiosus*, particularly for MBXb, MBXm, MBXj, MBXk, MBXl and MBXn, and not consecutive positions of the putative orthologous along the genomes. Considering these evidences, we may not assume the presence of an MBX complex in *T. naphthophila*, *T. petrophila*, *Pseudothermotoga lettingae*, and *Pseudothermotoga thermarum* genomes.

2.3 Molecular regulation induced by oxidative vs reductive S species

In order to identify molecular mechanisms regulating CLF upon different oxidative status induced by S sources, we selected cyst (ON = -1) and Na₂SO₄ (ON = +6) samples for a qRT-PCR approach (**Figure 5**). We selected genes coding for the CLF core enzymes namely pFOR subunit alfa (CTN_RS03385), lactate dehydrogenase (LDH, CTN_RS03950), hydrogenase subunit alfa (HYDa, CTN_RS05285), acetate kinase (ACK, CTN_RS02020), and phosphate acetyltransferase (PTA, CTN_RS07210). In addition, genes coding for S metabolism, cysteine synthase (CTN_RS09565) and cystathionine δ synthase (CTN_RS09565) and genes coding for bifurcating enzymes RFN (CTN_RS02165) and NFN/SuD (CTN_RS04020) were investigated. As reported in **Figure 5A**, ACK and PORa showed no significant differences between Na₂SO₄ and cyst. In according with H₂ and organic acid productions, HYDa showed -1.7 fc while LDH showed a +1.86 fc in Na₂SO₄ compared with cyst. The CLF link enzyme PTA showed an increased expression up to +4.84 fc. It is worth to point out that HYDa, PFORa and PTA increased their molecular expression by the N₂/CO₂ switch as insufflations gas [d'Ippolito et al., 2020]. This suggests that Na₂SO₄ hides the molecular effects of the CO₂ on the hydrogenase expression while strengthens the expression of PTA. By contrast, the molecular functioning of the pFOR remains unaltered upon Na₂SO₄.

Intriguingly, both analyzed genes coding for bifurcating enzymes NFN and RFN showed a decrease of expression in presence of Na₂SO₄ compared with cyst. The expression of these two genes showed a down-regulation about -2.1 and -2.7, respectively. The entire NFN and RFN complex enhanced their expression upon CO₂ vs N₂ insufflations [d'Ippolito et al., 2020] therefore, similar to HYDa, Na₂SO₄ stops the molecular regulation induced by CO₂. Finally, genes related to S organication namely, cysteine synthase and cystathionine δ synthase showed up-regulation in Na₂SO₄. These two genes were usually up-regulated upon CO₂ thus the substitution of cyst with Na₂SO₄ in the cultivation medium reinforce the molecular regulation triggered by CO₂.

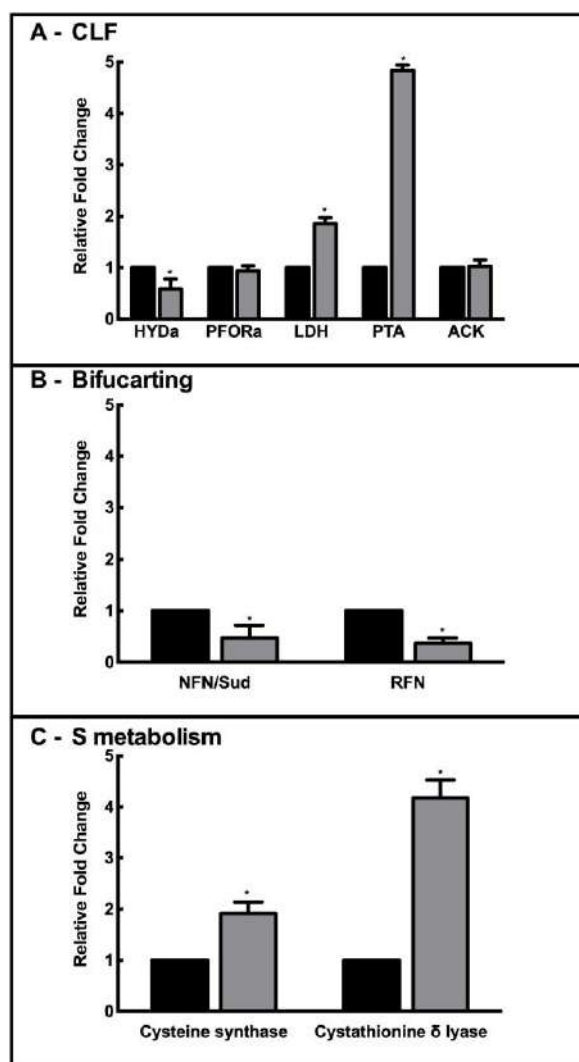


Figure 5. Changes in the gene expression of pFOR subunit alfa (CTN_RS03385), lactate dehydrogenase (LDH, CTN_RS03950), hydrogenase (HYD, CTN_RS05285), acetate kinase (ACK, CTN_RS02020), phosphate acetyltransferase (PTA, CTN_RS07210), cysteine synthase (CTN_RS09565), cystathionine δ synthase (CTN_RS09565), RFN (CTN_RS02165) and NFN (CTN_RS04020), in Na₂SO₄ and cysteine *Tne* treated samples, measured by qRT-PCR. Variations are indicated as relative fold-change in Na₂SO₄ (gray bars) with respect to cysteine (black bars). mRNA levels were calculated relatively to the expression of the RNA 16S used as calibrator. Asterisks indicate significantly different values in different S compounds vs cysteine samples at $p \leq 0.05$ (*) and $p \leq 0.001$ (**).

3. Discussion

In recent years, the management of S compounds showed an increased commercial interest considering that a number of novel microorganisms used for biotechnologies live in extreme environments and are extensively involved in S biogeochemical cycles [Lens and Kuenen, 2001; Lin et al., 2018]. Among extremophiles, *Tnea* shows innovative potentiality for the simultaneous production of H₂ and L-LA using CLF pathway [d'Ippolito et al., 2014; Dipasquale et al., 2014; Pradhan et al., 2017a; Nuzzo et al., 2019; Esercizio et al., 2021]. The molecular basis of CLF pathway was recently clarified but some energetic steps still remain unknown [d'Ippolito et al., 2014; d'Ippolito et al., 2020]. Particularly, the elemental source of the electronic force driving the entire CLF process was not identified. S certainly plays a role in *Thermotoga* metabolism, in fact upon classic anaerobic condition in presence of sulfur, glucose is ineffectually used but fermentation productions remain unaltered and hydrogen sulfide is produced instead of H₂ [Schröder et al., 1994]. Recently, Boileau et al. [2016] used different S compounds to assay the potentiality of *T. maritima* (*Tnea* very close specie) [Jannasch et al., 1988]. The authors reported a necessary requirement of S sources in the culture medium for conventional growth and H₂ production. Suitable S sources included sulfide, cysteine or thiosulfate [Boileau et al., 2016]. Similar evaluations were reported for mesophilic member of the *Thermotogales* phylum, such as *Mesotogae prima* [Fadhlaoui et al., 2018]. Different strains of this species are incapable to ferment glucose in absence of S, producing acetate only in presence of this element. It has been proposed the crucial role of S in order to eliminate an excess of reducing equivalents generated by a sugar obligatory oxidative pathway [Fadhlaoui et al., 2018].

In the present study cultures of the strain *Tnea* (substr. *capnolactica*) were characterized upon CLF condition (CO₂ insufflation instead of N₂) using different S compounds namely cyst, Na₂S, S₀, Na₂S₂O₃, Na₂SO₃, Na₂SO₄, and in absence of S compounds (No S). The S species were selected based on the different ON from -2 to +6. This study clearly showed that different S compounds significantly affect growth, metabolism and fermentation pathways of *Tnea* upon CLF condition. Interestingly, the reported modifications appear to be related to the oxidation state of the S compounds. Higher oxidation state of Na₂SO₄ (ON = +6), Na₂SO₃ (ON = +4) drastically modified the fermentation yields of *Tnea* inhibiting the CLF pathway. Similar effects were reported in absence of S. These conditions lead to a remarkable increase of LA productions and yields. Furthermore, cyst (ON = -1) and Na₂S (ON = -2) showed less differences leading both to the CLF phenotype. Intermediate conditions were S₀ and Na₂S₂O₃. Contrarily, CO₂ recycling action induced upon CLF condition, appear to be slightly influenced by different S compounds, thus indicating that S does not influence the reversal pFOR activity upon CO₂.

Different authors proposed that S reduction acts as an electron sink reaction to avoid the inhibitory effects of the accumulation of fermentation products [Huber et al., 1986; Janssen and Morgan, 1992; Childress and Noll, 1994; Fadhlaoui et al., 2018]. The pathway of glucose fermentation upon anaerobic condition drives the electrons from the glycolytic pathways to reduce protons and yielding H₂. When the H₂ concentration totally inhibits the activity of hydrogenase, sulfur reduction supplies an alternative mechanism for electron excess recycling [Jansen and Morgan, 1992]. These evidences suggest that S oxidants compounds could rivalry with CLF for the electron potential. The role of the S oxidation state was confirmed comparing gene expressions in Na₂SO₄ and Cyst. The challenge between these two pathways may be accelerate comparing CO₂ insufflation and simple anaerobic condition because CO₂ increased the speed of the H₂ production processes showing a faster inhibition of the hydrogenase. Accordingly with fermentation yields results, CLF core genes showed a modification of the expression justifying the decreased of H₂ production by a down-regulation of the HYDa and the increase of LA yield by the up-regulation of the LDH. At the same time, a number of studies reported a sulfhydrogenase ability of the *Tnea* hydrogenase [Childress and Noll, 1994; Kaslin et al., 1998]. This evidence suggests possible effects on the hydrogenase activity changing the S compound in the cultivation medium.

It is worth to point out that a critical step of CLF pathway induction is the increase of expression and protein occurrences of pFOR [d'Ippolito et al., 2014; d'Ippolito et al., 2020]. Accordingly, with labeled- CO_2 incorporation, pFOR expression has been not showed significant difference. This is in agreement with the idea that S compounds accessibility could slow down the CLF pathway. A reduced organic S availability could play an additional role in hydrogenase maturation, which required 4Fe-4S clusters [Albertini et al., 2015]. In fact, both cysteine and sulfide stimulate the in-vitro maturation of hydrogenase [Kuchenreuther et al., 2009]. These evidences further justifying the reduced H_2 yield. It is worth to point out that modification in the sparging gas (from N_2 to CO_2) induced molecular up-regulations of LDH, pFOR, HYDa PTA cysteine synthase, cystathionine δ synthase, RFN and NFN genes [d'Ippolito et al., 2020]. Interestingly, the Na_2SO_4 treatment further regulated the expression of LDH, PTA, cysteine synthase and cystathionine δ synthase strengthening their up-regulation.

Unexpectedly, bioinformatic analysis reports the absence of genes coding for conventional S reductive and oxidative pathways in *Tnea*. This genomic condition could in part explain the negative effects of the oxidant species to the CLF pathway and justifying the similarity between the Na_2SO_4 and No S phenotypes. Investigations on different *Thermotogales* and on the archaea *P. furiosus* highlighted that this is a common condition among this class of thermophiles and particular all *Thermotogae* and *Pseudothermotogae* bacteria showed the presence of putative sulfide dehydrogenase and NSR which are recognized archeal enzymes used for oxidoreduction of S derived products [Schut et al., 2007; Wu et al., 2018]. Interestingly, the major *P. furiosus* actor involved in S derived products oxidoreduction was recently identified in the membrane bound oxidoreductase complex (MBX) [Bridger et al., 2011; Santangelo et al., 2011; Wu et al. 2018]. This complex catalyzes the production of H_2S using the presence of S_0 or polysulfide in the medium and ferredoxin as electron donor. This activity practically changes the name of MBX to MBS [Wu et al. 2018]. Intriguingly, *P. furiosus* MBS uses reduced ferredoxin from glycolysis to reduce the experimental substrate dimethyl trisulfide to reduce the organic and anionic polysulfide. Our bioinformatics investigation retrieved the presence of putative MBX(S) complex in *Tnea* (as well as in *T. maritima* and *T. RQ7*) but this alternative S reducing activity is not yet experimentally demonstrate. This putative MBX complex of *Tnea* showed not differential expression upon CO_2 [d'Ippolito et al., 2020]. The presence of these S reducing complex in *Tnea* could be also suggested by the genomic similarities between *Tnea* and *P. furiosus*. Interestingly the 24% of the *T. maritima* ORF showed an archeal origin while phylogeny highlighted a strictly correlation between *thermotogales* and *P. furiosus* [Nesbo et al., 2001]. Genes such as glutamate synthase (gltB) and myo-inositol 1P synthase gene (ino1) were acquired during the divergence of the *Thermotogales* from archaea, particularly from *Pyrococcus* order [Nesbo et al., 2001]. These examples suggest a possible similar evolution for MBX and sulfide dehydrogenase genes retrieved in *Tnea*.

Among the investigated candidate genes related to S redox pathways, the subunits of NFN enzymes, CTN_RS04020 and CTN_RS04025, were now also identified as subunits of sulfide dehydrogenase. This enzyme is double linked with S metabolism catalyzing both the reducing equivalents supplying (from ferredoxin or NADH to NADPH) both the S oxidoreduction [Ma and Adams, 1994; Childress and Noll, 1994; Kaslin et al., 1998; Nesbo et al., 2019]. It is worth to point out that SudAB subunits were recently identified also in *Mesotogae prima* suggesting this complex as putative thiosulfate reducers. [Nesbo et al., 2019]. Based on transcriptomic evidences we suggest a reductans recovery cycle to sustain the CLF requirements [d'Ippolito et al., 2020]. This cycle is based on the reactions catalyzed by the bifurcating enzyme NFN and RFN. The double action of NFN in S oxidoreduction and as reduced ferredoxin and NADH supplier would explain the additional electronic burden required to equilibrate the deviation from dark fermentation to CLF about carbon and hydrogen balance. The energetic link provided by NFN identified S as key chemical element for CLF functioning. Interestingly, Na_2SO_4 condition down-regulated the expression of NFN and RFN genes thus suggesting an electronic potential deviation for the S reduction and organication.

4. Conclusions

Our study clearly indicated a key role of sulfur in CLF pathway. These results indicated that CO₂ insufflation is necessary but not sufficient to trigger CLF if the growth medium contains S oxidants species or an absence of S. Upon CLF condition, reductive S species increased *Tnea* metabolism addressing the enhanced electron force for the H₂ and LA production through CLF pathway. On the other hand, upon CLF condition, the presence of S oxidant species completely drives *Tnea* metabolism to LA production. S plays a key role in hydrogen production through electron providing/sequestering. Alternatively, our data indicated that the management of S compounds in *Tnea* is an efficient strategy to select the desired fermentative products. The key role in *Tnea* S oxidoreductive metabolism could be played by the putative SuDAB and/or MBS putative complexes. Further studies will be necessary to clarify the effective roles of these proteins.

4. Materials and Methods

4.1 Biological material

Tnea subsp. capnolactica (DSM 33003) derives from the DSMZ 4359T strain that was stimulated in our laboratory under saturating concentration of CO₂ for several years [Pradhan et al., 2017]. Bacterial cells were grown in a modified ATCC 1977 culture medium containing 10 ml/l of filter-sterilized vitamins and trace element solutions (DSM medium 141) together with 10 g/L NaCl, 0.1 g/L KCl, 0.2 g/L MgCl₂·6H₂O, 1 g/L NH₄Cl, 0.3 g/L K₂HPO₄, 0.3 g/L KH₂PO₄, 0.1 g/L CaCl₂·2H₂O, 0.5 g/L cysteine-HCl, 2 g/L yeast extract, 2 g/L tryptone, 5 g/L glucose, 0.001 g/L resazurin (d'Ippolito et al., 2010). In order to study the S effects, bacteria were also growth upon different conditions using several sulfur compounds replacing cysteine: Na₂S (0.32g/L), S₀ (0.13 g/L), Na₂S₂O₃ (0.33 g/L), Na₂SO₃ (0.52 g/L), Na₂SO₄ (0.59 g/L), and in absence of sulfur compounds. The grams of the S species were selected to perform each experiment using an equal mMoles of S (4.13).

4.2 Bacterial growth

Pre-cultures (30 mL) were incubated overnight at 80°C without shaking and used to inoculate (6% v/v) the samples. Standard culture medium was distributed into six separated bottles (120 ml total volume) using 30 ml of medium. Oxygen was removed by heating until the solution was colorless. Experimental bacterial cultures were inoculated at 6% (v/v). The culture medium was initially sparged with CO₂ gas (to obtain CLF condition) for 5 min at 30 mL/min. Sparging was repeated after 24h of culture; pH was monitored and adjusted to approximately 7.5 by 1 M NaOH at 0h and 24h. The culture bottles were growth into an heater (Binder ED720) set at 80°C. Gas chromatography was performed after 24h and 48h. Cell growth was determined by optical density (OD) at 540 nm (UV/Vis spectrophotometer DU 730, Beckman Coulter). Aliquots of 2 ml of medium were collected from each samples after 0h, 24h and 48h, centrifuged at 16000 g 15 min (Hermle Z3236K) and kept to -20°C until analysis.

4.3 CO₂ labeling experiments

In order to evaluate the incorporation of the CO₂ in the final LA produced by *Tnea*, we performed an in-vitro reaction to generate labeled-CO₂. For ¹³C-labelling experiments in 120mL serum bottles, 30 mL of bacterial cultures were firstly sparged with N₂ and then saturated with oxygen-free ¹³CO₂ generated by the neutralization of 600mg (3 mmol) of Ba¹³CO₃ with 3M HCl (5 mL). ¹³CO₂ saturation of head space was verified by GC analysis.

4.4 Gas analysis

Gas (H₂ and CO₂) measurements were performed by Gas chromatography (GC) on an instrument (Focus GC, Thermo Scientific) equipped with a thermoconductivity detector (TCD) and

fitted with a 3 m molecular sieve column (Hayesep Q). N₂ was used as carrier gas. Analyses were carried out after 24h and 48h prior to gas sparging.

4.5 Chemical analysis

Glucose concentration was determined by the dinitrosalicylic acid method calibrated on a standard solution of 2 g/L glucose [Bernfeld, 1995]. Organic acid was measured by ERETIC 1H NMR as described by Nuzzo et al. [2019]. All experiments were performed on a Bruker DRX 600 spectrometer equipped with an inverse TCI CryoProbe. Peak integration, ERETIC measurements and spectrum calibration were obtained by the specific subroutines of Bruker Top-Spin 3.1 program. Spectra were acquired with the following parameters: flip angle = 90°, recycle delay = 20 s, SW = 3000 Hz, SI = 16K, NS = 16, RG = 1. An exponential multiplication (EM) function was applied to the FID for line broadening of 1 Hz. No baseline correction was used.

4.6 Mass spectrometry

For MS analysis, 500 µL sample of culture medium of each culture were acidified at pH 3 with HCl. The solutions were extracted with 1 volume of ethyl acetate three times. The organic extracts were evaporated and dissolved in methanol to a final concentration of 20 µg/mL and directly analyzed by means of an LC-MS instrument equipped with a micro-Quadrupole TOF analyzer using an electrospray ionization (ESI) source in negative ion mode. Lactate ion [M – H][–] was detected at m/z≈87 due to the artefactual in-source formation of pyruvate described by Trefely et al. [2018].

4.7 RNA extraction and Real-Time PCR

An aliquot of 20 ml of culture cells were collected after 24h both from Cyst and Na₂SO₄ bottles. Total RNA was extracted using the standard RNA extraction method with TRIzol (Invitrogen, Carlsbad, CA, USA) and cDNA synthesis were performed using the Quantitech® RNA reverse transcription kit (Quiagen, Hilden Germany). RNA amount was measured by NanoDrop ND-1000 spectrophotometer (NanoDrop Technologies). Gene expression analysis was carried out by qRT-PCR. Triplicate quantitative assays were performed using an ABI 7900 HT (Applied Biosystems, Foster City, CA, USA) and Platinum SYBR Green qPCR SuperMix (Life Technologies, Carlsbad, CA, USA). *Thermotoga* cells growth using Cyst were used as calibrators; RNA 16S served as endogenous reference gene [Okonkwo et al., 2017]. Calculation of gene expression was carried out using the 2^{–ΔΔCt} method as in Livak and Schmittgen [2001]. For each sample, mRNA amount of selected genes was calculated relatively to the calibrator sample for corresponding genes.

4.8 Bioinformatics

Sequences of proteins related to sulfur reductive/oxidative pathways were found using keywords searches on UniProt. These were selected using representing bacteria for each sulfur related pathways. *Thermotogales* genomes were obtained on the ensambl bacteria database (<https://bacteria.ensembl.org/index.html>) (access on October 2020). Comparison were performed using the ensambl BLASTp and NCBI BLASTp software (<https://blast.ncbi.nlm.nih.gov/Blast.cgi>).

4.9 Statistics

Each experiment was made in at least three replicates. Values were expressed as mean ± standard deviation (SD). The statistical significance of comparison between the different S compounds and cysteine was calculated through Student's t-test (p ≤ 0.05) for qRT-PCR, sugar consumption, H₂ cumulative production and OD 540. In addition, analysis of variance (ANOVA) was utilized to calculate the statistical significance of the differences between different S treatments for H₂ yield, organic acids mM and yields (ANOVA calculations correspond to α = 0.05). Differences between means were evaluated for significance using the Tukey–Kramer test.

Author Contributions: Conceptualization, SL, GD and AF; Experimental activity, SL, MV, NE, ML, GN and LC; Data analysis, SL, NE, MV and GD; Data curation, SL and GD; Writing, SL and GD Supervision, GD and AF; Funding acquisition, AF and GD. All authors have read and agreed to the published version of the manuscript.

Funding: This research was funded by BioRECO2VER_H2020NMBP-BIO-2017 project, grant number 760431.

Acknowledgments:

Conflicts of Interest: The authors declare no conflict of interest

References

- Albertini, M.; Berto, P.; Vallese, F.; Di Valentin, M.; Costantini, P.; Carbonera, D. Probing the Solvent Accessibility of the [4Fe-4S] Cluster of the Hydrogenase Maturation Protein HydF from *Thermotoga neapolitana* by HYSCORE and 3p-ESEEM. *J Physical Chem*, **2015**; *119*, 13680–13689.
- Belkin, S.; Wirsén, C.; Jannasch, H.W. A New Sulfur-Reducing, Extremely Thermophilic Eubacterium from a Submarine Thermal Vent. *Appl Environ Microbiol*, **1986**, *51*(6), 1180–1185.
- Bernfeld, P. Amylases a and b. *Methods Enzymol*. **1995** *1*:149e58
- Boileau, C.; Auria, R.; Davidson, S.; Casalot, L.; Christen, P.; Liebgott, P.P.; Combet Blanc, Y. Hydrogen production by the hyperthermophilic bacterium *Thermotoga maritima* part I: effects of sulfured nutrients, with thiosulfate as model, on hydrogen production and growth. *Biotechnol for Biofuel*. **2016**, *9*:269.
- Childers, S.E.; Noll, K.M. Characterization and Regulation of Sulfur Reductase Activity in *Thermotoga neapolitana*. *Appl Environ Microbiol*. **1994**, *60*: 2622–2626.
- Dipasquale, L.; d'Ippolito, G.; Fontana, A. Capnophilic lactic fermentation and hydrogen synthesis by *Thermotoga neapolitana*: An unexpected deviation from the dark fermentation model. *Inter J Hydrogen Ener*. **2014**.
- Dipasquale, L., Adessi, A., d'Ippolito, G. *et al*. Introducing capnophilic lactic fermentation in a combined dark-photo fermentation process: a route to unparalleled H₂ yields. *Appl Microbiol Biotechnol* **99**, 1001–1010 (2015).
- d'Ippolito, G.; Dipasquale, L.; Vella, F.M.; Romano, I.; Gambacorta, A.; Cutignano, A.; Fontana, A. Hydrogen metabolism in the extreme thermophile *Thermotoga neapolitana*. *Inter J Hydrogen Ener*. **2010**
- d'Ippolito, G.; Dipasquale, L.; Fontana, A. Recycling of Carbon Dioxide and Acetate as Lactic Acid by the Hydrogen Producing Bacterium *Thermotoga neapolitana*. *ChemSusChem*. **2014**.
- d'Ippolito, G.; Landi, S.; Esercizio, N.; Lanzilli, M.M.; Vastano, M.; Dipasquale, L.; Nirakar, P.; Fontana, A. CO₂-induced transcriptional reorganization: molecular basis of Capnophilic lactic fermentation in *Thermotoga neapolitana*. *Front. Microbiol*. **2020**.
- Esercizio, N.; Lanzilli, M.; Vastano, M.; Landi, S.; Xu, Z.; Gallo, C.; Nuzzo, G.; Manzo, E.; Fontana, A.; d'Ippolito, G. Fermentation of Biodegradable Organic Waste by the Family *Thermotogaceae*. *Resources* **2021**, *10*, 34.
- Esercizio, N.; Lanzilli, M.; Vastano, M.; Xu, Z.; Landi, S.; Caso, L.; Gallo, C.; Nuzzo, G.; Manzo, E.; Fontana, A.; d'Ippolito, G. Improvement of CO₂ and Acetate Coupling into Lactic Acid by Genetic Manipulation of the Hyperthermophilic Bacterium *Thermotoga neapolitana*. *Microorganisms*. **2021** Aug 9;9(8):1688.
- Esercizio, N.; Lanzilli, M.; Landi, S.; Caso, L.; Xu, Z.; Nuzzo, G.; Gallo, C.; Manzo, E.; Esposito, S.; Fontana, A.; d'Ippolito, G. Occurrence of Capnophilic Lactic Fermentation in the Hyperthermophilic Anaerobic Bacterium *Thermotoga* sp. Strain RQ7. *Int J Mol Sci*. **2022** Oct 10;23(19):12049.
- Han, D.; Xu, Z. (2017). Development of a pyrE-based selective system for *Thermotoga* sp. strain RQ7. *Extremophiles*. **21**, 297–306.
- Huber, R.; Langworthy, T.A.; König, H.; Thomm, M.; Woese, C.R.; Sleytr, U.B.; et al. *Thermotoga maritima* sp. nov. represents a new genus of unique extremely thermophilic eubacteria growing up to 90 °C. *Arch Microbiol*. **1986**; *144*(4):324–33.
- Jannasch, H.W.; Huber, R.; Belkin, S.; Stetter, K.O. *Thermotoga neapolitana* sp. nov. of the extremely thermophilic, eubacterial genus *Thermotoga*. *Arch Microbiol*. **1988**; *150*(1):103–4.
- Janssen, P.H.; Morgan, H.W. Heterotrophic sulfur reduction by *Thermotoga* sp. Strain FjSS3.B1. *FEMS Microbiol Lett*. **1992** *96*. 212–218.
- Juturu, V.; Wu, J.C. Microbial production of lactic acid: the latest development. *Crit Rev Biotechnol*. **2016**, *36*(6), 967–977.
- Kaslin, S.; Childers, S.E.; Noll, K.M. Membrane-associated redox activities in *Thermotoga neapolitana*. *Arch Microbiol*. **1998** *170*, 297–303.
- Lanzilli, M.; Esercizio, N.; Vastano, M.; Xu, Z.; Nuzzo, G.; Gallo, C.; Manzo, E.; Fontana, A.; d'Ippolito, G. Effect of Cultivation Parameters on Fermentation and Hydrogen Production in the Phylum *Thermotogae*. *Int J Mol Sci*. **2020** Dec 30;22(1):341.
- Lens, P.N.; Kuenen, J.G. **2001**. The biological sulfur cycle: novel opportunities for environmental biotechnology. *Water Sci Technol*. *44*(8):57–66.
- Lin, S.; Mackey, H.R.; Hao, T.; Guo, G.; van Loosdrecht, M.C.M.; Chen, G. Biological sulfur oxidation in wastewater treatment: A review of emerging opportunities. *Water Research*. **2018**; *143*, 399–415.

23. Livak, K.J.; Schmittgen, T.D. Analysis of relative gene expression data using real-time quantitative PCR and the 2- $\Delta\Delta$ CT method. *Methods*, **2001**; *25*.
24. Ma, K.; Adams, M.W.W. Sulfide Dehydrogenase from the Hyperthermophilic Archaeon *Pyrococcus furiosus*: a New Multifunctional Enzyme Involved in the Reduction of Elemental Sulfur. *J. Bacteriol.* **1998**, *176*, 6509–6517.
25. Nuzzo, G.; Landi, S.; Esercizio, N.; Manzo, E.; Fontana, A.; d'Ippolito, G. Capnophilic Lactic Fermentation from *Thermotoga neapolitana*: A Resourceful Pathway to Obtain Almost Enantiopure L-lactic Acid. *Fermentation*, **2019** *5*, 34.
26. Okonkwo, O.; Lakaniemi, A.M.; Santala, V.; Karp, M.; Mangayil, R. Quantitative real-time PCR monitoring dynamics of *Thermotoga neapolitana* in synthetic co-culture for biohydrogen production. *Int J Hydrog Energy*. **2017**, *43*, 3133–3141.
27. Pradhan, N.; Dipasquale, L.; D'Ippolito, G.; Panico, A.; Lens, P. N. L.; Esposito, G.; Fontana, A. Hydrogen production by the thermophilic bacterium *Thermotoga neapolitana*. *Int J Hydrog Energy*. **2015**.
28. Pradhan, N.; Dipasquale, L.; d'Ippolito, G.; Panico, A.; Lens, P. N. L.; Esposito, G.; Fontana, A. Hydrogen and lactic acid synthesis by the wild-type and a laboratory strain of the hyperthermophilic bacterium *Thermotoga neapolitana* DSMZ 4359T under capnophilic lactic fermentation conditions. *Int J Hydrog Energy*, **2017**.
29. Pradhan, N.; Rene, E. R.; Lens, P. N. L.; Dipasquale, L.; D'Ippolito, G.; Fontana, A.; Esposito, G. Adsorption behaviour of lactic acid on granular activated carbon and anionic resins: Thermodynamics, isotherms and kinetic studies. *Energies*, **2017** *10*(5), 1–16.
30. Pradhan, N.; D'Ippolito, G.; Dipasquale, L.; Esposito, G.; Panico, A.; Lens, P. N. L.; Fontana, A. Simultaneous synthesis of lactic acid and hydrogen from sugars via capnophilic lactic fermentation by *Thermotoga neapolitana* cf *capnolactica*. *Biomass and Bioenergy*, **2019**, 125:17–22.
31. Schröder, C.; Selig, M.; Schönheit, P. Glucose fermentation of acetate, CO₂ and H₂ in the anaerobic hyperthermophilic eubacterium *Thermotoga maritima*: involvement of the Embden-Meyerhof pathway. *Arch Microbiol.* **1994**; *161*(6):460–70.
32. Schut, G.J.; Adams M.W. The iron-hydrogenase of *Thermotoga maritima* utilizes ferredoxin and NADH synergistically: a new perspective on anaerobic hydrogen production. *J. Bacteriol.* **2009**; *191*:4451–7.
33. Klentzin, A.; Urich, T.; Muller, F.; Bandejas, T.M.; Gomes, C.M. Dissimilatory oxidation and reduction of elemental sulfur in thermophilic archaea. *J. Bioenerg Biomembr.* **2004**, *36*, 77–91.
34. Zeng, X.; Zhang, X.; Shao, Z. Metabolic Adaptation to Sulfur of Hyperthermophilic *Palaeococcus pacificus* DY20341T from Deep-Sea Hydrothermal Sediments. *Int J. Mol. Sci.* **2020** *21*, 368.
35. Rabus, R.; Hansen, T.A.; Widdel, F. Dissimilatory Sulfate- and Sulfur-Reducing Prokaryotes. IN *The Prokaryotes*, Fourth Edition, ED Rosenberg, E.; DeLong, E.F.; Lory, S.; Stackebrandt, E.; Thompson, F. Springer.
36. Nesbo, C.M.; L'Haridon, S.; Stetter, K.O.; Doolittle, F.W. Phylogenetic Analyses of Two "Archaeal" Genes in *Thermotoga maritima* Reveal Multiple Transfers Between Archaea and Bacteria. *Mol Biol Evo.* **2001** *18*, 362–375.
37. Santangelo, T.J.; Cubonova, L.; Reeve, J.N. Deletion of alternative pathways for reductant recycling in *Thermococcus kodakarensis* increases hydrogen production. *Mol. Microbiol.* **2011**, *81*, 897–911.
38. Singh R, White D, Demirel Y, Kelly R, Noll K, Blum P. (2018). Uncoupling Fermentative Synthesis of Molecular Hydrogen from Biomass Formation in *Thermotoga maritima*. *Applied and Environmental Microbiology*. 84: e00998-18.
39. Wu, C.H.; Schut, G.J.; Poole, F.L.; Haja D.K.; Adams, M.W.W. Characterization of membrane-bound sulfane reductase: A missing link in the evolution of modern-day respiratory complexes. *J Biol. Chem.* **2018**.
40. Bridger, S.L.; Clarkson, S.M.; Stirrett, K.; DeBarry, M.B.; Lipscomb, G.L.; Schut, G.J.; Westpheling, J.; Scott, R.A.; Adams, M.W.W. Deletion strains reveal metabolic roles for key elemental sulfur-responsive proteins in *Pyrococcus furiosus*. *J. Bacteriol.* **2011**, *193*, 6498–6504.
41. Schut, G.J.; Bridger, S.L.; Adams M.W. Insights into the metabolism of elemental sulfur by the hyperthermophilic archaeon *Pyrococcus furiosus*: characterization of a coenzyme A- dependent NAD(P)H sulfur oxidoreductase. *J. Bacteriol.* **2007**, *189*, 4431–4441.
42. Trefely, S.; Mesaros, C.; Xu, P.; Doan, M.T.; Jiang, H.; Altinok, O.; Orynbayeva, Z.; Snyder, N.W. Artefactual formation of pyruvate from in-source conversion of lactate, *Rapid Commun Mass Spectrom.* **2018**; *32*:1163–1168.

43. Dipasquale, L.; Pradhan, N.; d'Ippolito, G.; Fontana, A. Potential of hydrogen fermentative pathways in marine thermophilic bacteria: dark fermentation and capnophilic lactic fermentation in *Thermotoga* and *Pseudothermotoga* species, **2018**. In *Grand Challenges in Marine Biotechnology*, eds P. H. Rampelotto, and A. Trincone, (Berlin: Springer), 217–235.
44. Buckel, W.; Thauer, R.K. Flavin-based electron bifurcation, ferredoxin, flavodoxin, and anaerobic respiration with protons (Ech) or NAD⁺(Rnf) as electron acceptors: a historical review. *Front. Microbiol.* **2018** 14:401.
45. Angel, A. M.; Brunene, M.; Baumeister, W. The functional properties of Ompb, the regularly arrayed porin of the hyperthermophilic bacterium *Thermotoga neapolitana*. *FEMS Microbiol.* **1993**, 109, 231–236.
46. Kuchenreuther JM, Stapleton JA, Swartz JR (2009) Tyrosine, Cysteine, and S-Adenosyl Methionine Stimulate *In Vitro* [FeFe] Hydrogenase Activation. *PLoS ONE* 4(10): e7565.
47. Fadhlou, Khaled et al. "Obligate sugar oxidation in *Mesotoga* spp., phylum *Thermotogae*, in the presence of either elemental sulfur or hydrogenotrophic sulfate-reducers as electron acceptor." *Environmental Microbiology* 20 (2018): 281–292.
48. Nesbø, Camilla L. et al. "Genomic analysis of the mesophilic *Thermotogae* genus *Mesotoga* reveals phylogeographic structure and genomic determinants of its distinct metabolism." *Environmental Microbiology* 21 (2019): 456–470
49. Wu B, Lui F, Fang W, Yang T, Chen GH, He Z, Wang S. Microbial sulfur metabolism and environmental implications. *Science of the Total Environment*, **2021**, 778, 146085.

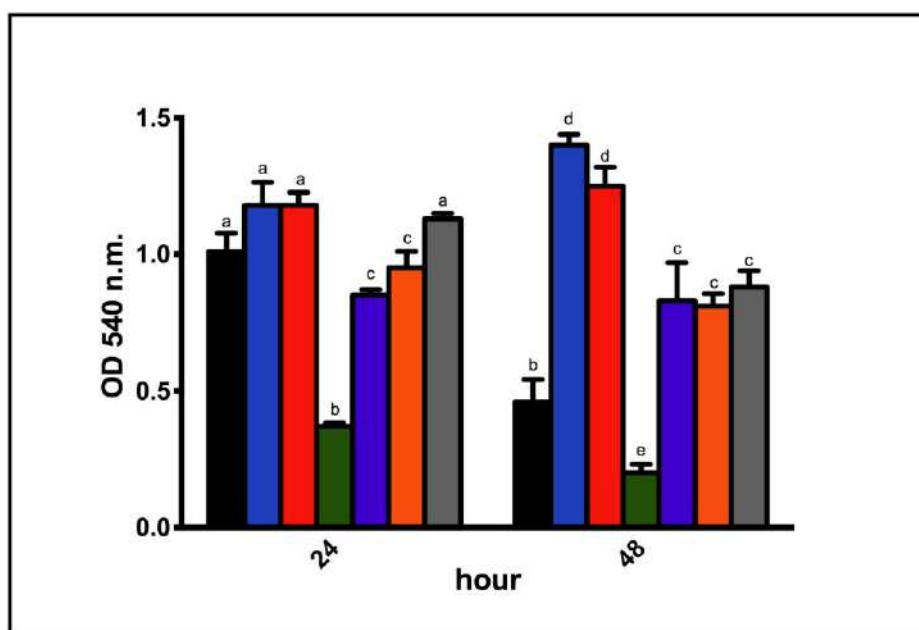


© 2020 by the authors. Submitted for possible open access publication under the terms and conditions of the Creative Commons Attribution (CC BY) license (<http://creativecommons.org/licenses/by/4.0/>).



Supplementary Materials

Supplemental Figure S1: Glucose consumption of *Tnea* growth in presence of cysteine (black bars/lines), Na_2S (blue bars/lines), S_0 (grey bars/lines), $\text{Na}_2\text{S}_2\text{O}_3$ (red bars/lines), Na_2SO_3 (green bars/lines), Na_2SO_4 (purple bars/lines) and in absence of S compounds (No S – orange bars/lines). Letters indicate ANOVA significances among S species.



610

611 **Supplemental Table S1.** BLASTp analysis of S bacterial metabolic pathways vs *thermotogales* genome
 612 (*neapolitana*, *maritima*, *petrophila*, *naphthophila*, *RQ*, *Pseudothermotoga* *thermarum* and
 613 *Pseudothermotoga* *lettingae*).

614

Enzymes	<i>T. neapolitana</i>	<i>T. maritima</i>	<i>T. petrophila</i>	<i>T. naphthophila</i>	<i>P. thermarum</i>	<i>P. lettingae</i>	<i>RQ7</i>
Sulfate adenyltransferase	Absent	Absent	Absent	Absent	Absent	Absent	Absent
Adenylylsulfate kinase	Absent	Absent	Absent	Absent	Absent	Absent	<u>Present</u>
P phosphosulfate reductase	Absent	Absent	<u>Present</u>	Absent	Absent	Absent	Absent
Sulfate adenyltransferase	Absent	Absent	Absent	Absent	Absent	Absent	Absent
Adenylylsulfate reductase	Absent	Absent	Absent	Absent	Absent	Absent	Absent
Sulfite reductase	Absent	Absent	Absent	Absent	Absent	Absent	Absent
L-cysteine S-thiosulfotransferase	Absent	Absent	Absent	Absent	Absent	Absent	Absent
Sulfate thiol esterase	Absent	Absent	Absent	Absent	Absent	Absent	Absent
Sulfite dehydrogenase	Absent	Absent	Absent	Absent	Absent	Absent	Absent
Sulfur oxidation c-type cytochrome	Absent	Absent	Absent	Absent	Absent	Absent	Absent
Thiosulfate oxidation carrier protein	Absent	Absent	Absent	Absent	Absent	Absent	Absent
Sulfur compound chelating protein	Absent	Absent	Absent	Absent	Absent	Absent	Absent
Sulfide-quinone reductase	Absent	Absent	Absent	Absent	Absent	Absent	Absent
Sulfur oxygenase/reductase	Absent	Absent	Absent	Absent	Absent	Absent	Absent
Sulfide oxidase	Absent	Absent	Absent	Absent	Absent	Absent	Absent
Sulfide dehydrogenase sub alfa	<u>Present</u>	<u>Present</u>	<u>Present</u>	<u>Present</u>	<u>Present</u>	<u>Present</u>	<u>Present</u>
Sulfide dehydrogenase sub beta	<u>Present</u>	<u>Present</u>	<u>Present</u>	<u>Present</u>	<u>Present</u>	<u>Present</u>	<u>Present</u>
CoA dep NAD(P)H sulfur reductase	<u>Present</u>	<u>Present</u>	<u>Present</u>	<u>Present</u>	<u>Present</u>	<u>Present</u>	<u>Present</u>

615



Supplemental Table S2. BLASTp analysis of MBX complex from *P. furiosus* vs *thermotogales* genome (*maritima*, *petrophila*, *naphthophila*, *RQ*, *Pseudothermotoga thermarum* and *Pseudothermotoga lettingae*. QC = Query coverage; I = Identities. Consecutive loci were highlighted in blue.

	<i>Maritima</i>		<i>Naphthophila</i>		<i>Petrophila</i>		<i>Lettingae</i>		<i>Thermarum</i>		<i>RQ7</i>	
Genes	Locus	Stats	Locus	Stats	Locus	Stats	Locus	Stats	Locus	Stats	Locus	Stats
MBX a	AAD36281	QC = 92%; I=48%	ADA67466	QC = 78%; I=27%	ABQ46352	QC = 78%; I=27%	ABV34578	QC = 63%; I=29%	AEH51578	QC = 83%; I=31%	AJG41443	QC = 92%; I=45%
MBX b	AAD36282	QC = 84%; I=47%	ADA66319	QC = 22%; I=39%	ABQ46723	QC = 27%; I=38%	ABV34608	QC = 70%; I=28%	AEH51579	QC = 75%; I=26%	AJG41442	QC = 75%; I=25%
MBX d	AAD36283	QC = 77%; I=37%	ADA67159	QC = 77%; I=31%	ABQ47048	QC = 77%; I=31%	ABV33475	QC = 59%; I=37%	AEH51580	QC = 59%; I=37%	AJG41441	QC = 91%; I=35%
MBX f	AAD36284	QC = 89%; I=41%	ADA67726	QC = 49%; I=28%	ABQ47639	QC = 49%; I=28%	ABV33694	QC = 58%; I=24%	AEH51581	QC = 66%; I=28%	AJG41440	QC = 89%; I=41%
MBX g	AAD36285	QC = 87%; I=46%	ADA67732	QC = 80%; I=36%	ABQ47645	QC = 80%; I=36%	ABV34604	QC = 87%; I=37%	AEH51582	QC = 87%; I=37%	AJG41439	QC = 91%; I=44%
MBX h	AAD36287	QC = 90%; I=29%	ADA67731	QC = 59%; I=26%	ABQ47644	QC = 59%; I=26%	ABV34605	QC = 53%; I=21%	AEH51577	QC = 62%; I=25%	AJG41437	QC = 72%; I=32%
MBX h	AAD36286	QC = 99%; I=33%	ADA67731	QC = 64%; I=26%	ABQ47644	QC = 64%; I=26%	ABV34605	QC = 64%; I=25%	AEH51575	QC = 73%; I=22%	AJG41438	QC = 86%; I=31%
MBX m	AAD36288	QC = 98%; I=38%	ADA66609	QC = 16%; I=38%	ABQ47745	QC = 18%; I=27%	ABV32958	QC = 17%; I=26%	AEH51987	QC = 17%; I=23%	AJG41436	QC = 98%; I=38%
MBX j	AAD36289	QC = 91%; I=58%	ADA66239	QC = 13%; I=44%	ABQ46162	QC = 13%; I=44%	ABV34038	QC = 29%; I=24%	AEH50444	QC = 27%; I=27%	AJG41435	QC = 91%; I=58%
MBX k	AAD36290	QC = 76%; I=38%	ADA66261	QC = 42%; I=31%	ABQ46577	QC = 44%; I=31%	ABV34526	QC = 14%; I=53%	AEH50766	QC = 28%; I=34%	AJG41434	QC = 76%; I=38%

MBX l	AAD36291	QC = 93%; I=48%	ADA67876	QC = 17%; I=24%	ABQ47814	QC = 17%; I=24%	ABV34500	QC = 11%; I=33%	AEH50607	QC = 15%; I=36%	AJG41433	QC = 93%; I=48%
MBX n	AAD36292	QC = 50%; I=45%	ADA67144	QC = 27%; I=39%	ABQ47062	QC = 27%; I=39%	ABV34076	QC = 27%; I=37%	AEH51620	QC = 31%; I=35%	AJG41432	QC = 48%; I=45%



Supplemental Figure S2: Alignments of sulfide dehydrogenase (SudA-B) amino acid sequences from *Pyrococcus furiosus* vs the corresponding sequences of the *Thermotoga neapolitana* genome (CTN_RS04020 and CTN_RS04025).

A - SudA	
Tnea_CTN_RS04020 P.fur_SudA	---MSKKTFMREQSPDVRKRNFEVALGYTLEEAVAEARCLQCPTH--PCVSGCPVGI MPRLIKDRVPTPERSVGERVDFGEVNLGYSWELALREAERCLQCFVEYAPCIKGCFFVHI :....* *.* . * :*,** ***: * : * :*****. ** :**** *
Tnea_CTN_RS04020 P.fur_SudA	DIPGFIRELREGR-----LEESYRILKSYNNLPAVCGRVCPQEVQCEFRVVGKMKDSE NIPGFIKALRENDRNPSKAVREALRIIWRDNTLPAITGRVCPQEEQCEGACVVGKVGVD-- :*****. ***,* : * : **:. * :***: ***** ** :**** *
Tnea_CTN_RS04020 P.fur_SudA	FVAIGRLERFVADWAAEN-LEEK--VEESAGQRK--EKVAIVGSGPAGLTAADLAKIGY PINIGKLERFVADYAREHGIDDELLLEEIKGKRNGKKVAIIAGAPAGLTCAADLAKMGV * : ** :*****: * * : : : : : ** * .. :****:*****:*****: **
Tnea_CTN_RS04020 P.fur_SudA	NVDVFEALHKPGGVLYVYGIPEFRLPKRIVEREVNIEKLGVRIFLNTIVVGKTIKVKDLLE EVTIYEALHQPGGVLYVYGIPEFRLPKRIVEREVNIEKLGVRIFLNTIVVGKTIKVKDLLE :* : :*****:*****:***** ** :*,* : : ,***,* * :*****:*** *
Tnea_CTN_RS04020 P.fur_SudA	EYDAIFIGTGAGIPKFMGIPGTNLNGVYSANEFLTRVNLKAYLFPDYDTPVRVGRKRVAV EYDAIFIGTGAGIPRIYFPWGVNLNGIYSANEFLTRINLMKAYKFPEYDTPIKVGRKRVAV *****:***: * :*,** :*****:***** ** :*****:*****
Tnea_CTN_RS04020 P.fur_SudA	IGAGNTAMDAARSALRLGAERKVIYVYRTENEMPARREYHHALEEGIEFLWLILFVRYL IGGNTAMDAARSALRLGAE-VWILYRRTKEMTAREEEIKHAEEGVKFMFLVTPKRFI ** :*****:***** * :*,** :*** ** :** ***:***. * * : :
Tnea_CTN_RS04020 P.fur_SudA	GDANGNVEAMECVRMELKGVDRSGRPKPFVVEGSMFVLEIDMVIEAIGQGPNRVLSEFP GDENGNLKAIIELEKMKLGEPEDESGRRRPIPT-GETFIMEFDTAIIAIGQTPNKTFLFETVP ** ***:*** * :* * *** :*,* . :*,** :*** * :*** ** :***. *
Tnea_CTN_RS04020 P.fur_SudA	GLELNERGYINTDRDTGATSVRGVFAGGDIVTGAATVIEAMGAGKRAAQFIHSLSGEWD GLKVDENGRIVVDEML-MTSPGVFAGGDAIRGEATVILAMGDGRKAIAHQLYSKE-- ***** * * * * ** :***** . * **** * * * * ** * * * *
B - SudB	
Tnea_CTN_RS04025 P.fur_Sudb	MNEIVVKRLAFDVFDFVHSPSISKEAKPGQFVIIRLHEKGERIPTVADTKPEEGLFR MFRILRKERLAPGINLFEIESPRIARHAKPGQFVMIRLHERGERIPTIADVDISKGSIT * :* : * :*** . : * : * * * * :*****:*****:***. . :* :
Tnea_CTN_RS04025 P.fur_Sudb	MVVRVVGKTHLSLRKEGDTILDVVGPLGNPSEIRNYGRVLLVGGGVGIATLYPIAKAL IVAQEVGKTTRELGTYEAGDYILDVLGPLGKPSHIDYFGTVVMIGGGVGVAEIYPVAKAM :*,* :*****:***. : * * ***:*****:*** * :* * : :*****: * :*,***:
Tnea_CTN_RS04025 P.fur_Sudb	KNSGNEVVAVLGARTKDYLMVDFEKEIS-EVFLVTDGSGAGMKGVVTDAMDRLFREG-S KEGNYVISILGFRKDLVFWEDKLSVSDEVIVTNDGSGYGMKGFTHALQKLEEGRK * :*,* * : :*,* *** : : * : :*,* * :*,* * :*,* * :*,* * :*,* * :*,* *
Tnea_CTN_RS04025 P.fur_Sudb	FDCVWAIGPTIMMKFCTLKAMEYGVPIWVSLNPIIMVDGTGMCACRVTVSGQMKFACVDG IDLHVAVGPAIMMKAVAEITKPYGIKTVASLNPIMVDGTGMCACRVTVSGGEVKFACVDG :*,* :*,* :***** : : * : * :*****:*****:***:*****
Tnea_CTN_RS04025 P.fur_Sudb	PEFRGEEVDWDELLKRLAQYRQERISYERFLKTAGETK PEFDAHLVDWDQLMNRLAYRDLEKISLEKWERERRMV- *** . ***:***:*** ** :*,* * : . . .



Consiglio Nazionale
delle Ricerche



9. Adaptive laboratory evolution of *Thermotoga neapolitana* in minimal medium containing glucose as unique organic source

Nunzia Esercizio¹ et al.,

¹ Institute of Biomolecular Chemistry (ICB), Consiglio Nazionale delle Ricerche (CNR), Via Campi Flegrei 34, 80078 Pozzuoli, Italy; n.esercizio@icb.cnr.it

² Department of Biology, University of Naples "Federico II", Via Cinthia, I-80126 Napoli, Italy



Adaptive laboratory evolution of *Thermotoga neapolitana* in minimal medium containing glucose as unique organic source

Nunzia Esercizio ¹ et al.

¹ Institute of Biomolecular Chemistry (ICB), Consiglio Nazionale delle Ricerche (CNR), Via Campi Flegrei 34, 80078 Pozzuoli, Italy; n.esercizio@icb.cnr.it (N.E.); m.lanzilli@icb.cnr.it (M.L.); l.caso@icb.cnr.it (L.C.); afon-tana@icb.cnr.it (A.F.)

² Department of Biology, University of Naples "Federico II", Via Cinthia, I-80126 Napoli, Italy.

Abstract: *Thermotoga neapolitana* subsp. *capnolactica* is a mutant strain in which capnophilic lactic fermentation (CLF) was elucidated for the first time. This anaplerotic mechanism couples exogenous acetate and CO₂ to synthesize lactic acid without affecting hydrogen production. One of the main factors that could influence the fermentation rate is the presence in the complete medium of yeast extract and tryptone as extra organic carbon and nitrogen source. Here we describe for the first time the possibility of adapting *T. neapolitana* in a minimal medium without yeast extract and tryptone by the adaptive laboratory evolution (ALE) strategy. The adapted strain was subjected to CLF condition and phenotypically characterized.

Keywords: adaptive laboratory evolution; yeast extract; tryptone; carbon balance; electron balance

1. Introduction

Thermotoga neapolitana is an anaerobic, hyperthermophilic bacteria, able to metabolize a variety of mono- and polysaccharides as carbon and energy source to produce hydrogen at high yields (d'Ippolito et al., 2010; Esercizio et al., 2021a). Along with the classical Dark fermentation, *T. neapolitana* was also recognized for its ability to assimilate exogenous CO₂ through the activation of an unprecedented anaplerotic pathway called Capnophilic lactic fermentation (CLF), by which the hydrogen production is accompanied with the concomitant synthesis of value-added products as lactic acid (Dipasquale et al., 2014; d'Ippolito et al., 2014; Pradhan et al., 2016; Nuzzo et al., 2019).

Among the cultivation parameters that surely affect the growth rate and carbohydrate metabolism in *Thermotogae* members, yeast extract and tryptone have a crucial role, since represent an essential source of nitrogen and amino acids, necessary for the synthesis of cellular components like nucleic acids, proteins and enzymes (Lanzilli et al., 2021). However, yeast extract composition is always unknown, thus making its replacement with other alternative substrates hard (Van Niel et al., 2002). A surplus of NH₄Cl in the culture medium only partially restore the effect of yeast extract and tryptone in *Thermotoga* sp.RQ7 (Han et al., 2017). Moreover, experiments with high concentrations of both yeast extract and tryptone in *Caldicellulosiruptor saccharolyticus* and *Thermotoga elfi* significantly improved hydrogen production, while lower concentrations reduced both hydrogen and acetic acid yields (Van Niel et al., 2002). *Thermotoga neapolitana* did not growth on modified medium without yeast extract and tryptone, while cultures without glucose partially produced hydrogen at the beginning of the fermentation process, suggesting the importance of these components in the initial growth phase (d'Ippolito et al., 2010). Biomass increased along with the increase of yeast extract concentrations (up to 4.0 g/L), while concentrations around 2–4 g/L are still able to support productivity and bacterial growth (Van Niel et al., 2002; Nguyen et al., 2008; Maru et al., 2012). Labeling experiments

Citation: Lastname, F.; Lastname, F.; Lastname, F. Title. *Fermentation* **2021**, *7*, x. <https://doi.org/10.3390/xxxxx>

Academic Editor: Firstname Lastname

Received: date

Accepted: date

Published: date

Publisher's Note: MDPI stays neutral with regard to jurisdictional claims in published maps and institutional affiliations.



Copyright: © 2021 by the authors. Submitted for possible open access publication under the terms and conditions of the Creative Commons Attribution (CC BY) license (<https://creativecommons.org/licenses/by/4.0/>).

with 6-¹³C-glucose in *T. neapolitana* with 2g/L of both yeast extract and tryptone allowed to estimate at 10-15% their contribution in the production of acetate, and therefore hydrogen during fermentation (d'Ippolito et al., 2010). The aim of the present work was to push *T. neapolitana* towards an adaptation in a minimal growth medium without yeast extract, tryptone and cysteine (the latter was replaced by Na₂S as inorganic sulfur source), and only glucose as carbon organic source. The adaptive laboratory evolution (ALE) approach was used, and represent a systematic and prolonged exposure to a perturbed environment that could result in phenotypic and genetic changes in bacterial strain (Latif et al., 2015). Few examples of ALE are known in *Thermotogales*, as in *T. maritima* and *T. sp. RQ7*, with different limitations (Latif et al., 2015; Singh et al., 2018; Gautam et al., 2022). In this context, *Thermotoga neapolitana* subsp. *capnolactica* was pushed to adapt its metabolism in a minimal medium without yeast extract and tryptone but under CO₂-saturated atmosphere, in order to study and evaluate the effect under capnophilic lactic fermentation condition and in a "cleaner" context, excluding other organic sources. This represent the first example of *T. neapolitana* adaptation, especially because this technique has allowed to overcome the constraints for the cultivation in minimal medium without yeast extract and tryptone discussed previously.

2. Materials and Methods

2.1. Bacterial strain and culture medium

Basal *Thermotoga neapolitana* subsp. *capnolactica* (Tncf) (DSM 33003) strain was used in this study as control. For the adaptive laboratory experiments, the strain was grown anaerobically in a modified version of the culture medium without other carbon sources (cysteine, yeast extract and tryptone) except glucose, containing (g L⁻¹): NaCl 10.0; KCl 0.1; MgCl₂·6H₂O 0.2; NH₄Cl 1.0; K₂HPO₄ 0.3; KH₂PO₄ 0.3; CaCl₂·2H₂O 0.1; glucose 5.0; resazurin 0.001; 10.0 mL of filter-sterilized vitamins and trace element solutions (DSM medium 141) in 1.0 L distilled H₂O (D'Ippolito et al., 2010; Dipasquale et al., 2014). Cysteine was replaced by Na₂S in sulfur equivalent to ensure the same growth conditions. Aliquots (30 mL) of culture medium were distributed into 120 mL serum bottles. Excess oxygen was removed by heating until the solution was colorless. The serum bottles were immediately capped with butyl rubber stoppers and sterilized by autoclaving for 15 min at 110°C. For the experiments with pH control, different form of filtered Hepes solutions (Hepes sodium salt, Hepes acid, Hepes buffer) were added after autoclave in final concentration of 100 mM to ensure the maintenance of the pH constant around 7.5.

2.2. Adaptive laboratory experiments

Adaptive laboratory experiments were conducted in the modified medium described before, under CO₂ saturated atmosphere. *Thermotoga neapolitana* subsp. *capnolactica* (Tncf) (DSM 33003) inoculum was centrifuged at 16,000 × g for 10 min (Hermle Z3236K), and then washed with fresh modified medium, to remove residues of yeast extract and tryptone. Bacterial cultures were inoculated at 6% (v/v) in serum bottle with fresh modified medium and sparged with CO₂ to remove oxygen. The initial pH was adjusted to approximately 7.5 by 1 M NaOH. The temperature of the medium was constantly maintained at 80°C in a heater (Binder ED720). Cells were allowed to growth till mid-log phase first every 48h and then every 24h and then the culture was transferred in new fresh serum bottle, sparged again and allowed to growth again. For ALE, a total of about 100 serial subcultures were carried out at least twice a week. Every month the subcultures were tested for their ability of producing hydrogen and organic acids compared to the wild type strain.

2.3. Standard growth condition

For phenotypic analysis, the adapted strain and the wild type strain were sparged with CO₂ gas for 3 min at 30 mL/min in order to create an anaerobic atmosphere. Bacterial cultures were inoculated with the pre-culture inoculum at 6% (v/v). The initial pH was adjusted to approximately 7.5 by 1 M NaOH. The temperature of the medium was constantly maintained at 80°C in a heater (Binder ED720). Sparging followed by pH adjustment was repeated after 24h. Cell growth was determined by optical density (OD) at 540 nm (UV/Vis Spectrophotometer DU 730, Beckman Coulter). Samples (2 ml of medium) were collected from each bottle after 0, 24, and 48 h. After centrifugation at 16,000 × g for 15 min (Hermle Z3236K), residues and supernatants were kept at −20°C until analysis. Cell morphology was monitored by microscope observation (Axio VertA1, Carl Zeiss, magnification of 100×).

2.4. Chemical Analysis

Hydrogen production were performed by gas chromatography (GC) on an instrument (Focus GC, Thermo Scientific) equipped with a thermoconductivity detector (TCD) and fitted with a 3 m molecular sieve column (Hayesep Q). N₂ was used as carrier gas. Gas sampling was carried out at 24 and 48 h. Glucose concentration was determined by the dinitrosalicylic acid method calibrated on a standard solution of 2 g/L glucose (Bernfeld, 1995). Organic acids were measured by ERETIC ¹H NMR as described by Nuzzo et al. (2019). All experiments were performed on a Bruker DRX 600 spectrometer equipped with an inverse TCI CryoProbe. Peak integration, ERETIC measurements, and spectrum calibration were obtained by the specific subroutines of Bruker Top-Spin 3.1 program. Spectra were acquired with the following parameters: flip angle = 90°, recycle delay = 20 s, SW = 3000 Hz, SI = 16K, NS = 16, RG = 1. An exponential multiplication (EM) function was applied to the FID for line broadening of 1 Hz. No baseline correction was used.

2.5. Determination of Carbon and Energy Balance

Carbon balance and electron equivalents balance for each culture were calculated based on the methods described below. For carbon balance, the moles of carbon for a compound are calculated by multiplying the number of carbon molecules in the molecular formula by the number of moles of the compound that were experimentally measured (e.g., 6 for glucose, 2 for acetate, 3 for lactate etc.) (Munro et al., 2009). The moles of biomass were calculated considering the empirical formula C₅H₈O₃NS_{0.05} of *T.maritima* (Munro et al., 2009). The mole of CO₂ was estimated by considering that one mole of CO₂ was produced per mole of acetate. The balance equations were determined by the ratio of carbon derived from the end-products and the carbon from substrate consumed. For electron equivalents balance, the numbers of moles of glucose and end-products were converted to electron equivalents based on their degree of reduction (glucose, 24; H₂, 2; lactate, 12; acetate, 8; butyrate, 20; biomass). The balance was calculated by dividing the number of electron equivalents from the end-products by the number of electron equivalents provided as the substrate (Oh et al., 2008; Esquivel-Elizondo et al., 2017).

2.6. ¹³C-labeling experiments and NMR analysis

The adapted strain was grown as described above using a culture medium supplemented with 5 g/L of 1,2-¹³C₂-glucose (Sigma-Aldrich, Italy). Serum bottles were incubated at 80°C for 48h with pH correction. Gas samples from the headspace were regularly analyzed by GC, and the supernatant for NMR analysis was collected by centrifugation. For the labelled patterns analysis and signals attribution ¹H and ¹³C NMR were performed on

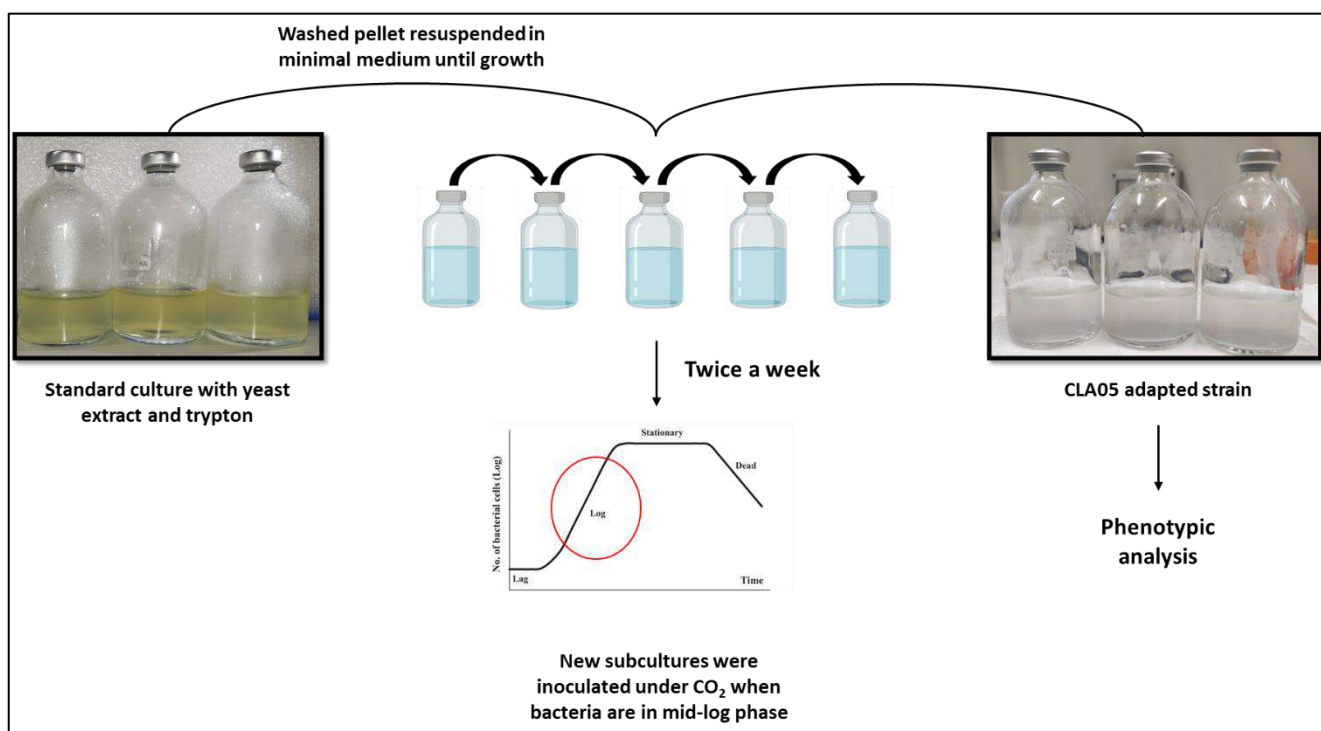
culture broth after dilution of supernatant (0.6 mL) with 0.1 mL of D₂O and transfer to an NMR tube.

3. Results and Discussion

3.1. Evolutionary adaptation of *Thermotoga neapolitana*

As shown in the **Fig. 1**, the experiments started in November 2018 and are currently ongoing, as the strain shows a phenotyping instability and evolution. The adapted strain was called CLA-05 (Capnolactic strain n.05). Periodically, the CLA-05 strain was checked to verify the fermentation rate and production yields, compared to the wild type strain. A total of 250 transfers were completed, resulting in around 205 batches of evolved bacterial populations, named as CLA-05_1 – CLA-05_205.

Fig. 1 Graphical representation of the adaptive laboratory evolution strategy adopted



in this paper on *Thermotoga neapolitana* subsp. *capnolactica*

In the first year of adaptation, the strain grew badly, and weekly transfers were needed for about 12 months to have an interesting phenotypic first response. On January 2020, the obtained strain seemed efficiently capable of metabolizing glucose producing hydrogen and lactic acid according to the yields of a classical CLF activation (**Table 1**). The same performances seem to be repeated at each monthly check until September 2020, suggesting that CLA-05 was an adapted CLF-performing strain (**Table 1**). However, from October 2020 the strain is undergoing a new phase of evolution, as its performances has significantly changed. As showed in **Table 1**, in fact, when CLA-05 was exposed to CO₂, the classical CLF phenotype was no longer observed: hydrogen yields are increased from an average of 2.3 mol H₂/mol glucose in January to 3.3 mol H₂/mol glucose in October, while lactate yields are drastically reduced, from around 0.55 mol lactate/mol glucose to 0.08 mol lactate/mol glucose. The ratio between acetate and lactate production shifted

from 0.60-0.70 to 0.10-0.20, these latter values are comparable to those observed in the wild type strain with N₂ sparge (no CLF condition). These data suggest that CLA-05 strain has again modified its metabolism, becoming CO₂-insensitive and switching to a dark fermentation model (Table 1).

Table 1 Yields of the main products of fermentation of CLA05 adapted strain under CO₂. AL, lactate; AA, acetate.

	Yields			
	H ₂	Acetate	Lactate	AL/AA
January	2.33 ± 0.27	0.79 ± 0.00	0.53 ± 0.03	0.66 ± 0.04
February	2.73 ± 0.20	0.89 ± 0.07	0.25 ± 0.04	0.33 ± 0.09
March	2.13 ± 0.62	0.60 ± 0.00	0.59 ± 0.00	0.95 ± 0.00
September	2.60 ± 0.38	0.81 ± 0.13	0.41 ± 0.20	0.71 ± 0.07
October	3.37 ± 0.13	0.89 ± 0.34	0.08 ± 0.04	0.11 ± 0.05
November	2.74 ± 0.10	0.96 ± 0.02	0.21 ± 0.04	0.22 ± 0.05

3.2. Carbon and energy balance in the adapted strain CLA-05

When the adapted strain CLA-05 performed CLF at high yields, the possibility of retracing the carbon and electron flux in this “cleaner” system was investigated. In a minimal medium without other carbon sources, in fact, the fermentation end-products obtained could come only from glucose consumption. Munro et al., 2009 described for the first time the carbon and electron balance in *Thermotoga neapolitana* in a complete medium at different growth temperature, to establish the fermentation stoichiometry of glucose (Munro et al., 2009).

The analysis of the carbon and electron content in biomass and in the broth on *Thermotoga neapolitana* CLA05 was conducted considering the mmol of glucose consumed and the mmol of carbon obtained in biomass and end-products (acetate, lactate, alanine and CO₂). The carbon and electron content in biomass was estimated empirically with the formula indicated in Materials and Methods from the absorbance values at 540nm. Organic acids concentrations were determined by ¹H NMR analysis. Alongside this classical quantification of the fermentation products, Total Organic Carbon analysis (TOC) has been performed on the fermentation broth to evaluate the carbon recovery efficiency of our methods. Interestingly, considering the standard deviations related to the high number of replicates and the instrumental measurements, the difference in C-balance with and without TOC analysis is around 20%, and the balance was almost completely closed at around 89 ± 9% with TOC analysis (Table 2). This discrepancy could be attributed to a better resolution of the CO₂ content in TOC analysis, since its percentage is the sum of dissolved CO₂ from the medium sparge, and CO₂ from fermentation, whereas our CO₂ estimation is only the result related to the acetate production.

For the electron equivalents balance, this is completely closed, with a 93% recovery rate (Table 2). This confirms that no other secondary products are obtained from glucose fermentation in this metabolic condition. The normalization of products related to the glucose consumed allows us to observe how the same amount of equivalents is dedicated to the production of both hydrogen and lactic acid (around 0.19-0.25 for hydrogen-acetate production and 0.26 for lactic acid production), sustaining the classical CLF-phenotype in which the concomitant production of hydrogen and lactic acid has been described (Table 2). These data confirm again the presence of an extra reducing power to satisfy the energy

demand under CO₂, and this could be derived from the activation of different glycolytic pathway for glucose fermentation, as Entner-Doudoroff or pentose phosphate pathway (d'Ippolito et al., 2020).

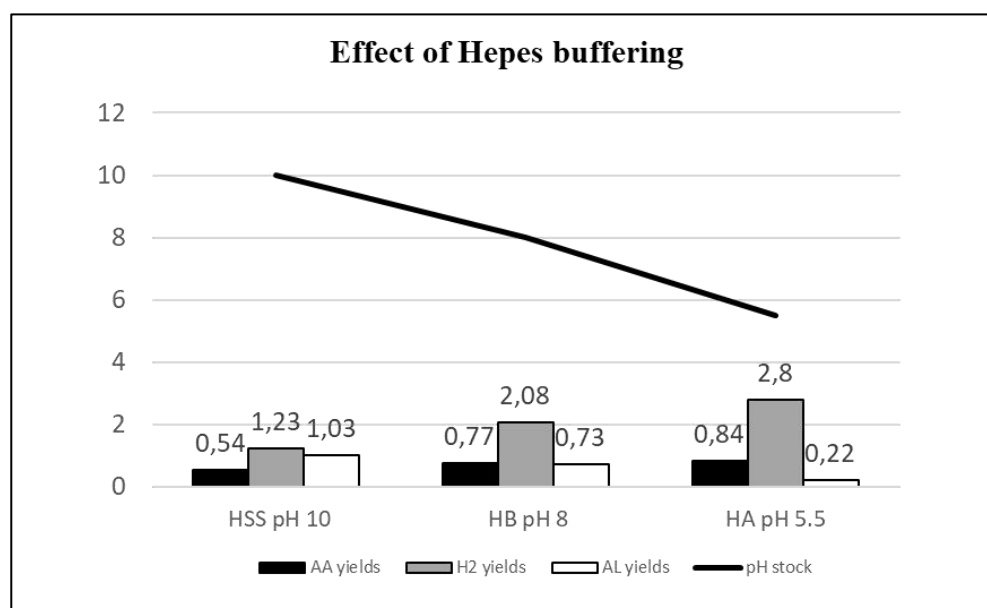
Table 2. Carbon and electron equivalents balances of *Thermotoga napolitana* CLA05 adapted strain after 48h in serum bottles.

	mM	Carbon equivalent	Electron equivalents	Normalization Electron equiv.
Reactant				
Glucose consumed	28.14 ± 0.14	168.83 ± 0.85	0.68 ± 0.003	1
Products				
H ₂	65.29 ± 2.69		0.13 ± 0.005	0.19
Acetate	20.73 ± 0.53	41.47 ± 1.06	0.17 ± 0.004	0.25
Lactate	14.72 ± 0.94	44.17 ± 2.81	0.18 ± 0.011	0.26
Alanine	1.16 ± 0.06	3.48 ± 0.17	0.01 ± 0.001	0.02
CO ₂	20.73 ± 0.53	20.73 ± 0.53		
Biomass	7.20 ± 0.47	7.20 ± 0.47	0.14 ± 0.009	0.21
Total products in broth	-	109.85 ± 4.57		
Total products and Biomass	-	117.05 ± 5.04		0.93
C-Balance %	-	69.33 ± 4.30		
TOC broth analysis	-	122.11 ± 9.32		
Total products and Biomass	-	150.04 ± 10.33		
C-Balance %	-	88.90 ± 8.61		
E-Balance %			93.44 ± 1.10	

3.3. The effect of the pH on *Thermotoga napolitana* CLA05 fermentation

When the phenotypic analysis of the adapted CLA05 strain clearly shown a drastic change in metabolism under CO₂, becoming as a "CO₂-insensitive strain", several strategies were adopted in order to push the strain again to CLF performances. One of the strategies involved the pH control of the culture medium, since it is reported to be a determining factor for the metabolism of *Thermotoga* (Pradhan et al., 2019; Lanzilli et al., 2021). According to the data obtained in Pradhan et al., 2019 in the wild type strain under CLF conditions, Hepes has been selected as buffering agent for CLA05 experiments. Different forms have been tested: Hepes sodium salt pH 10, Hepes acid pH 5 and Hepes equimolar buffer pH 8, in concentration of 100mM.

Fig. 2 Effect of different Hepes forms on the fermentation yields in *Thermotoga napolitana* CLA05, under CLF condition after 48h. HSS, Hepes sodium salt; HB, Hepes buffer, HA, Hepes acid, AA, acetate, AL, lactate.



litana CLA05, under CLF condition after 48h. HSS, Hepes sodium salt; HB, Hepes buffer, HA, Hepes acid, AA, acetate, AL, lactate.

As shown in **Fig. 2**, variations in pH values significantly impact on the fermentation parameters: when the initial pH of the buffering agent passes from 10 to 5.5, hydrogen and acetate yields increase from 1.23 mol H₂/mol glucose to 2.8 mol H₂/mol glucose and from 0.54 mol acetate/mol glucose to 0.84 mol acetate/mol glucose respectively. In contrast, pH decrease decreases lactate yields, from 1.03 mol lactate/mol glucose at pH 10, to 0.22 mol lactate/mol glucose (**Fig. 2**). When the equimolar solution of acid and sodium salt of Hepes was used, fermentation yields seem to assume intermediate values, similar to those obtained in March 2020 (see **Table 1**): 2.08 mol H₂/mol glucose, 0.77 mol acetate/mol glucose and 0.73 mol lactate/mol glucose, restoring lactate yields not completely breaking down hydrogen yields. These data indicates that in CLA05 adapted strain no significant genomic mutations occurred, as its metabolism changes continuously according to the metabolic condition in which it is found.

Changes in the fermentation yields at different pH could be attribute to the different equilibrium created by the Hepes forms in solution, which could affect the availability of CO₂ (**Fig.3**): using the Hepes Acid form (pH 5.5), the strength in proton release by the acid group is greater than the tendency to accept a proton by the basic group, and a more acidic environment has been created. In this context, the dissociation of CO₂ into carbonic acid in solution was less, thus reducing the organization process of CO₂, and the fermentation is directed towards the exclusive production of hydrogen, as in a dark fermentation system, while the effect of CO₂ is hidden. On the other hands, using Hepes sodium salt (pH 10), Na⁺ are released in solution and the Hepes form subtracts protons, and the pH of the medium is higher (around 9): in this context, the prevailing form of CO₂ is the hydrogen carbonate HCO₃⁻, which release protons, changing the pH of the medium that reaches 7.3 (**Fig.3**). The buffering action pushes to lactate production while hydrogen yields are reduced.

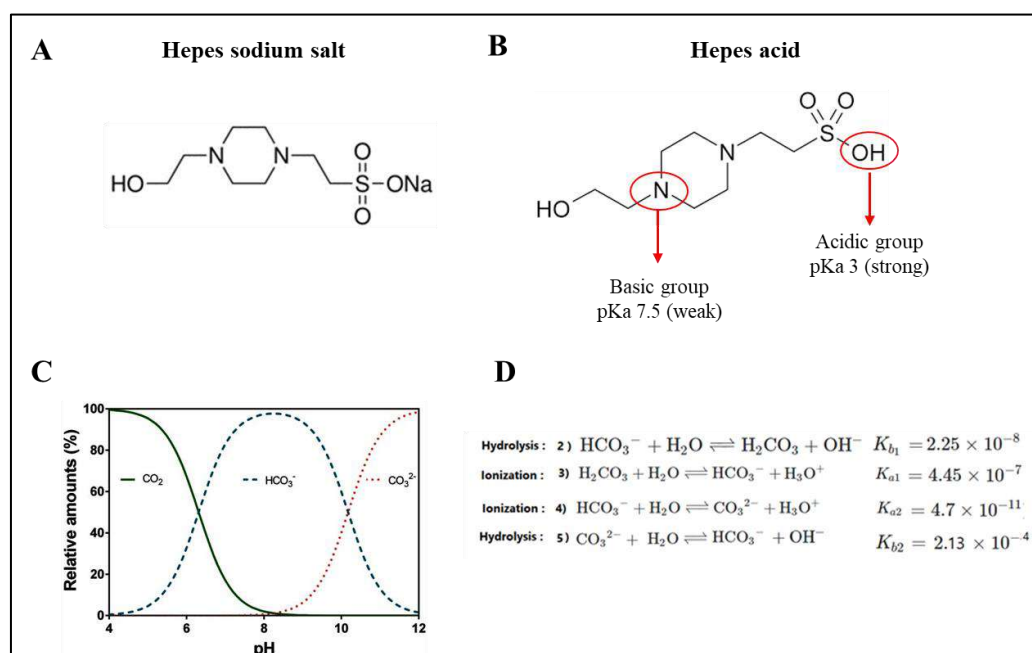


Fig. 3 Different forms of Hepes and CO₂ equilibrium in solution. A, structure of Hepes sodium salt pH 10; B, structure of Hepes acid pH 5.5; C, relative amounts of different forms of CO₂ depending on pH values; D, reactions involving the different forms of CO₂ in solution.

3.4. Analysis of the glycolytic pathways active in *Thermotoga napolitana* CLA05

Preliminary labeling experiments were conducted on CLA-05 to investigate the possible activation of another glycolytic pathway, together with the classical Embden-Meyerhof-Parnas (EMP) pathway. ¹H and ¹³C NMR analysis on the fermentation broth supplied with 1,2-¹³C₂-glucose and Hepes sodium salt pH 10 (one of the extreme condition tested) clearly demonstrated the activation of EMP, since the presence of the major EMP products, the 2,3-¹³C₂-lactate and 1,2-¹³C₂-acetate, is highlighted in 1H NMR (Fig.XXX): the 2,3-¹³C₂-lactate was detected as a “doublet of doublets”, around the unlabelled doublets of methyl group of lactate (δ=1.30ppm, 1J_{βH-αH} = 7 Hz), with splitting 1J_{βH-βC} = 128 Hz (Lloyd et al., 2004), while the presence of 1,2-¹³C₂-acetate was shown by the doublets around the singlet signal at 1.9 ppm, with J_{βH-βC} = 127 Hz, which is the signal of the coupling between the protons of the methyl group and the carboxyl function of acetate (Fig.XXX). At the same time, ¹³C NMR analysis confirm the presence of 2,3-¹³C₂-lactate and 1,2-¹³C₂-acetate as main product, since doublets at 21 ppm and 68.8 ppm with J_{αC-βC} = 37 Hz described the coupling between the methyl group and the alcoholic function of lactate (2,3-¹³C₂-lactate), and the doublets at 24 ppm and 181 ppm with J_{αC-βC} = 52 Hz are characteristic of the coupling between the methyl group and the carboxyl function of acetate (1,2-¹³C₂-acetate). Surprisingly, in ¹³C NMR spectrum is also observable another doublet around the peak at 182 ppm, diagnostic of the carboxyl group of lactate, with J_{CO-αC} = 55 Hz, that represent the 1,2-¹³C₂-lactate. This labeled product clearly come from the activation of the Entner-Doudoroff pathway (Fig.XXX).

These data confirm that a metabolic switch from EMP to ED pathway occur in *Thermotoga napolitana* CLA05 adapted strain when the metabolism is completely directed to lactate production, in contrast with the wild type strain, in which the activation of ED has

been excluded (d'Ippolito et al., 2010; Esercizio et al., manuscript in preparation). Further experiments with the other Hepes forms are necessary to understand the metabolic switch that occur in every condition tested.

4. Conclusions

Thermotoga neapolitana subsp. *capnolactica* was pushed to adapt in a minimal medium without yeast extract and tryptone as extra carbon and nitrogen source. This represent the first example of Adaptive laboratory evolution (ALE) in *T. neapolitana*, with several limitation related to the continuous metabolic changes, and therefore phenotypic changes, that do not yet allow a precise characterization of how the strain has really evolved. The analyses carried out on the current CLA05 adapted strain are, therefore, only the basis for further studies, and provide important information to how the metabolism of *Thermotoga neapolitana* varies in function of external stimuli.

Author Contributions: Conceptualization, GD; Experimental activity, NE, ML, and LC; Data analysis, NE, SL and GD; Data curation, NE, SL and GD; Writing, NE and GD Supervision, GD and AF; Funding acquisition, AF and GD. All authors have read and agreed to the published version of the manuscript.

Funding: This research was funded by BioRECO2VER_H2020NMBP-BIO-2017 project, grant number 760431.

Acknowledgments:

Conflicts of Interest: The authors declare no conflict of interest

References

1. G. d'Ippolito et al., "Hydrogen metabolism in the extreme thermophile *Thermotoga neapolitana*," *Int. J. Hydrogen Energy*, vol. 35, no. 6, pp. 2290–2295, 2010.
2. N. Esercizio et al., "Fermentation of biodegradable organic waste by the family thermotogaceae," *Resources*, vol. 10, no. 4, 2021.
3. L. Dipasquale, G. D'Ippolito, and A. Fontana, "Capnophilic lactic fermentation and hydrogen synthesis by *Thermotoga neapolitana*: An unexpected deviation from the dark fermentation model," *Int. J. Hydrogen Energy*, vol. 39, no. 10, pp. 4857–4862, 2014.
4. G. d'Ippolito, L. Dipasquale, and A. Fontana, "Recycling of Carbon Dioxide and Acetate as Lactic Acid by the Hydrogen-Producing Bacterium *Thermotoga neapolitana*," *ChemSusChem*, vol. 7, no. 9, pp. 2678–2683, 2014.
5. N. Pradhan et al., "Model development and experimental validation of capnophilic lactic fermentation and hydrogen synthesis by *Thermotoga neapolitana*," *Water Res.*, vol. 99, no. April, pp. 225–234, 2016.
6. G. Nuzzo, S. Landi, N. Esercizio, E. Manzo, A. Fontana, and G. D'Ippolito, "Capnophilic lactic fermentation from *Thermotoga neapolitana*: A resourceful pathway to obtain almost enantiopure L-lactic acid," *Fermentation*, vol. 5, no. 2, 2019.
7. M. Lanzilli et al., "Effect of cultivation parameters on fermentation and hydrogen production in the phylum thermotogae," *Int. J. Mol. Sci.*, vol. 22, no. 1, pp. 1–34, 2021.
8. E. W. J. Van Niel, M. A. W. Budde, G. De Haas, F. J. Van der Wal, P. A. M. Claassen, and A. J. M. Stams, "Distinctive properties of high hydrogen producing extreme thermophiles, *Caldicellulosiruptor saccharolyticus* and *Thermotoga elfii*," *Int. J. Hydrogen Energy*, vol. 27, no. 11–12, pp. 1391–1398, 2002.
9. D. Han and Z. Xu, "Development of a pyrE-based selective system for *Thermotoga* sp. strain RQ7," *Extremophiles*, vol. 21, no. 2, pp. 297–306, Mar. 2017.
10. T. A. D. Nguyen, J. Pyo Kim, M. Sun Kim, Y. Kwan Oh, and S. J. Sim, "Optimization of hydrogen production by hyperthermophilic eubacteria, *Thermotoga maritima* and *Thermotoga neapolitana* in batch fermentation," *Int. J. Hydrogen Energy*, vol. 33, no. 5, pp. 1483–1488, Mar. 2008.
11. B. T. Maru, A. A. M. Bielen, S. W. M. Kengen, M. Constantí, and F. Medina, "Biohydrogen Production from Glycerol using *Thermotoga* spp.," *Energy Procedia*, vol. 29, pp. 300–307, 2012.
12. H. Latif et al., "Adaptive evolution of *Thermotoga maritima* reveals plasticity of the ABC transporter network," *Appl. Environ. Microbiol.*, vol. 81, no. 16, pp. 5477–5485, 2015.

13. R. Singh, D. White, Y. Demirel, R. Kelly, K. Noll, and P. Blum, "Uncoupling fermentative synthesis of molecular hydrogen from biomass formation in *Thermotoga maritima*," *Appl. Environ. Microbiol.*, vol. 84, no. 17, pp. 998–1016, Sep. 2018.
14. J. Gautam et al., "Adapted laboratory evolution of *Thermotoga* sp. strain RQ7 under carbon starvation," *BMC Res. Notes*, vol. 15, no. 1, pp. 1–7, Mar. 2022.
15. P. Bernfeld, "Amylases, A and B Methodology," *Enzymology*, p. 1986, 1986.
16. S. A. Munro, S. H. Zinder, and L. P. Walker, "The fermentation stoichiometry of *Thermotoga neapolitana* and influence of temperature, oxygen, and pH on hydrogen production," *Biotechnol. Prog.*, vol. 25, no. 4, pp. 1035–1042, 2009.
17. Y. K. Oh et al., "Carbon and energy balances of glucose fermentation with hydrogenproducing bacterium *Citrobacter amalonaticus* Y19," *J. Microbiol. Biotechnol.*, vol. 18, no. 3, pp. 532–538, 2008.
18. S. Esquivel-Elizondo, Z. E. Ilhan, E. I. Garcia-Peña, and R. Krajmalnik-Brown, "Insights into Butyrate Production in a Controlled Fermentation System via Gene Predictions," *mSystems*, vol. 2, no. 4, Aug. 2017.
19. N. Pradhan et al., "Simultaneous synthesis of lactic acid and hydrogen from sugars via capnophilic lactic fermentation by *Thermotoga neapolitana* cf *capnolactica*," *Biomass and Bioenergy*, vol. 125, pp. 17–22, Jun. 2019.

10. Electrostimulation of hyperthermophilic *Thermotoga neapolitana* cultures

Giuliana d'Ippolito ^a, Gaetano Squadrito ^b, Matteo Tucci ^{c,d}, **Nunzia Esercizio** ^a, Angela Sardo ^a,
Marco Vastano^a, Mariamichela Lanzilli ^a, Angelo Fontana ^a and Pierangela Cristiani ^{e,*}

^a Institute of Biomolecular Chemistry (ICB), Consiglio Nazionale delle Ricerche (CNR), Via Campi Flegrei 34, 80078 Pozzuoli, Italy

^b Institute of Advanced Technologies for Energy (ITAE), Consiglio Nazionale delle Ricerche (CNR), Messina, Italy

^c Water Research Institute (IRSA), Consiglio Nazionale delle Ricerche (CNR), Monterotondo, Rome, Italy

^d e-Bio Center, Department of Environmental Science and Policy, Università degli Studi di Milano, Italy

^e Ricerca sul Sistema Energetico - RSE S.p.A., Milano, Italy

* Correspondence: pierangela.cristiani@rse-web.it (P. Cristiani)

Citation:

G. d'Ippolito, G. Squadrito, M. Tucci, **N. Esercizio**, A. Sardo, M. Vastano, M. Lanzilli, A. Fontana, P. Cristiani. Electrostimulation of hyperthermophile *Thermotoga neapolitana* cultures, *Bioresource Technology*, **2021** Vol 319, 2021,124078, ISSN 0960-8524.



Electrostimulation of hyperthermophile *Thermotoga neapolitana* cultures

G. d'Ippolito^a, G. Squadrito^b, M. Tucci^{c,d}, N. Esercizio^a, A. Sardo^a, M. Vastano^a, M. Lanzilli^a, A. Fontana^a, P. Cristiani^{e,*}

^a Institute of Biomolecular Chemistry (ICB), National Research Council (CNR), Pozzuoli, Na, Italy

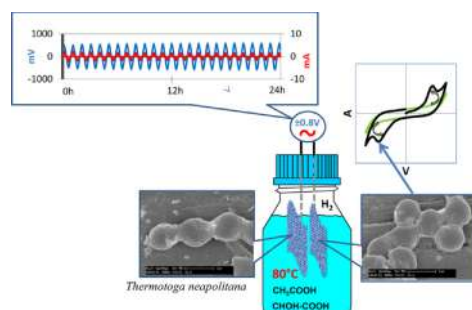
^b Institute of Advanced Technologies for Energy (ITAE), National Research Council (CNR), Messina, Italy

^c Water Research Institute (IRSA), National Research Council (CNR), Via Salaria km29, 300 00015 Monterotondo, Rome, Italy

^d e-Bio Center, Department of Environmental Science and Policy, Università degli Studi di Milano, via Celoria 2, 20133 Milan, Italy

^e Ricerca sul Sistema Energetico - RSE S.p.A., via Rubattino, 54, 20134 Milano, Italy

GRAPHICAL ABSTRACT



ARTICLE INFO

Keywords:

Bio-hydrogen
Thermotoga neapolitana
Electrochemical microbial stimulation
Hyperthermophiles
Capnophilic lactic fermentation

ABSTRACT

Hyperthermophile bioelectrochemical systems are seldom investigated although their superior control of microbial consortium and thermodynamic advantages. Hyperthermophilic *Thermotogales*, for instance, are able to produce hydrogen and lactic acid from wastes better than mesophilic bacteria. Here, the electrostimulation of *Thermotoga neapolitana* in single-chamber electrochemical bioreactors is studied.

The glucose fermentation under CO₂ pressure, as model metabolism, was tested at 80 °C.

Results show that a dynamic polarization (± 0.8 to ± 1.2 V) drives glucose fermentation and biofilm stasis on electrodes. Under this condition, production of lactic acid (33 vs 12 mM) and yields of acetate and hydrogen (with lactic/acetic acid ratio of 1.18) were higher than those achieved with static polarization or open-circuit.

Dynamic polarization is possibly exploitable to stimulate *T. neapolitana* in a hyperthermophile electrochemical system for various applications including control of power-to-gas processes or production of value-added products (hydrogen and lactic acid) from sugary wastes.

1. Introduction

The environmental impact of unsustainable growth has led researchers to increasingly address the technologies able to supply clean

energy and to minimize wastes. In this new vision, hydrogen is considered a suitable energy vector of renewable energy sources since its utilization is carbon-free and produces only water as a by-product. Moreover, hydrogen is largely used in the chemical industry like in the

* Corresponding author.

E-mail address: pierangela.cristiani@rse-web.it (P. Cristiani).

<https://doi.org/10.1016/j.biortech.2020.124078>

Received 1 July 2020; Received in revised form 30 August 2020; Accepted 31 August 2020

Available online 06 September 2020

0960-8524/ © 2020 Elsevier Ltd. All rights reserved.

production of ammonia-fertilizers, methanol and the production of polymers. Not least, the increased attention to reduce waste and the electrical power consumption induced increasing attention to the biological production of hydrogen (Nikolaïdis and Poullikkas, 2017; Stephen et al., 2017). Particularly, the emerging power-to-gas concept addresses great expectancy to innovative electromethanogenesis process, which effectively can combine conventional anaerobic digestion (AD) process to an electrochemical bio-methane production in thermophilic condition (Aryal et al., 2018). Electromethanogenesis consists in a biogenic version of the Sabatier reaction, exploiting the capability of bacteria to produce and convert hydrogen and CO₂ gases into methane, by a syntrophic metabolism between hydrogenogenic and methanogenic bacteria in bioelectrochemical systems (Geppert et al., 2016). In a Power-to-gas logic, CO₂-rich industrial discharged gases and organic sludge could be switched by (dispersed) renewable electric energy in values, thus contributing to solve emission issues storing energy vectors (Ceballos-Escalera et al., 2020).

According to operating temperature, the fermentative H₂ production can be classified in mesophilic (usually 30–45 °C), thermophilic (50–60 °C), and hyperthermophilic (over 60 °C). Thermotogales represents one of the most hyperthermophilic organotroph (> 80 °C) within the bacterial branch of the phylogenetic tree. This group includes *Thermotoga neapolitana* (DSM 4359, ATCC 49049), a rod-shaped, gram-negative, non-sporulating bacterium, isolated from the shallow marine hydrothermal vents in the Gulf of Naples, that can simultaneously release hydrogen and L-lactic acid from waste organic matter by a novel anaerobic process, named Capnophilic Lactic Fermentation (CLF), in marine water (d'Ippolito et al., 2010; d'Ippolito et al., 2014; Pradhan et al., 2019).

Hyperthermophilic microorganisms are simple to operate in single culture or coculture, as the extreme conditions of temperature reduce the risk of contamination by other strains. Furthermore, it has been reported that *T. neapolitana* can reach hydrogen yield close to the theoretical 4 molecules of H₂ per molecule of metabolized glucose (Dipasquale et al., 2014). Considering the significant industrial request of lactate, these facts make *T. neapolitana* particularly promising for biotechnological and energy recovering applications, in a circular economy vision.

On the other hand, hyperthermophilic strains have seldom been explored within electrochemical systems. A single experiment recently investigated the hydrolysis of starch by *Thermotoga maritima* (Hirano and Matsumoto, 2017). This experiment was carried out in a double chamber electrochemical system by using an electron mediator (Anthraquinone-2,6-disulfonate) to enhance the bacteria interaction with electrodes. Applied potentials of −0.6 V and −0.8 V vs. Ag/AgCl reduced the lag phase of *T. maritima*, and enhanced sugar consumption and lactic acid production.

The tendency of thermophilic bacteria to form a biofilm on solid substrates has been also rarely reported, in spite of the technical advantages for fermentation processes. Pisz and co-workers reported that *T. maritima* can attach on glass walls, nylon meshes, and polycarbonate filters in maltose-based media at 80 °C (Pysz et al., 2004). The observed biofilm exhibited increased transcription of genes involved in iron and sulphur transport, as well as in the biosynthesis of NAD and isoprenoid side chains of quinones. Other authors showed significant differences in the growth phase of *T. maritima* even in conditions of coculture with the hyperthermophilic archaea *Methanococcus jannaschii*, which syntrophic metabolism to form methane has already been demonstrated (Johnson et al., 2006). *Thermotoga neapolitana* cells have been immobilized on stable cationic hydrogel bearing amine groups (Basile et al., 2012) or sintered glass and ceramic supports (Cappelletti et al., 2012; Belkin et al., 1986) but evidence of the capability of this organism to interact with conductive materials forming biofilm has not been reported so far.

Aiming at exploring the electrostimulation of biofilm growth and hyperthermophile metabolism, here we investigated *T. neapolitana* in simple single-chamber electrochemical bioreactors. Different types of

polarization, potentiostatic and potentiodynamic, are experimented in a range around 1 V. Capnophilic glucose metabolism of *T. neapolitana* at already well-characterized conditions (Pradhan et al., 2019; Dipasquale et al., 2014) is investigated, as fermentation model. Results of biofilm tests carried out on carbon cloth (and other conductive materials which are not discussed here) are reported in Squadrito et al. (2020). Carbon cloth (CC), a woven carbon fibres fabric with a partial graphite structure, was selected for electrodes as it is largely used since long time in fuel cell technology. Its high electric conductivity, flexibility, mechanical properties and affinity to bacteria make it a good material for non-plain electrodes and application in bioelectrochemical systems (Guo et al., 2017; Wang et al., 2013; Santoro et al., 2014; Sharma et al., 2019).

2. Materials and methods

2.1. Strain and culture medium

Thermotoga neapolitana subsp. *capnolactica* (DSM 33003) derives from the DSMZ 4359T strain under saturating concentration of CO₂ (Pradhan et al., 2019). Bacterial cells were grown in a modified ATCC 1977 culture medium containing 10 ml/L of filter-sterilized vitamins and trace element solution (DSM medium 141) together with 10 g/L NaCl, 0.1 g/L KCl, 0.2 g/L MgCl₂·6H₂O, 1 g/L NH₄Cl, 0.3 g/L K₂HPO₄, 0.3 g/L KH₂PO₄, 0.1 g/L CaCl₂·2H₂O, 1 g/L cysteine-HCl, 2 g/L yeast extract, 2 g/L tryptone, 5 g/L glucose, and 0.001 g/L resazurin (d'Ippolito et al., 2010; Pradhan et al., 2016). Aliquots of the medium were splitted into 120 ml serum bottles. Excess oxygen was removed by heating batch reactors while sparging its content with a stream of O₂-free N₂ gas until the solution was colourless. Then serum bottles were sealed, capped and sterilized by autoclaving for 10 min at 110 °C. After the inoculum with 1 ml of batch culture, the serum bottles were incubated at 80 °C. All transfers and sampling of cultures were performed with sterile syringes and needles.

2.2. Reactors set-up and operation

T. neapolitana cells were cultured in a fed-batch mode, at 80 °C, in two different type of bioreactors (Fig. 1a and b) suitably equipped with electrodes, under stirring (250 rpm).

Before to start the test, cultures were sparged for 5 min with 30 ml min^{−1} of pure CO₂ gas. The pH was corrected to 7.5 (measured at room temperature) with a solution 1 N NaOH, for all experiments before the start. Tests in the large bioreactor lasted 24 h.

Experimentation was prolonged for 72 h in small bioreactors, without additional feeding. Biofilm tests described in Squadrito et al. (2020) were performed without stirring. The same Carbon Cloth (SAATI, Legnano, Italy) was used for electrostimulation tests in small bioreactors and for biofilm tests. Pt electrodes were used for the preliminary screening in the large bioreactor.

In the case of small reactors (Glass 315 ml DURAN bottles filled with 200 ml of sterilized Tn culture medium) the cap was substituted after the sterilization process with another cap equipped with two identical electrodes (working and counter) made of carbon cloth and set-up as shown in Fig. 1b and described in Squadrito et al. (2020), that was previously sterilized with acetone and dried. A carbon cloth piece of 10 × 10 cm was used for setting up each electrode. The carbon cloth piece was wrapped-around and thigh fixed to a titanium wire and then wrapped again with a plastic net so to avoid short-circuits when pressed close to the opposite electrode. Electrodes were dimensioned to geometrically occupy, when immersed almost completely in the reactor, almost 1/5 of the liquid volume of reactors.

The small reactors were operated in a two-electrode configuration and in triplicates. One of the triplicate bioreactors was also equipped with a reference electrode (Amel, Ag/AgCl 3 M), to measure the single electrode potential during the polarization. Each set of triplicated

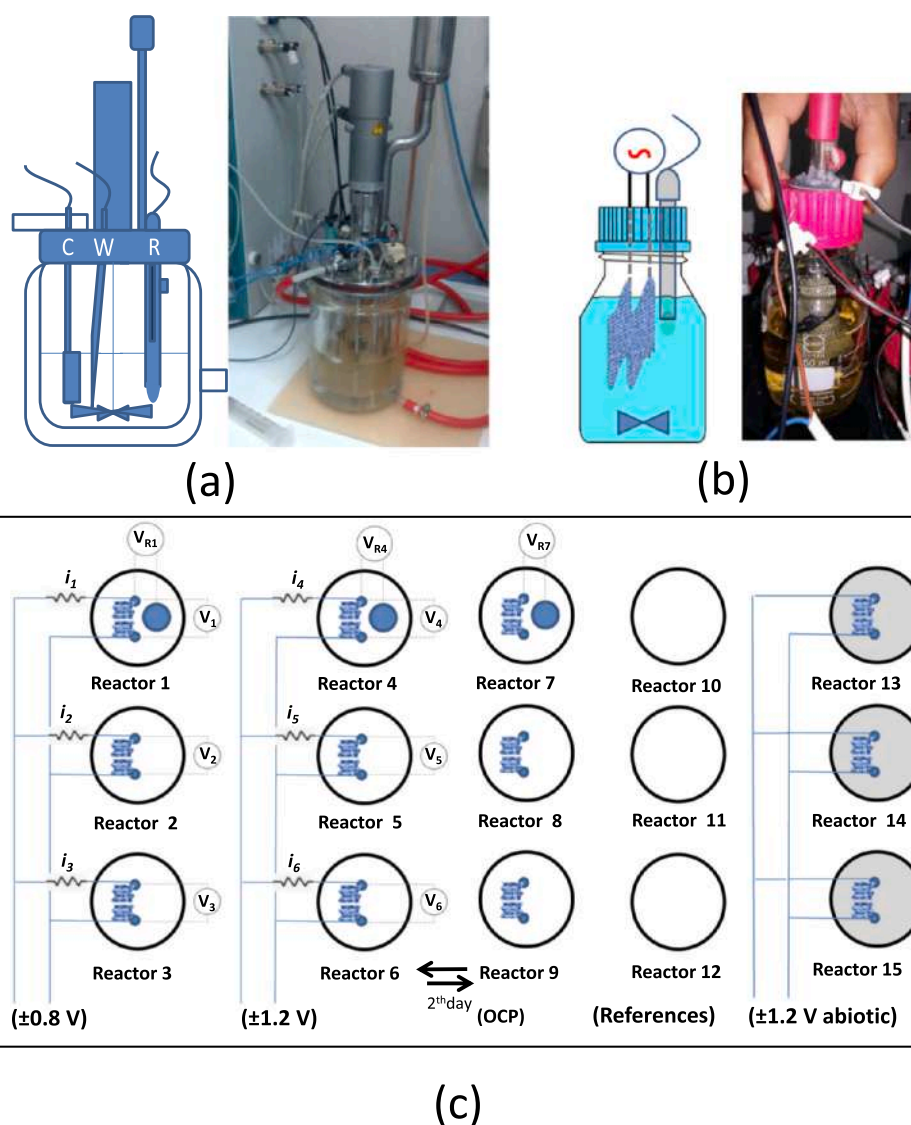


Fig. 1. Schematics and picture of: a) the large electrochemical reactor; b) the small electrochemical reactor. c) Set-up of tests with small reactors.

electrochemical reactors were polarized in parallel, using a single potentiostat (Fig. 1c).

2.3. Electrostimulation tests

All tested conditions are detailed in Table 1.

A screening of electrochemical conditions was firstly performed using the large glass bioreactor (volume of 2.8 L) previously used for similar experimentation with same *T. neapolitana* strain (d'Ippolito

et al., 2010) but without electrodes (reference condition for this experimentation). Due to the presence of a metallic stirrer posed in the middle of the reactor, small and rigid Pt electrodes were used for this first electrostimulation screening, to avoid probable short circuits during the test. The same liquid culture volume (1 L) and environmental condition (CO_2 gas pressure, pH 7.5 and 80°C as in the previous tests (d'Ippolito et al., 2010) were used. A Pt rod (length 4.5 cm, Φ 0.5 cm, active immersed area of 7.2 cm^2) working electrode, a Pt-platinized plate (2.5×3 cm, projected area of 7.5 cm^2) as counter and an

Table 1

Tested conditions.

Test type*	Polarization*	Label
- Control without electrodes (large and small bioreactors)	–	Reference
- Control without bacteria (small reactors)	± 1.2 V, W vs C, 0.5 mVs^{-1}	Abiotic
- Unpolarized electrodes (large and small bioreactors)	OCP (No polarization)	OCP
- Potentiostatic polarizations (large bioreactor, Pt electrodes)	-0.8 V, W vs Ag/AgCl & -1.2 V, W vs Ag/AgCl	Pstatic
- Potentiodynamic polarizations (large bioreactor, Pt electrodes)	$-0.8-0$ V, W vs Ag/AgCl, 0.2 mVs^{-1} & ± 0.8 V, W vs Ag/AgCl, 0.2 mVs^{-1}	Pdynamic
- Potentiodynamic polarizations (small bioreactor, CC electrodes)	± 0.8 V, W vs C, 0.5 mVs^{-1}	± 0.8 V
	± 1.2 V, W vs C, 0.5 mVs^{-1}	± 1.2 V
- Switched condition (small bioreactors)	From OCP to ± 1.2 V, W vs C	OCP/ ± 1.2 V ± 1.2 V/OCP
- Biofilm settlement (small bioreactors, CC samples)	From ± 1.2 V to OCP	CC

* CC: Carbon cloth; OCP: Open Circuit Potential; W: Working electrode; C: Counter electrode

Ag/AgCl 3 M (Amel, E = 203 mV vs NHE) reference electrode were added in the bioreactor (Fig. 1a, b), geometrically disposed at a distance of 8 cm one each other. The selected polarizations, summarized in Table 1, were: i) potentiostatic polarization (Pstatic) of -0.8 V and -1.2 V vs Ag/AgCl; ii) cyclic-potentiodynamic polarization (Pdynamic) between -0.8 and 0 V (W vs Ag/AgCl), and between -0.8 and $+0.8$ V (W vs Ag/AgCl), at the scan rate of 0.2 mVs $^{-1}$.

Subsequent tests of sole dynamic polarization were then performed in smaller reactors.

Five different conditions, and 15 small reactors, were contemporaneously tested for 72 h (as detailed in the scheme of Fig. 1c and in Table 1). The cyclic potentiodynamic polarization ± 0.8 V was applied to reactors n. 1, 2 and 3 for all tests. The slight higher polarization of ± 1.2 V was applied to reactors n. 4, 5 and 6, while electrodes of the reactors n. 7, 8 and 9 were not polarized (OCP), but one of the triplicate (Reactor n. 6 and Reactor n. 9) were inverted the second day, so that polarization resulted switched from one condition to the other (± 1.2 V/OCP reactor n. 6; OCP/ ± 1.2 V reactor n. 9) for the remaining two days. The conditions of the other reactors (n. 4, 5, 7, and 8) were unchanged during the test. Reactors n. 10, 11, and 12 (Reference reactors) were operated without electrodes for all time. Reactor n. 13, 14 and 15 were operated with electrodes polarized at ± 1.2 V as reactor n. 6, but in abiotic condition (without bacteria), for one day.

Polarization of electrodes was imposed by potentiostats IVIUM, CompactStat plus. Potentials and currents circulated in each electrochemical reactor were measured and stored using a data logger Graphtec GL840.

2.4. Cyclic voltammetry

Four cycles of Cycling Voltammetry (CV) at a scan rate of 50 mVs $^{-1}$, in the range of ± 1.2 V, in a two (working vs counter) and three (working vs Reference) electrodes configuration, depending on the reactor, were performed at the beginning (0–1 h), after 24 h, and after 48 h of testing. Electrostimulation was temporarily interrupted in all the replicates to perform CVs.

2.5. Chemical analyses

The analysis of generated H_2 in the bioreactors was performed sampling the headspace of the bioreactors by a sterile gas-tight syringe and equilibrating the samples at room temperature before the analysis.

Gas (H_2) analysis was performed by gas-chromatography using a gas-chromatographer (Focus GC, Thermo Scientific) equipped with a thermo-conductivity detector (TCD) and fitted with a 3 m molecular sieve column (Hayesep Q). Nitrogen was used as gas carrier. Acetic acid (AA) and lactic acid (LA).

Glucose concentration was determined by the dinitrosalicylic acid method calibrated on a standard solution of 1 g/L glucose (Bernfeld, 1995). Organic acids were measured by ERETIC 1H NMR as described by Nuzzo et al. (2019). All experiments were performed on a Bruker DRX 600 spectrometer equipped with an inverse TCI CryoProbe. Peak integration, ERETIC measurements, and spectrum calibration were obtained by the specific subroutines of Bruker Top-Spin 3.1 program. Spectra were acquired with the following parameters: flip angle = 90° , recycle delay = 20 s, SW = 3000 Hz, SI = 16 K, NS = 16, RG = 1. An exponential multiplication (EM) function was applied to the FID for line broadening of 1 Hz. No baseline correction was used. Cell growth was determined as Optical Density (O.D.) at 540 nm wavelength with a spectrophotometer (Perkin Elmer Lambda 950).

3. Results and discussion

Several micrographs of pristine carbon cloth and the consistent biofilm grew on carbon fibres after different time of exposition to the *T.*

neapolitana culture during the biofilm tests are reported in Squadrito et al. (2020).

Images of CC samples simply dried and covered by gold underline the relevance of biofilm that covers the material fibres (Squadrito et al., 2020). Samples treated with 2% glutaraldehyde evidence the presence of coccoid and rod-shaped bacterial cells and a filamentous, structured, bacterial networks under a thick biofilm. SEM analysis globally demonstrated an evident tendency of *T. neapolitana* to form biofilm on carbon cloth. Electrochemical, biological, and chemical data underlined significant differences in the bacterial behaviour among different tests, particularly for the cases of dynamic polarization. The OCP condition also significantly differed from the reference without electrodes, especially the first day of test in small bioreactors, as the fermentation only started in reference tests.

3.1. Electrostimulation tests

The redox potential of the culture media (open circuit potential of Pt electrodes vs Ag/AgCl) was measured during preliminary tests carried out in the large bioreactor. It stabilized in a few hours at about -0.6 V vs Ag/AgCl due to the strict anaerobic condition of the culture. In a first test, a potentiostatic polarization (Pstatic) of -0.8 V vs Ag/AgCl was imposed between the Pt Working (W) electrode and the Reference electrode, corresponding to a difference of about 0.4 V between Working and Counter (C) electrode. The low redox potential of the medium justifies the almost negligible current that was detected in the bioreactor (Fig. 2a). More current, although still low, circulated between the electrodes when the reactor was polarized at -1.2 V (W vs. Ag/AgCl, about 1.2 V between the electrodes) as cathodic values were about -6 mA at the beginning of the test and gently decreased to -2 mA (Fig. 2b). Cyclic potentiodynamic polarization (Pdynamic) was hence tested in the large bioreactor, which generated currents of the same order of magnitude as in previous Pstatic tests, although differently decreasing. The current trends of Pdynamic tests cycling -0.8 to 0 V and ± 0.8 V (W vs Ag/AgCl) are reported in Fig. 2c and d, where the first and last polarization cycle of each test (lasting 1.2 and 2.4 h respectively) are shown.

To enhance the circulating current and the interaction of bacteria with the electrode surface, further polarization tests were performed using smaller bioreactors and larger electrodes of carbon cloth, having a geometric surface of ~ 100 cm 2 . The catalytic properties of the two materials (Pt and CC) substantially differ. Nevertheless, the active surface of new electrodes was orders of magnitudes increased due to the microfiber-texture of carbon cloth.

Only cyclic potentiodynamic polarizations were tested, as negligible differences in chemical data vs the reference tests were observed for potentiostatic polarizations. Reference electrodes were added only in one of the three replicated bioreactors to limit the risk that an excessive leaking of gas (CO_2 and hydrogen) could affect chemical data. Potential trends of Working (W) and Counter (C) electrodes measured vs the Ag/AgCl in those differently polarized bioreactors (n. 1, 4 and 7) are shown in Fig. 3. The OCP potential measured in the large bioreactor (varying among tests) reached values lower than the OCP measured in the small bioreactors. Since OCP of Pt and carbon cloth are similarly and passively affected by traces of oxygen (as documented in microbial fuel cells experimentations, i.e. Cristiani et al., 2013; Roustazadeh Sheikhyouse et al., 2017), a poor sealing of bioreactor equipped with a reference electrode is likely to occur.

Although the absolute values of the circulated current were almost similar in the different (large and small) bioreactors, the OCP potential of Pt measured in the large bioreactor (varying among tests) reached lower values than the OCP of the carbon cloth measured vs Ag/AgCl in the small bioreactors. This result confirms a probable poorer sealing of these type of bioreactor equipped with reference electrode, as well the possibility of entrapping oxygen traces in the carbon cloth. Hence, it can be assumed that absolute potentials were not identically

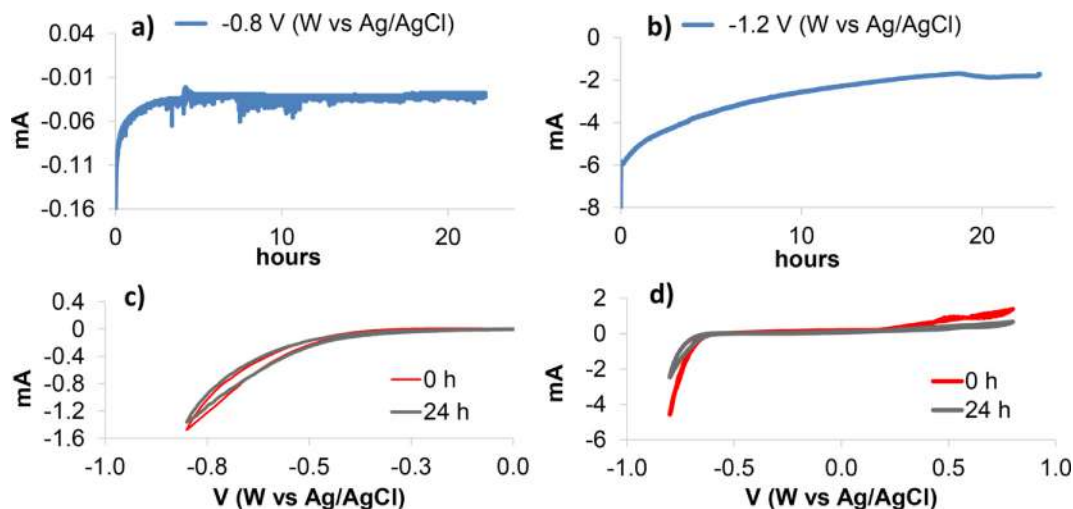


Fig. 2. Current trends of: a) Pstatic test at -0.8 V (W vs Ag/AgCl); b) Pstatic test at -1.2 V (W vs Ag/AgCl). First and last cycle of: c) Pdynamic test at $-0.8 - 0$ V (W vs Ag/AgCl) and d) Pdynamic test at ± 0.8 V (W vs Ag/AgCl), each cycle lasting 1.2 and 2.4 h respectively.

reproduced in the replicated small bioreactors without reference electrode, nevertheless, the actual applied voltage between the electrodes and current trends were almost similar for each triplicate (the first day at least, Fig. 4), oscillating in a different range, depending on the imposed polarization (± 0.8 V or ± 1.2 V). Fig. 3 shows that working electrodes moved around the OCP, while Counter electrodes had more positive values than the OCP, especially for ± 1.2 V polarization. At the beginning of the second day, the twisting of one ± 1.2 V replicate (reactor 6) with one from OCP condition (reactor 9) affected the current distribution between the other two replicates (Reactors 4 and 5 in Fig. 4) polarized with the same potentiostat in parallel mode. Different electric properties of the electrode kept the first day in OCP, developed as consequence of the bacteria settlement, may have induced the unbalancing in current distribution between those triplicates. Polarization were continued for one day more after twisting, for all small bioreactors, although missing replicates. Minor disturbs in the electrical oscillating trends were due to a temporary interruption of the polarization to perform specific cyclic voltammetry at high speed (50 mVs^{-1}) between the electrodes. The effect of these perturbations

was considered negligible in comparison to the regular oscillating polarization imposed between electrodes and was neglected.

Typical trends of the Cyclic Voltammetry (CV) performed at the beginning, after almost 24 h and after 48 h are shown in Fig. 5. The graphics clearly outlook a change in the catalytic properties of electrodes, depending on the bacteria presence and on the polarization mode. Indeed, abiotic electrodes operated in OCP show an increased capacitive current in time, more pronounced after 24 h in the abiotic media than at the beginning (Fig. 5a). On the contrary, electrodes kept in OCP condition, but subjected to the bacteria colonization, show a significant decrease of capacitive current during the 24 and 48 h of testing (Fig. 5b). Electrodes of ± 0.8 V tests less decreased the capacitive current and developed two pronounced and symmetrical peaks in the CV curve, which tend to gradually disappear in following cycles of the CV (data not reported for simplicity). The most evident peak of each triplicate cell is reported in Fig. 5c. An additional CV performed in the cell equipped with the reference electrode reveals that peaks, not present in the cathodic branch of the curve, are due to enhanced oxidation processes, at potential of about -410 mV and about -290 mV vs Ag/

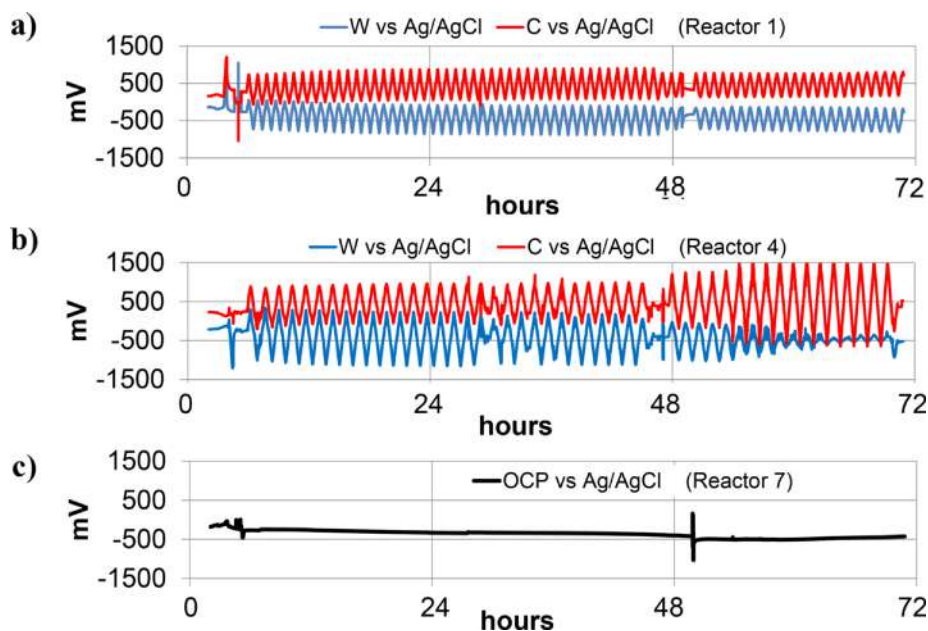


Fig. 3. Potential trends measured vs Ag/AgCl in: a) reactor 1 (± 0.8 V test); b) reactor 4 (± 1.2 V test); reactor 7 (OCP test).

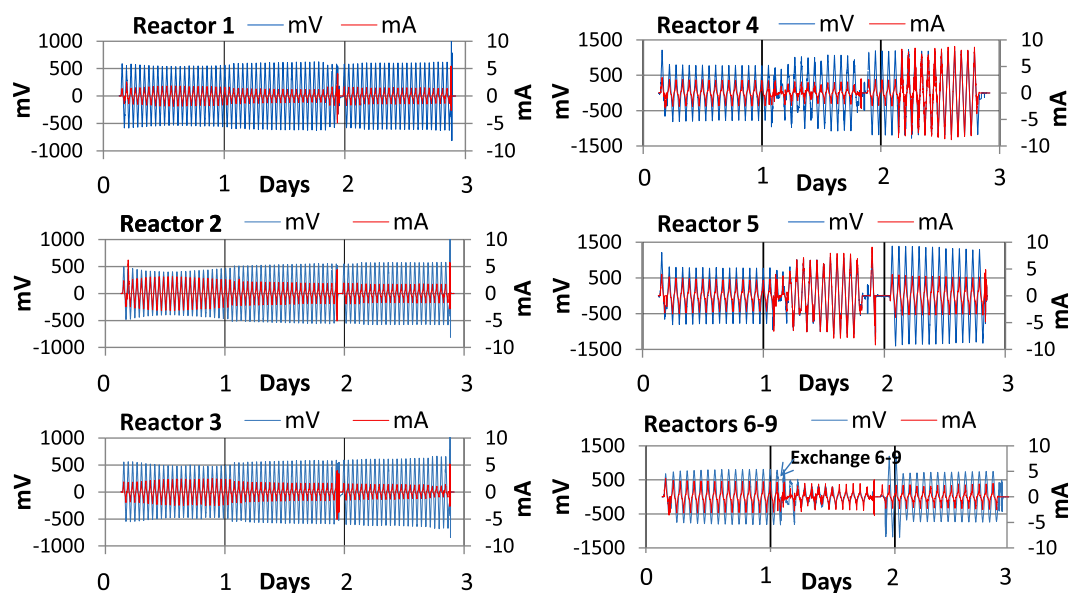


Fig. 4. CV curves (W vs C) of differently polarized electrodes at 0 h, 1 h, 24 h, and 48 h: a) Abiotic; b) OCP; c) ± 0.8 V; d) ± 1.2 V. CV curve of W vs Ag/AgCl for ± 0.8 V at 48 h is also reported in c).

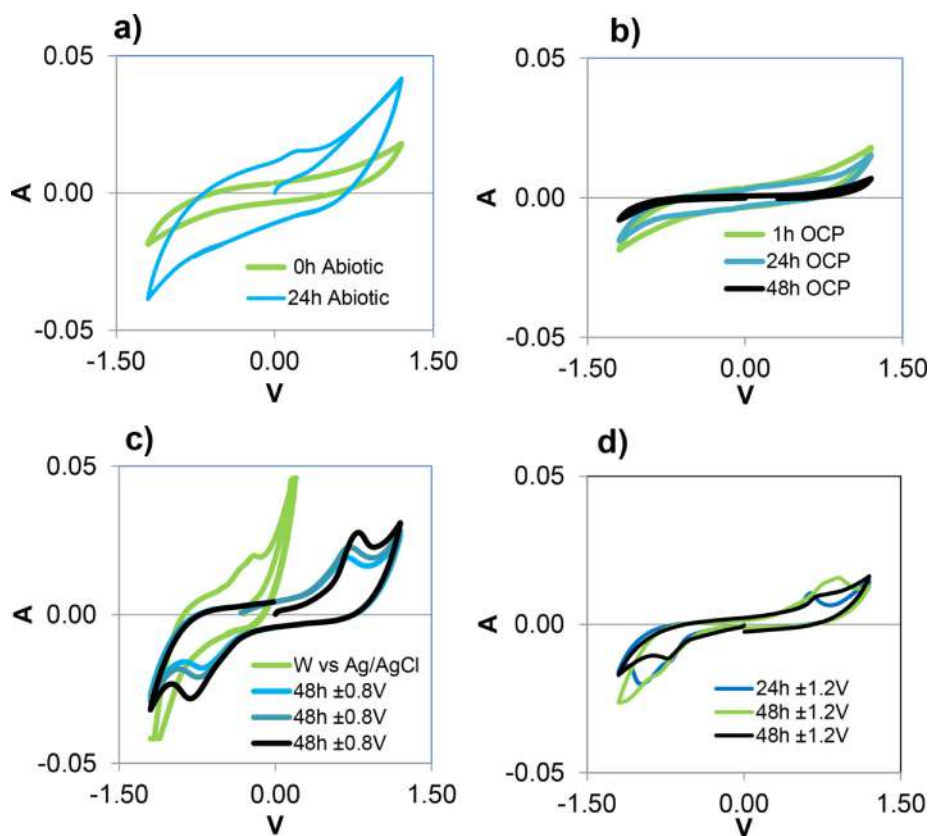


Fig. 5. Trends of potentials and currents of each polarized cell: ± 0.8 V in Cell 1, Cell 2, and Cell 3; ± 1.2 V in Cell 4, Cell 5, and Cell 6.

AgCl of the anodic branch.

Electrodes of ± 1.2 V polarized bioreactors show CV curves with an intermediate behaviour (Fig. 5d). After 24 h, similar peaks as for ± 0.8 V cells appear in this case, but with lower currents, decreasing in time. This behaviour can be correlated to increased current that circulated in those cells the second day of testing (Fig. 4). The switched cells also behave intermediate (Squadrito et al., 2020), evolving current trends in agreement with the new polarization condition.

3.2. Chemical analyses

Glucose consumption and fermentation products, namely hydrogen, acetic and lactic acid, were analysed every 24 h. Data are expressed as production (mM) and yield (moles of product/moles of consumed sugar). Results from Pstatic and Pdynamic tests performed in the large bioreactor, compared to a single test in OCP and reference tests are reported in Fig. 6a. Averages and error bars of grouped Pstatic tests (at

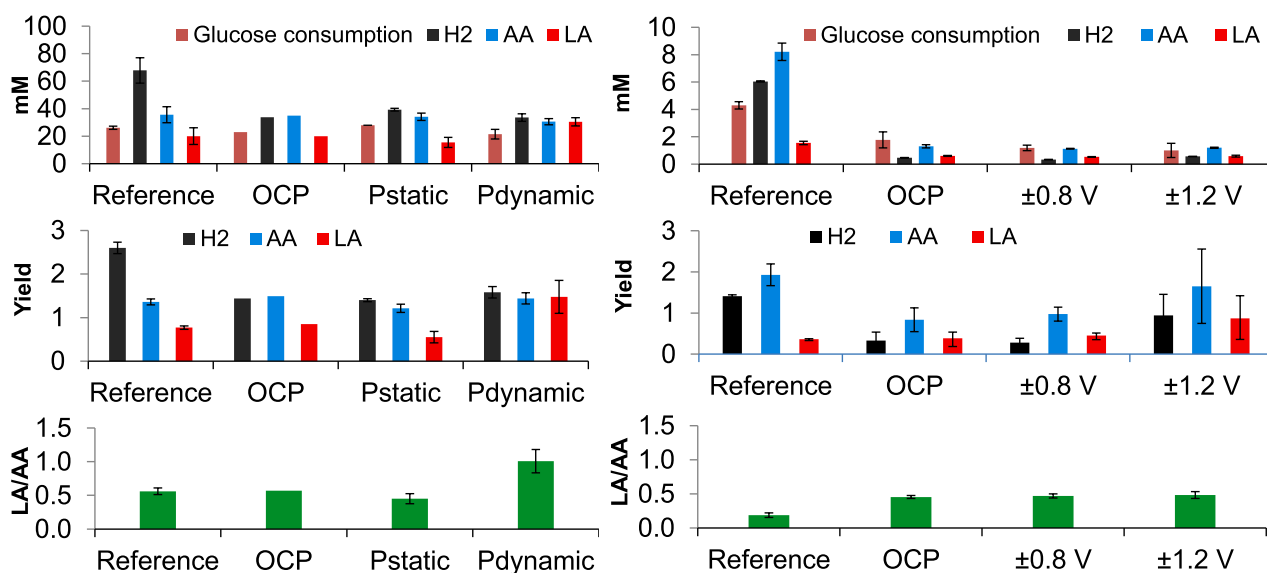


Fig. 6. Chemical analyses performed after 24 h: a) in large bioreactors and b) in small bioreactors. Averages of replicates and error bars are reported.

–0.8 V and at –1.2 V vs Ag/AgCl) and Pdynamic tests (from –0.8 V –0 V and of ± 0.8 V vs Ag/AgCl) are reported.

The glucose consumption marginally increased for Pstatic tests and marginally decreased for Pdynamic tests in comparison with reference and OCP. Hydrogen production was generally low with respect to reference tests (d'Ippolito et al., 2010). Indeed, the average of 67 mM of hydrogen from reference tests was about the double than in the other experiments. This result, however, might be affected by possible gas leaking due to inefficient sealing (under pressure) of the bioreactor cap hosting electrical collectors and the reference electrode. Acetic acid did not significantly varied. On the contrary, lactic acid of Pdynamic tests doubled in comparison to the average from other tests, reaching a value of 33 mM in one case, while the minimum was 12 mM in OCP and in one case of Pstatic tests. The lactic acid/acetic acids ratio was the highest for Pdynamic tests, reaching 1.18 vs the reference, which typical value of such test is 0.41.

Only a little decrease of the O.D (0.8 for Pdynamic tests vs 1.1 for reference) was observed (Squadrito et al., 2020) and equally vital microorganisms randomly dispersed in the media, for all test conditions.

Chemical results from tests carried out for 24 h in small bioreactors are reported in Fig. 6b. Switched condition (reactors n. 6 and n. 9) and ± 1.2 V condition after 72 h were not replicated. Integrated fermentation data calculated after 72 h of test, for each condition, are reported in the Table 2 (Glucose consumption and H₂, acetic and lactic acid production). Relative yields are reported in Table 3.

Relevant differences in the glucose metabolism between different polarized small bioreactors is noticed, although the first day the fermentation started only in reference tests (Fig. 6b). With some exceptions, fermentation started during the third day in polarized bioreactors (Table 2). Accordingly, optical density, glucose consumption and

Table 2

Cumulative glucose consumption and fermentation products for three days tests in small bioreactors.

	G* (mM)	H ₂ (mM)	AA* (mM)	LA* (mM)
Reference	18,88 \pm 0,49	13,1 \pm 0,55	18,50 \pm 0,86	4,14 \pm 0,11
OCP	13,76 \pm 0,35	18,1 \pm 1,02	11,57 \pm 1,55	3,43 \pm 0,10
± 0.8 V	3,87 \pm 1,11	8,01 \pm 1,52	8,32 \pm 1,82	1,95 \pm 0,68
± 1.2 V	14,71	11,58	12,97	3,77
OCP/ ± 1.2 V	13,96	10,86	13,55	4,28
± 1.2 V/OCP	20,17	25,35	16,04	5,13

* G: glucose consumption; AA: Acetic Acid; LA: Lactic Acid

Table 3

Cumulative yields of cumulative fermentation products for three days tests in small bioreactors.

	LA/AA ^a	AA ^a yield	LA ^a yield	H ₂ yield
Reference	0,22 \pm 0,04	0,98 \pm 0,83	0,22 \pm 0,11	1,10 \pm 0,04
OCP	0,29 \pm 0,11	0,84 \pm 0,47	0,24 \pm 0,07	1,15 \pm 0,33
± 0.8 V	0,23 \pm 0,13	1,07 \pm 0,12	0,25 \pm 0,25	1,07 \pm 0,64
± 1.2 V	0,29	0,88	0,26	0,79
± 1.2 V_OCP	0,32	0,80	0,25	1,26
OCP_ ± 1.2 V	0,32	0,97	0,31	0,78

^a AA: Acetic Acid; LA: Lactic Acid

concentration of metabolites were negligible at the end of the first two days for all the bioreactors with electrodes, independently of polarization. In the case of ± 0.8 V, the glucose consumption was still very low at the end of the third day (72 h).

The highest production of hydrogen (15.5 mM, with a low yield of 0.89) was achieved when the polarization was switched from OCP to ± 1.2 V condition. Continuing the test (second day after switching), this cell had a very low consumption of glucose (1.19 mM) and released 9.91 mM hydrogen, with 14.72 mM acetic acid and 4.42 mM lactic acid. High acetic acid (12.5 mM) and lactic acid (3.94 mM) were also produced in ± 1.2 V polarized bioreactors, although this condition had high variability between replicates and different glucose consumption during the three days of test. Replicates of ± 1.2 V condition, which did not still consumed much glucose during the third day, increased product yields and ratio of lactic/acetic acid. Fermentation also increased in the switched cells from ± 1.2 V to OCP condition, that showed a glucose consumption (13.88 mM) as large as the reference at the second day, with a little more metabolites production the third day (second day after switch: 9.2 mM hydrogen, 11.6 mM acetic acid and 3.45 mM of lactic acid, with a fermentation yield (0.66) more lower than the day before).

The high variability of the chemical data under similar polarization conditions suggests that noticed differences mostly depend on the start of the fermentation process.

3.3. Fermentation inhibition

After being inoculated, the culture media of small bioreactors equipped with electrodes remained more transparent than references, changing colour in some cases, and showing a negligible O.D.

(Squadrito et al., 2020). Most probably, oxygen trace might penetrate into the bioreactor in absence of fermentation, changing the culture media colour. It must be noted that O.D. significantly and similarly varied during all tests in large bioreactors, as polarization performed with little Pt electrodes and a high volume media probably did not affected the whole microbial pool.

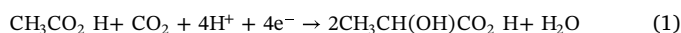
Comparing the results from reference tests in large and small bioreactors (Fig. 6a, b), it can be noticed that the glucose fermentation was faster in the large bioreactor, where glucose was almost completely consumed in one day. Glucose was slowly metabolized in polarized small reactors. Indeed, a partially and generally low glucose consumption occurred only in the second day. The different ratio between volume media and head space (0.36 and 0.57, in the large and small bioreactors respectively), which not linearly influenced gas partial pressure in the bioreactor, could justify this behaviour to some extent. A possible oxygen traces persisting at the beginning (increasing redox potential) also might have inhibited the bacteria metabolism in the small bioreactors.

Despite the above underlined concerns about fermentation rate and start, the comparison of results from polarization tests vs the respective references leads to some relevant considerations. Potentiostatic polarizations carried out in the large bioreactor did not significantly affect the glucose metabolism, as chemical data were very similar to references. Differently, potentiodynamic polarizations carried out in the same large bioreactor caused a significant increase of lactic acid production, especially for the highest polarization. This result is further confirmed by tests carried out in small bioreactors, where also acetic acid production was significantly increased, especially in coincidence with start of the fermentation process. Product yields were generally affected even if more experiments and higher product concentrations are necessary to determine a clear and univocal tendency. Most evidently, the very low glucose consumption and low hydrogen production during the first day of culture in small bioreactors suggest that bacteria preferred to attach to the carbon cloth, in a condition of stasis, than to ferment glucose. It seems reasonable to deduce that bacteria activated the glucose fermentation after a lag phase on the electrode, which can vary significantly depending on polarization. A more persisting lag phase affected bacteria culture under ± 0.8 V polarization, as glucose consumption and fermentation products were actually negligible for 48 h. The peaks in the CV curves of Fig. 5 suggest that bacteria approached electrode instead glucose for their energetic metabolism, even though it cannot be excluded that the polarization (although light) could have induced morphological changes of bacterial cells hampering glucose uptake. Nutrients can income in the bacteria cells only crossing the complex and protective cell wall, which is composed of three different layers in the case of gram negative bacteria such as *Thermotogales*. Limited permeability to small solutes, such as glucose, is available through the outer membrane by way of channels, constituted of a special class of substrate-nonspecific or substrate-specific proteins (Ames, 1986). This way is of particular relevance in the case of hyperthermophile microorganisms, where the presence of a higher composition of ionic components allow the activities of the enzymes at high temperature such as 80 °C (Unsworth et al., 2007). It might be, therefore, speculated that these channels could be modified by the polarization becoming impermeable to glucose.

High polarization (> 1 V between electrodes, Fig. 3) did not inhibit the stationary phase and biofilm growth, but induced a relevant bacteria stress both in large and small bioreactors, that is underlined by the increased production of lactic acid. The hydrogen and acetic acid production, as well as the lactic acid production, did not directly correlate to the glucose consumption in some of these cases. In the switched cell from OCP to ± 1.2 V, the high hydrogen production were associated with unexpectedly low yields of acetic and lactic metabolites in coincidence with a drastic increase of the optical density. An exceptional production of hydrogen and acetated was noticed (the third day) in this case. This result, although not replicated, suggests that the unexpected

applied polarization could have caused a shock in the microbial community settled under unpolarized condition, stimulating hydrogen acetate and lactate synthesis beneath biofilm. Fermentation products were, probably, slowly released from biofilm into solution the day after. Acetic and lactic acids were not produced in the other reversed switched bioreactor (from ± 1.2 V to OCP) also, but this result was associated with a negligible glucose consumption and hydrogen production, as one could expect by the induction of a bacterial stasis with low metabolism. Indeed, when the metabolism started in this bioreactor (during the third day), yields did not differ significantly from references.

For high polarization, it cannot be excluded that alternative assimilatory pathway are activated in bacteria attached to the electrode. In fact, *T. neapolitana* can actuate an interesting process under capnophilic condition such as the reaction (1), which requires carbon dioxide and a still unknown electron donor. Such metabolism allows for the conversion of carbon dioxide into L-lactic without biomass deconstruction (d'Ippolito et al., 2014). These metabolic changes, possibly induced by bacterial colonization of electrodes, deserve systematic and detailed future investigation to be confirmed.



3.4. Effect of dynamic polarization

It is worthy to underline that the chemical data from potentiostatic polarization tests and references tests without electrodes carried out in the large electrochemical bioreactor did not differ (Fig. 6a). This result slightly contrasts with the observations of other authors (Hirano and Matsumoto, 2017) that detected a significant increase (20%) of lactate production from the related species of *T. maritime* with the same potentiostatic polarization of -0.8 V vs Ag/AgCl. The cathodic chamber of the electrochemical bioreactor was enhanced, in that case, with a known electron mediator (Anthraquinone-2,6-disulfonate) already used for methane fermentation stabilization (Sasaki et al., 2010). The absence of mediator, a limited current, and limited electrodes surface (small Pt electrodes of few cm² in a culture media volume of 1 L) could have inhibited the effect of the potentiostatic polarization in the present work. Nevertheless, cyclic potentiodynamic polarization performed with the same large bioreactor and similarly low current, but dynamic (Fig. 2), induced a significant effect on the bacteria metabolism (Fig. 6a). Dynamic polarizations carried out in smaller bioreactors with high surface electrodes further revealed the major impact of a variable than a static electrostimulation of the *T. neapolitana* fermentation process (Fig. 6b). Furthermore, it is assumed that the stirring condition of the media allowed a large number of bacteria to approach the electrodes being affected by the polarization in both small and large bioreactors.

Due to the relatively low values of circulating current, it is supposed that electrochemically produced species such as Reactive Oxygen Species (ROS) at the anode and hydrogen at the cathode were effectively controlled varying continuously the applied potential. ROS, therefore, could have affected the electrode-solution interfaces but not the liquid media, despite the co-presence of anodic and cathodic electrodes in the same bulk. Furthermore, the hydrogen production on the polarized electrodes, measured at the beginning of the tests (before to introduce bacteria into the solution) in the large bioreactor and in the small bioreactors operated for 1 day without bacteria was negligible.

Based on these considerations, it can be inferred that the dynamic polarization conditions preserved the electrode surfaces active and attractive for bacteria more than a static polarization of the same entity.

3.5. Bacterial and biofilm morphology

Differences in biofilm morphology on carbon cloth were noticed between differently polarized electrodes. Coccoid form, instead of rod-

like shape, characterized almost all the visible bacteria in most of the carbon cloth samples (Squadrito et al., 2020). More uniform biofilm grew on the samples operated at ± 0.8 V, while a more fragmented and corpuscular biofilm was evident on the sample operated at ± 1.2 V. Evidence of bacteria detachment is underlined in the micrograph of the switched electrode from OCP to ± 1.2 V condition. Coccoid forms were not detected on the switched condition from ± 1.2 V to OCP, where rare and depressed rod cells are instead visible. It may take into account that the detected difference in the biofilm morphologies could be due, for some extent, to the sample preparation. Nevertheless, the results globally suggest that bacteria tend to directly interact with polarized electrode surfaces, preferentially in a coccoid form.

From literature, *T. neapolitana* cells are rod-shaped, occurring singly and in pairs, although they can exhibit different morphological characteristics in different growth media (Belkin et al. 1986). Usually, they are about 1.5–2 μm long and 0.5–0.6 μm in width, insofar as long shaped structures up to 100 μm have been observed. It was also reported that in the case of the related *T. maritima* cells become coccoid in the stationary phase. A significant growth phase-dependent differences were noted in the transcriptome of this bacterium in co-culture with the hydrogenotrophic archaeon *Methanococcus jannaschii*, with concomitant formation of exopolysaccharide (EPS)-based cell aggregates for the interspecies H_2 transfer (Johnson et al., 2006). Therefore, the same mechanism could have induced the structural modification of biofilm on slightly positively polarized electrodes noticed in the present study. Carbon cloth electrodes, instead of methanogenic archaea, could be the final electron sink in this case.

3.6. Electroactive enzymes

The peaks in the CV of Fig. 5c, eventually, suggest a probable enzymatic involvement in the electrostimulation of the oxidation process at the anode, similar to the case of acetate oxidation on polarized anodes mediated by cytochromes from *Geobacter* sp. (Jian et al., 2014; Katuri et al., 2012; Virdis et al., 2014). In *T. neapolitana*, peculiar [FeFe]-hydrogenases (Vargas et al., 1998; Eriksen et al., 2008) could promote (directly or hydrogen mediate) exchange of electrons with polarized anodes. L(+)-lactate dehydrogenases (LDH) could be also involved, considering the high production of lactic acid achieved as reaction to the excess of anodic polarization. LDH is a well-known enzyme of the *T. neapolitana* membrane that catalyses the conversion of pyruvate to lactate with the concomitant oxidation of NADH. This hyperthermophilic enzyme, already used in electrochemical sensor of lactate (Karkovska et al., 2015), is characterized by an increased number of intra-subunit ion pairs and a lower ratio of hydrophobic to charged surface area (Auerbach et al., 1998). Therefore, the modulation of the electrode charge could affect LDH performance.

Other enzymes can also act in case of an excessive anodic polarization like in a defensive strategy against ROS. Indeed, despite their strict anaerobic nature, *T. neapolitana* has been shown to survive in partially oxygenated hot sediments and fluids in hydrothermal vent ecosystems (van Ooteghem et al., 2004; le Fourn et al., 2008). The related specie *T. maritima* developed biochemical mechanisms to deal with temporary exposures to oxygen, reducing the glucose metabolism (Lakhal et al., 2010). Under oxidative conditions, an oxidoreductase flavoprotein homologous to the rubredoxin-oxygen reductase of *Desulfovibrio* species (Chen et al., 1993) was observed overproduced, concomitantly with enzymes iron-sulfur-cluster synthesis/repair, and the cysteine biosynthesis pathway. This mechanism can also be used to encode proteins involved in the biosynthesis of polysaccharides participating to biofilm formation (Lakhal et al., 2010). The same strategy of trapping the cells in the polysaccharide-matrix biofilm in reaction to the oxidative stress could be, therefore, thought used by *T. neapolitana* to protect themselves from an excessive imposed positive potential.

These currently speculative considerations globally deserve future studies to be elucidated. Nevertheless, they encourage the study of *T.*

neapolitana in hyperthermophile bio-electrochemical systems. New insight on the thermophilic metabolism of bacteria will surely help to develop improved power-to-gas biotechnologies for methane and bio-hydrogen production, and to drive carbon conversion and electron flux in value-added products, such as lactic acid.

4. Conclusion

The glucose fermentation of *T. neapolitana* as a model in hyperthermophile single-chamber bioelectrochemical system has been studied for the first time. Bacteria are able to form electroactive biofilm on carbon electrodes at 80 °C, reacting to a dynamic, rather than static, applied electrostimulation.

A cyclic potentiodynamic polarization of ± 0.8 V sustains stationary bacterial attachment and the growth of an electroactive biofilm. Higher dynamic voltage (± 1.2 V) induces bacteria detachment from electrodes and cause overproduction of lactic acid and hydrogen. Driving the bacteria metabolism in hyperthermophilic bioelectrochemical systems, innovative power-to-gas technologies and the recovering of value-added products from sugar rich wastes could be thus promoted.

CRediT authorship contribution statement

G. d'Ippolito: Methodology, Formal analysis, Visualization, Writing - original draft. **G. Squadrito:** Investigation, Writing - review & editing. **M. Tucci:** Investigation. **N. Esercizio:** Investigation. **A. Sardo:** Investigation. **M. Vastano:** Investigation. **M. Lanzilli:** Investigation. **A. Fontana:** Validation, Writing - original draft, Supervision. **P. Cristiani:** Conceptualization, Writing - review & editing, Supervision.

Declaration of Competing Interest

The authors declare that they have no known competing financial interests or personal relationships that could have appeared to influence the work reported in this paper.

Acknowledgments

This work was financed by the Italian Ministry of University and Research (MIUR) and by the Research Fund for the Italian Electrical System in compliance with the Decree of March, 19th 2009. It was also partially funded by the SIR 2014 Grant (PROJECT RBSI14JKU3), Italian Ministry of University and Research (MIUR). These funding sources had no other involvement in this study. Authors were grateful to Lucio Caso for technical assistance. GS like to thanks Dr. Lidia Pino for her friendly support to the research.

References

- Ames, G.F., 1986. Bacterial periplasmic transport systems: structure, mechanism, and evolution. *Annu. Rev. Biochem.* 55, 397–425.
- Aryal, N., Kvist, T., Amman, F., Pant, D., Ottosen, L.D., 2018. An overview of microbial biogas enrichment. *Bioresour. Technol.* 264, 359–369.
- Auerbach, G., Ostendorf, R., Prade, L., Korndörfer, I., Dams, T., Huber, R., Jaenicke, R., 1998. Lactate dehydrogenase from the hyperthermophilic bacterium *Thermotoga maritima*: the crystal structure at 2.1 Å resolution reveals strategies for intrinsic protein stabilization. *Structure* 6, 769–781.
- Basile, M.A., Carfagna, C., Cerruti, P., Gomez, d'Ayala, G., Fontana, A., Gambacorta, A., Malinconico, M., Dipasquale, L., 2012. Continuous hydrogen production by immobilized cultures of *Thermotoga neapolitana* on an acrylic hydrogel with pH-buffering properties. *RSC Adv.* 2, 3611–3614.
- Belkin, S., Wirsén, C.O., Jannash, H.W., 1986. A new sulfur-reducing, extremely thermophilic eubacterium from a submarine thermal vent. *Appl. Environ. Microbiol.* 51 (6), 1180–1185.
- Bernfeld, P., 1995. Amylases a and b. *Methods Enzymol.* 1, 149–158.
- Cappelletti, M., Bucchi, G., De Sousa Mendes, J., Alberini, A., Fedi, S., Bertin, L., Frascari, D., 2012. Biohydrogen production from glucose, molasses and cheese whey by suspended and attached cells of four hyperthermophilic *Thermotoga* strains. *J. Chem. Technol. Biotechnol.* 87, 1291–1301.

- Ceballos-Escalera, A., Molognoni, D., Bosch-Jimenez, P., Shahparasti, M., Bouchakour, S., Luna, A., Guisasaola, A., Borràs, E., Della Pirriera, M., 2020. Bioelectrochemical systems for energy storage: a scaled-up power-to-gas approach. *Appl. Energy* 260, 114138.
- Chen, L., Liu, M.Y., LeGall, J., Fareira, P., Santos, H., Xavier, A.V., 1993. Rubredoxin oxidase, a new flavo-hemo-protein, is the site of oxygen reduction to water by the 'strict anaerobe' *Desulfovibrio gigas*. *Biochem. Biophys. Res. Commun.* 193 (1), 100–105.
- Cristiani, P., Carvalho, M.L., Guerrini, E., Daghighi, M., Santoro, C., Li, B., 2013. Cathodic and anodic biofilms in single chamber microbial fuel cells. *Bioelectrochemistry* 92, 6–13.
- Dipasquale, L., d'Ippolito, G., Fontana, A., 2014. Capnophilic lactic fermentation and hydrogen synthesis by *Thermotoga neapolitana*: an unexpected deviation from the dark fermentation model. *Int. J. Hydrogen Energy* 39, 4857–4862.
- d'Ippolito, G., Dipasquale, L., Vella, F.M., Romano, I., Gambacorta, A., Cutignano, A., Fontana, A., 2010. Hydrogen metabolism in the extreme thermophile *Thermotoga neapolitana*. *Int. J. Hydrogen Energy* 35, 2290–2305.
- d'Ippolito, G., Dipasquale, L., Fontana, A., 2014. Recycling of carbon dioxide and acetate as lactic acid by the hydrogen-producing bacterium *Thermotoga neapolitana*. *ChemSusChem* 7, 2678–2683.
- Eriksen, N.T., Nielsen, T.M., Iversen, N., 2008. Hydrogen production in anaerobic and microaerobic *Thermotoga neapolitana*. *Biotechnol. Lett.* 30 (1), 103–109.
- Geppert, F., Liu, D., van Eerten-Jansen, M., Weidner, E., Buisman, C., Ter Heijne, A., 2016. Bioelectrochemical power-to-gas: State of the art and future perspectives. *Trends Biotechnol.* 34, 879–894.
- Guo, K., PrévotEAU, A., Patil, S.A., Rabaey, K., 2017. Materials and their surface modification for use as anode in microbial bioelectrochemical systems, in *Functional Electrodes for Enzymatic and Microbial Electrochemical Systems*. Ed. N. Brun and V. Flexer. 403–427.
- Hirano, S., Matsumoto, N., 2017. Electrochemically applied potentials induce growth and metabolic shift changes in the hyperthermophilic bacterium *Thermotoga maritima* MSB8. *Biosci. Biotechnol. Biochem.* 201781, 1619–1626.
- Karkovska, M., Smutoka, O., Stasyuka, N., Gonchar, M., 2015. L-Lactate-selective microbial sensor based on flavocytochrome b₂-enriched yeast cells using recombinant and nanotechnology approaches. *Talanta* 144, 1195–1200.
- Katuri, K.P., Rengaraj, S., Kavanagh, P., O'Flaherty V and Leech D., 2012. Charge Transport through *Geobacter sulfurreducens* Biofilms Grown on Graphite Rods. *Langmuir*, 28, 7904–7913. [dx.doi.org/10.1021/la2047036](https://doi.org/10.1021/la2047036).
- Jian, S., Liu, X., Sun, H., Hou, S., 2014. The electrochemical studies of cytochrome c incorporated in 3D porous calcium alginate films on glassy carbon electrodes. *RSC Adv.* 4, 6165–6172.
- Johnson, M., Conners, S., Montero, C., Chou, C., Shockley, K., Kelly, R., 2006. The *Thermotoga maritima* phenotype is impacted by syntrophic interaction with *Methanococcus jannaschii* in hyperthermophilic coculture. *Appl. Environ. Microbiol.* 72 (1), 811–818.
- Lakhal, R., Auria, R., Davidson, S., Ollivier, B., Dolla, A., Hamdi, M., Combet-Blanc, R., 2010. Effect of oxygen and redox potential on glucose fermentation in *thermotoga maritima* under controlled physicochemical conditions. *Int J Microbiol.* 896510, 10 pages. <https://doi.org/10.1155/2010/896510>.
- Le Four, C., Fardeau, M.L., Ollivier, B., Lojou, E., Dolla, A., 2008. The hyperthermophilic anaerobe *Thermotoga maritima* is able to cope with limited amount of oxygen: insights into its defence strategies. *Environ. Microbiol.* 10 (7), 1877–1887.
- Nikolaïdis, P., Poullikkas, A., 2017. A comparative overview of hydrogen production processes. *Renew Sust En Rev.* 67, 597–611.
- Nuzzo, G., Landi, S., Esercizio, N., Manzo, E., Fontana, A., d'Ippolito, G., 2019. Capnophilic lactic fermentation from *Thermotoga neapolitana*: a resourceful pathway to obtain almost enantiopure L-lactic acid. *Fermentation* 5 (2), 34. <https://doi.org/10.3390/fermentation5020034>.
- Pradhan, N., Dipasquale, L., d'Ippolito, G., Fontana, A., Panico, A., Lens, P.N.L., Pirozzi, F., Esposito, G., 2016. Kinetic modeling of fermentative hydrogen production by *Thermotoga neapolitana*. *Int. J. Hydrogen Energy* 41, 4931–4940.
- Pradhan, N., d'Ippolito, G., Dipasquale, L., Esposito, G., Panico, A., Lens, P.N.L., Fontana, A., 2019. Simultaneous synthesis of lactic acid and hydrogen from sugars via capnophilic lactic fermentation by *Thermotoga neapolitana* cf *capnolactica*. *Biomass Bioenergy* 125, 17–22. <https://doi.org/10.1016/j.biombioe.2019.04.007>.
- Pysz, M.A., Conners, S.B., Montero, C.I., Shockley, K.R., Johnson, M.R., Ward, D.E., Kelly, R.M., 2004. Transcriptional analysis of biofilm formation processes in the anaerobic, hyperthermophilic bacterium *Thermotoga maritima*. *Appl. Environ. Microbiol.* 70, 6098–6112.
- Roustazadeh Sheikhyouse, P., Nasr Esfahany, M., Colombo, A., Franzetti, A., Trasatti, S.P., Cristiani, P., 2017. Investigation of different configurations of microbial fuel cells for the treatment of oilfield produced water. *Appl. Energy* 192, 457–465.
- Santoro, C., Artyushkova, K., Babanova, S., Atanassov, P., Ieropoulos, I., Greenman, J., Cristiani, P., Grattieri, M., Li, B., 2014. Parameters characterization and optimization of activated carbon (AC) cathodes for microbial fuel cell applications. *Bioresour. Technol.* 163, 54–63.
- Sasaki, K., Sasaki, D., Morita, M., Hirano, S., Matsumoto, N., Ohmura, N., Igarashi, Y., 2010. Bioelectrochemical system stabilizes methane fermentation from garbage slurry. *Bioresour. Technol.* 101 (10), 3415–3422. <https://doi.org/10.1016/j.biortech.2009.12.076>.
- Sharma, M., Alvarez-Gallego, Y., Achouak, W., Pant, D., Sarma, P.M., Dominguez-Benetton, X., 2019. Electrode material properties for designing effective microbial electrosynthesis systems. *J. Mater. Chem. A*, accepted. DOI:10.1039/C9TA04886C.
- Squadrito, G., Cristiani, P., d'Ippolito, G., Tucci, M., Esercizio, N., Sardo, A., Vastano, M., Ianzilli, M., Fontana, A., 2020. Hyperthermophilic biofilms of *Thermotoga neapolitana* on different materials and electrostimulated: SEM micrographs and chemical data of the glucose fermentation in electrochemical reactors. *Data Brief* (in press).
- Stephen, A.J., Archer, S.A., Orozco, R.L., Macaskie, L.E., 2017. Advances and bottlenecks in microbial hydrogen production. *Microbial Biotech.* 10, 1120–1127.
- Unsworth, L.D., van der Oost, J., Koutsopoulos, S., 2007. Hyperthermophilic enzymes - stability, activity and implementation strategies for high temperature applications. *FEBS J.* 274, 4044–4056.
- van Ooteghem, S.A., Jones, A., van der Lelie, D., Dong, B., Mahajan, D., 2004. H₂ production and carbon utilization by *Thermotoga neapolitana* under anaerobic and microaerobic growth conditions. *Biotechnol. Lett.* 26 (15), 1223–1232.
- Vargas, M., Kashefi, K., Blunt-Harris, E.L., Lovley, D.R., 1998. Microbiological evidence for Fe (III) reduction on early Earth. *Nature* 395 (395), 65–67.
- Virdis, B., Millo, D., Donose, B.C., Batstone, D.J., Permyakov, E.A., 2014. Real-time measurements of the redox states of c-type cytochromes in electroactive biofilms: a confocal resonance raman microscopy study. *PLoS ONE* 9 (2), e89918. <https://doi.org/10.1371/journal.pone.0089918>.
- Wang, X., Santoro, C., Cristiani, P., Squadrito, G., Lei, Y., Agrios, A.G., Pasaogullari, U., Li, B., 2013. Influence of electrode characteristics on coulombic efficiency (CE) in microbial fuel cells (MFCs) treating wastewater. *J. Electrochem. Soc.* 160, G3117–G3122.



6. *Conclusions and future perspectives*

The objectives of this PhD project are part of the European BioRECO₂VER project in which *Thermotoga neapolitana* was selected as one of the microbial platforms for the non-photosynthetic process of capture and conversion of CO₂ into value-added products, as isobutene and lactate. In this context, Capnophilic lactic fermentation (CLF) represents a promising process to achieve CO₂ mitigation and target the climate change effects.

To this aim, the PhD research mostly focused on the study and characterization of the main metabolic and technological factors that affect the sequestration of CO₂ and the conversion of CO₂ into L-lactic acid by *Thermotoga neapolitana*. Within this frame, I also explored molecular approaches to manipulate the microbial strains and enhance the coupling reaction catalyzing the CO₂ fixation into lactic acid by capnophilic lactic fermentation.

According to the transcriptional analysis, CO₂ changes the microbial bioenergetics and increases production of biological reductants, namely NADPH and reduced ferredoxin, to sustain the concomitant production of hydrogen and lactic acid. The bacterial cells perform a deep metabolic rewiring to sustain the redox requirements needed by this synthesis, including variation in central carbon metabolism, expression of oxidoreductive enzymes, triggering of ion and/or proton pumps across the cellular membranes, and activation of energy conservation mechanisms based on the bifurcating enzymes NFN and RNF.

Labeling experiments with labeled precursors in *T. neapolitana* cultures demonstrated for the first time the activation of the pentose phosphate (PP) pathway under CO₂. The PP pathway takes place in the cytosol and generates ribose-5-phosphate and NADPH. The involvement of PP pathway in CLF provides first molecular evidence of the change in the redox status that is needed to sustain the concomitant synthesis of hydrogen and lactic acid production. To the best of our knowledge, the PP



pathway has been never described in hyperthermophiles, thus its identification in *T. neapolitana* has also a general significance in the study of bacteria and archaea thriving in hot or very hot environments.

Energy conservation mechanism in biological organisms involves separation of reactions and transport of charges, usually H^+ and Na^+ , across membranes to build electrochemical gradients driving ATP synthesis. NFN and RNF are two flavin-based transporters that have been recently characterized as bifurcating enzymes in *Thermotoga maritima* and in some species of acetogens, respectively. The up-regulation of these complexes in *T. neapolitana* suggests a role to overcome the energy limitations due to CLF. NFN and RNF operate in combination with membrane-bound ATPases to establish effective energy conservation mechanisms. Notably, the bioinformatic analysis revealed that proton-dependent F-type ATPases are widespread in *Thermotogaceae* but sodium-dependent V-type ATPases are restricted to *T. neapolitana* and *T. sp.* strain RQ7. Since these species are the only ones to operate CLF, the co-existence of V- and F-type ATPases might be crucial to make operational the mechanism of energy conservation linked to NFN and RNF,

Another interesting aspect that opens new scenarios in the study on the CLF pathway is represented by the discovery of *T.sp.*RQ7 as CLF-performing strain. *T. neapolitana* is considered a recalcitrant to genetic manipulation and many efforts have been devoted to achieve its genetic transformation during the PhD thesis. The development of the entire transformation strategy was based on the previously studies in *T. maritima* and *T.sp.*RQ7. A very important contribution in the resolution of the major issues related to the genetic transformation has been given by professor Zhaohui Xu, from the University of Bowling Green (OH-USA), who kindly hosted me for a few months in her laboratory and donated a strain of *T.sp.*RQ7. The heterologous expression of the ACS gene from *T. thermophilus* in *T. neapolitana* ACS03 is the first example of transformation of this bacterium. The significant



increase of lactic acid from exogenous ^{13}C -labeled acetate performed by the mutant strain proves the acetate uptake during CLF and corroborates the biochemical mechanism reported in previous studies carried out in the laboratory of my supervisors. The increased synthesis of L-lactic acid by *T. neapolitana ACS03* also reveals for the first time the possibility to manipulate this bacterium to develop bio-based processes for the non-photosynthetic fixation of CO_2 .

The analysis of sulfur inorganic compounds in *T. neapolitana* showed a significative effect on CLF performances, and also the adapted laboratory strain obtained from the wild type strain in a selected medium without yeast extract and tryptone showed an important rearrangement of the entire metabolism that has to be further investigated. In this perspective, the adaptive laboratory evolution strategy described here for the first time on *T. neapolitana* could represent another important tool to push the system through a phenotypic selection of mutants, useful when the classical molecular approaches are ineffective.

The success of the electrostimulation experiments in bioelectrochemical systems on *T. neapolitana*, and the documented capability of *Thermotoga* and *Pseudothermotoga spp* in fermenting organic wastes originated from food, glycerol, lignocellulosic, and microalgal biomass demonstrated again the enormous biotechnological potential of these hyperthermophilic bacteria in innovative power-to-gas and value-added recovery technologies.

In addition to the biotechnological perspectives, the findings of this PhD thesis open interesting opportunities to target the physiological importance of CLF metabolism. The preliminary results about the co-existence of V-type and F-type ATPases in *T. neapolitana* represent a good starting point in the study of energy conservation and functioning of these complexes in hyperthermophilic bacteria. Experiments with antibodies against F- and V-ATPases are already underway to confirm



Consiglio Nazionale
delle Ricerche



the regulation observed in the transcriptomic analysis. Further research programs involve knockout of CLF pathway genes in *T.sp.RQ7* to provide molecular confirmation of key steps in this unconventional fermentation.